Design and Synthesis of Novel Benzodiazepines

Stephanie Lee MacQuarrie

Dissertation submitted to the Faculty of the Virginia Polytechnic Institute and State University in partial fulfillment of the requirements for the degree of

Doctor of Philosophy

In

Chemistry

Dr. Paul R. Carlier, Chairman

Dr. Paul A. Deck

Dr. David G.I. Kingston

Dr. Timothy E. Long

Dr. James M. Tanko

November 30, 2005

Blacksburg, Virginia

Keywords: Bivalent Ligand, Agonist, Benzodiazepine, Heterodimer, $GABA_A$ Receptor, Asymmetric Synthesis, 1,4-Benzodiazepin-1,5-dione, Memory of Chirality, Density Functional Theory

Design and Synthesis of Novel Benzodiazepines

Stephanie Lee MacQuarrie

ABSTRACT

Bivalent drug design is an efficient strategy for increasing potency and selectivity of many drugs. We devised a strategy to prepare agonist-benzodiazepine heterodimers that could simultaneously bind to agonist and BZD sites of the $GABA_AR$. We synthesized a benzodiazepine-MPEG model compound that relied on physiological GABA to elicit flux. We established that a tether at the N1 position of the BZD would not prevent binding to the receptor. However, coupling of GABA amides with long chain PEG tethers studied by another group member resulted in complete loss of agonist activity. We therefore ceased research in this particular area.

1,4-Benzodiazepin-2,5-diones display a wide range of pharmacological activities. Compounds containing the tricyclic proline-derived subtype have received attention as potent anxiolytic agents and as starting materials for anthramycin-inspired anticancer agents. More recently enantiopure (*S*)-proline-derived 1,4-benzodiazepin-2,5-diones have been recognized as selective α5 $GABA_A$ receptor ligands. Despite the impressive diversity of 1,4-benzodiazepine-2,5-diones prepared to date, enantiopure examples possessing a quaternary stereogenic center have been largely unexplored.

"Memory of chirality" (MOC) is an emerging strategy for asymmetric synthesis. This technique enables the memory of a sole chiral center in the substrate to be retained in a process that destroys that center. We have used this technique to prepare a library of quaternary proline-derived, thioproline-derived and hydroxyproline-derived 1,4-benzodiazepin-2,5-diones, in high ee. We have developed an efficient synthetic method

for preparing oxaproline-derived 1,4-benzodiazepin-2,5-diones in high yields, and by applying the MOC strategy we have prepared quaternary derivatives in acceptable %ee. We envision oxaproline-derived 1,4-benzodiazepin-2,5-diones may exhibit similar or more potent pharmacological properties than proline-derived 1,4-benzodiazepin-2,5-diones. Using density functional theory (DFT) methods, we modeled the formation of an enantiopure, dynamically chiral enolate intermediate and the slow racemization of the enolate on the alkylation reaction time scale.

Acknowledgments

I would like to thank my advisor, Dr. Paul Carlier for his guidance, enthusiasm, and his great efforts to explain things clearly and simply. Throughout the term of my graduate program, he has provided encouragement, sound advice, and good teaching. I would like to express gratitude to Dr. Paul A. Deck, Dr. David G.I. Kingston, Dr. Timothy E. Long and Dr. James M. Tanko for the time they have spent on my committee. I would also like to thank Dr. Jeffery Bloomquist for teaching me how to perform bioassays and understand the results.

I am grateful to Mr. Tom Glass and Mr. Bill Bebout for their analytical services. I acknowledge the financial support of the Department of Chemistry at Virginia Tech.

I am indebted to the Carlier group members past and present for providing a stimulating and fun environment in which to learn and grow.

Finally, I am forever grateful to my husband, son and parents whose constant encouragement and love I have relied on throughout my time at graduate school.

Table of Contents

List of Figures

List of Schemes

List of Tables

Chapter 1. Introduction and Background of Benzodiazepines

1.1 Benzodiazepines as anxiolytic drugs

The discovery of new, anxiolytic drugs that are fast-acting and free from the unwanted side effects associated with traditional benzodiazepines (BZD) continues to be an important scientific concern. Many neuroactive drugs, including benzodiazepines, interact with the $GABA_A$ receptor, the major inhibitory ion-channel in the mammalian central nervous system.[1-6] Benzodiazepines display not only anxiolytic action, but also sedative, hypnotic, and anticonvulsant actions.[1, 7, 8] It would be desirable to separate these divergent actions and to learn more about their interaction with the $GABA_A$ receptor. To understand the need for this class of improved medicinal agents, it is essential to understand the history of benzodiazepines as well as their mechanism of action at the $GABA_AR$.

1.2 Discovery of benzodiazepine drugs

Benzodiazepines remain a long-standing subject of lively scientific interest.[6, 9-14] In the mid 1950's, knowledge of the processes occurring in the brain was limited, making the design of new therapeutic agents that affected the central nervous system a formidable challenge to chemists.[15] In the past, the molecular modification of already existing drugs led to vastly improved medicines. The tranquilizing drugs that were already on the market had been intensively studied,[15] so the only option was to search

for a new class of drugs with similar biological activity. Sternbach had made some easily modified compounds called benzoheptoxdiazines (**1**) during his postdoctoral work at the University of Cracow, Poland, in the early 1930's (Figure 1.1).[15] At that time, very little had been published on this group of compounds, a fact that increased their appeal.

Figure 1.1 Benzoheptoxdiazines

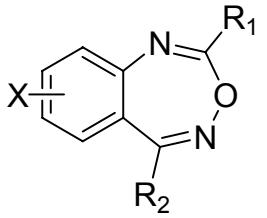

1

It seemed relatively trivial to synthesize a library of benzoheptoxdiazines with varying R_1 and R_2 substituents. Yet, in the midst of preparing these analogues, a problem surfaced. During hydrogenation experiments, the oxygen in the 7-membered ring of the heptoxdiazine was removed easily and quinazoline was formed in excellent yield. Upon further investigation, the structure proposed for compounds like that shown in Figure 1.1 was disproved. The products formed from these reactions were actually quinazoline-3-oxides (**2**) (Figure 1.2).

Figure 1.2 Quinazoline-3-oxides

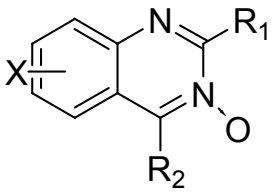

2

The fact that these compounds were easily accessible and interesting led to the synthesis of a novel set of compounds for pharmacological testing.[16] Unfortunately, this

set of compounds did not show biological activity. No further work was done in this field until 1957, when Sternbach and coworkers happened upon a crystalline amine (Scheme 1.1). This compound (**4**) had not been submitted for pharmacological testing in 1955, but it had the expected composition of the other compounds that had been tested at that time.

Scheme 1.1 Preparation of quinazoline-3-oxide (**4**)

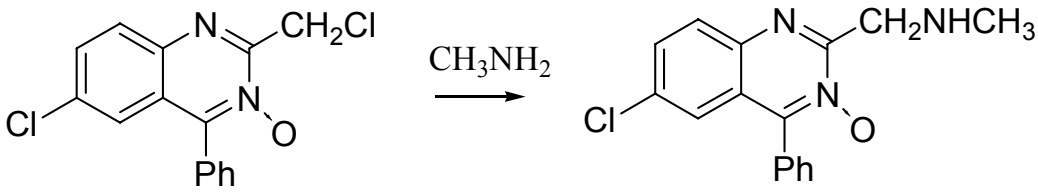

3 **4**

Anticipating negative pharmacological results, but still hopeful, Sternbach submitted the water-soluble salt for testing. The compound showed interesting properties in six tests that were commonly used in the screening of tranquilizers and sedatives.[15]

While the biological screening and testing was being performed, chemists were troubled by the spectral data that was available for this compound (**4**). The UV and IR spectra did not resemble previously synthesized quinazoline-3-oxides, however analytical data ensured it had the correct molecular weight and chemical composition of the expected product (**4**) shown in Scheme 1.1. Work to determine the correct structure of this compound was difficult during this time, as NMR and mass spectrometry were not yet available. Specific degradative studies shown in Scheme 1.2 led to the determination of the reaction product (**4**) as a benzodiazepine-4-oxide (**5**) (Scheme 1.2).

Scheme 1.2 Degradative studies

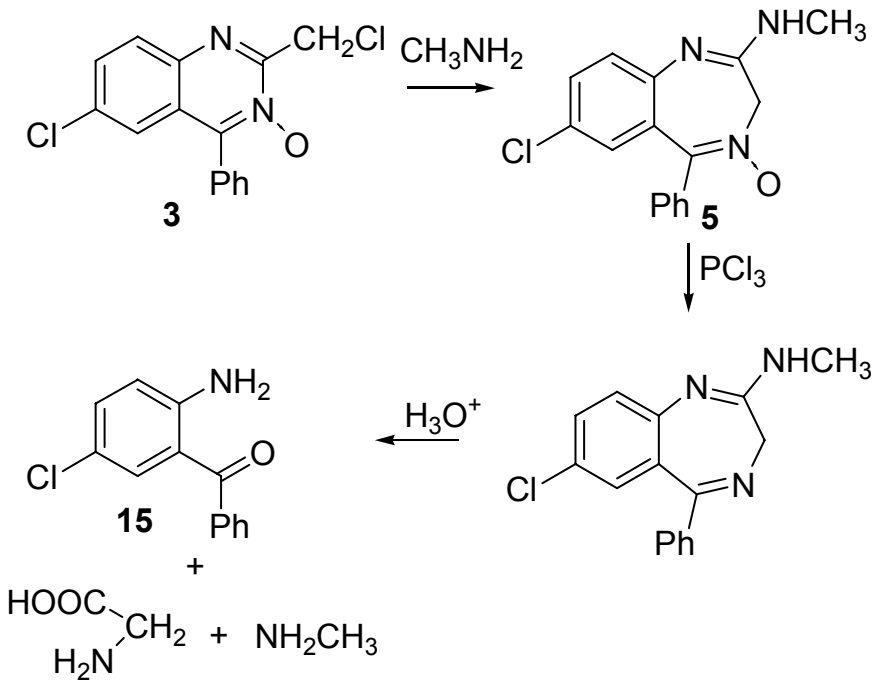

The exciting pharmacological results from this compound led to the synthesis of another library of analogues and homologues.[17] In 1959, a patent was granted claiming the preparation of novel 2-amino-1,4-benzodiazepine-4-oxides (**5**) with various substituents.[15] Unfortunately, none of the analogues or homologues that were prepared showed as much biological activity as the methylamino derivative (**5**). After intensive clinical studies, and two and half years after the first pharmacological testing was done, 7-chloro-2 (methylamino)-5-phenyl-3H-1,4-benzodiazepine-4-oxide (**5**) was introduced, as an anxiolytic drug, into the pharmaceutical market under the trade mark Librium (chlordiazepoxide).[15]

Valuable drugs are often either bitter, hygroscopic, or unstable. Librium (**5**) had all three problems. The next challenge was to find a more suitable form of the drug. The

instability was related to the substituent at the 2-position, which was easily removed by hydrolysis (Scheme 1.3).[18]

Scheme 1.3 Hydrolysis of chlordiazepoxide

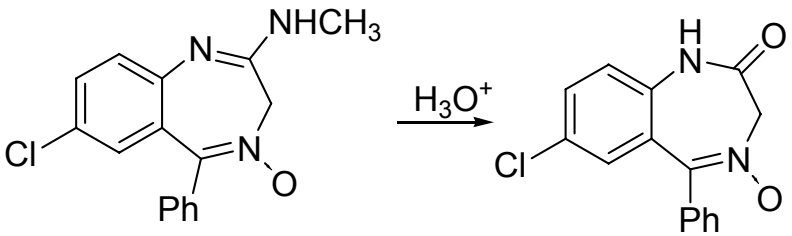

5 **6**

The pharmacological results from testing the hydrolysis product (**6**) showed that it had the same biological activity as Librium (**5**).[15] Removing the N-oxide moiety actually enhanced the activity (Scheme 1.4).[15] The only features that all the biologically active compounds had in common were the 1,4-benzodiazepine ring with a chlorine at the 7 position and a phenyl at the 5 position (**7**).

Scheme 1.4 Removal of the N-oxide moiety

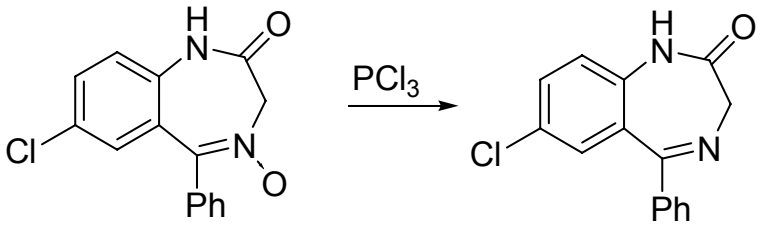

6 **7**

Once the clinical value of Librium was known, it became important to find more selective and more potent products. Most of the compounds that had been tested had similar or weaker potency, except one. 7-Chloro-1,3-dihydro-1-methyl-5-phenyl-2H-1,4

benzodiazepin-2-one (**8**) (Figure 1.3) was significantly more potent than chlordiazepoxide. After thorough clinical and toxicological testing, the first benzodiazepinone exhibiting high biological activity was introduced into clinical practice in 1963. This drug showed anxiolytic behavior and was given the generic name diazepam. It was introduced to the medicinal community as Valium (**8**).[15]

Figure 1.3 Diazepam, Valium

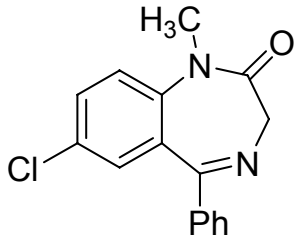

8

Since this time, a huge library of 1,4-benzo-, and hetero-diazepinones have been developed and tested for biological activity. [15] Research in this area is still active and since the first introduction of benzodiazepines (some 37 years ago) they have become one of the most widely used drugs. [1]

1.3 Uses of benzodiazepines in medicine

Benzodiazepines (BZDs), as a class of antianxiety, hypnotic, and muscle relaxing agents, have replaced traditional barbiturates. Benzodiazepines are more effective in alleviating anxiety and stress and they have fewer and less severe side effects. [19, 20] Consequently, BZD's continue to be used to treat such conditions as phobic and panic disorders, as well as depression and migraines. [21]

In addition to treating anxiety, BZD's are often prescribed for treating insomnia, alcohol withdrawl and more recently, epilepsy.[22, 23] Due to the possible adverse effects such as sedation and amnesia, however, research in this area continues.[22] Superior drugs with increased potency or more specific properties will hopefully be discovered.[15] The widespread use of eight benzodiazepine derivatives throughout the U.S. proves their acceptance as clinical drugs.[15] These benzodiazepine derivatives shown in Figure 1.4 are all anxiolytics with the exception of flurazepam (**10**), which is a hypnotic, and clonazepam (**12**), which is marketed as an antiepileptic. Outside the U.S. at least 14 different BZD drugs are available for clinical use, mostly as anxiolytics or hypnotics.[19] The usage of these drugs can differ between countries as well. For example, oxazepam (**9**), is prescribed to treat anxiety in the U.S.. In some European countries, however, it is used as a hypnotic.[24]

Figure 1.4 Benzodiazepine drugs and (half-life values) [24]

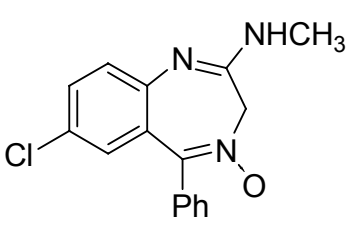

5 chlordiazepoxide
(long)

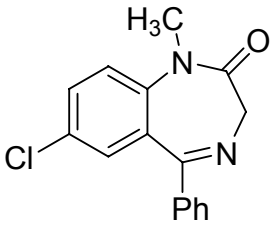

8 diazepam
(long)

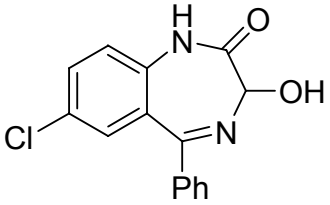

9 oxazepam
(intermediate)

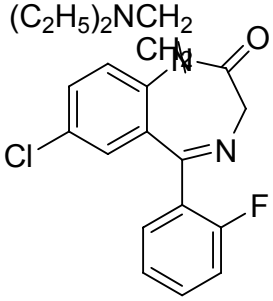

10 flurazepam
(long)

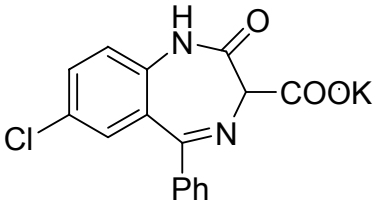

11 clorazepate
(long)

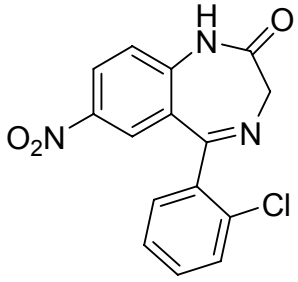

12 clonazepam

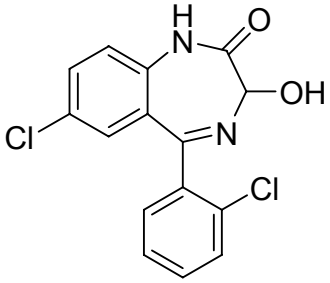

13 lorazepam

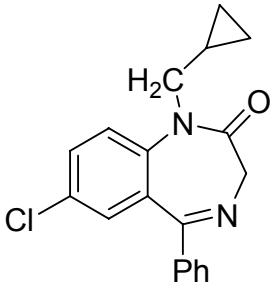

14 prazepam
(long)

Besides the differences in their potency, BZD drugs mainly differ in their pharmacokinetic properties. Their rate of absorption and rate and extent of distribution after a single dose determines the time required for an effect to begin in the body as well as their duration of action. Some of the drugs that are widely used in the U.S. (shown in

Figure 1.4) are often characterized as having a long (half-life of > 24 hours), intermediate (half-life of 5-24 hours) or short (half-life of < 5 hours) duration of action. Half-lives are noted under the compounds that had available data in Figure 1.4. [24] The implications of the half-life for each drug have been studied intensely. Compounds with shorter half-lives are less likely to affect the patient in the morning after taking an evening dosage, so these compounds are often prescribed for sleep aids.[24] Yet when anxiolytic activity is desired, it would make the most sense to use a drug with a longer half-life and hence a longer duration of action.[25]

Depression is the most prevalent psychiatric illness, and yet it is often mis-diagnosed. Insomnia is a common symptom of depression and hypnotics are often prescribed as a treatment for people that actually require antidepressant treatment.[24] This has led to some of the misuse of BZD drugs, as well as the psychological dependence that sometimes develops, especially after long term use.[24, 26]

1.4 Synthetic route to benzodiazepines

The most extensively used methods for preparing 1,4-benzodiazepines begins with an ortho-aminobenzophenone (**15**) (Figure 1.5). The first method involves a two step synthesis. The first step involves treatment of the appropriate aminobenzophenone with haloacetyl halide to afford the amide (**16**), followed by the addition of ammonia to first displace the chlorine giving the glycinamide (**17**). Then cyclization by imine formation will give the benzodiazepine (**18**).[27, 28] The other method involves treating the o-aminoketone with an amino acid ester hydrochloride in pyridine to yield (**18**). Generally,

the first method gave a higher percent yield of clean product, while the second method facilitated the conversion of o-aminoketones to benzodiazepines in one step, with a variety of substituents.[27, 29]

Scheme 1.5 Synthetic routes to BZD's

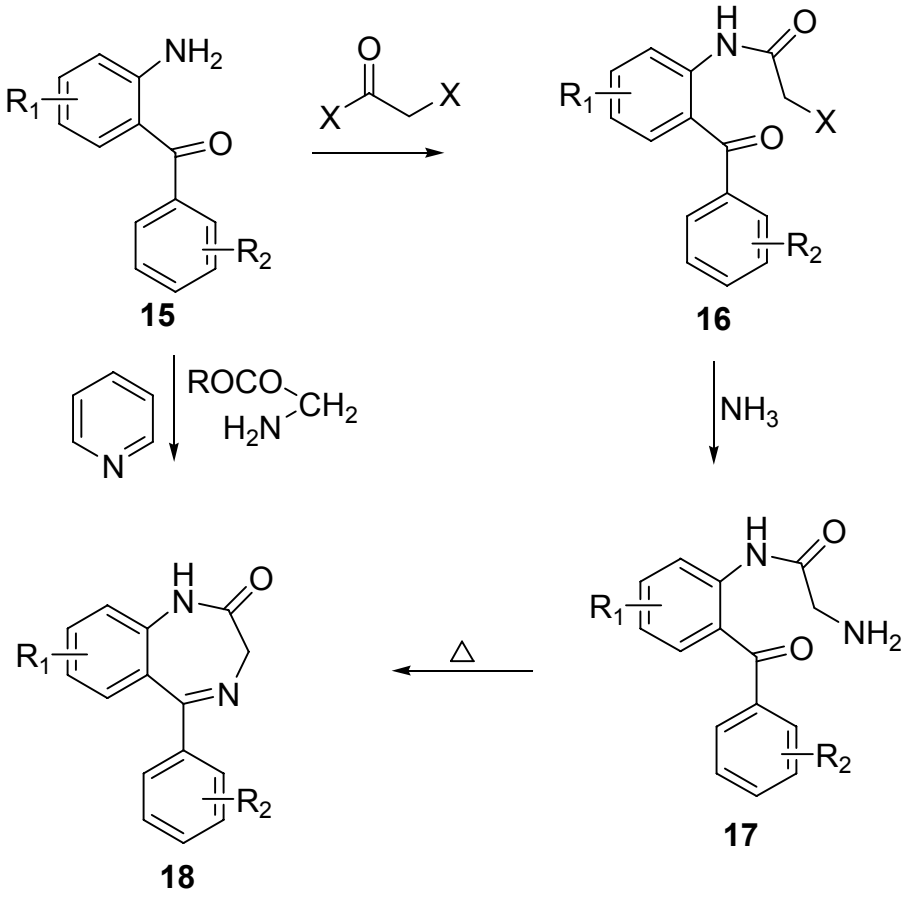

Some other interesting routes for synthesizing 1,4-benzodiazepines have been developed. One of these synthetic methods involves indole derivatives, which form aminoacetoamido compounds when the double bond in the five membered ring is oxidized. They will then cyclize to benzodiazepines under proper reaction conditions (Scheme 1.6).[30]

Scheme 1.6 Formation of indole derivatives by oxidation

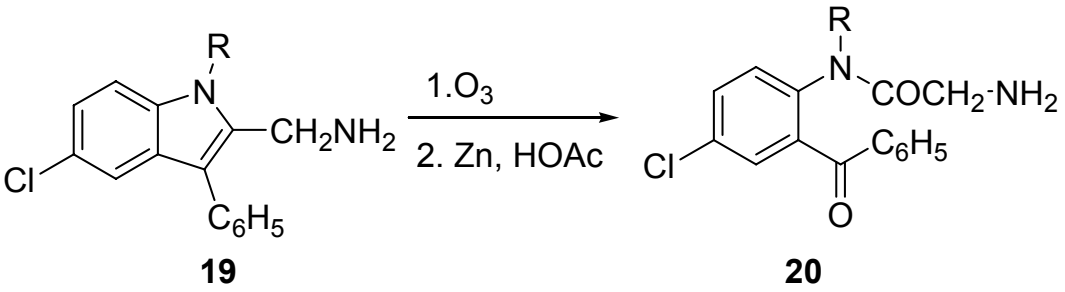

19 **20**

Most of the available alternative routes for the construction of the 7-membered ring involve intermediates that have protected or potential glycine moieties. Some of these are shown in Figure 1.5.[30] Compounds **21** and **22** can be directly synthesized via condensation of 2-aminobenzophenone and the appropriate α-amino protected glycine unit.

Figure 1.5 Glycine moieties intermediates

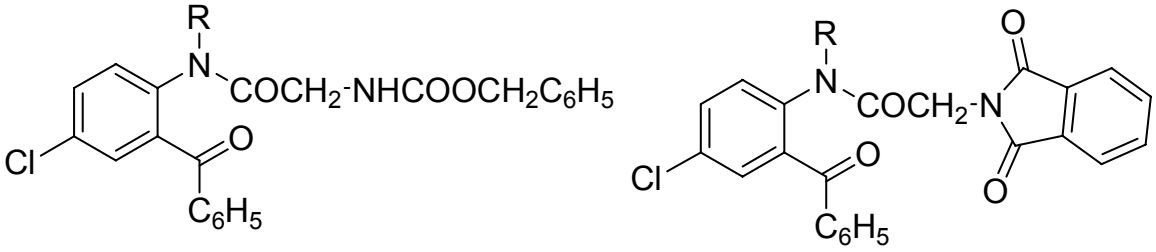

21 **22**

A more recent solid support synthesis of 1,4-benzodiazepines was described by Ellman.[31] Initially, 1,4-benzodiazepin-2-ones were synthesized using standard 2-aminobenzophenones, amino acids and alkylating agents. Scheme 1.7 shows the 2-*N*-Fmoc aminobenzophenone coupled to the acid-cleavable acetic acid (HMP) linker. The

linker can be attached by either a hydroxyl or a carboxyl group on either aromatic ring of the aminobenzophenone. Using standard amide bond formation methodology, the linker (**23**) is then coupled to the solid support yielding (**24**).

Scheme 1.7 Aminobenzophenone coupled to the solid support

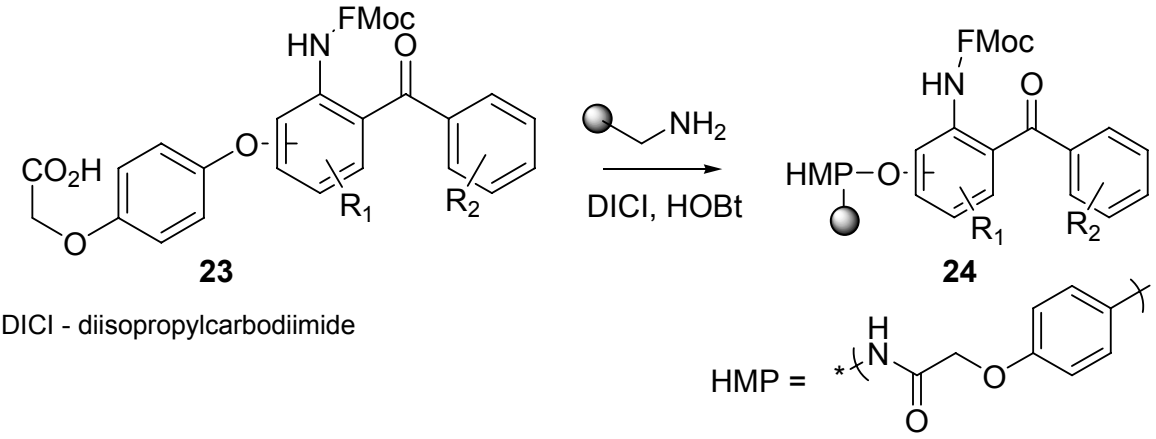

The synthesis of benzodiazepines on the solid support begins with removal of the 9-fluorenyl-methoxycarbonyl (Fmoc) protecting group, followed by a coupling of the unprotected 2-aminobenzophenone with α-*N*-Fmoc amino acid fluorides to give the amide product (**25**) (Scheme 1.8).[31]

Finally removal of the Fmoc group and treatment with 5% acetic acid in *N*-methylpyrrolidinone yields the benzodiazepine derivative (**26**). It is then possible to alkylate the anilide of (**26**) by using either lithiated acetanilide or lithiated 5-(phenylmethyl)-2-oxazolidinone as the base, and an alkylating agent to provide 1,4-benzodiazepines (**27**). Treatment with trifluoroacetic acid (TFA) affords the 1,4-benzodiazepine in high yield (**28**) (Scheme 1.8).[31]

Scheme 1.8 Ellman's synthesis of 1,4-benzodiazepines[31]

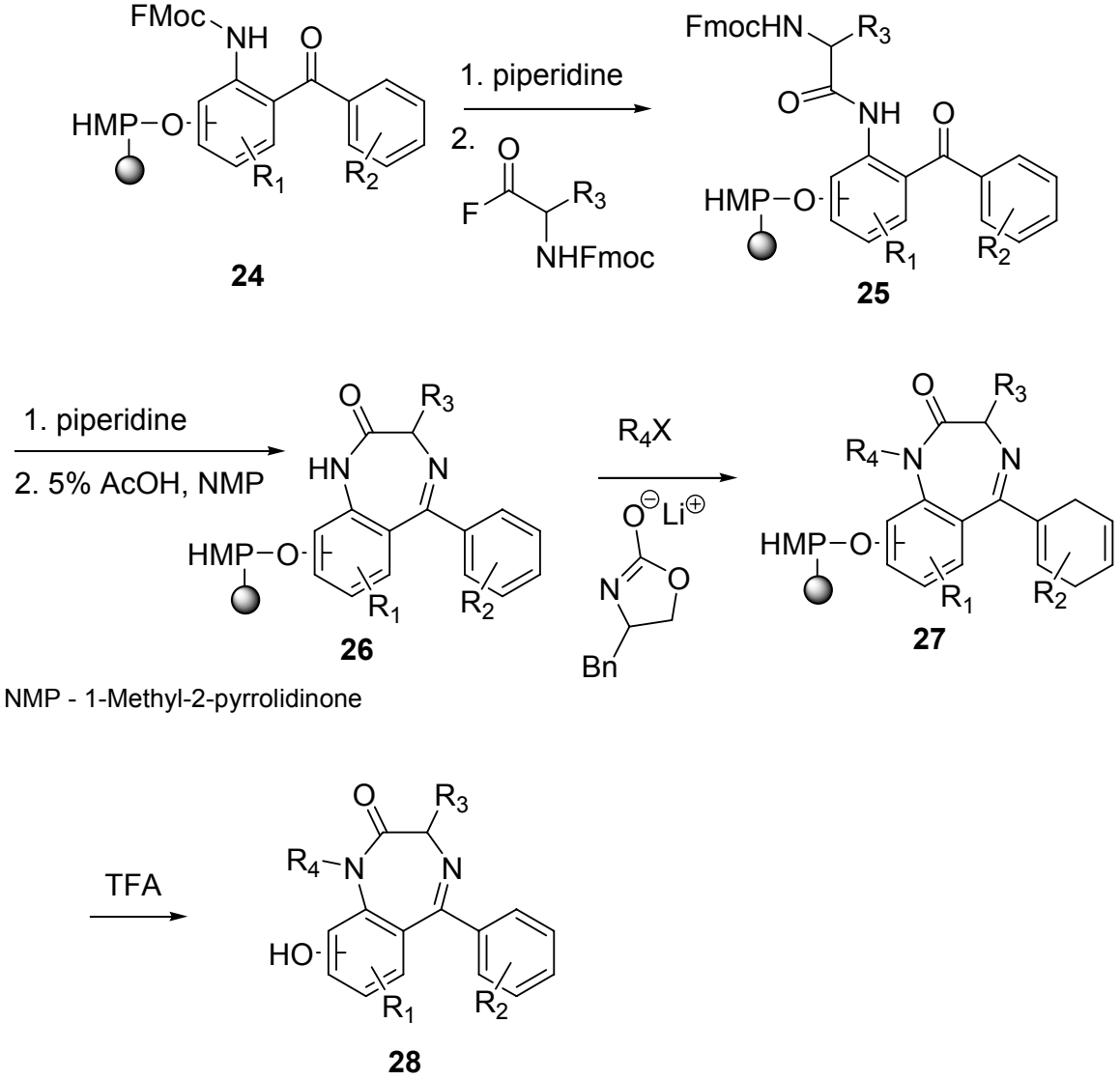

Due to the fact that few 2-aminobenzophenones were commercially available, an improved synthetic strategy was devised. To increase the diversity of 1,4-benzodiazepin-2-ones available for solid support synthesis, Stille coupling was used to synthesize a library of 2-aminoaryl ketones on solid support.[31] The 2-(4-biphenyl) isopropyloxycarbonyl (Bpoc) protected (aminoaryl)stannane (**29**) is prepared from commercially available starting material, and is coupled to the support using the HMP

linker. Stille coupling is employed with a variety of acid chlorides in the presence of the catalyst Pd_2-$(dba)_3$·$CHCl_3$. The Bpoc group is removed with treatment of 3% TFA, CH_2Cl_2 solution affording the support-bound aminoaryl ketone (**30**) (Scheme 1.9). 1,4-benzodiazepine derivatives are then synthesized following the previously described synthesis (Scheme 1.8). Utilizing this strategy, a library of 11,200 1,4-benzodiazepines was synthesized from 20 different acid chlorides, 35 amino acids and 16 alkylating agents. [31]

Scheme 1.9 Ellman's synthesis of BZDs using Stille coupling[31]

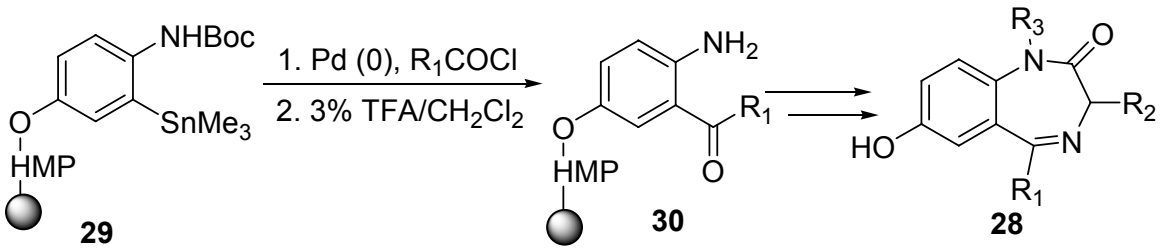

1.5 Structure activity relationships of benzodiazepines

With such a large library of benzodiazepines available, structure activity relationships have been studied thoroughly.[15, 32-35] The set of "rules" that were established by Sternbach proved to be very valuable in the synthesis of more potent and selective benzodiazepines.[15, 36]

The tests that were used to make these observations include the inclined screen, foot shock, and the unanesthetized cat assay.[37] The inclined screen test involved giving male mice a maximum dose of 500 mg of the drug per kg of body weight. The mice were then left on an inclined screen for at least 4 hours to observe any paralyzing effects severe

enough to cause the mouse to slide off of the screen. The foot shock test involves shocking the feet of a pair of mice to induce fighting. One hour before the second shocking the mice were treated with the drug. At least three pairs of mice at three different dose levels were examined. The dose which prevents fighting in the three pairs of mice is considered to be 100% effective. The final test that was used was the unanesthetized cat assay, in which the drug being tested was administered to cats. At least three cats were used per dose of the drug and three different doses were administered. The cats were then observed for behavioral changes and limpness in the legs. The minimum effective dose is the lowest dose at which muscle relaxation was observed. The structure activity relationship which follows was based on the results of these three assays.[37]

Substitution on the rings had a pronounced effect on biological activity. Substitution at the R_2 position of ring A with electron withdrawing groups, (halogens and nitro groups) imparted high activity, while having electron donating groups (methyl and methoxy) at this position causes a significant activity decrease (Figure 1.6).

Figure 1.6 Effects of substituents on the biological activity of BZDs

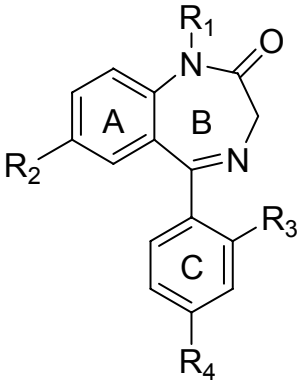

31

Summary

R1 Positive Effect: H, CH_3, Et, i-Bu
Negative Effect:t-Bu
R2 Positive Effect: Cl, F, NO_2, CF_3
Negative Effect: Me, OMe
R3 Positive Effect: H, F, Cl
R4 Positive Effect: H
Negative Effect: anything else

The nitrogen atom at the R_1 position in ring B tolerates substitution by a methyl group, whereas larger groups in this position such as tertiary butyl led to significantly decreased activity.[15, 30] Substitution of the R_3 position on ring C with halogens leads to increased activity, but any substitution at the R_4 position strongly decreases anxiolytic activity.[15]

Based on these findings a library was prepared, consisting of over 80 benzodiazepines with varying substitution at the R_1 and R_2 positions. Eventually one of the most potent benzodiazepines to date was synthesized combining all the moieties that induce high activity. The compound, Flunitrazepam (**32**), has a methyl group at R_1, a nitro group at R_2 and a fluorine at the R_3 position (Figure 1.7). It is prescribed in Switzerland as a potent hypnotic.[15]

Figure 1.7 Flunitrazepam[38, 39]

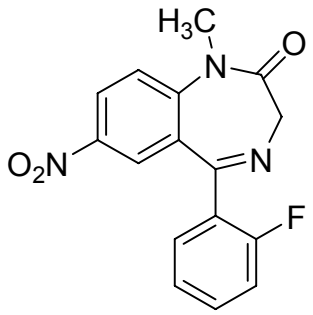

32

Although benzodiazepines were first introduced into clinical practice in 1960, their specific binding to receptor sites was unknown until 1977.[40] The discovery of high-affinity benzodiazepine binding sites in the CNS directed researchers to the $GABA_A$ receptor as a likely site of action.[1] To understand BZD's exact mechanism of action, GABA and the $GABA_A$ receptor must thoroughly be discussed.

References for Chapter 1

[1] Sigel, E., Buhr, A., The benzodiazepine binding site of $GABA_A$ receptors., *Trends Pharm. Sci.* **1997**, *18*, 425.

[2] Togashi, H., Mori, K., Kojima, T., Matsumoto, M., Ohashi, S., Different effects of anxiolytic agents, diazepam and 5-HT1A agonist tandospirone, on hippocampal long-term potentiation in vivo, *Pharmacol. Biochem. Behav.* **2001**, *69*, 367.

[3] Mohler, H., Okada, T., Benzodiazepine receptor: demonstration in the central nervous system., *Science* **1977**, *198*, 849.

[4] Mombereau, C., Kaupmann, K., van der Putten, H., Cryan, J., Altered response to benzodiazepine anxiolytics in mice lacking GABA B receptors, *European Journal of Pharmacology* **2004**, *497*, 119.

[5] Basile, A., Lippa, A. S., Skolnick, P., Anxioselective anxiolytics: can less be more?, *European Journal of Pharmacology* **2004**, *500*, 441.

[6] Berezhnoy, D., Nyfeler, Y., Gonthier, A., Schwob, H., Goeldner, M., Sigel, E., On the benzodiazepine binding pocket in GABA A receptors, *J. Biological Chemistry* **2004**, *279*, 3160.

[7] Brandao, R. C., Aguiar, J. C., Graeff, F. G., GABA mediation of the anti-aversive action of minor tranquilisers, *Pharmacol. Biochem. Behav.* **1982**, *16*, 397.

[8] Marinelli, S., Gatta, F., Sagratella, S., Effects of GYKI 52466 and some 2,3-benzodiazepine derivatives on hippocampal in vitro basal neuronal excitability and 4-aminopyridine epileptic activity, *European Journal of Pharmacology* **2000**, *391*, 75.

[9] Pritchett, D. B., Seeburg, P. H., γ-Aminobutyric acid A receptor α-5-subunit creates novel type II benzodiazepine pharmacology, *J. Neurochem.* **1990**, *54*, 1802.

[10] Triet, D., Animal models for the study of anti-anxiety agents: a review, *Neurosci. Biobehav. Rev.* **1985**, *9*, 203.

[11] Chiu, T., Rosenberg, H. C., Benzodiazepine--specific and nonspecific tolerance following chronic flurazepam treatment, *Trends Pharm. Sci.* **1983**, *4*, 348.

[12] Mandel, P., DeFeudis, F. V. *Advances in Experimental Medicine and Biology*; Plenum Press: New York, 1979; Vol. 123.

[13] Geller, I., Kulak, J. T., Seifter, J., The effects of chlordiazepoxide and chlorpzomazine on a punished discrimination, *Psychopharmacologia* **1962**, *3*, 374.

[14] Lopes, D. V. S., Caruso, R. R. B., Castro, N. G., Costa, P. R. R., da Silva, A. J. M., Noel, F., Characterization of a new synthetic isoflavonoid with inverse agonist activity at the central benzodiazepine receptor, *European Journal of Pharmacology* **2004**, *502*, 157.

[15] Sternbach, L. H., The benzodiazepine story, *J. Med. Chem.* **1979**, *22*, 1.

[16] Sternbach, L. H., Kaiser, S., Reeder, E., Quinazoline 3-oxide structure of compounds previously described in the literature as 3,1,4-benzoxadiazepines, *J. Am. Chem. Soc.* **1960**, *82*, 475.

[17] Sternbach, L. H., Reeder, E., Keller, O., Metlesics, W., Quinazolines and 1,4-benzodiazepines III. Substituted 2-amino-5-phenyl-3H-1,4-benzodiazepine 4-oxides, *J. Org. Chem.* **1961**, *26*, 4488.

[18] Sternbach, L. H., Reeder, E., Quinazolines and 1,4-benzodiazepines IV. Transformations of 7-chloro-2-methylamino-5-phenyl-3H-1,4-benzodiazepine 4-oxide, *J. Org. Chem.* **1961**, *26*, 4936.

[19] Venter, J. C., Harrison, L. C. *Benzodiazepine/GABA Receptors and Chloride Channels*; Alan R. Liss, Inc, 1986; Vol. 5.

[20] Rudolph, U., Benzodiazepine actions mediated by specific gamma-aminobutyric acid(A) receptor subtypes, *Nature* **1999**, *401*, 796.

[21] Covelli, V., Maffione, A. B., Nacci, C., Tato, E., Jirillo, E., Strees, neuropsyciatric disorders and immunological effects exerted by benzodiazepines, *Immunopharmacol. and Immunotoxicol.* **1998**, *20*, 199.

[22] Tecott, L. H., Designer genes and anti-anxiety drugs, *Nature Neurosci.* **2000**, *3*, 529.

[23] Costa, E., Guidotti, A., Benzodiazepines on trial: a research strategy for their rehabilitation, *Trends Pharm. Sci.* **1996**, *17*, 192.

[24] Trimble, M. R. *Benzodiazepines Divided*; John Wiley and Sons: New York, 1983.

[25] Lader, M., Antianixety drugs: clinical pharmacology and therapeutic use., *Drugs* **1976**, *12*, 362.

[26] Woods, J. H., Winger, G., Current benzodiazepine issues, *Psychopharmacology* **1995**, *118*, 107.

[27] Sternbach, L. H., Fryer, R. I., Metlesics, W., Reeder, E., Sach, G., Saucy, G., Stemple, A., Quinazolines and 1,4-benzodiazepines VI. Halo-, methyl-, and methoxy-substituted 1,3- dihydro-5-phenyl-2H-1,4-benzodiazepin-2-ones., *J. Org. Chem.* **1962**, *27*, 3788.

[28] Lednicer, D. *The Organic Chemistry of Drug Synthesis*; Wiley-Interscience: New York, 1998.

[29] Lednicer, D., Mitschev, L. A. *The Organic Chemistry of Drug Synthesis*; Wiley-Interscience: New York, 1977.

[30] Sternbach, L. H. *The Benzodiazepines*; Raven Press: New York, 1973.

[31] Ellman, J. A., Design, synthesis, and evaluation of small-molecule libraries, *Acc. Chem. Res.* **1996**, *29*, 132.

[32] Fryer, R. I., Schmidt, R. A., Sternbach, L. H., Quinazolines and 1,4-benzodiazepines, *J. Pharmaceutical Sci.* **1964**, *53*, 264.

[33] Sternbach, L. H., 1,4-Benzodiazepines. Chemistry and some aspects of structure-activity relationship, *Angew. Chem.* **1971**, *10*, 34.

[34] Fernandez, M., Fernandez, E. M., Imperial, S., Centelles, J. J., Structural requirements of benzodiazepines for the inhibition of pig brain nitric oxide synthase, *Mol. Brain. Res.* **2001**, *96*, 87.

[35] Zappala, M., Grasso, S., Micale, N., Polimeni, S., De Micheli, C., Synthesis and structure-activity relationships of 2,3-benzodiazepines as AMPA receptor antagonists, *Mini-Rev. Med. Chem.* **2001**, *1*, 243.

[36] Gilman, N. W., Sternbach, L. H., Quinazolines and 1,4-benzodiazepines. Synthesis of the tert-butyl analog of diazepam, *J. Heterocycl. Chem.* **1971**, *8*, 297.

[37] Garattini, S., Mussini, E., Randall, L. O. *The Benzodiazepines*; Raven Press: New York, 1973.

[38] DeSarro, G., Gitto, R., Rizzo, M., Zappia, M., DeSarro, A., 1,4-Benzodiazepine derivatives as anticonvulsant agents in DBA/2 mice, *Gen. Pharmac.* **1996**, *27*, 935.

[39] Negrusz, A., Moore, C. M., Hinkel, K. B., Stockham, T. L., Verma, M., Strong, M. J., Janicak, P. G., Deposition of 7-aminoflunitrazepam and flunitrazepam in hair after a single dose of Rohypnol, *J. Forensic Sci.* **2001**, *46*, 1143.

[40] Olsen, R. W., GABA-benzodiazepine-barbiturate interactions, *J. Neurochem.* **1981**, *37*, 1.

Chapter 2. The $GABA_A$ Receptor as the Target of Action for Benzodiazepines and a Review of Multi-valent Ligands

2.1 Introduction to GABA and GABA receptors

The amino acid gamma-aminobutyric acid (GABA) is the major inhibitory neurotransmitter in the mammalian central nervous system.[1] GABA (**1**) was first discovered when scientists noticed the abundance of a particular amino acid in mouse brain, that other tissue, urine or blood lacked. A study of the properties of this substance showed it to be GABA (**1**) (Figure 2.1).[2]

Figure 2.1 GABA

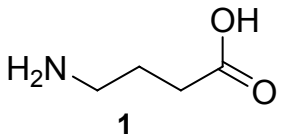

1

The idea that such a simple compound could actually be responsible for inhibitory neurotransmission met with much resistance. Yet, with the persistence of a few determined scientists, clinical studies began to test the role of GABA in conditions such as epilepsy, schizophrenia and other such mental disorders.[2] It was soon discovered that the majority of central neurons are GABA-controlled, and the apparent importance of understanding the GABA system led to intensive research in this area.[2] The overall activity of the brain is determined by two superior functions. The first is excitation by the major excitatory amino acid transmitter, glutamic acid, which depolarizes neurons via

multiple receptor types. The second function is inhibition by GABA, which hyperpolarizes neurons, also through many different receptors.

GABA is an agonist at three major classes of receptors: $GABA_A$, $GABA_B$ and $GABA_C$.[1] The most abundant receptors, $GABA_A$, are ligand gated ion channel receptors, as are $GABA_C$R. These receptors are classified as ionotropic receptors. The $GABA_A$R and $GABA_C$R differ in their sensitivity and location. $GABA_C$ receptors are primarily located in the vertebrate retina, are composed of ρ-subunits, and are insensitive to modulatory drugs (benzodiazepines, barbiturates and neurosteroids).[3, 4] The more abundant receptors $GABA_A$R, are present in all CNS regions, have modulatory binding sites for benzodiazepines, barbiturates and neurosteroids, and are composed of α-, β-, and γ- subunits.[3] $GABA_C$R are more sensitive to physiological GABA then the $GABA_A$R, supporting the presence of five ligand binding sites on $GABA_C$R, compared to the two that appear to be present on the $GABA_A$R.[3-5] Both ionotropic ($GABA_A$R and $GABA_C$R) receptors have similar Cl^- channel pore size (5.6 Å and 5.1 Å, respectively) and exhibit high anion (Cl^-) selectivity.[3, 5] The other GABA receptor, the $GABA_B$ receptor, is a G-protein coupled receptor and is classified as a metabotropic receptor. The $GABA_A$ and $GABA_B$ receptors are insensitive to baclofen (**3**) and (+)-bicuculline (**2**) respectively (Figure 2.2).[3, 4] $GABA_C$R does not respond to either drug. Some $GABA_B$R agonists exhibit important therapeutic properties for the treatment of asthma and also gastroinstetinal disorders.[6] The $GABA_A$R is the target of action for many medicinally important drugs (anxiolytic, anticonvulsants, antidepressants, anesthetics,[7] sedative - hypnotics,[3] insecticides,[8-10] and anthelmintics[7]), hence it continues to be a subject of investigation.

Figure 2.2 (+)-Bicuculline (**2**) and Baclofen (**3**)

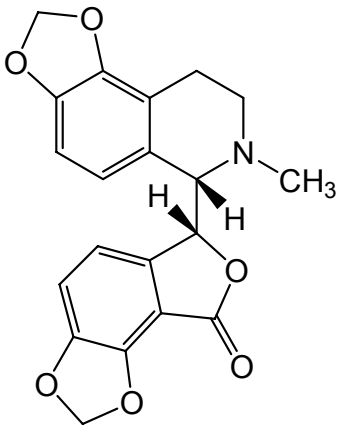

2

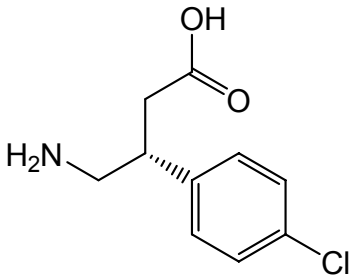

3

2.2 Structure of $GABA_A$ receptor and proposed location of binding sites on $GABA_AR$

The $GABA_AR$ shares similar structural features with other ligand-gated ion channels, such as the nicotinic acetylcholine and glycine receptors.[11, 12] Electron microscopy of the $GABA_AR$ suggests that it is a pentameric arrangement of protein subunits approximately 70 Å wide, having a central water-filled pore.[11] The existence of six α, four β, three γ, one δ, one ε, and one π subunit suggests that an array of heteropentameric isoforms may occur.[13-16] Despite the potentially bewildering complexity, it appears that the major isoform in the brain is: $(\alpha 1)_2(\beta 2)_2(\gamma 2)_1$ (Figure 9).[17-19]

Figure 2.3 Top view of the proposed $GABA_A$ receptor[17]

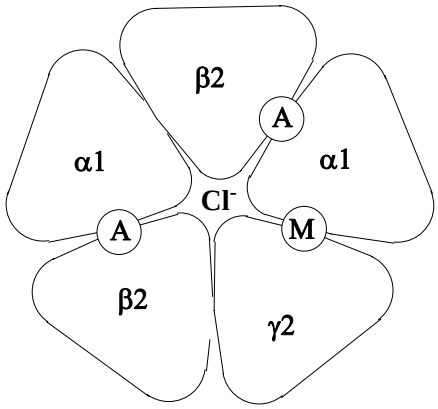

A – functional agonist sites

M- BZD modulator binding site

Earlier evidence suggested the native $GABA_AR$ had both high and low affinity agonist binding sites,[20] which greatly differed in their affinities for agonists.[20, 21] It is assumed that GABA exerts its physiological effect by binding at the low affinity site since micromolar concentrations of GABA or other agonists are required to activate the Cl^- ion channel, and to modulate other binding sites. [7, 22, 23] It has been postulated that the low affinity binding sites are located at the two β-α subunit interfaces. [13, 14, 17, 24] More recently Sigel published a convincing argument that suggested that the high and low affinity sites are identically located and that these two classes of sites interconvert when an agonist binds. Sigel also suggested that these sites exhibit different affinities towards agonists depending on the method of tissue preparation.[25] We agree with Sigel's conclusion that high- and low-affinity sites are interconvertible sites on the $GABA_AR$. Similar to the GABA binding site, binding sites for barbiturates, steroids, and channel-

blocking convulsants are located at $GABA_AR$ subunit interfaces. Not all the various binding sites, however, may be present on each $GABA_AR$ isoform.[7]

Benzodiazepines exert their clinically important action by enhancing the effects of GABA binding at the $GABA_AR$, and increasing the frequency of the Cl^- ion channel opening in response to GABA.[26-28] Benzodiazepines cannot open the chloride ion channel in the absence of GABA. The existence of a specific high affinity binding site for benzodiazepines has been demonstrated, and is believed to occur at the α-γ interface (M shown on Figure 2.3).[7, 25] The BZD site and the functional GABA binding site could be anywhere from 10-40 Å apart depending on where the binding is located with respect to the ion channel.

2.3 Agonist and modulators of the $GABA_AR$

It is possible to group GABA receptor ligands according to their structure and function. Two important classes of ligands are agonist and agonistic modulators, examples of which are shown in Figure 2.4.

Figure 2.4 GABA receptor ligands

Agonists

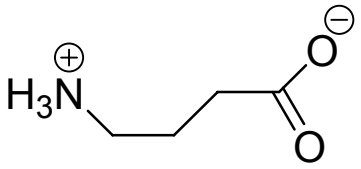

GABA **1**

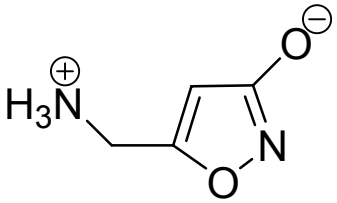

muscimol **4**

Agonistic Modulators

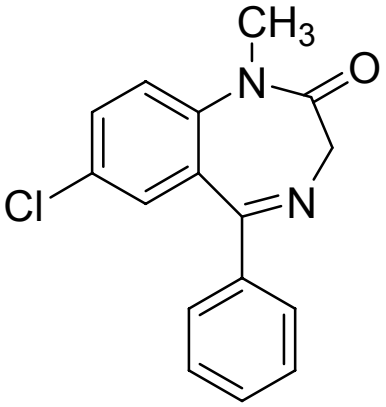

diazepam **5**

A large number of GABA analogues have been prepared in order to determine the structural requirements necessary for binding to the receptor. By systematically altering some of the structural parameters that characterize the GABA molecule, medicinal chemists and pharmacologists concluded that GABA agonist analogues must be zwitterions. Recent studies published in our laboratory by Dr. Ella Clement, however show that appropriately functionalized GABA amides are effective GABA agonists despite their non-zwitterionic structures.[29, 30] The GABA amide superagonist synthesized and tested by Dr. Clement is shown in figure 2.5 (**6**).[29, 30] Zwitterionic GABA analogues developed prior to our work are shown in Figure 2.6. The structural similarity of dihydromuscimol (**8**) to GABA (**1**) explains its pronounced potency.

Figure 2.5 GABA amide superagonist

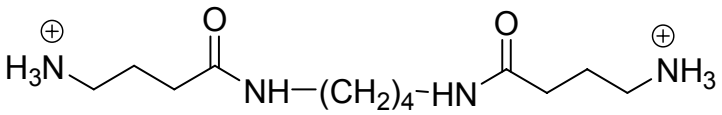

6

Figure 2.6 The structures of some GABA analogues

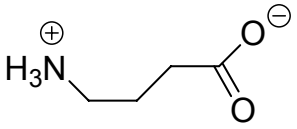

GABA **1**

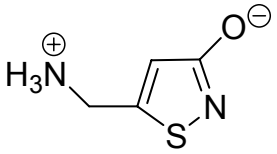

Thio-muscimol **7**

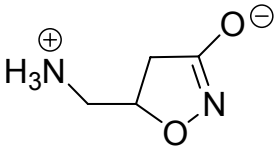

Dihydro-muscimol **8**

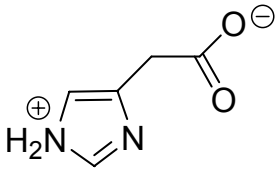

Imidazole-4-acetic acid **9**

Some potent or moderately potent GABA agonists

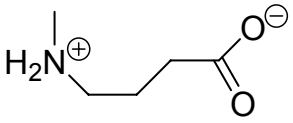

N-Methyl-GABA **10**

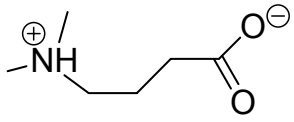

N,N-Dimethyl-GABA **11**

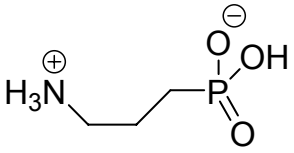

3-Amino-propanephosphonic acid **12**

Some GABA analogues with little or no GABA agonist activity

Replacement of the $-CH_2-CH_2-CO_2^{\ominus}$ group of GABA by a conformationally restricted functionality has resulted in more potent agonists than GABA itself.[31]

Important examples include muscimol (**4**) (Figure 2.4), dihydro-muscimol (**8**) and thiomuscimol (**7**) (Figure 2.6).

The phosphonic acid analogue (**12**) is almost devoid of GABA agonist activity. This is possibly due to the presence of two acid functionalities (Figure 2.6).[32] It is also possible to replace the primary amino group of GABA with other functionalities and maintain GABA agonist activity, as can be seen in imidazole-4-acetic acid (**9**). The N-methyl derivatives of GABA (**10**), however, are virtually inactive.[33]

Benzodiazepines are distinct in that they do not bind to the agonist site and cannot induce channel opening in the absence of agonist. They do, however, exert a positive cooperative effect on GABA binding to its receptor.[34-36]

2.4 Proposed gating schemes for $GABA_AR$

The $GABA_AR$ is a heteropentameric protein complex with binding sites for both GABA and BZD's. Hill Slope measurements are indicative of the minimum number of individual molecules required to bind to a receptor for significant activation,[37-41] and are obtained from dose response curves (Figure 2.5).[42] The dose response curves shown in Figure 12 are described by Equation 2.1.[43] The number of sites that must be occupied in order to activate the receptor is expressed as the exponent n. The slope of the curve gets steeper as n (number of binding sites) increases. At a constant EC_{50} the effect of the Hill number (n) can be observed. A Hill number of 2 results in less activation than a Hill number of 1 when the concentration is less than the EC_{50}. At concentrations above the EC_{50}, however, a Hill number of 2 results in greater activation (Figure 2.7).

Figure 2.7 Dose response curves (n = 1, n = 2)

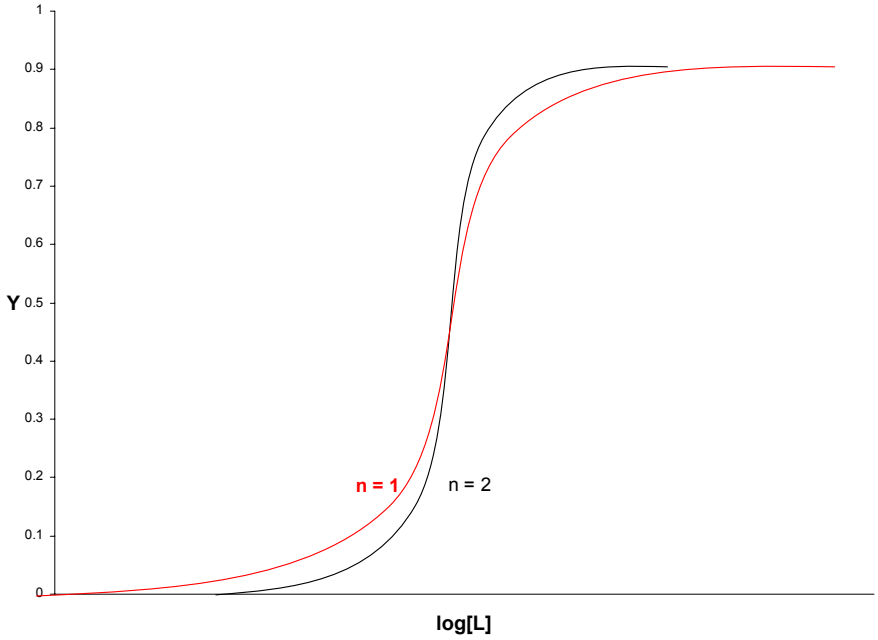

Equation 2.1 Equation describing dose response curves

$$Y = 1/ (K_D/[L]^n + 1)$$

According to patch-clamp studies[41] for GABA, the dose response curve for $GABA_AR$ activation has a Hill Slope of 2. This indicates that there are two functional agonist binding sites that must be occupied before gating will occur. A simplified model for gating is presented in Figure 2.8.

Figure 2.8 Proposed gating scheme for $GABA_AR$

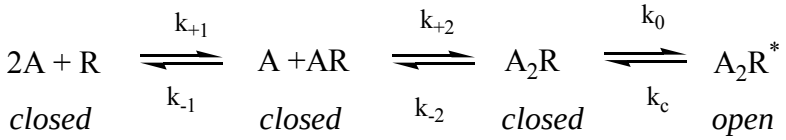

In Figure 2.8, A represents the agonist while R represents the $GABA_A$ receptor with the two functional agonist sites unoccupied. When one agonist binds to the receptor, the GABA channel remains closed. When the GABA receptor is bound by two agonists the GABA channel is in equilibrium between open and closed states (A_2R is closed and A_2R^* is open).[39]

Benzodiazepines do not mediate chloride flux in the absence of GABA. They do, however, enhance the GABA-mediated channel opening. A possible gating scheme that explains the increase in maximum ion flux in the presence of BZD is shown in Figure 2.9.[39, 44] In the figure below, M represents the BZD modulator, R again represents the receptor and A represents agonists. While it is still true that two bound molecules are required to gate the channel, one of these can be a BZD. If a BZD modulator binds to one of the channel gating sites, and an agonist binds to the other GABA binding site, the channel will be in equilibrium between an open (RMA^*) and closed state (RMA). It is also true that two agonists can bind and gate the channel as shown above in Figure 2.8.

Figure 2.9 Proposed gating scheme for $GABA_AR$ in the presence of BZD and agonist

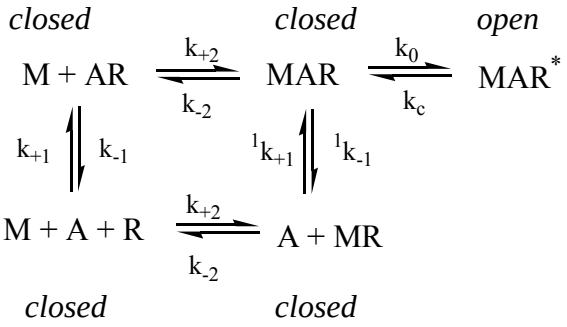

2.5 Assay methods for $GABA_A$ agonists and modulators (BZD)

In early studies of benzodiazepine and receptor interactions, all physiological effects were assessed by monitoring animal behavior. No functional studies were done using isolated organs, or in any system where the concentration of drug in the receptor could be assessed.[32] Two benzodiazepines, for example, may have had the same affinity for the receptor, but if one had low bioavailability, fast metabolism or other such traits, it would show low potency in experimental animal testing. Two important assay methods have since become available for studying GABA agonist and modulators. These methods are functional and binding assays.

One type of functional assay, chloride influx measurements, measures ^{36}Cl uptake into brain vesicles and provides a measurement of the action of GABA agonists. Chloride uptake assays were first described by Harris and Allan in 1985[45] and have been used extensively to characterize the effects of drugs that act at the GABA receptor. [3, 46, 47] GABA stimulates an influx of chloride ions into the central pore. Flux does not continue indefinitely; it is attenuated within a few seconds by desensitization of the receptor.[48] The effect of an agonist on receptor activation can be shown by means of a dose response

curve. Dose response curves are a plot of the log of the concentration of the drug versus the net counts per minute of ^{36}Cl uptake (Figure 2.10).

Figure 2.10 Dose Response curve for GABA (green), GABA & positive allosteric modulator (black), and GABA & negative allosteric modulator (red).

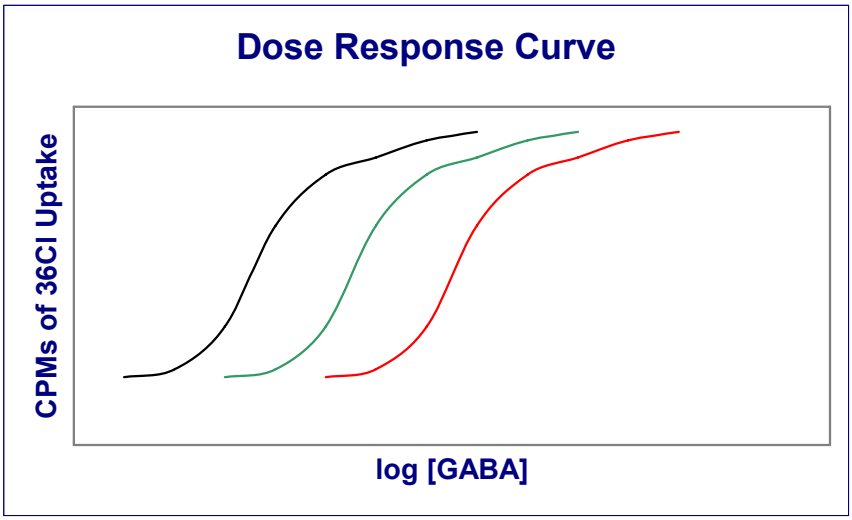

Agonists (such as GABA) bind to a specific site, and this leads to gating of the chloride channel. It is also possible that an antagonist will bind to this site and prevent gating of the channel; such compounds are referred to as competitive antagonists. When competitive antagonists (such as bicuclline) bind to the GABA receptor, they block the binding of agonists (GABA) to the functional agonist site, hence inhibiting GABA-gated chloride ion flux.[45] Other antagonists can prevent channel gating without actually binding to the agonist site (such as α,α-diisopropyl-γ-butyrolactone),[49] by blocking the channel; these are called noncompetitive antagonists.[49]

Other compounds can prevent GABA from gating the chloride ion channel (such as ethyl β-carboline-3-carboxylate), allosterically antagonizing GABA, and binding to an allosteric binding site.[48] This type of compound is known as a negative allosteric

modulator, meaning it inhibits the effect of GABA binding at the agonist site. As mentioned before, there are also positive allosteric modulators that increase the effect of GABA binding at the agonist site, such as benzodiazepines.

The graph in Figure 2.10 shows the effect of allosteric modulators on the dose response curve for the log [GABA] versus the counts per minute of ^{36}Cl uptake into mouse brain vesicles. The green curve in the middle shows the effect of GABA on gating the ion channel allowing for ^{36}Cl flux. The curve to the left (black) indicates the effect when a positive allosteric modulator is present, such as diazepam. The parallel left-ward shift relative to the GABA-only curve indicates an overall improved efficiency for channel opening by GABA. The curve to the right (red) demonstrates the effect of negative allosteric modulators on gating the ion channel. This parallel right-ward shift indicates decreased efficiency of GABA to open the channel.

Another important type of functional assay is termed electrophysiology. Sakmann and Neher first described a method for measuring the currents that flow through a single activated AChE channel in 1976 and were awarded a Nobel Prize in 1991 for their efforts.[43] Since this time, patch-clamping has been developed into a very useful tool for understanding the physiology, pharmacology and molecular biology of single ion channels. Patch-clamping works by isolating a tiny patch of membrane beneath a microelectrode so that the only signal recorded is that from the patch-clamp. The microelectrodes are coated with a hydrophobic resin that reduces capacitance. Once the microelectrode is placed on the surface of the cell, a gentle suction is applied, creating a seal between the cell and the electrode. It is then possible to see current measurements showing the channel switching between open and closed states. Channel gating of ligand gated ion channels (such as $GABA_AR$) can be observed by applying a solution of agonist

to the cell. Ideally, each dip represents a single channel opening and closing. Patch-clamping is time resolved and is therefore a powerful tool that provides gating information.[40, 41, 43, 50]

In order for an agonist or modulator to effect the $GABA_AR$, it must first bind. The method for using radioligand-binding assays to characterize receptors and receptor subtypes has become widespread since it was first introduced in 1971.[42] Radioligand-binding assays provide detailed information on the binding of agonists to receptors, by measuring membrane-bound radioligands. The use of radioligands can also be helpful when isolated tissue preparations are difficult, such as when studying CNS receptors.[43, 51] This method can provide a way of determining the density or number of receptors in a particular tissue sample. This approach requires many assumptions to be made and met before useful data can be obtained. The first is that pseudo-first-order conditions operate, i.e. [drug]>>[receptor]. Secondly, competition for binding of non-labeled ligands must be accounted for, and it must be assumed that the radioligand is bound before the competing ligands reach equilibrium.[9, 42]

Binding studies have demonstrated the existence of specific high affinity binding sites for BZD's. A high affinity binding site for [^{3}H]flunitrazepam (receptor affinity (K_d) ~2 nM), was observed when all three $GABA_AR$ subunits (α, β, γ) were present. Binding of [^{3}H]flunitrazepam to the membrane was stimulated by GABA and inhibited by bicuculline.[7] BZD's also increased the binding of GABA to the $GABA_AR$. The binding of [^{3}H]flunitrazepam (nM range) was completely blocked in the presence of 1μM diazepam, indicating these drugs bind to the same site. [52]

Many approaches have been developed for determining benzodiazepine-receptor binding in the brain of living mice.[32, 53] Most of these methods are quite similar in that

they involve a tritium-labeled benzodiazepine (^{3}H-diazepam) that is administered through the tail vein. After enough time has elapsed so that the radiolabeled drug has reached the receptor, the mouse is decapitated. The brain is removed and the cells are isolated and examined for radioactivity due to the radioligand binding at the receptor. This procedure must be carried out quickly so that the measurement reflects the amount of binding present when the mouse was alive. This method is known as the occupancy method.[32] These methods allow measurement of the *in vivo* occupancy of benzodiazepine receptors by the drug administered and any of its active metabolites that are also present. *In vivo* radiolabeling assays involve a number of problems, such as affinity, diffusion and availability of the ligand.[54]

The *in vivo* occupancy of the benzodiazepine receptor has been investigated using a variety of ligands. The values that are obtained are usually expressed as ED_{50} values, which indicate the dose of a given test substance at which the ligand occupies 50% of the benzodiazepine receptor sites.[55]

2.6 A brief review of multi-valent ligands

Since we plan to prepare molecules that span sites on the $GABA_AR$, it is worthwhile to review earlier examples of both bi- and multi-valent ligands. Much work has been done in this area, and the following is a review of only a few examples.

2.6.1 Bivalent ligands for opioid receptors

Portoghese *et al.* are responsible for the most successful examples to date of bivalent ligands that bind to the different opioid receptors.[56-59] Portoghese and

coworkers synthesized a variety of bivalent ligands (Figure 2.11) containing either the oxymorphamine (**13b-e**) or naltrexamine (**14b-e**) pharmacophores that were connected via spacers of varying lengths.[59] The oxymorphamine bivalent ligands (**13b-e**) behaved as agonists at the μ-opioid receptor. A good correlation was shown between agonist activity and binding as a function of spacer length, with the spacer that conferred peak agonist activity containing four glycyl units (**13c**). Agonist potencies and affinities for **13b-e** were greater than double those of the corresponding monovalent agonist (**13a**, Figure 2.11). The naltrexamine bivalent ligands (**14b-e**) were effective antagonists at the μ-opioid receptor, there was however no correlation of activity and binding as a function of spacer length. The absence of such correlation signified a fundamental difference between μ agonist and antagonistic recognition sites. [56-59] This work provides an impressive example of how bivalent ligands can be used as molecular probes of receptor structure.

Figure 2.11 Bivalent opioid receptor ligands

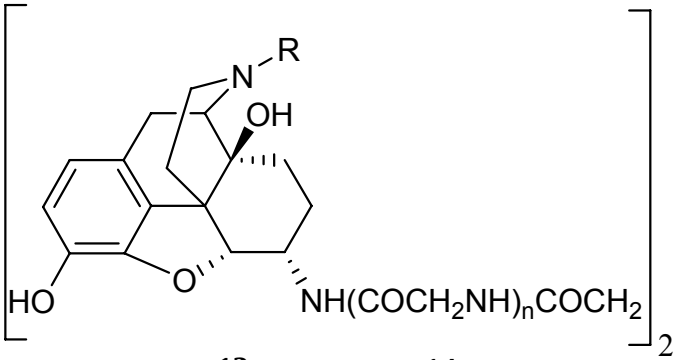

13 **14**

R = CH_3 R = $CH_2CH(CH_2)_2$

n = 0 - 4

2.6.2 Acetylcholinesterase (AChE)

It has been known since the early 1950's that there are two inhibitor binding sites on AChE (acetylcholinesterase). The existence of these binding sites was deduced based on the finding that of decamethonium (**15**) was much more potent than tetramethyl ammonium for inhibiting hydrolysis of acetylcholine (ACh) (**16**).

Figure 2.12 Decamethonium

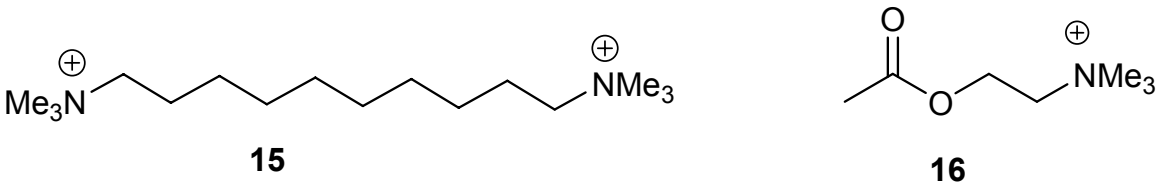

15 **16**

The fact that decamethonium exhibited very weak potency at BChE (butyrylcholinesterase) suggested that this enzyme did not possess two cation-binding domains. The 1993 crystal structure of the Torpedo AChE binding with decamethonium provided the first hard evidence for the location of a peripheral site at the mouth of the gorge that leads to the catalytic site.[60, 61] This structure revealed that the cations of decamethonium interacted with the aromatic residues that are present in AChE, and provided early evidence for the cation-pi effect.[62-64]

Figure 2.13 Tacrine and bivalent amine ligands [65-67]

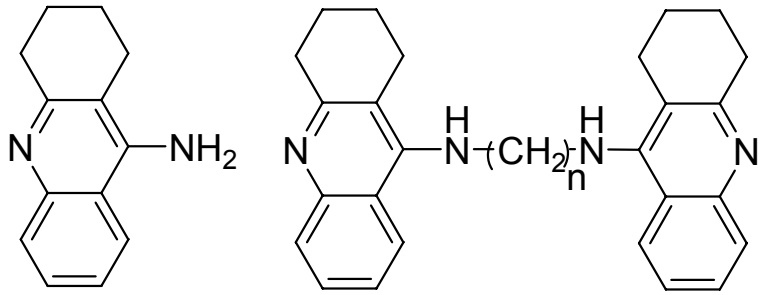

tacrine **17** bis(n)-tacrine: n=2-10 **18a-i**

a: n=2; b: n=3; c: n=4; d: n=5; e: n=6; f: n=7; g: n=8; h: n=9; i: n=10

Based on the crystal structure of the AChE-decamethonium complex, and on his own docking studies, Pang prepared tacrine dimers bis(n)-tacrine (**18g-i)**, linked by 7-10 methylenes.[63] As hoped, these dimers were up to 1000 fold more potent than tacrine for AChE inhibition. To confirm that the potency and selectivity of these compounds was indeed due to dual site binding, Carlier prepared shorter dimers (**18a-f**), having 2-6 methylenes, hoping to see a tether length dependency on potency and selectivity. As the tether was shortened, there should be a point when the dimer can no longer span both sites, therefore making it only as active as the monomer.[65] The results from this study showed that when the tether was shorter than 5 methylenes, the dimer potency approached that of the monomer (Figure 2.11).[65] The L-shaped curve that is evident in the graph of IC_{50} versus number of methylenes will be used as diagnostic feature of dual site binding to determine if it is occurring on the $GABA_AR$.

Figure 2.14 Plot of AChE IC_{50} values as a function of tether length of bis(n)-tacrines[65]

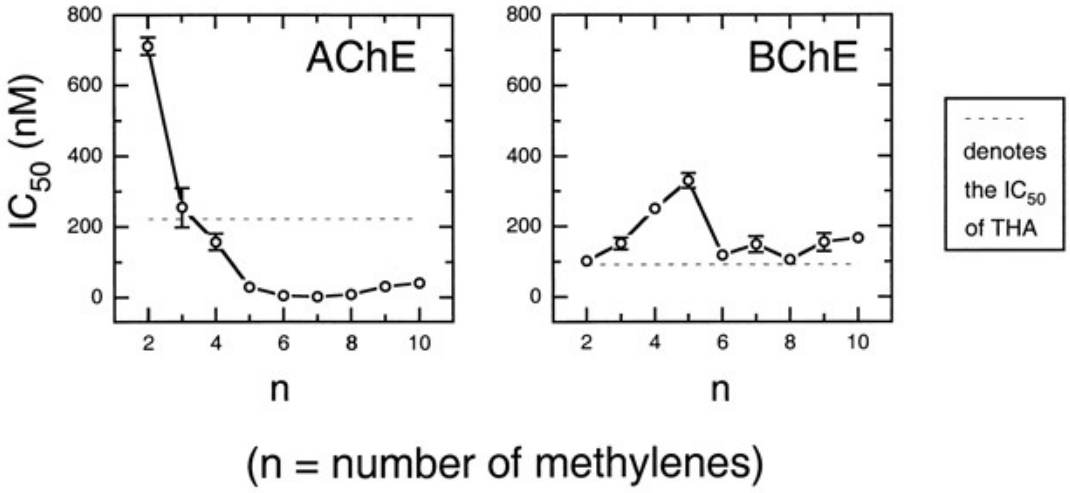

Carlier prepared a collection of blood-brain-barrier permeable bivalent amine-based ligands (**19-21**) (based on tacrine and huperzine A) that could be used as therapeutic agents for Alzheimer's disease.[65-69] Both homo- and hetero-dimers were tested for their ability to inhibit AChE and in each case tether-length dependence was noted, supporting the proposal of dual site binding.[69] The optimum tether length was found to vary between 7-10 methylenes, giving a distance of 12.4-14.8 Å which corresponds to the distance between catalytic and peripheral sites on AChE, determined by X-ray crystallography.[70] The narrow cleft that leads to the catalytic site prevents dimers from dual site binding in a folded-up state, therefore the extended length of the dimer is most relevant for determining binding site distances in AChE.

Figure 2.15 Bivalent amine-based ligands prepared by Carlier[69]

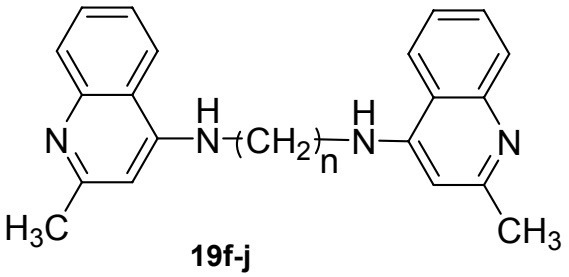

19f-j

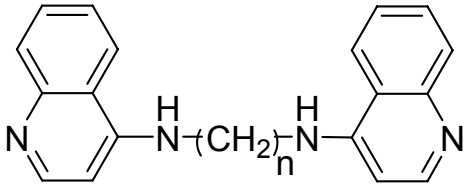

20e-i,k

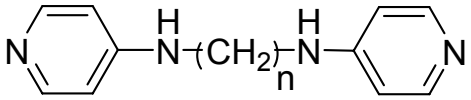

21e-k

a: n=2; b: n=3; c: n=4; d: n=5; e: n=6; f: n=7; g: n=8; h: n=9; i: n=10, j: n=11, k: n=12

2.6.3 Cyclic nucleotide gated channels.

Most of the examples of bivalent or multivalent ligand design implement a flexible hydrophobic tether structure of less than 14 Å and are designed to be potent inhibitors.[66, 71, 72] In 1998 Kramer and Karpen prepared flexible variable length polymer linked ligand dimers (PLD's with cGMP moieties on each end -PEG-$(cGMP)_2$ **22**, Figure 2.16) for proteins with multiple binding sites. The improved water solubility and low toxicity of polyethylene glycol (PEG) made it a superior choice for spanning the distance between binding sites. A more hydrophobic or peptide spacer would likely undergo hydrophobic collapse.

Figure 2.16 Polymer-linked dimer containing two cGMP moieties and a PEG linker

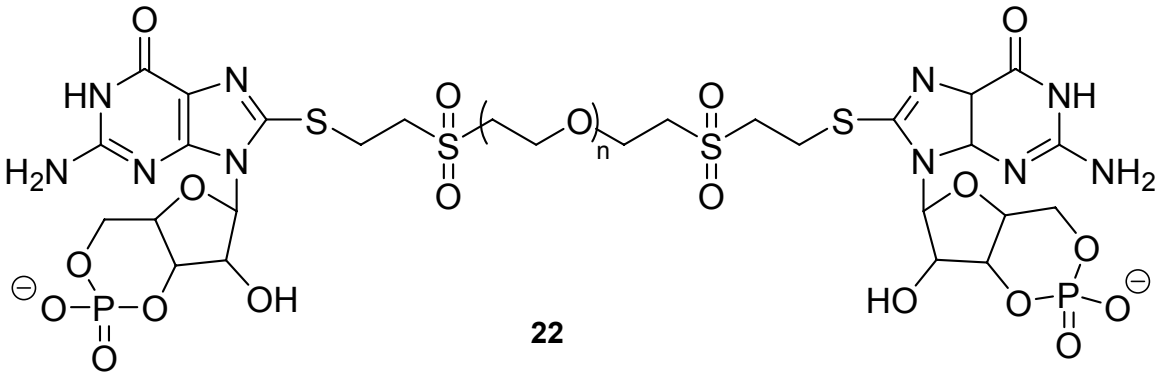

22

They predicted that the tether length of the PLD would have a direct effect on binding to a protein with multiple binding sites (Figure 2.16). If the average length of the tether is much shorter than the distance between binding sites (Figure 2.16 A) then the molar affinity for the PLD should be about twice that of cGMP (since it is a dimer) . When the average length of the PLD matches the distance between binding sites (Figure 2.16 C), the apparent affinity for the cGMP binding moiety should increase significantly. Once one cGMP was bound, the other will be constrained to a radius equal to the r.m.s. length of the polymer, due to its tether. In other words, it is already in close proximity to the binding site, so diffusion is limited and there is a greater chance of binding. In order to test this theory they prepared an impressive library of PLDs with average molecular weights ranging from 282 to 20000 daltons (corresponding to average lengths ranging from 15-123 Å), as well as a polymer linked monomer (PLM) containing one cGMP tethered to a 5000 dalton PEG. They compared the binding affinities of the various length PLD's with the PLM by fitting the dose-response curves with the Hill equation to determine Hill coefficients. They found that the Hill coefficient indicative of the minimum number of molecules required for activation of the CNG channel was

comparable for cGMP (1.7) , PLM (2.0) and the shortest PLD prepared 282 PEG-$(cGMP)_2$ (2.0). For the larger PLDs 3400 PEG-$(cGMP)_2$ and 20000 PEG-$(cGMP)_2$, however, the Hill coefficients (1.1 and 0.8 respectively) were about half as large as for cGMP. This result indicates that the larger PLDs simultaneously occupy two binding sites, while the smaller PLD does not.

Figure 2.17 Schematic of PLD's binding to a channel with 4 binding sites. PLD's are shown with average lengths too short (A), too long (B) and just right for spanning two binding sites.

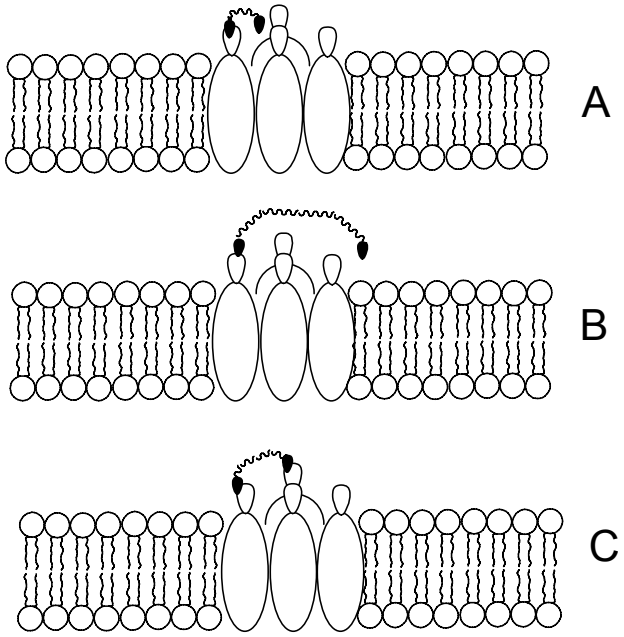

All CNG channels have four binding sites, however the distance between these binding sites may differ depending on the particular protein. In order to determine these distances Kramer and Karpen used the series of PLDs they had prepared (282 PEG-$(cGMP)_2$ -2000PEG-$(cGMP)_2$) with average lengths ranging from 15-123 Å. The average polymer length is assumed to be proportional to the square root of the number of monomers (r.m.s).[38, 73] They examined three cyclic-nucleotide-activated proteins:

photoreceptor and olfactory channels and cGMP dependent protein kinase (PKG). Each protein showed tether length dependence and responded optimally to polymers with different average lengths. The results showed that the optimal PLD for activating the olfactory CNG channels was 2000 PEG-$(cGMP)_2$ (average length equal to 39 Å). An optimum radius of 39 Å permitted the first cGMP to bind to the olfactory protein, and greatly increased the probability of the other cGMP binding as they had predicted it would. The 1200PEG-$(cGMP)_2$ corresponding to an average length of 30 Å, was optimal for activating the photoreceptor CNG channels. These results indicated that there is wider spacing between the binding sites in the olfactory channel, compared with the photoreceptor channel. Finally, the optimal PLD for PKG was determined to be 282PEG-$(cGMP)_2$ corresponding to an average length of 15 Å. These results demonstrated that optimal binding occurred when the length of the PEG tether matched the distance between neighboring cGMP binding sites on the CNG channels. This method of fine tuning polymer lengths and choosing optimal ligands to estimate the average distances between binding sites on receptors has also been applied by Fan *et al.* [71]

2.6.4 Pentavalent ligands

There has been a significant amount of successful work done in the area multivalent ligand design.[38, 73-75] Fan and coworkers have demonstrated a particularly interesting example using structure-based ligand design to target multimeric bacterial toxins.[71] The design of pentavalent ligands was based on the heat-labile enterotoxin (LT) from *Escherichia coli*, which exists as a symmetrical arrangement of five β subunits.[71, 72] Fan demonstrated that the design of such pentavalent systems (**23**) leads to very significant gains in affinity when compared to the monovalent ligand D-galactose (**24**) (Figure 2.18). D-galactose is a terminal sugar unit of LT's natural receptor ganglioside GM1. It interacts very specifically with the toxin via hydrogen bonding and it has a very high affinity for binding at LT's receptor site (IC_{50} = 58000 μM). The IC_{50} value for these pentavalent ligands was 10^5–fold better than galactose.

Figure 2.18 Fan's pentavalent ligand and D-galactose

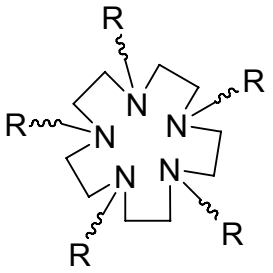

23

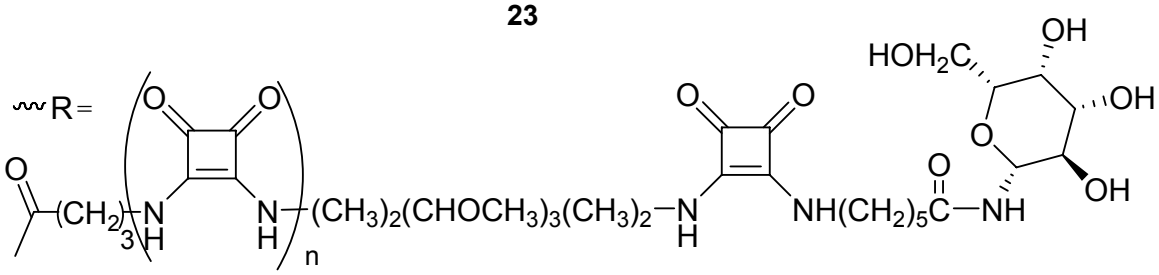

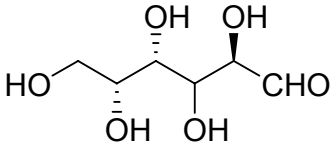

24

Approximately 14 compounds were synthesized and tested, demonstrating that there is in fact a large gain in affinity by pentavalent relative to monovalent ligands.[71] Fan's work also agreed with Kramer and Karpen's idea that in order to gain affinity, the linkers must span the binding sites precisely.[73] Also, this distance must be based on the linker's effective length rather than its extended length, since these linkers are quite flexible. When the effective length of the linker (n = 1-3) was shorter than the distance between binding sites they saw a dramatic decrease in binding affinity. In contrast, when n = 4 (**23**) the effective length of the linker matched the distance between binding sites and the highest gain in binding affinity was noted. The effective dimensions of the

pentavalent ligands were determined using the same equation that Kramer and Karpen[73] used, which is based on a polymer model described by Knoll and Herman.[76] In this case the effective dimensions of the ligand are taken to be equal to the square root of the molecular weight between two fingers

This approach has allowed for efficient synthesis of a variety of large molecular weight protein ligands. It has also led to a better understanding of the receptor or protein to which these compounds are binding, and more specifically the actual location of the relative binding sites.

In conclusion a large amount of work has been done in the area of bivalent drug design, and a plethora of evidence indicates that it is an effective strategy for increasing the potency and selectivity of many drugs.

2.7 Proposed direction of research

In 2000 we envisioned constructing molecules that can simultaneously bind to the agonist and BZD sites of the $GABA_AR$. Such an approach was unprecedented and entailed a high degree of risk. However the successful work of Kramer and Karpen in spanning sites 39 Å apart inspired us to attempt this research. Unlike other BZD's these compounds would not require physiological GABA or agonist to gate the receptor, so they could activate chloride ion flux with sub-micromolar concentrations of GABA. Thus, once the built-in agonist binds, the probability of binding the BZD is increased because it is already in place. If this is the case, these heterodimers would have more potent or novel anxiolytic, antinociceptive, or even antiepileptic properties. We devised a

strategy to prepare a series of heterodimers with different tether lengths that will be discussed in the following chapter.

References for Chapter 2

[1] Chebib, M., Johnston, A. R., GABA- activated ligand gated ion channels: medicinal chemistry and molecular biology, *J. Med. Chem.* **2000**, *43*, 1427.

[2] Krogsgaard-Larsen, P., Frolund, B., Flemming, S., Schousboe, A., $GABA_A$ receptor agonists, partial agonists, and antagonists. Design and therapeutic prospects, *J. Med. Chem.* **1994**, *37*, 2489.

[3] Bormann, J., The "ABC" of GABA receptors, *Trends Pharm. Sci.* **2000**, *21*, 16.

[4] Johnston, G. A. R., $GABA_C$ receptors: relatively simple transmitter-gated ion channels?, *Trends Pharm. Sci.* **1996**, *17*, 319.

[5] Bormann, J., Feigenspan, A., $GABA_C$ receptors, *Trends Neurosci.* **1995**, *18*, 515.

[6] Enna, S. J., Bowery, N. G., GABAA receptor alterations as indicators of physiological and pharmacological function, *Biochemical Pharmacology* **2004**, *68*, 1541.

[7] Sieghart, W., $GABA_A$ receptors: ligand-gated Cl^- ion channels modulated by multiple drug-binding sites, *Trends Pharm. Sci.* **1992**, *13*, 446.

[8] Bloomquist, J. R., Jackson, J. L., Karr, L. L., Ferguson, H. J., Gajewski, R. P., Spirosultam LY219048: A new chemical class of insecticide acting upon the GABA receptor/ chloride ionophore complex, *Pestic. Sci.* **1993**, *39*, 185.

[9] Bloomquist, J. R., Toxicology, mode of action and target site-mediated resistance to insecticides acting on chloride channels, *Comp. Biochem. Physiol.* **1993**, *106C*, 301.

[10] Bloomquist, J. R., Soderlund, D. M., Neurotoxic insecticides inhibit GABA-dependent chloride uptake by mouse brain vesicles, *Biochemical and Biophysical Research Communications* **1985**, *133*, 37.

[11] Luddens, H., Korpi, E. R., Seeburg, P. H., $GABA_A$/Benzodiazepine receptor heterogeneity: neurophysiological implications, *Neuropharmacology* **1995**, *34*, 245.

[12] McKernan, R. M., Rosahl, T. W., Reynolds, D. S., C., S., Wafford, K. A., Atack, J. R., Farrar, S., Myers, J., Cook, G., Ferris, P., Garrett, L., Bristow, L., Marshall, G., Macaulay, A., Brown, N., Howell, O., Moore, K. W., Carling, R. W., Street, L. J., Castro, J. L., Ragan, C. I., Dawson, G. R., Whiting, P. J., Sedative but not anxiolytic properties of benzodiazepines are mediated by the $GABA_A$ receptor α_1 subtype, *Nature Neurosci.* **2000**, *3*, 587.

[13] Smith, G. B., Olsen, R. W., Functional domains of $GABA_A$ receptors, *Trends Pharm. Sci.* **1995**, *16*, 162.

[14] Boileau, A. J., Evers, A. R., Davis, A. F., Czajkoski, C., Mapping the agonist binding site of the $GABA_A$ receptor: evidence for a β-Strand, *J. Neuro. Sci.* **1999**, *19*, 4847.

[15] Haung, Q., He, X., Ma, C., Liu, R., Yu, S., Dayer, C. A., Wegner, G. R., R.M., M., Cook, J. M., Pharmacophore/receptor models for $GABA_A$/BzR subtypes ($\alpha1\beta3\gamma2$, $\alpha5\beta3\gamma2$, and $\alpha6\beta3\gamma2$) via a comprehensive ligand-mapping approach, *J. Med. Chem.* **2000**, *43*, 71.

[16] Kash, T. L., Trudell, J. R., Harrison, N. L., Structural Elements involved in activation of the g-aminobutryic acid type A (GABAA) receptor, *Biochem. Soc. Trans* **2004**, *32*, 540.

[17] Sigel, E., Buhr, A., The benzodiazepine binding site of $GABA_A$ receptors., *Trends Pharm. Sci.* **1997**, *18*, 425.

[18] Nayeem, N., Green, T. P., Martin, I. L., Barnard, E. A., Quaternary structure of the native $GABA_A$ receptor determined by electron microscopic image analysis, *J. Neurochem.* **1994**, *62*, 815.

[19] Mohler, H., Rudolph, U., Selective GABAA circuits for novel CNS drugs., *Drug Discovery Today: Ther. Strategies* **2004**, *1*, 162.

[20] Agey, M. W., Dunn, M. J., [3H]Muscimol binding to the GABAA receptor in bovine brain membranes, *Biochemistry* **1989**, *28*, 4200.

[21] Newell, J. G., Davies, M., Bateson, A. N., Dunn, M. J., Tyrosine 62 of the γ–aminobutyric acid type A receptor β2 subunit is an important determinant of high affinity agonist binding, *J. Biol. Chem.* **2000**, *275*, 14198.

[22] Segal, M., Barker, J. L., Rat hippocampal neurons in culture: properties of GABA-activated chlorine ion conductance., *J. Neurophysiol.* **1984**, *51*, 500.

[23] Squires, R. F., Casida, J. E., Richardson, M., Saederup, E., [35S]t-butylbicyclophosphorothionate binds with high affinity to brain-specific sites coupled to gamma-aminobutyric acid-A and ion recognition sites., *Mol. Pharmacol.* **1983**, *23*, 326.

[24] Smith, G. B., Olsen, R. W., Identification of a [^{3}H]muscimol photoaffinity substrate in the bovine γ-aminobutyric $acid_A$ receptor α subunit, *J. Biol. Chem.* **1994**, *269*, 20380.

[25] Baur, R., Sigel, E., On high and low-affinity agonist sites in GABAA Receptor, *J. Neuro. Sci.* **2003**, *87*, 325.

[26] Walters, R. J., Hadley, S. H., Morris, K. D. W., Amin, J., Benzodiazepines act on $GABA_A$ Receptors via Two Distinct and Separable Mechanisms, *Nature Neurosci.* **2000**, *3*, 1274.

[27] Lan, N. C., Kelvin, W. G., Bolger, M. B., Chen, J. S., Differential Responses of Expressed Recombinant Human γ-Aminobutyric $Acid_A$ Receptors to Neurosteroids, *J. Neurochem.* **1991**, *57*, 1818.

[28] Dekermendjian, K., Kahnberg, P., Witt, M. R., Sterner, O., Nielsen, M., Liljefors, T., Structure-activity relationships and molecular modeling analysis of flavonoids binding to the benzodiazepine site of the rat brain $GABA_A$ receptor complex., *J. Med. Chem.* **1999**, *42*, 4343.

[29] Chow-Clement, E., Ph.D. thesis, Virginia Polytechnic and State University, Blacksburg VA, 2005.

[30] Carlier, P. R., Chow, E. S. H., Barlow, R. L., Bloomquist, J. R., Discovery of non-zwitterionic GABAAR receptor full agonists and a superagonist, *Bioorg. Med. Chem. Lett.* **2002**, *12*, 1985.

[31] Mandel, P., DeFeudis, F. V. *Advances in Experimental Medicine and Biology*; Plenum Press: New York, 1979; Vol. 123.

[32] Venter, J. C., Harrison, L. C. *Benzodiazepine/GABA Receptors and Chloride Channels*; Alan R. Liss, Inc: New York, 1986; Vol. 5.

[33] Curtis, D. R., Watkins, J. C., The excitation and depression of spinal neurons by structurally related amino acids, *J. Neurochem.* **1960**, *6*, 117.

[34] DeSarro, G., Gitto, R., Rizzo, M., Zappia, M., DeSarro, A., 1,4-Benzodiazepine derivatives as anticonvulsant agents in DBA/2 Mice, *Gen. Pharmac.* **1996**, *27*, 935.

[35] Boileau, A. J., Kucken, A. M., Evers, A. R., Czajkoski, C., Molecular dissection of benzodiazepine binding and allosteric coupling using chimeric γ-aminobutyric $acid_A$ receptor subunits, *Mol. Pharmacol.* **1998**, *53*, 295.

[36] Bowling, A. C., De Lorenzo, R. J., Micromolar affinity benzodiazepine receptors: identification and characterization in central nervous system, *Science* **1982**, *216*, 1247.

[37] Kardos, J., Maderspach, K., Simonyi, M., Towards a more physiological approach in GABA binding, *Neurochem. Int.* **1985**, *7*, 737.

[38] Kramer, R. H., Tibbs, G. R., Antagonists of cyclic nucleotide-gated channels and molecular mapping of their site of action., *J. Neuro. Sci.* **1996**, *16*, 1285.

[39] Amin, J., Weiss, D. S., $GABA_A$ receptor needs two homologous domains of the β-subunit for activation by GABA but not by pentobarbital, *Nature* **1993**, *366*, 565.

[40] Sakmann, B., Hamill, O. P., Bormann, J., Patch-clamp measurements of elementary chloride currents activated by the putative inhibitory transmitters GABA and glycine in mammalian spinal neurons, *Neural Transmission Suppl.* **1983**, *18*, 83.

[41] Bormann, J., Clapham, D. E., γ-Aminobutyric acid receptor channnels in adrenal chromaffin cells: A patch-clamp study, *Proc. Natl. Acad. Sci. USA* **1985**, *82*, 2168.

[42] Siegel, G. J., Agranoff, B. W., Albers, R. W., Molinoff, P. B. In *Basic Neurochemistry*; Raven Press: New York, 1994, pp 1086.

[43] Matthews, J. C. *Fundamentals of Receptor, Enzyme, and Transport Kinetics*; CRC Press: Boca Raton, 1993.

[44] Serfozo, P., Cash, D. J., Effect of benzodiazepine (chlordiazepoxide) on a $GABA_A$ receptor from rat brain. Requirement of only one bound GABA molecule for channel opening., *FEBS Lett.* **1992**, *310*, 55.

[45] Harris, R. A., Allan, A. M., Functional coupling of γ-aminobutyric acid receptors to chloride channels in brain membranes., *Science* **1985**, *228*, 1108.

[46] Soderlund, D. M., Adam, P. P., Bloomquist, J. R., Differences in the action of advermectin B_{1a} on the $GABA_A$ receptor complex of mouse and rat., *Biochem. and Biophys. Res. Commun.* **1987**, *146*, 692.

[47] Bloomquist, J. R., Adams, P. M., Soderlund, D. M., Inhibition of γ-aminobutyric acid - stimulated chloride flux in mouse brain vesicales by polychlorocycloalkane and pyrethroid insecticides, *NeuroToxicology* **1986**, *7*, 11.

[48] Bloomquist, J. R., Grubs, R. E., Soderlund, D. M., Knipple, D. C., Prolonged exposure to GABA activates GABA-gated chloride channels in the presence of channel-blocking convulsants, *Comp. Biochem. Physiol.* **1991**, *99C*, 397.

[49] Kerr, D. I. B., Ong, J., GABA agonists and antagonists, *Medicinal Research Reviews* **1992**, *12*, 593.

[50] Revest, P., Longstaff, A. *Molec. Neurosci.*; BIOS Scientific Publishers Lim., 1998.

[51] Dixon, R., Glover, W., Earley, J., Specific radioimmunoassay for flunitrazepam, *J. Pharm. Sci.* **1981**, *70*, 230.

[52] Pritchett, D. B., Sontheimer, H., Shivers, B. D., Ymer, S., Kettenmann, H., Schofield, P. R., Seeburg, P. H., Importance of novel $GABA_A$ receptor subunit for benzodiazepine pharmacology, *Nature* **1989**, *338*, 582.

[53] Skolnick, P., Paul, S. M., Rice, K. C., Barker, J. C., Interactions of barbiturates with benzodiazepine receptors in the central nervous system, *Brain Research Reviews* **1982**, *233*, 143.

[54] Fernandez-Lopez, A., Chinchetru, M. A., Fernandez, P. C., The autoradiographic perspective of central benzodiazepine receptors: A short review, *Gen. Pharmac.* **1997**, *29*, 173.

[55] Rowlett, J. K., Woolverton, W. L., Assessment of benzodiazepine receptor heterogeneity in vivo: apparent pA_2 and pK_B analyses from behavioral studies, *Psychopharmacology* **1996**, *128*, 1.

[56] Han, D., Forsterling, F. H., Li, X., Deschamps, J. R., Cao, H., Cook, J. M., Determination of the stable conformation of GABAA-benzodiazepine receptor bivalent ligands by low temperature NMR and X-ray analysis, *Bioorg. Med. Chem. Lett.* **2004**, *14*, 1465.

[57] Erez, M., Takemori, A. E., Portoghese, P. S., Narcotic antagonistic potency of bivalent ligands which contain β-naltrexamine, *J. Med. Chem.* **1982**, *25*, 847.

[58] Portoghese, P. S., Larson, D. L., Yim, C. B., Sayre, L. M., Ronsisvalle, G., Lipkowski, A. W., Takemori, A. E., Rice, K. C., Tam, S. W., Stereostructure-activity relationship of opioid agonist and antagonist bivalent ligands, *J. Med. Chem.* **1985**, *28*, 1140.

[59] Portoghese, P. S., Larson, D. L., Sayre, L. M., Yim, C. B., Ronsisvalle, G., Tam, S. W., Takemori, A. E., Opioid agonist and antagonist bivalent ligands, *J. Med. Chem.* **1986**, *29*, 1855.

[60] Harel, M., Schalk, I., Ehret-Sabatier, L., Bouet, F., Goeldner, M., Hirth, C., Axelsen, P. H., Silman, I., Sussman, J. L., Quaternary ligand binding to aromatic residues in the active-site gorge of acetylcholinesterase, *Proc. Natl. Acad. Sci. USA* **1993**, *90*, 9031.

[61] Miyazawa, A., Fujiyoshi, Y., Stowell, M., Unwin, N., Nicotinic acetylcholine receptor at 4.6A resolution: Transverse tunnels in the channel wall, *J. Mol. Biol.* **1999**, *288*, 765.

[62] Unwin, N., Acetylcholine receptor channel imaged in the open state, *Nature* **1995**, *373*, 37.

[63] Pang, Y. P., Quiram, P., Jelacic, T., Hong, F., Brimijoin, S., Highly potent, selective, and low cost bis-tetrahydroaminacrine inhibitors of acetylcholinesterase., *J. Biol. Chem.* **1996**, *27*, 23646.

[64] Ma, C., Dougherty, D. A., The cation-pi interaction, *Chem. Rev.* **1997**, *97*, 1303.

[65] Carlier, P. R., Han, Y. F., Chow, E. S. H., Li, C. P. L., Wang, H., Lieu, T. X., Wong, H. S., Pang, Y. P., Evaluation of short-tether bis-THA AChE inhibitors. A further test of the dual binding site hypothesis, *Bioorg. Med. Chem.* **1999**, *7*, 351.

[66] Carlier, P. R., Chow, E. S. H., Han, Y., Liu, J., Yazal, J. E., Pang, Y. P., Heterodimeric tacrine-based acetylcholinesterase inhibitors: Investigating ligand-peripheral site interactions, *J. Med. Chem.* **1999**, *42*, 4225.

[67] Carlier, P. R., Du, D. M., Han, Y. F., Liu, J., Pang, Y. P., Potent, Easily Synthesized Huperazine A-Tacrine Hybrid Acetylcholinesterase Inhibitors, *Bioorg. Med. Chem.* **1999**, *9*, 2335.

[68] Carlier, P. R., Du, D. M., Han, Y. F., Liu, J., Perola, E., Williams, I. D., Pang, Y. P., Dimerization of an inactive fragment of huperzine A produces a drug with twice the potency of the natural product., *Angew. Chem.* **2000**, *39*, 1775.

[69] Han, Y. F., Li, C. P. L., Chow, E. S. H., Wang, H., Pang, Y. P., Carlier, P. R., Dual-site binding of bivalent 4-aminopyridine and 4-aminoquinoline-based AChE inhibitors: contribution of the hydrophobic alkylene tether to monomer and dimer affinities, *Bioorg. Med. Chem.* **1999**, *7*, 2569.

[70] Arias, H. R., Topology of ligand binding sites on the nicotinic acetylcholine receptor, *Brain Research Reviews* **1997**, *25*, 133.

[71] Fan, E., Zhang, Z., Minke, W. E., Hou, Z., Verlinde, C. L. M. J., Hol, W. G. J., High-affinity pentavalent ligands of ezcherichia coli heat-labile enterotoxin by modular structure-based design, *J. Am. Chem. Soc.* **2000**, *122*, 2663.

[72] Kitov, P. I., Sadowska, J. M., Mulvey, G., Armstrong, G. D., Ling, H., Pannu, N. S., Read, R. J., Bundle, D. R., Shiga-like toxins are neutralized by tailored multivalent carbohydrate ligands., *Nature* **2000**, *403*, 669.

[73] Kramer, R. H., Karpen, J. W., Spanning binding sites on allosteric proteins with polymer-linked dimers, *Nature* **1998**, *395*, 710.

[74] Mammen, M., Choi, S.-K., Whitesides, G. M., Polyvalent interactions in biological systems: implications for design and use of multivalent ligands and inhibitors., *Angew. Chem. Int. Ed.* **1998**, *37*, 2754.

[75] Choi, S.-K., Mammen, M., Whitesides, G. M., George, G., Generation and in situ evaluation of libraries of poly(acrylic acid) presenting sialosides as side chains as polyvalent inhibitors of influenza-mediated hemagglutination., *J. Am. Chem. Soc.* **1997**, *119*, 4103.

[76] Knoll, D., Hermans, J., Polymer-protein interactions. Comparison of experiment and excluded volume theory, *J. Biol. Chem.* **1983**, *258*, 5710.

Chapter 3. Synthesis of Bivalent Ligands

Benzodiazepines (BZD) have long been known to exhibit anxiolytic activity by having an effect at the $GABA_AR$.[1-5] Specifically, BZDs are agonist modulators, meaning they require an agonist (such as GABA) to be present in order to gate the Cl^- ion channel and show this anxiolytic behavior.[6] The $GABA_AR$ is the target of action for many medicinally important drugs (anxiolytic, anticonvulsants, antidepressants, anesthetics, sedative-hypnotics, insecticides, and anthelmintics), and therefore it has become the target of intense studies in this area. The location of the agonist and modulator binding sites on the $GABA_AR$, however, are not precisely known.[7] In view of this ambiguity there continues to be great interest in the structure of $GABA_AR$.[7, 8]

As mentioned in Chapter 2, we envisioned constructing molecules that could bind to the agonist and BZD sites of the $GABA_AR$ at the same time. In pursuit of this endeavor, we were able to develop a model compound that relied on physiological GABA to elicit flux. Although no agonist is bound to the tether this compound provided us with valuable information on whether the tether would have an effect on binding.

3.1 Synthesis of Benzodiazepine-methoxy terminated poly(ethylene glycol) (BZD-MPEG) model compound

The growing medical need for new anxiolytic drugs brought about the idea that benzodiazepine-agonist heterodimers may suit this purpose. A previous study[9, 10] showed the effects of BZD substituents on their anxiolytic activity. The anilide nitrogen is quite tolerant to substitution, as shown in Figure 1.6, Chapter 1 and for this reason we made the connection to the tether at this position.

We began with the synthesis of the linker, *N*-Boc-3-tosyl-propanamine (**2**) (Scheme 3.1). Commercially available 3-amino-1-propanol was Boc-protected using the method described by Mattingly[11] affording compound **1** in 80% yield (Scheme 3.1). Conversion to the tosylate (**2**) involved treatment of **1** with tosyl chloride in pyridine (Scheme 3.1).

Scheme 3.1 Synthesis of linker **2**

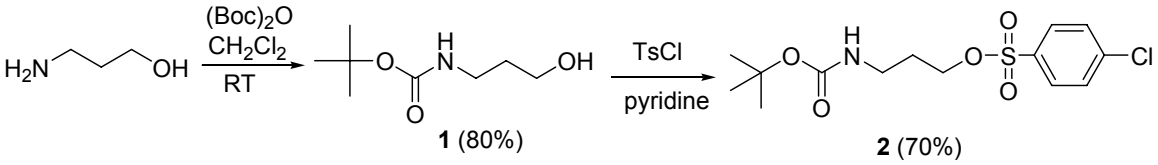

Synthesis of the diazepam ring began with commercially available 2-aminobenzophenones (**3**).[10] This method involved treatment of (**3**) with glycine ethyl ester in dry pyridine leading directly to (**4**) (Scheme 3.2).[12]

Scheme 3.2 Synthesis of diazepam **4**

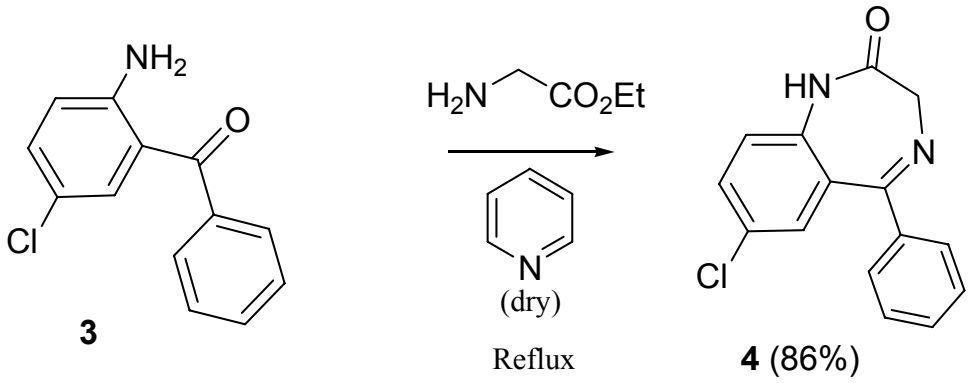

We attempted to install the linker (**2**) at the *N*1 position of **4** using a variety of different reaction conditions outlined in Table 3.1. Attempted deprotonation with LiHMDS in THF or DMF followed by addition of *N*-Boc-3-tosyl-propanamine (**2**) yielded no desired product (**5**) (Table 3.1, entries 1-2). Switching to sodium methoxide in methanol/DMF afforded **5** in only 15% yield (Table 3.1, entry 3). Treating **4** with KH or KHMDS in DMF to make the benzodiazepine salt, and then adding *N*-Boc-3-tosyl-propanamine (**2**), afforded amino-functionalized BZDs (**5**) in an improved 40% yield (Table 3.1, entries 4-5).

Table 3.1 Synthesis of amino-functionalized BZD **5**

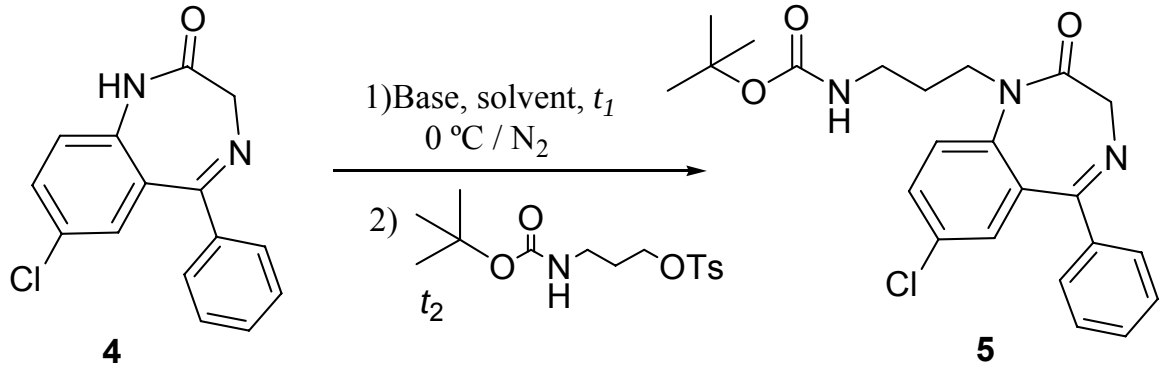

Entry	Base	Solvent	t_1 (min)	t_2 (min)	Yield of **5**
1	LiHMDS	THF	30	30	0 [a]
2	LiHMDS	DMF	30	30	0 [a]
3	MeONa	MeOH/DMF	30	60 [b]	15%
4	KH	DMF	30	60	40%
5	KHMDS	DMF	30	120	40%

[a] recovered a significant quantity of **4** [b] reaction was warmed to room temperature

Quantitative removal of the Boc-protecting group using trifluoroacetic acid gave the trifluoroacetic acid salt (**6**) (Scheme 3.3) which was then ready to be coupled to the methoxy terminated poly(ethylene glycol) (MPEG) linker**.**

Scheme 3.3 Removal of the Boc-protecting group from **5**

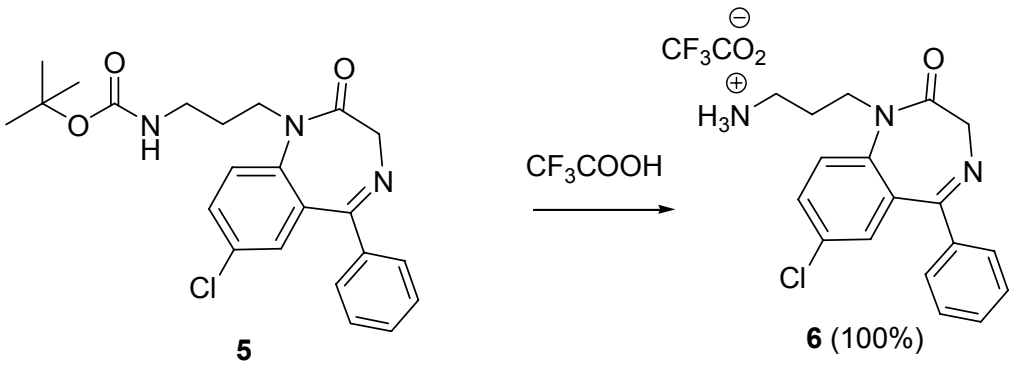

Our original intent was to prepare a series of heterodimers with different tether lengths. We therefore enlisted PEG-type linkers to accommodate for the potentially long distances between binding sites.

The activated methoxy terminated poly(ethylene glycol) (MPEG) linker (**8**) was prepared from commercially available PEG monomethyl ether (**7**) (average M_n=2000 rms length of 38 Å). We converted the PEG monomethyl ether to the *p*-nitrophenyl carbonate following the procedure optimized by Dr. Polo Lam.[13] Bis-(*p*-nitrophenyl) and PEG monomethyl ether were dissolved in dichloromethane and diisopropylethylamine was used as the base. The activated MPEG-linker (**8**) was obtained in 89% yield, 100% incorporation.

Scheme 3.4 Synthesis of activated methoxy terminated poly(ethylene glycol) (MPEG) linker (**8**).

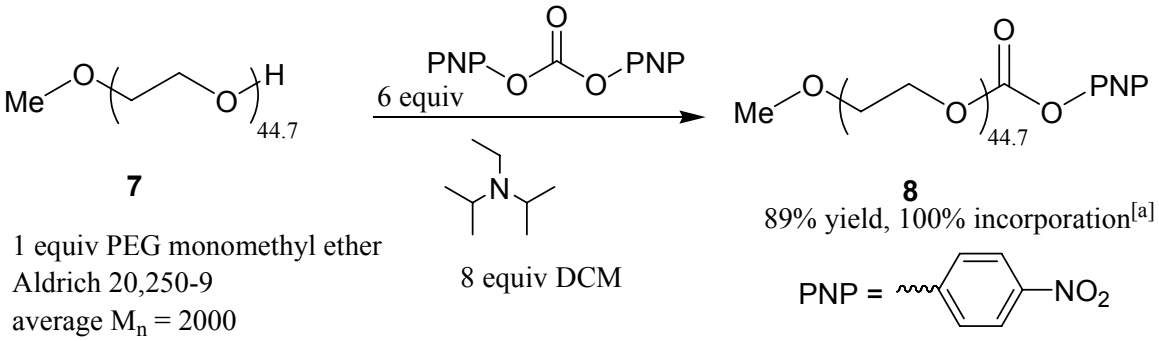

[a] explanation of % incorporation found in section 3.4

We were then able to couple the activated MPEG (**8**) with the amino functionalized BZD (**6**) to form the BZD-methoxy terminated poly(ethylene glycol) (MPEG) model compound (**9**).

Dr. Polo Lam developed a protocol for coupling baccatin-III with (*p*-nitrophenyl)-PEG carbonate (Scheme 3.5). He found that direct coupling of baccatin-III with MPEG

(M_n=2000) would only occur in the presence of DMAP, and even then the reaction proceeds slowly taking more than 3 days at room temperature to achieve 31% yield (Scheme 3.5).[13]

Scheme 3.5 Coupling of MPEG (**8**) with Baccatin III[13]

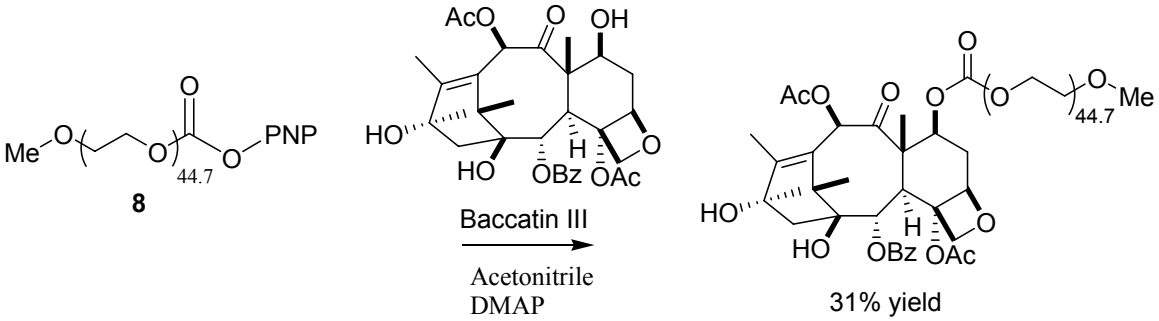

Dr. Ella Chow Clement successfully coupled PNP activated MPEGs with a GABA amide to afford MPEG-linked GABA amide with efficient incorporation without the addition of DMAP and only stirring at room temperature for 1 day.[14]

Given the previous success of the Carlier group to couple PNP activated PEG's with a variety of compounds,[13, 14] we were confident that we could couple the PNP activated MPEG with the amino functionalized BZD **6**. We initially attempted to couple **8** and **6** in acetonitrile without the addition of DMAP (Table 3.2, entry 1)[14] and obtained no product. We incorporated the protocol optimized by Dr. Lam and were able to couple the PNP activated MPEG and **6** (Table 3.2, entry 2-4), however despite prolonged reaction times the best yield we were able to achieve was 30% (Table 3.2, entry 4).

Table 3.2 Synthesis of BZD-methoxy terminated poly(ethylene glycol) (MPEG) model compound (**9**).

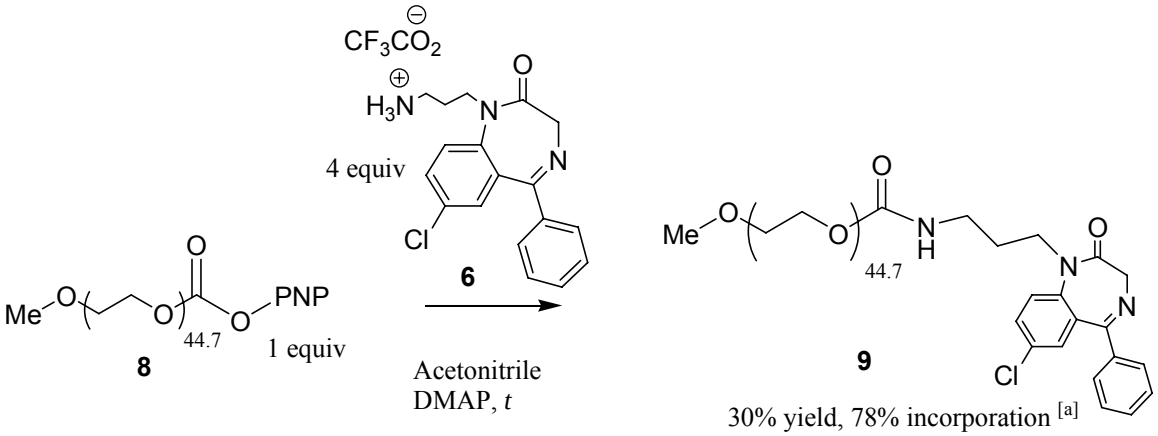

[a] explanation of % incorporation found in section 3.4

Entry	DMAP	*t* (days)	Yield of **9**
1	no	1	0
2	yes	3	20 %
3	yes	4	26%
4	yes	5	30%

We began collaboration with Dr Bloomquist (Entomology, Virginia Tech) where I learned methods for preparing striatal synaptoneurosomes from mice and running binding assays on the $GABA_AR$.

3.2 Bioassay results of two model compounds: BZD-BOC (5) and BZD-MPEG (9)

The BZD-methoxy terminated poly(ethylene glycol) (MPEG) model compound (**9**) and the Boc-protected precursor (**5**) were screened for their activity as $GABA_AR$ modulators using a dissociation binding assay in mouse-brain synaptoneurosomes. Details describing the assay method are discussed in section 3.4.2.

Radioligand binding assays provide detailed information about binding to the receptor by measuring the membrane-bound radioligands. The tissue containing the $GABA_A$ receptors was incubated with both [^{3}H]diazepam and the drug being tested (**5** or **9**). [^{3}H]diazepam (K_D = 40.0 nM)[15] binds to the modulator site of the $GABA_AR$. If the tether at the N1 position has no effect on binding to the $GABA_A$ receptors, then we anticipate that compounds **5** and **9** will also bind to the modulator site. The displacement of [^{3}H]diazepam indicates binding of the drug to the receptor, so we are interested in seeing a decrease in counts per minute of radioactivity (CPM).

Binding to the receptor of interest is called specific binding.[17] In addition to binding to the $GABA_AR$, [^{3}H] diazepam may also bind to other proteins or it may stick to the filter apparatus, a phenomenon called non-specific binding. Nonspecific binding is detected by measuring the binding of a radioligand ([^{3}H] diazepam) in the presence of a saturating concentration of an unlabeled drug, (Flunitrazepam **32**) that has a high affinity (K_D = 2.2 nM) to bind to the receptor. Under these condition all the specific binding sites are occupied by the unlabeled drug (Flunitrazepam) so the [^{3}H] diazepam can only bind to nonspecific sites.[17] By subtracting the nonspecific binding from the total binding of the [^{3}H] diazepam we can determine the specific binding (Figure 3.1).

Figure 3.1 shows the results from the first binding assay with the Boc-protected compound (**5**). Each bar shows the average CPM from three different trials. When only the "hot" ligand ([^{3}H] diazepam) is present (Figure 3.1, bar 1) we see a very high CPM (average = 19444). When we add the "cold" Flunitrazepam (Figure 3.1, bar 2) the CPM is significantly decreased indicating that the "cold" ligand has displaced all of the specifically bound [^{3}H] diazepam. The remaining CPM (roughly 5000) is due to nonspecific binding. Based on these experiments we determined the average specific binding of [^{3}H] diazepam to be roughly 14000 CPM. As can be seen from Figure 3.1 the Boc-protected model compound displaced a significant amount of the radiolabeled diazepam at quite low concentrations. The approximate IC_{50} value for compound **5** is less than 1 nM. This experiment confirmed that a moderately long substituent at the N1 position would not preclude binding at the $GABA_A$ receptor.

Figure 3.1 Binding assay results for BZD-BOC **5**.

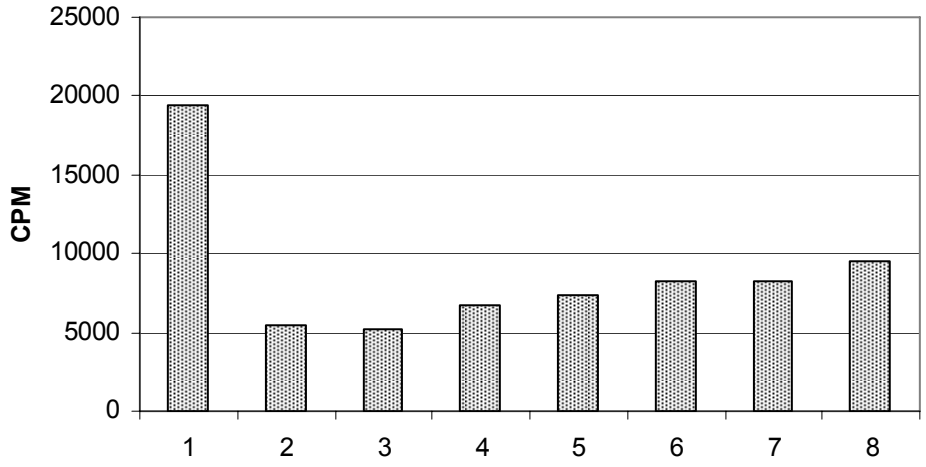

1: 1nM [^{3}H] diazepam
2: 1nM [^{3}H] diazepam + 12 nM Flunitrazepam
3: 1nM [^{3}H] diazepam + 100 μM **5**
4: 1nM [^{3}H] diazepam + 10 μM **5**
5: 1nM [^{3}H] diazepam + 1 μM **5**
6: 1nM [^{3}H] diazepam + 0.1 μM **5**
7: 1nM [^{3}H] diazepam + 0.01 μM **5**
8: 1nM [^{3}H] diazepam + 0.001 μM

BZD-MPEG model compound **9** was screened for activity using the same binding assay described above. The results are outline in Figure 3.2. We observed significant displacement of the [^{3}H] diazepam with the addition of 100 μM of BZD-MPEG **9** (Figure 3.2, bar 3). We continued to see displacement of the "hot" ligand at concentrations equal to 10 μM and 1 μM of **9** (Figure 3.2, bars 4-5). The benzodiazepine bound to the MPEG tether and [^{3}H] diazepam both bind at the modulator site on the $GABA_AR$. We see displacement of [^{3}H] diazepam by BZD-MPEG **9** at concentrations equal to 1-100 μM, therefore we can conclude that the MPEG tether would not prevent the benzodiazepine from binding to the modulator site on the $GABA_A$ receptor. Concentrations lower than 1 μM of **9** showed no significant displacement of [^{3}H] diazepam. Based on these experiments we determined that the IC_{50} value for compound **9** is between1 μM and 10 μM.

Figure 3.2 Binding assay results for BZD-MPEG **9**

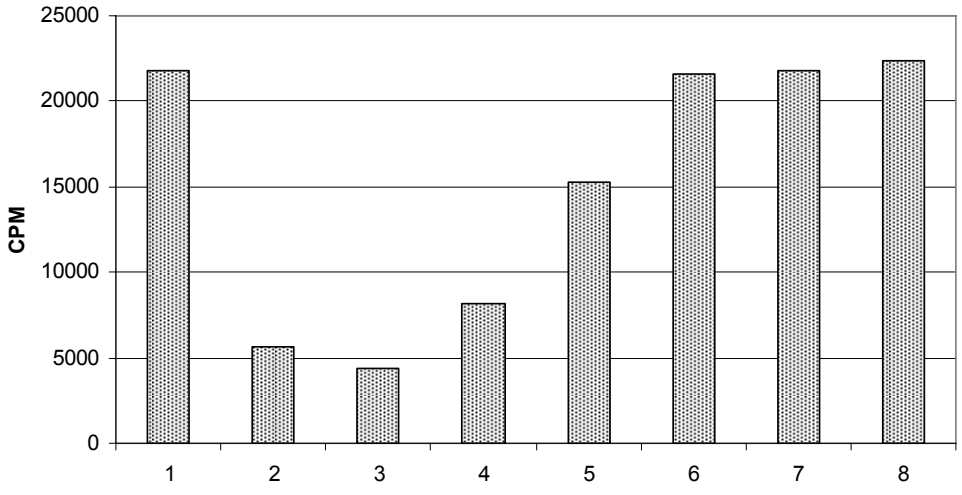

1: 1nM [^{3}H] diazepam
2: 1nM [^{3}H] diazepam + 12 nM Flunitrazepam
3: 1nM [^{3}H] diazepam + 100 μM **9**
4: 1nM [^{3}H] diazepam + 10 μM **9**
5: 1nM [^{3}H] diazepam + 1 μM **9**
6: 1nM [^{3}H] diazepam + 0.1 μM **9**
7: 1nM [^{3}H] diazepam + 0.01 μM **9**
8: 1nM [^{3}H] diazepam + 0.001 μM **9**

3.3 Conclusions

We were able to develop a BZD-methoxy terminated poly(ethylene glycol) (MPEG) model compound **9** from the Boc-protected precursor **5**. With these two compounds in hand we were able to obtain valuable information on whether the tether would have an effect on binding. We chose a tether with an average rms length of 38 Å and coupled the activated MPEG with the amino functionalized BZD (**5**). We enlisted the most potent benzodiazepine (Flunitrazepam) as a control. We first tested the Boc-protected compound and as can be seen from Figure 3.1 the compound displaced a significant amount of the radiolabeled diazepam at quite low concentrations. We found the approximate IC_{50} value for compound **5** is less than 1nM. Finally, addition of 100μM to 0.001μM of the BZD-MPEG model compound **9** also displaced the [^{3}H] diazepam confirming that a tether of this length would not prevent binding to the receptor. The IC_{50} value for compound **7** is between 1μM and 10μM.

The original intent of this project was to design and test benzodiazepine-agonist heterodimers (section 2.7, Chapter 2). To achieve this goal we not only have to link the benzodiazepine to the tether, but also an agonist such as GABA. Unfortunately, unlike the BZD-MPEG compound **9**, addition of an MPEG tether to GABA amide did affect the potency of the agonist, GABA.[14] Dr. Ella Chow Clement determined that coupling GABA amides with long chain PEG-linkers resulted in complete loss of agonist activity at the $GABA_AR$.[14] Without the tethered agonist we can not make modulator-agonist heterodimers, therefore we did not pursue further research in this particular area. Fortunately, exciting asymmetric methodology on 1,4-benzodiazepin-2-ones was being

successfully developed in our labs. We decided to turn our focus to this productive area, specifically 1,4-benzodiazepin-2,5-diones.

3.4 Experimental details

3.4.1 Chemistry

General

2-Aminobenzophenone (**1**) was obtained from Acros. PEG monomethyl ether (**5**) (average M_n=2000) was obtained from Aldrich. *N*-Boc-3-tosyl-propanamine was prepared according to the literature methods.[11, 18] ^{1}H and ^{13}C NMR were recorded on Bruker JEOL 500 MHz spectrometer. Identity and purity of the synthesized compounds were further confirmed in the following way. High resolution mass spectra recorded under FAB conditions (NBA, PEG), in each case gave the expected molecular formula (M+1) as the closest match among all possible formulas. Analytical thin-layer chromatography (TLC) was performed using aluminum coated RDH silica gel 60 F254. VWR silica gel 60 (60-240 mesh) was used for flash chromatography.

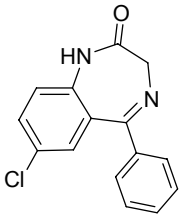

Synthesis of 1,4-benzodiazepine-2-one (4)[10, 12]

2-Aminobenzophenone (1.00 g, 4.3 mmol) and glycine ethyl ester hydrochloride (750.0 mg, 5.38 mmol) were combined in dry pyridine (20 mL) and heated to reflux for 15 hours. Solvent was removed via vacuum distillation. The residue was dissolved in

diethyl ether (50 mL) and extracted with H_2O (50 mL). The aqueous layer was made alkaline (2M NaOH) and extracted with diethyl ether (50 mL). The combined diethyl ether layers were washed once more with H_2O (50 mL) and dried over Na_2SO_4. The crude product was recrystallized from toluene and petroleum ether. 1,4-Benzodiazepin-2-one (**4**) was obtained as a white solid (1.01 g, 86 %). The ^1H and ^{13}C spectra closely matched the spectra for compound **4** found in the literature.[10, 12] ^1H NMR ($CDCl_3$) δ 4.33 (bs, 2H), 7.06 (d, *J* = 8.7 Hz, 1H), 7.31 (s, 1H), 7.45 (m, unassigned aromatic protons, 5H), 7.53 (d, *J* = 8.7 Hz, 1H), 8.54 (bs, 1H); ^{13}C NMR ($CDCl_3$) δ 56.66, 122.57, 128.48, 129.00, 129.63, 130.73, 130,82, 131.92, 169.82, 171.57; HRMS (FAB) calcd for $C_{15}H_{11}N_2OCl$ $[M + H]^+$ 270.0559, found 270.100 (+0.9 ppm, +0.3 mmu).

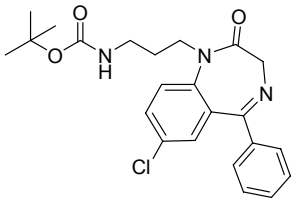

Synthesis of N-Boc protected amino functionalized 1,4-benzodiazepin-2-one (5)

N-H-1,4-Benzodiazepin-2-one (**4**) (350.0 mg, 1.29 mmol) was dissolved in dry DMF (20 mL) and deprotonated with KH (35% w/w, 190.0 mg, 1.66 mmol) at 0 °C under a nitrogen atmosphere to afford the benzodiazepine potassium salt. *N*-Boc-3-tosyl-propanamine[11] (1.27 g, 3.87 mmol) was dissolved in dry DMF (5 mL) and added dropwise to the reaction flask. The reaction mixture was stirred at 0 °C for 2 hours. The reaction was quenched with saturated NH_4Cl. Diethyl ether (100 mL) was added and the solution was extracted with H_2O (3 x 100 mL). The organic layer was dried with $MgSO_4$, filtered and evaporated under reduced pressure. The crude product was purified via flash

column chromatography (60:40 EtOAc:Hexane) to yield the corresponding amino functionalized 1,4-benzodiazepin-2-one (**5**) as a foamy solid (241.5 mg, 44 %).[1]H NMR (CD_3OD) δ 1.38 (s, 9H), 1.59 (m, 1H), 1.69 (s, 1H), 2.82 (m, 1H), 2.84, (m, 1H), 3.74 (m, 1H), 3.82 (d, *J* = 10.7, 1H), 4.40 (m, 1H), 4.61 (d, *J* = 10.7, 1H), 7.22 (s, 1H), 7.46-7.63 (m, unassigned aromatic protons, 7H); ^{13}C NMR (CD_3OD) δ 13.19, 27.47, 27.94, 31.55, 36.98, 37.21, 44.16, 56.43, 59.14, 60.21, 78.62, 124.34, 128.26, 128.38, 129.34, 129.63, 129.87, 130.84, 131.47, 131.88, 137.99, 141.20, 156.89, 169.45, 171.57; HRMS (FAB) calc for $C_{23}H_{26}N_3O_3Cl$ $[M + H]^+$ 427.166, found 427.210 (-4.0 ppm, -1.1 mmu).

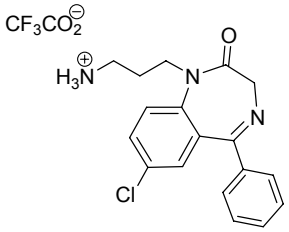

Synthesis of the deprotected amino functionalized 1,4-benzodiazepin-2-one (6)

Quantitative removal of the Boc protecting group of **5** was achieved by treatment of the *N*-Boc protected amino functionalized 1,4-benzodiazepin-2-one (50.0 mg, 0.117 mmol) with an excess of trifluroacetic acid (1 mL) stirred at room temperature under N_2 for 1 h. The product was concentrated in vacuum to yield the desired deprotected compound **6** as the trifluoroacetic acid salt (38.0 mg, 100 %). ^1H NMR (CD_3OD) δ 1.84 (m, 1H), 1.91 (s, 1H), 2.78 (m, 2H), 2.84, (m, 1H), 3.74 (m, 1H), 3.89 (m, 1H), 3.95 (d, *J* = 11.0, 1H), 4.38 (m, 1H), 4.65 (d, *J* = 11.0, 1H), 7.22 (s, 1H), 7.46-7.63 (m, unassigned aromatic protons, 7H); ^{13}C NMR (CD_3OD) δ 33.22, 39.71, 46.76, 56.43, 122.34, 127.26, 127.38, 129.34, 129.68, 129.97, 131.84, 131.55, 133.88, 136.99, 140.20, 156.90, 169.58, 172.07; HRMS (FAB) calc for $C_{23}H_{26}N_3O_3Cl$ $[M + H]^+$ 327.1138, found 327.1109 (+6.0 ppm, +1.6 mmu).

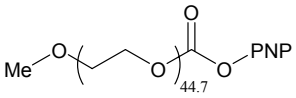

Synthesis of PNP (*p*-nitrophenyl carbonate) activated methoxy-terminated poly(ethylene glycol) (MPEG) linker (8)[13]

Methoxy-terminated poly(ethylene glycol) (Average M_n = 2000) (1.000 g, 0.5 mmol) was dissolved in dichloromethane (10.0 mL). Bis(4-nitrophenyl) carbonate (912.6 mg, 3.0 mmol) and *N*,*N*-diisopropylethyl amine (0.192 mL, 2.0 mmol) were added to the reaction flask and the mixture was stirred at room temperature for 3 days. The organic layer was washed with H_2O (10 mL fractions) until the aqueous layer remained clear. The crude product was purified using flash chromatography (10:90 CH_3OH:CH_2Cl_2) to afford the desired PNP activated MPEG **8** (1.09 g, 86% yield, 100% incorporation).^{1}H NMR ($CDCl_3$) δ 3.37 (s, 3H), 3.63 (m, 188H), 7.38 (d, *J* = 8.5 Hz, 2H), 8.28 (d, *J* = 8.5 Hz, 2H). The experimental ^{1}H NMR integration ratio of the methoxy protons at 3.37 ppm to the phenyl protons ortho to the nitro group at 8.28 ppm is equal to 3:2, which corresponds to 100% incorporation. The molecular weight of the PEG purchased from Aldrich is an average; therefore there is often discrepancy between the predicted internal CH_2 integral and the actual internal CH_2 integral. ^{1}H NMR analysis confirms that n = 44.7 for the MPEG linker **8**, as follows: we selected the phenyl proton ortho to the nitro group at 8.28 ppm as an internal reference for 2 protons, since there are 188 methylene protons in the internal repeating unit, we confirm that n = 44.7 as predicted by the average molecular weight. A more detailed description of integral analysis for PEG tethers can be found in Dr. Polo Lam's thesis.[13]

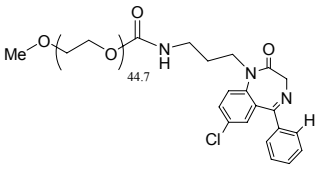

Synthesis of BZD-methoxy terminated poly(ethylene glycol) (MPEG) model compound (9).[13]

Amino functionalized 1,4-benzodiazepin-2-one (**6**) (50.0 mg, 0.152 mmol) was dissolved in acetonitrile (1 mL). Previously prepared PNP activated MPEG (83.3 mg, 0.030 mmol) and DMAP (0.9 mg, 0.007 mmol) were added to the reaction flask and the mixture was stirred at room temperature for 5 days. Dichloromethane (10 mL) was added to the reaction flask and the organic layer was extracted with HCl (0.1M, 10 mL). The organic layer was washed with 10 mL portions of $NaHCO_3$ until no more yellow color was visible in the aqueous layer. The organic layer was dried using $MgSO_4$, filtered and the solvent was evaporated under reduced pressure. The crude product was purified using preparatory thin layer chromatography (10:90 CH_3OH:CH_2Cl_2) to afford the desired BZD-methoxy terminated poly(ethylene glycol) (MPEG) model compound (**9**) (16.6 mg, 30% yield, 78% incorporation as described below) ^{1}H NMR ($CDCl_3$) δ 1.54 (m, 1H), 1.74 (m, 1H), 2.76 (m, 1H), 3.14 (m, 1H), 3.36 (s, 3H), 3.63 (m, 188H), 4.13 (d, *J* = 11.0, 1H), 4.39 (m, 1H), 4.80 (d, *J* = 11.0, 1H), 5.11 (m, 1H), 7.04-7.42 (m, unassigned aromatic protons, 12H). Incorporation calculation: the experimental ^{1}H NMR integration ratio of the methoxy protons (3.33 ppm) to the benzodiazepine proton (2.76) equals 3:0.78, which corresponds to 78% incorporation. Choosing the benzodiazepine methylene proton (2.76 ppm) for our internal reference again resulted in 188 methylene protons in the internal repeating unit, therefore n = 44.7 as expected.

3.4.2 Biological Assay

The procedure we used for performing radioligand displacement binding assays[19] is illustrated step by step in Figure 3.3. Synaptoneurosomes were prepared from one male ICR mouse brain (Harlan Sprague Dawley, Dublin, VA). The brain was removed after cervical dislocation, and homogenized in 1.25 mL of cold low-Cl buffer. The buffer solution contains 118 mM NaCl, 5 mM KCl, 1.2 mM $MgSO_4$, 2.5 mM $CaCl_2$, 54 mM glucose and 20 mM HEPES adjusted to pH = 7.4. Using a Dounce glass-glass homogenizer the brain tissue is homogenized with exactly 5 strokes. The brain tissue is then diluted with 6.0 mL of cold low-Cl buffer and filtered through 3 layers of 100 mesh nylon to remove any solids. The membrane filtrate is divided into two centrifuge tubes and then spun in the centrifuge for 15 minutes at 3000 g. The supernatant is removed and each pellet is resuspended in 1.5 mL of low-Cl buffer (with 1mg/mL BSA). Stock solutions of flunitrazepam (12 nM), and compounds **3** and **7** (various concentrations) in HEPES buffer were prepared prior to synaptoneurosome preparation. The stock solution of [^{3}H] diazepam in HEPES buffer was prepared immediately before the assay.
Each sample was run in triplicate as demonstrated in Figure 3.3. The first set of 3 test tubes each contain 5 μL of [^{3}H] diazepam. This allows us to see how much binding occurs when only radiolabeled ligand is bound at the modulator site on the $GABA_AR$. The second set of test tubes is charged with both [^{3}H] diazepam (5 μL each) and flunitrazepam (5 μL each). As previously stated flunitrazepam is a very potent benzodiazepine and will displace a significant amount of the [^{3}H] diazepam at this concentration. The data obtained from this set provides us with a nice control and also ensures that the assay was performed properly. Finally, the last triplicate of test tubes

contains the [^{3}H] diazepam (5 μL each) as well as 5 μL the compound being tested (**3** or **7**). The synaptoneurosomes are warmed to room temperature. The binding reactions are initiated when 90 μL of synaptoneurosomes are added to each test tube which is then incubated at 20 °C for 10 minutes. Addition of 2.5 mL of cold buffer terminates the binding reaction and the tissue is the collected on Whatman GF/C filters using a vacuum filtration apparatus. Each filter paper is washed twice with 2.5 mL cold buffer to guarantee that the only [^{3}H] diazepam that is on the filter is bound to the receptors. Each filter paper is put in a scintillation vial and filled with scintillation cocktail (xylenes). Radioactivity is determined using scintillation counting.

Figure 3.3 Radiolabeled ligand displacement binding assay diagram

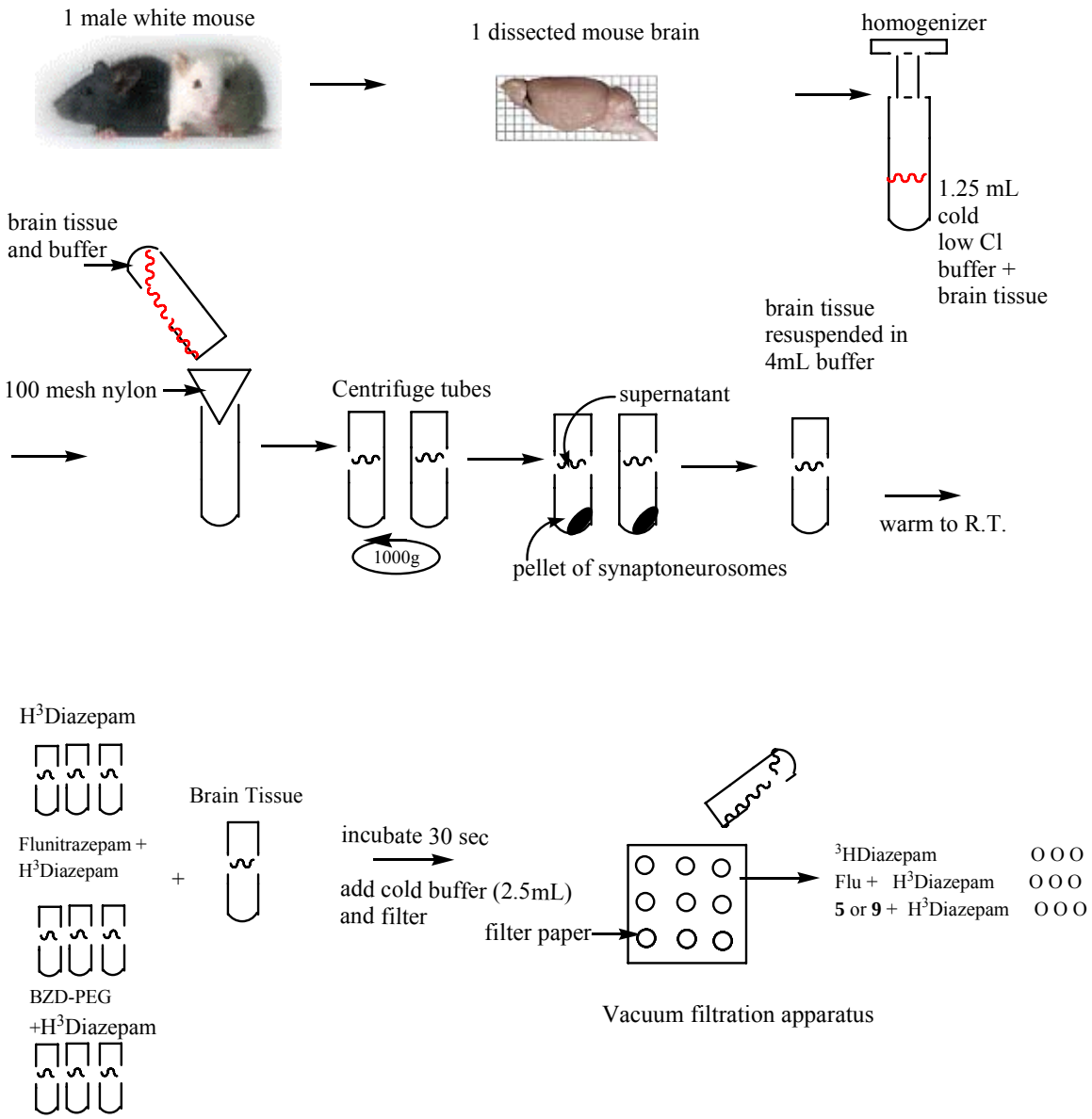

References for Chapter 3

[1] Pritchett, D. B., Seeburg, P. H., γ-Aminobutyric acid A receptor α-5-subunit creates novel type II benzodiazepine pharmacology, *J. Neurochem.* **1990**, *54*, 1802.

[2] Triet, D., Animal models for the study of anti-anxiety agents: a review, *Neurosci. Biobehav. Rev.* **1985**, *9*, 203.

[3] Chiu, T., Rosenberg, H. C., Benzodiazepine--specific and nonspecific tolerance following chronic flurazepam treatment, *Life Science* **1983**, *4*, 348.

[4] Mandel, P., DeFeudis, F. V. *Advances in Experimental Medicine and Biology*; Plenum Press: N.Y., 1979; Vol. 123.

[5] Geller, I., Kulak, J. T., Seifter, J., The effects of chlordiazepoxide and chlorpzomazine on a punished discrimination, *Psychopharmacologia* **1962**, *3*, 374.

[6] Sigel, E., Buhr, A., The benzodiazepine binding site of $GABA_A$ receptors., *Trends Pharm. Sci.* **1997**, *18*, 425.

[7] Luddens, H., Korpi, E. R., Seeburg, P. H., $GABA_A$/Benzodiazepine receptor heterogeneity: Neurophysiological implications, *Neuropharmacology* **1995**, *34*, 245.

[8] Smith, G. B., Olsen, R. W., Functional domains of $GABA_A$ receptors, *Trends Pharm. Sci.* **1995**, *16*, 162.

[9] Covelli, V., Maffione, A. B., Nacci, C., Tato, E., Jirillo, E., Stree, Neuropsyciatric disorders and immunological effects exerted by benzodiazepines, *Immunopharmacol. and Immunotoxicol.* **1998**, *20*, 199.

[10] Sternbach, L. H., The benzodiazepine story, *J. Med. Chem.* **1979**, *22*, 1.

[11] Mattingly, P., Diagndiv, G., Mono-protected diamines. N-a-(tert-butoxycarbonyl)-α-ω-alkane diamine hydrochlorides from amino alcohols, *Synthesis* **1990**, *4*.

[12] Sternbach, L. H., Fryer, R. I., Metlesics, W., Reeder, E., Sach, G., Saucy, G., Stemple, A., Quinazolines and 1,4-benzodiazepines VI. Halo-, methyl-, and methoxy-substituted 1,3- dihydro-5-phenyl-2H-1,4-benzodiazepin-2-ones., *J. Org. Chem.* **1962**, *27*, 3788.

[13] Lam, P. C.-H., Ph.D. thesis, Virginia Polytechnic Institute and State University, Blacksburg VA, 2004.

[14] Clement Chow, E., Ph.D. thesis, Virginia Polytechnic and State University, Blacksburg VA, 2005.

[15] Li, M., Szabo, A., Rosenberg, H. C., Evaluation of native GABAA receptors containing an a5 subunit., *European Journal of Pharmacology* **2001**, *413*, 63.

[16] Boileau, A. J., Evers, A. R., Davis, A. F., Czajkoski, C., Mapping the agonsit binding site of the $GABA_A$ receptor: Evidence for a β-strand, *J. Neuro. Sci* **1999**, *19*, 4847.

[17] Revest, P., Longstaff, A. *Molecular Neuroscience*; BIOS Scientific Publishers Lim.: New York, 1998.

[18] Fieser, M. In *Fiesers' reagents for organic synthesis*; M. Fieser, Ed.; Wiley-Interscience: New York, 1980; Vol. 1, p 1180.

[19] Boileau, A. J., Kucken, A. M., Evers, A. R., Czajkoski, C., Molecular dissection of benzodiazepine binding and allosteric coupling using chimeric γ-aminobutyric $acid_A$ receptor subunits, *Mol. Pharmacol.* **1998**, *53*, 295.

Chapter 4. Introduction of 1,4-Benzodiazepin-2,5-diones and Memory of Chirality (MOC)

4.1 Medicinal importance of 1,4-benzodiazepin-2,5-diones

1,4-Benzodiazepines (**1**) are a fundamentally important class of drugs that display selective activities against a wide array of biological targets.[1-4] A subset of the 1,4-benzodiazepines, 1,4-benzodiazepin-2,5-diones (**2**) comprise a privileged structure that has also exhibited diverse biological activity.[5-9] Compounds containing the 1,4-benzodiazepin-2,5-dione skeleton have received attention as potential therapeutics for endocrine disorders (**3**).[10] Pyrrolobenzodiazepines (**4**) have been reported to exert potent and efficacious analgesic activity without displaying the serious undesirable side effects associated with morphine and its relative compounds.[11] Pyrrolo-derivatives are also important synthetic precursors to benzodiazepine receptor antagonists such as flumazenil (**5**) [12] and G5598 (**6**).[13] The benzodiazepine dione derivative G5598 has been shown to be a potent inhibitor of the binding of GpIIb/IIIa to fibrinogen as well as a potent inhibitor of platelet aggregation.[13]

Inverse agonists related to Ro 15-4513 (**7**) exhibit anxiogenic, somnolytic and convulsant/proconvulsant activity.[14] Finally, 1,4-benzodiazepin-2,5-diones such as **8** have been reported to be valuable pharmacological mimics of the tripeptide RGD (Arg-Gly-Asp).[15] [16]

Figure 4.1 Biologically active 1,4-benzodiazepin-2,5-diones

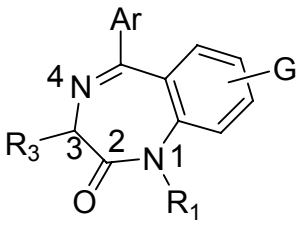

1,4-benzodiazepin-2-one

1

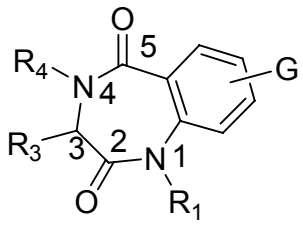

1,4-benzodiazepin-2,5-dione

2

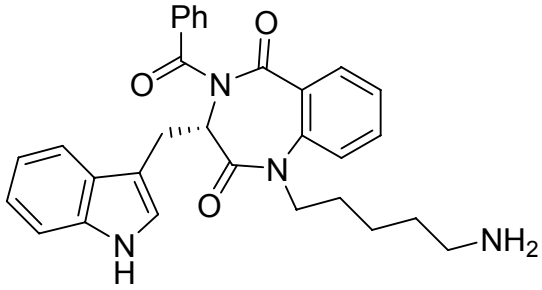

Somatostatin mimic

3

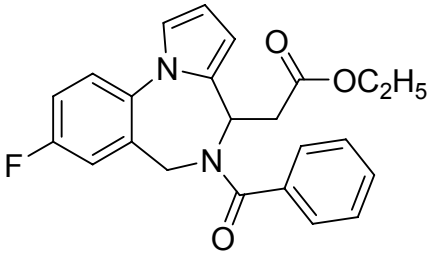

Analgesic agent

4

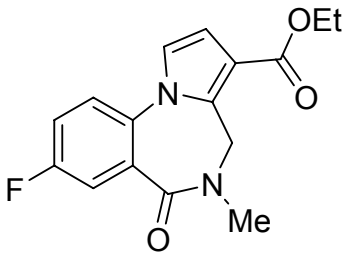

Flumazenil

5

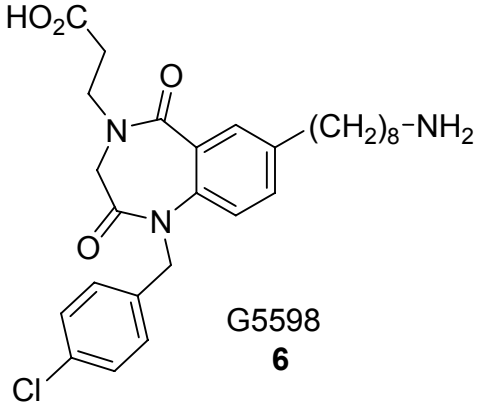

G5598

6

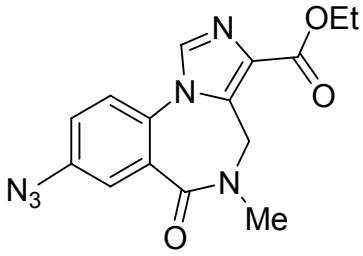

Ro 15-4513

7

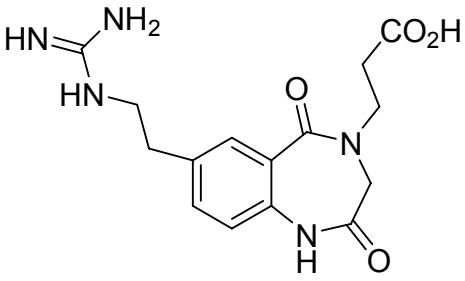

RGD analogue

8

Examples of compounds containing the tricyclic proline-derived 1,4 benzodiazepine-2,5-dione subtype have been reported as anxiolytic drugs (**9**),[5, 17] and as starting materials for the synthesis of anthramycin-inspired anticancer agents (e.g.,**10**). [1, 4, 17-20] More recently, however, they have been recognized as weaker non-covalent ligands (**11**) for the DNA minor groove[17] and have shown promise as herbicides (**12**).[17, 21]

Figure 4.2 Proline-derived 1,4-benzodiazepin-2,5-diones

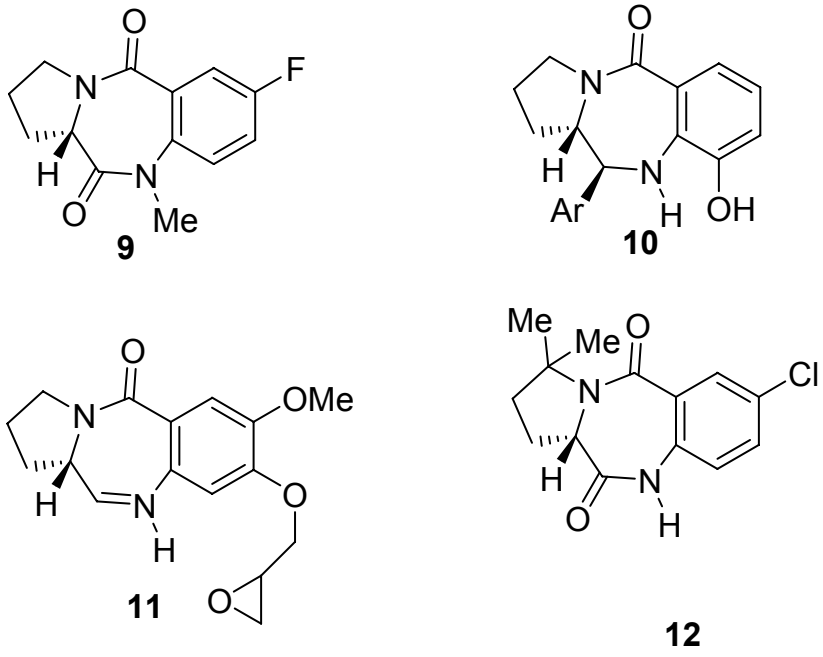

Despite the impressive diversity of 1,4-benzodiazepin-2,5-diones prepared to date, examples possessing a quaternary stereogenic center have been largely unexplored due to the limited commercial availability of enantiopure quaternary amino acids.

Enantiopure 3,3-disubstituted quaternary benzodiazepines have previously been difficult to synthesize and most examples mentioned in the literature thus far are prepared from the proteinogenic amino acids.

Previous to the work recently published by Carlier et al.,[22] lipase-catalyzed kinetic resolution was the only published method for preparing enantiopure 3,3-disubstituted 1,4-benzodiazepines.[23, 24] Avdagic and co-workers[24] enantioselectively acetylated a series of chiral 3-(hydroxyalkyl)-1,4-benzodiazepin-2-ones using the enzyme *Novozym 435*. In particular, they established the prevalent acetylation of **13** (uniformly disubstituted at C3) to **(3*R*)-14** in 90.2% ee**.** It is pertinent at this time to discuss the well known conformational properties of 1,4-benzodiazepin-2-ones in order to understand their rationalization of this noteworthy result.

Scheme 4.1 Lipase-catalyzed acetylation of 3-(hydroxyalkyl)-1,4-benzodiazepin-2-ones.

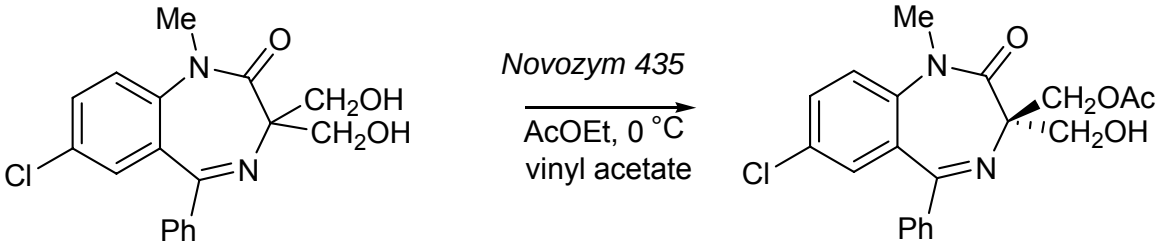

13 (3*R*)-**14**

Glycine derived 1,4-benzodiazepin-2-ones (**15**) such as diazepam (**15a**) are chiral, despite the absence of a stereogenic center. They exist as the conformational enantiomers shown in Table 4.1.[25] The helical descriptors *M* and *P* are used to describe the sense of chirality in the ring and are based on the sign of τ2345 torsional angle (*M*

denotes a negative dihedral and means minus and *P* denotes a positive dihedral and means plus). Inspection of the structure of **13** reveals that it exists as a pair of conformational enantiomers.

Table 4.1 Dynamic chirality of 1,4-benzodiazepin-2-ones **15a-d**

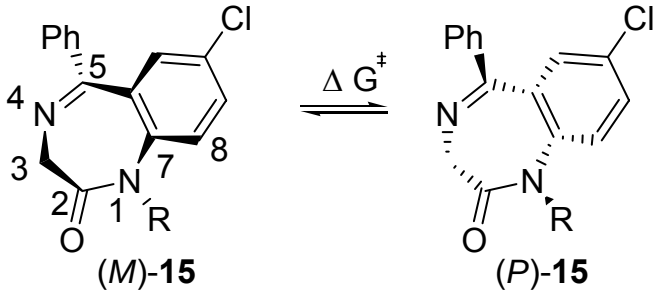

(*M*)-**15** (*P*)-**15**

R	ΔG‡ (kcal/mol)
H (**15c**)	12.3
Me (**15a**)	17.6
i-Pr (**15b)**	21.1
t-Bu (**15d)**	>24

* $\Delta G^{\ddagger}$ measured by Dr. Polo Lam

Table 4.1 shows that the barrier to inversion for these compounds does in-fact depend greatly on the size of the N1 substituent. When the N1 substituent is small such as H, Me and *i*-Pr (**15a-c**) racemization is fast at room temperature and these compounds cannot be resolved. However, when the N1 substituent is quite large (*t*-Bu, **15d**) resolution of the (*M*)- and (*P*) enantiomers is possible.[25]

Placement of a single substituent at C3 perturbs the conformational equilibrium of *N*-Me BZDs, the pseudoequatorial conformer **16** is preferred and therefore (3*S*)-

stereochemistry at C3 will induce the (*M*)-conformation of the diazepam ring (Scheme 4.2).

Scheme 4.2 Stereochemical cooperativity of 1,4-benzodiazepin-2-ones.

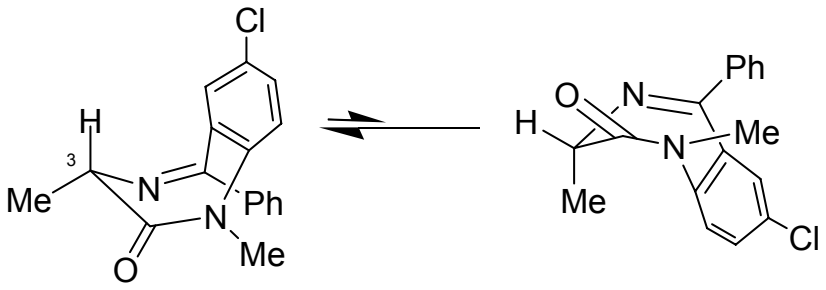

pseudoequatorial methyl in (*M*)-conformer of (*3S*)-**16**

pseudoaxial methyl in (*P*)-conformer of (*3S*)-**16**

The enantiomeric conformers of **13** ((*M*)-and (*P*)) are shown in Scheme 4.3. To rationalize the result depicted in Scheme 4.1 Avdagic proposed that the much less hindered pseudo-equatorial hydroxyl methyl group is readily acetylated at the active site of the enzyme. Since the Pro-(*R*) **13** is in the (*P*)-conformation, Avdagic proposed that the enzyme selectively binds and reacts with the (*P*)-conformation.

Scheme 4.3 Enantiomeric conformers of **13**

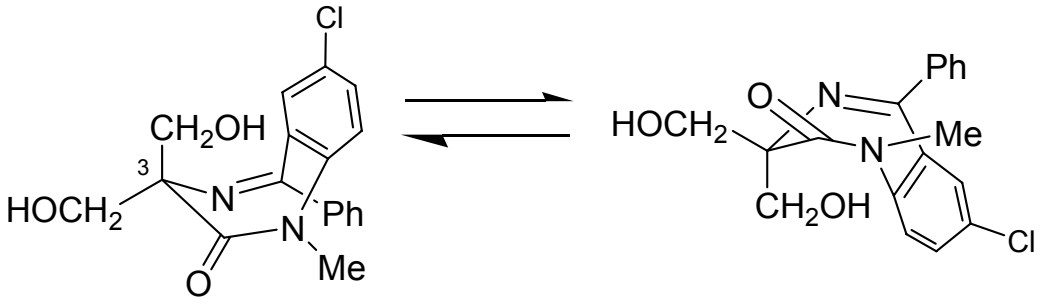

(*M*)-conformer of **13**

(*P*)-conformer of **13**

In addition to the importance of largely expanding the library of quaternary 1,4-benzodiazepin-2,5-diones known to date, enantiopure examples have assisted in the design of pharmacophore/receptor models for BzR subtypes of the GABA receptor.[26-28] Studies on a series of framework-constrained 4,5 substituted pyrroloimidazobenzodiazepines (**17a-d**) and azetidinylimidazobenzodiazepines (**18a,b**),[27] with both *R* and *S* configurations indicated that the *S* enantiomers were the only active conformers in this series of ligands (Table 4.2).[27, 29] The stereopreference for the *S* enantiomers of these ligands implied that the conformational topography at the recombinant receptor subtypes was well-conserved. It is well known that placement of a single substituent at C3 perturbs the conformational equilibrium of simple *N*-Me 1,4-benzodiazepin-2-ones, stabilizing the pseudoequatorial conformer thus, (3S)-stereochemistry induces the benzodiazepine ring to adopt the (*M*)-conformation.[25] The Carlier group has shown that (3S)-stereochemistry causes the benzodiazepine ring to adopt the (*M*) for quaternary 1,4-benzodiazepin-2-ones[22] and proline-derived 1,4-benzodiazepin-2,5-diones.[30] The rigid conformation of the active *S* enantiomers has lead to a better understanding of the conformational requirements of each receptor subtype.[27, 31] Determination of the differences among receptor pharmacophores of BzR subtypes will facilitate the design of more selective ligands, producing better drugs for treating anxiety, convulsions, sleep disorders and memory deficits.[31, 32]

Table 4.2 Affinities of framework-constrained **17a-b** and **18** at recombinant αxβ3γ2 (x = 1-3,5,6)[27]

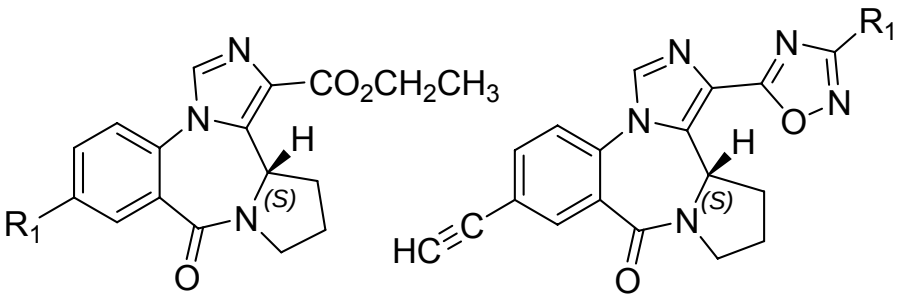

17a-b **18**

Compound	R_1	R_4	K_i (nM) α1	K_i (nM) α2	K_i (nM) α3	K_i (nM) α5	K_i (nM) α6
17a	Br	*(S)*	49	29	15	1	46
ent-17a	Br	(*R*)	<1000	<1000	<1000	<1000	<1000
17b	CCH	*(S)*	59	44	27	1.3	126
ent-17b	CCH	(*R*)	<1000	<1000	<1000	<1000	<1000
18	CH_3	*(S)*	89	70	91	3.7	301
ent-18	CH_3	(*R*)	<1000	<1000	<1000	157	<1000

* Data shown here are the means of two determinations which differed by less than 10%.[27]

1,4-Benzodiazepines and their subtypes display a wide range of pharmacological activities. A direct synthesis leading to quaternary benzodiazepines would be a key development in the search for more potent and more selective agents. The Carlier research group has developed a novel way to perform enantioselective α-alkylations on 1,4-benzodiazepines using a memory of chirality strategy.[22]

4.2 Introduction to Memory of Chirality

The general concept of "memory of chirality" (MOC) relies upon the idea that the memory of a single chiral center in the subtrate can be retained in a process that destroys that chiral center. Memory of chirality has been described as "a formal substitution at an sp^3 stereogenic center that proceeds stereospecifically, even though reaction proceeds by trigonalization of that center, and despite the fact that no other permanently chiral elements are present in the system" [33, 34]

Fuji was the first to design a reaction that utilized this phenomenon.[35, 36] He stated that the key to a MOC strategy was the preservation of static central chirality of the starting material in the form of transient or dynamic conformational chirality in the reactive intermediate. In summary, utilizing a MOC strategy requires going from static central chirality to dynamic transient chirality and back to static central chirality.

4.2.1 Static versus Dynamic Chirality

Enantiomers are defined as non-superimposible mirror images. Molecule **19** (Figure 4.3) posses a stereogenic center marked by a star and the two molecules shown are considered enantiomers because they can not interconvert without breaking and reforming a bond. These molecules have static central chirality.

Figure 4.3 Static central chirality

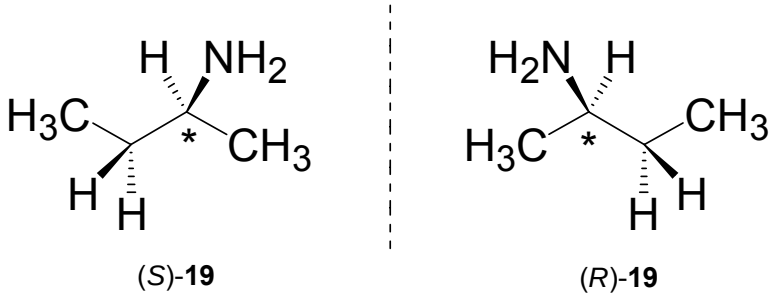

(*S*)-**19** (*R*)-**19**

Consider n-butane shown in Figure 4.4. Obviously n-butane is achiral in the anti conformation (**anti-20**). However, the individual gauche conformers are chiral; single bond rotation interconverts the enantiomeric g^- and g^+ conformers of **20.** This type of chirality is known as dynamic chirality and it depends on time and temperature. The formation of a dynamically chiral intermediate is one of several requirements that must be satisfied when implementing a successful MOC transformation.

Figure 4.4 *n*-Butane exhibits dynamic conformational chirality

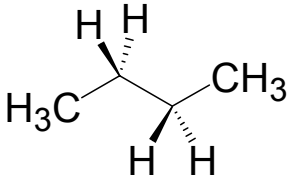

anti-20

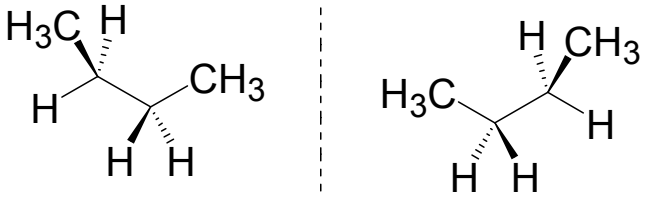

20 **ent-20**

g^- conformer g^+ conformer

4.2.2 Necessary Criteria for Successful MOC Transformations

The formation of a dynamically chiral intermediate is, in itself not sufficient for carrying out a MOC transformation. Successful MOC reactions depend upon three criteria. These criteria are illustrated in a deprotonation/alkylation scheme below (Scheme 4.4).

Scheme 4.4 Deprotonation/Alkylation outlining necessary criteria for successful MOC transformations

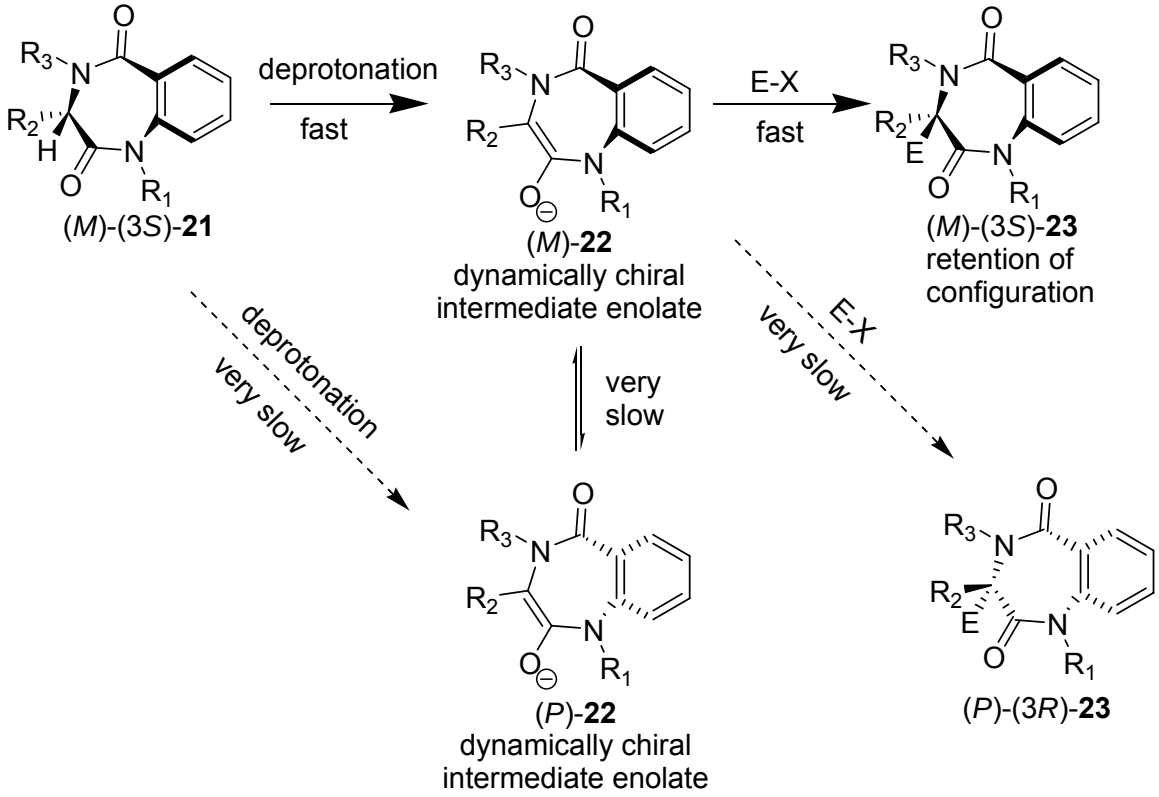

The starting material (**21**) in this example possesses static chirality arbitrarily depicted here as (*S*). The three requirements are:

1) Upon deprotonation of **21**, a dynamically chiral intermediate ((M)-**22**) must be formed in high enantioselectivity. The helical descriptors *M* and *P* are used here to describe the intermediate chirality.

2) Racemization of the intermediate ((*M*)-**22**) to its enantiomer ((*P*)-**22**) must be slow on the reaction timescale.

3) The dynamically chiral intermediate must react with the electrophile quickly and in high stereoselectivity to form the product (**23**) that contains static chirality.

All of these requirements must be met in order to yield highly enantiopure products.

How efficient transfer of chirality occurs in the first and last step is generally not well understood. What is more easily controlled and understood is the racemization rate of the reactive intermediate, which can be conveniently discussed in terms of the lifetime of the dynamically chiral intermediate.

If we assume a unimolecular racemization mechanism, the Eyring equation can be used to determine the racemization half life (Table 4.3) of the reactive intermediate.[37]

Table 4.3 Dependence of racemization $t_{1/2}$ on barrier and temperature

Racemization Barrier $\Delta G^{\ddagger}$ (kcal/mol)	**Racemization $t_{1/2}$ at -100 °C**	**Racemization $t_{1/2}$ at -78 °C**	**Racemization $t_{1/2}$ at 25 °C**
12	2.3 min	2.4 sec	$3.5 * 10^{-5}$ sec
14	13 h	7 min	$1.0 * 10^{-3}$ sec
16	181 d	20 h	$3.0 * 10^{-2}$ sec
18	167 y	148 d	0.9 sec
20	$5.6 * 10^{4}$ y	70 y	26 sec

* Eyring Equation $t_{½} = (\ln 2)/k_{rac}$, $k_{rac} = 2(k_B T/h)\exp(-\Delta G^{\ddagger}/RT)$[37]

As can be seen from this table, a racemization barrier of 12 kcal/mol will lead to a very short half life of $3.5*10^{-5}$seconds at room temperature, 2.4 seconds at -78 °C and 2.3 minutes at -100 °C. If we increase this barrier to 16 kcal/mol the reactive intermediate would have sufficient time at -78 °C to react with the electrophile without undergoing significant racemization. At -100 °C, however, it is possible to conduct MOC transformations with reactive intermediates that have inversion barriers as low as 12 kcal/mol. [38, 39] MOC strategies are rarely developed around sp^3-sp^3 bond rotation, because they have barriers to rotation of less than 7 kcal/mol. Alternatively, sp^2-sp^2 bonds can have barriers of rotation in excess of 16 kcal/mol and therefore make excellent candidates for MOC transformations.[40]

4.3 Examples of Memory of Chirality

4.3.1 The First Appearance of Memory of Chirality

MOC was first demonstrated in enolate chemistry.[35, 36] Fuji and Kawabata were the first to intentionally design and implement a MOC transformation. They converted the chiral ketone **24** into chiral alkylated ketones **25a-d** in 48-67% ee without any additional chiral source present in the reaction. They proposed that the central chirality at the carbon α to the carbonyl is preserved as transient axial chirality in the enolate intermediate and then regenerated as central chirality in the alkylated products.

Scheme 4.5 Fuji and Kawabata's first MOC transformation[36]

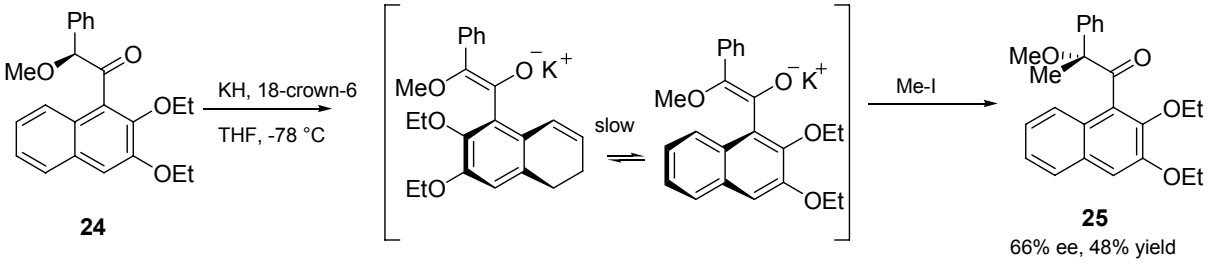

Subsequently, Fuji and Kawabata beautifully illustrated that MOC transformations provided a direct method for preparing α,α-disubsituted α-amino acids starting with commercially available proteinogenic α-amino acids without using an external chiral source.[41, 42] They reported the α-alkylation of the two phenylalanine derivatives shown in Scheme 4.6. When the phenylalanine ester is protected with two different groups such as Boc and MOM (**29a**), the methylated product (**31a**) is obtained in 81% ee despite the destruction of the stereogenic center during deprotonation. If, however, the phenylalanine ester is symmetrically protected (**29b**), the product (**31b**) that

is obtained is completely racemic. Fuji and Kawabata proposed that in the first example, where the starting material is asymmetrically protected, the enolate (**30a**) that is produced upon deprotonation exhibits axial chirality (along N1-C2) and is therefore chiral. The formation of this dynamically chiral intermediate leads to highly enantiopure products. Alternatively, the symmetrically protected phenylalanine ester **29b** yields an achiral enolate **30b** upon deprotonation and therefore yields racemic products.[41]

Scheme 4.6 MOC α-alkylation of α-amino acids

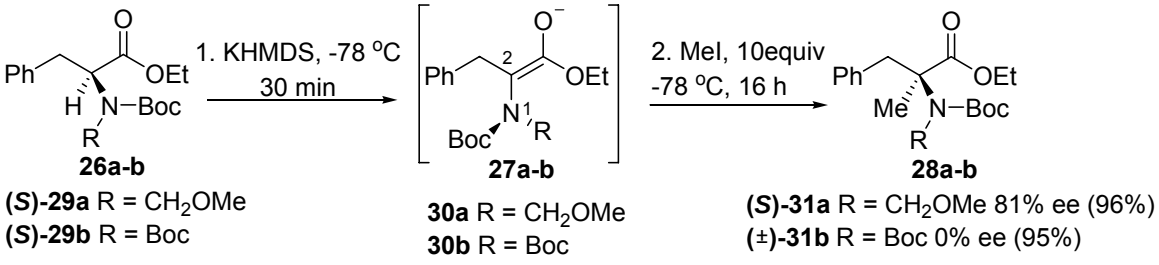

In 2000 Fuji and Kawabata published an interesting mechanistic study in which diastereomers **32a** and **33a** were separately deprotonated and alkylated.[43] As shown in Scheme 4.7, these diastereomers have the same (*S*) chirality at C3 but they possess opposite stereochemistry at C2. In the absence of memory of chirality **32a** and **33a** would generate the same enolate upon deprotonation. Upon alkylation they would give identical ratios of diastereomers **35a** and **36a**. If on the other hand, a chiral enolate is formed upon deprotonation, retentive alkylation of **32a** should yield mostly diastereomer **35a** and deprotonation and alkylation of **33a** should yield mostly **36a**. When **32a** was deprotonated and alkylated the product was obtained with a diastereomer ratio of **35a**:**36a**

equal to 93:7. When **33a** was reacted under the same conditions the ratio of products **35b**:**36b** that was obtained was 14:86.

These results suggest that the enolates that are formed upon deprotonation of **32a** and **33a** are different and that the stereochemical outcome for this reaction is controlled by the formation of a dynamically chiral C2-N axis rather than the statically chiral C3 center.[43] In contrast, if the nitrogen was symmetrically protected the C2-N axis would be achiral. Thus, when **32b** and **33b** are deprotonated they should generate identical enolates. As expected deprotonation/alkylation of **32b** and **33b** gave identical mixtures of **35b** and **36b**. In summary these studies on **32a,b** and **33a,b** provide additional strong evidence of Fuji and Kawabata's MOC proposal.

Scheme 4.7 Mechanistic study of MOC transformations on diastereomeric substrates[43]

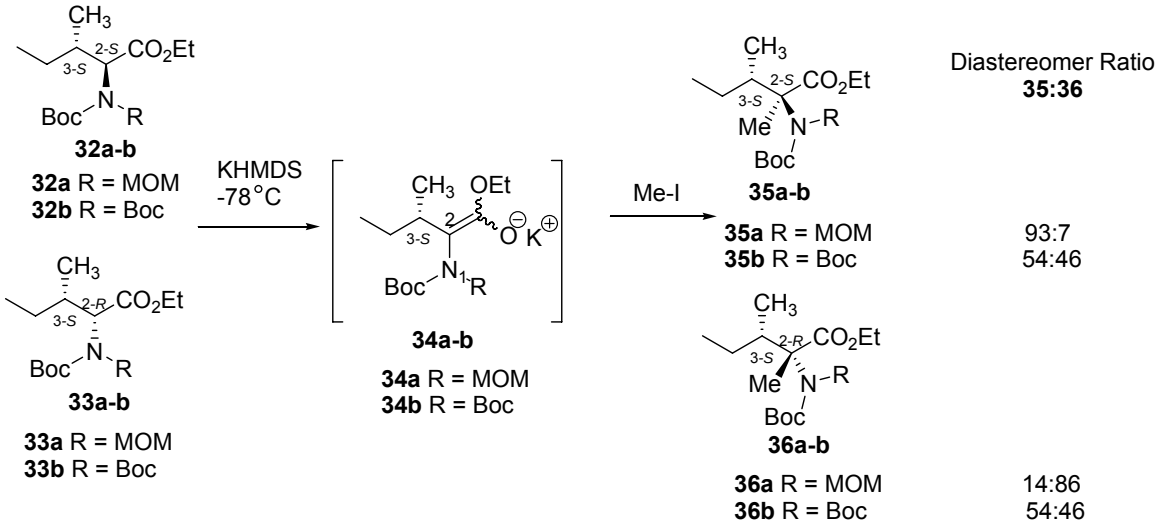

Since the successful MOC transformations developed by Fuji and Kawabata, [44] MOC protocols have been extended to include many other reactions besides those involving enolate chemistry. Rychnovsky applied a MOC strategy to radical chemistry in

cyclic systems.[45] Matsumura utilized MOC in the electrochemical oxidation of carbenium ions,[46] and Griesbeck described a decarboxylative photocyclisation that involved the formation of a biradical that underwent a memory of chirality transformation.[47] In addition to these examples described in the literature our group has recently published a method of asymmetrically alkylating a chiral center that is dependant on MOC.[22]

4.3.2 Applications of MOC in the Carlier Research Group

The Carlier group was the first to report a MOC route to quaternary 1,4-benzodiazepin-2-ones (BZD).[22] Our proposal was based on the stereochemical cooperativity demonstrated by 3-alkyl-1,4-benzodiazepin-2-ones as described in section 4.1. When 1,4-benzodiazepin-2-ones are substituted with a group at C3, the more stable pseudoequatorial conformer is preferred, therefore (3*S*) stereochemistry at C3 will induce the (*M*) conformation (Scheme 4.2) We proposed that upon deprotonation of **16** the resulting enolate would remain chiral, despite destruction of the chiral center, due to the non-planar nature of the benzodiazepine ring.

A concise summary of this work is shown in Scheme 4.8. [22] Notably, when deprotonated and alkylated at -78 °C the *N*-Me derivative (**16a**) affords the desired benzylated product (**37a**) in 72% yield but it is completely racemic. On the other hand, the *N*-*i*-Pr derivative (**16b**) yields the desired product (**37b**) in a 74% and a high enantiomeric excess of 97 %. We propose that the enolate formed upon deprotonation of the *N*-Me BZD **37a** has a low inversion barrier and racemizes quickly, yielding racemic products. On the other hand, the enolate that is formed from the *N*-*i*-Pr BZD (**37b**) has a

higher inversion barrier, presumably from the bulky isopropyl group, and the original chirality of the ring is preserved in the enolate yielding highly enantiopure products.

Scheme 4.8 Enantioselective synthesis of 1,4-benzodiazepin-2-ones illustrating a MOC transformation[22]

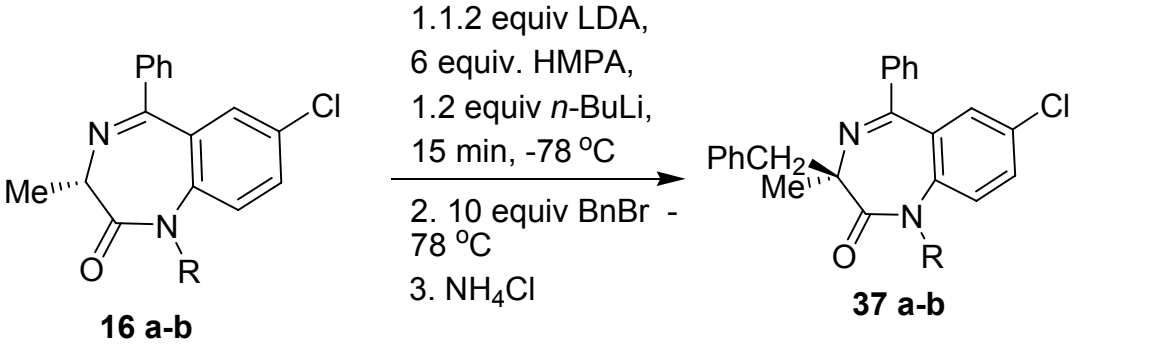

	R	%ee	%yield
37a	Me	0	72
37b	*i*-Pr	97(R)	74

As mentioned above the lack of enantioselectivity from the deprotonation/alkylation of **16a** was proposed to be a consequence of the smaller N1 substituent and a rapidly racemizing enolate at -78 °C.[22] In order to test this hypothesis and rule out the possibility that **16a** forms an achiral enolate, Dr. Polo Lam developed a technique to enantioselectively deprotonate and alkylate 1,4-benzodiazepin-2-ones bearing a small N1 substituent (*p*-methoxybenzyl (PMB)) (**38**).[38, 39] A low inversion barrier for the enolate derived from (**38**) was expected, given the small size of PMB and the racemic results obtained from the *N*-Me derivative **16a**, therefore the temperature of the reaction was lowered to -100 °C (Et_2O/CO_2).

Table 4.4 summarizes the results obtained from this study. After a 5 min deprotonation time (t_1) with KHMDS at -100 °C, addition of benzyl bromide afforded

completely racemic product **39** (Table 4.4, entry 1). This result led to the development of an in situ protocol (t_1 = 0), where the electrophile is already present upon deprotonation. In the presence of 100 equiv of BnBr the product was obtained in 80% ee (Table 4.4, entry 2). Improving the alkylation rate constant by using a more reactive electrophile (BnI), yielded the desired product in 88% ee. In this case, the stepwise protocol had to be implemented (t_1 = 10 s), due to rapid reaction of the base with the more reactive electrophile. Comparison of entries 2 and 3 (Table 4.4) indicates that BnI is more than 10 times as reactive as BnBr. It was apparent that even with short deprotonation times the enolate formed from **38** racemizes quickly at -100 °C, and improved enantioselectivity could not be achieved at this temperature. In order to achieve excellent enantioselectivity it was necessary to run these reactions at -109 °C (THF/N_2). Entry 4, in Table 4.4 shows that using a sequential deprotonation/alkylation protocol (t_1 = 20 min) with BnI as the electrophile yielded the product **39** in a very high 97% ee. The obvious dependence of % ee on temperature and time demonstrated from the above results provides further evidence that these transformations do rely upon memory of chirality.

Table 4.4 Memory of chirality trapping of a low inversion barrier 1,4-benzodiazepin-2-one

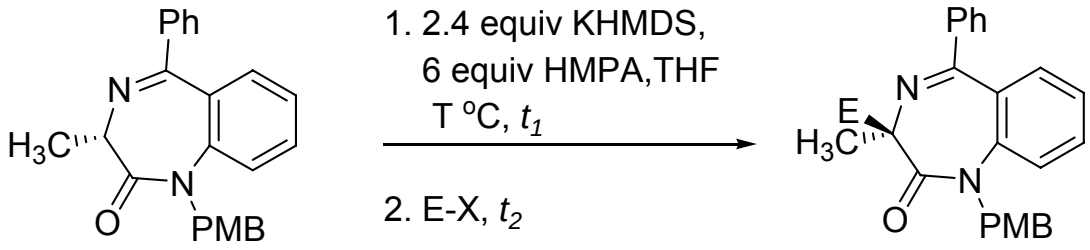

(*S*)-**38** (*R*)-**39**

Entry	E-X (equiv)	t_1	t_2 (min)	T °C	% ee	Yield (%)
1	Bn-Br (10)	5 min	120	-100	3	100
2	BnBr (100)	0 min	1	-100	80	46
3	BnI (10)	10 s	1	-100	88	61
4	BnI (20)	20 min	10	-109	97	93

Given the structural similarities of the 1,4 benzodiazepin-2-ones and 1,4 benzodiazpin-2,5-diones (Figure 4.1), we thought that they too could exhibit this intrinsic chirality, and that by implementing this successful MOC strategy they could be used as scaffolds for preparing enantiopure quaternary stereogenic centers.

References for Chapter 4

[1] Constantine, G., Boojamra, K. M., Lorin, A., Ellman, J. A., Solid-phase synthesis of 1,4-benzodiazepine-2,5-diones. Library, preparation and demonstration of synthesis generality, *J. Org. Chem.* **1997**, *62*, 1240.

[2] Ellman, J. A., Design, Synthesis and evaluation of small-molecule libraries, *Acc. Chem. Res.* **1996**, *29*, 132.

[3] Matthews, J. M., Dyatkin, A. B., Evangelisto, M., Gauthier, D. A., Hecker, L. R., Hoekstra, W. J., Liu, F., Poulter, B. L., Sorgi, K. L., Maryanoff, B. E., Synthesis, resolution and absolute configuration of novel tricyclic benzodiazepines, *Tetrahedron: Asymmetry* **2004**, *15*, 1259.

[4] Constantine, G., Boojamra, K. M., Burow, K., Ellman, J. A., An expedient and high yielding method for the solid-phase synthesis of diverse 1,4-benzodiazepine-2,5-diones, *J. Org. Chem.* **1995**, *60*, 5742.

[5] Wright, W., Brabander, H., Greenblatt, E., Day, I., Hardy, R., Derviatives of 1,2,3,11a-tetrahydro-5H-pyrrolo[2,1-c][1,4]benzodiazepine-5,11(10H)-dione as anxiolytic agents, *J. Med. Chem.* **1978**, *21*, 1087.

[6] Stuart, W., Howard, P., Forrow, S., Hartley, J., Adams, L., Jenkins, T., Kelland, L., Thurston, D., Design, synthesis and evalution of a novel sequence-selective epoxide-containing DNA cross-linking agent based on the pyrrolo[2,1-c][1,4]benzodiazepine system, *J. Med. Chem.* **1999**, *42*, 4028.

[7] Bi, Y., Schultz, P., Building blocks for peptide and carbamate libraries, *Bioorganic and Medicinal Chemistry Letters* **1996**, *6*, 2299.

[8] Kim, D. H., Derivatives of Tetrahydro-1,4-benzodiazpines as potential antihypertensive agents, *J. Med. Chem.* **1977**, *20*, 209.

[9] Sugimori, T., Okawa, T., Eguchi, S., Kakehi, A., Yashima, E., Okamoto, Y., The first total synthesis of (-)-benzomalvin B via the intramolecular aza-wittig reactions, *Tetrahedron* **1998**, *54*, 7997.

[10] Ishikura, M., Mori, M., Terashima, M. B., Y., A new synthesis of anthramycin via palladium-catalyzed carbonylation, *J. Chem. Soc. Chem . Commun.* **1982**, 741.

[11] Mai, A., Di Santo, R., Massa, S., Artico, M., Pantaleoni, G. C., Giorgi, R., Coppolino, M. F., Barracchini, A., Pyrrolobenzodiazepines with antinociceptive activity, *Eur. J. Med. Chem.* **1995**, *30*, 593.

[12] Goff, D. A., Zuckermann, R. N., Solid-phase synthesis of defined 1,4-benzodiazepine-2,5-dione mixtures, *J. Org. Chem.* **1995**, *60*, 5744.

[13] Webb II, R. R., Barker, P., Baier, M., Reynolds, M. E., Robarge, K. D., Blackburn, B. K., Tischler, M., Weese, K. J., Mono-N-alkylation of anthranilamides via quinazolinones, *Tetrahedron Letters* **1994**, *35*, 2113.

[14] Haung, Q., He, X., Ma, C., Liu, R., Yu, S. e. a., Pharmacophore/receptor models for GABAA/BzR subtypes via a comprehensive ligand-mapping approach, *J. Med. Chem.* **2000**, *43*, 71.

[15] Mc Dowell, R. S., Blackburn, B. K., Gadek, T. R., McGee, L. R., Rawson, T., Reynolds, M. E., K.D., R., Somers, T. C., Thorsett, E. D., Tischler, M., Webb II, R. R., M.C., V., From peptide to non-peptide. The de novo design of potent, non-peptidal inhibitors of the platelet aggregation based on a benzodiazepinedione scaffold, *J. Am. Chem. Soc* **1994**, *116*, 5077.

[16] Addicks, E., Mazitschek, R., Giannis, A., Synthesis and biological investigation of novel tricyclic bezodiazepinedione-based RGD analogues, *ChemBioChem* **2002**, *3*, 1078.

[17] Madani, H., Thompson, A., Threadgill, M. D., An expedient synthesis of 7-O-functionalized pyrrolo-1,4-benzodiazepine-2,11-diones, *Tetrahedron* **2002**, *58*, 8107.

[18] Pena, M. R., Stille, J. K., A total synthesis of anthramycin, *J. Am. Chem. Soc* **1989**, *111*, 5417.

[19] Confalone, P. N., Huie, E. M., Ko, S. S., Cole, G. M., Design and synthesis of potential DNA cross-linking reagents based on the anthramycin class of minor groove binding compounds, *J. Org. Chem.* **1988**, *53*, 482.

[20] Kamal, A., Enzymatic approach to the synthesis of the pyrrolo[1,4]benzodiazepine antibiotics, *J. Org. Chem.* **1991**, *56*, 2237.

[21] Karp, G. M., Manfredi, M. C., Guaciaro, M. A., Ortlip, C. L., Marc, P., Szamosi, I. T., Synthesis and herbicidal activity of 1,H-1,4-benzodiazepine-2,5-diones, *J. Agric. Food. Chem.* **1997**, *45*, 493.

[22] Carlier, P. R., Zhao, H., DeGuzman, J., Lam, P. C.-H., Enantioselective synthesis of "quaternary" 1,4-benzodiazepin-2-one scaffolds via memory of chirality, *J. Am. Chem. Soc* **2003**, *125*, 11482.

[23] Avdagic, A., Lesac, A., Sunjic, V., First examples of the solvent effect on absolute conformation of chiral 3,3-disubstituted 1,4-benzodiazepin-2-ones, *Tetrahedron* **1999**, *55*, 1407.

[24] Avdagic, A., Lesac, A., Majer, Z., Hollosi, M., Sunjic, V., Lipase-catalyzed acetylation of 3-substituted 2,3-dihydro-1H-1,4-benzodiazepin-2-ones. Effect of

temperature and conformation on enantioselectivity and configuration., *Helv. Chim. Acta.* **1998**, *81*, 1567.

[25] Gilman, N., Rosen, P., Earley, J. V., Cook, C., Todaro, L. J., Atropisomers of 1,4-benzodiazepines. Synthesis and resolution of a diazepam-related 1,4-benzodiazepine, *J. Am. Chem. Soc* **1990**, *112*, 3969.

[26] Han, D., Forsterling, F. H., Li, X., Deschamps, J., Cao, H., Cook, J. M., Determination of the stable conformation of GABA(A)-benzodiazepine receptor bivalent ligands by low temperature NMR and X-ray analysis, *Bioorg. Med. Chem. Lett.* **2004**, *14*, 1465.

[27] Haung, Q., He, X., Ma, C., Liu, R. Y., Yu, S., Dayer, C. A., Wenger, G. R., McKerna, R., Cook, J. M., Pharmacophore/receptor models for GABA(A)/BzR subtyoes via comprehensive ligand mapping approach, *J. Med. Chem.* **2000**, *43*, 71.

[28] Li, X., Cao, H., Zhang, C., Furtmueller, R., Fuchs, K., Huck, S., Sieghart, W., Deschamps, J., Cook, J. M., Synthesis, in vitro affinity, and efficacy of a bis 8-ethyl-4H-imidazo[1,5a]-[1,4]benzodiazepine analogue, the first bivalent α5 subtype selective BzR/GABA(A) antagonist, *J. Med. Chem.* **2003**, *46*, 5567.

[29] Liu, R., Zhang, P., Gan, T., McKerna, R., Cook, J. M., Evidence for the conservation of conformational topography at five major GABA(A)/benzodiazepine receptor subsites. Potent affinities of the *S*-enantiomers of the frame-work constrained 4,5-pyrroloimidazobenzodiazepines, *Med. Chem. Res.* **1997**, *7*, 25.

[30] MacQuarrie-Hunter, S., Carlier, P. R., Highly enantioselective synthesis of rigid, quaternary 1,4-benzodiazepine-2,5-diones derived from proline, *Organic Lett.* **2005**, *7*, 5305.

[31] Yu, S., Ma, C., He, X., McKerna, R., Cook, J. M., Studies in the search for alpha 5 subtype selective agonists for GABA(A)/BzR sites, *Med. Chem. Res.* **1999**, *9*, 71.

[32] Li, X. Y., Yu, J. M., Atack, J. R., Cook, J. M., Development of selective ligands for the benzodiazepine receptor subtypes by manipulating the substiuents at positions 3 and 7 of optically active BzR ligands, *Med. Chem. Res.* **2004**, *13*, 259.

[33] Carlier, P. R., Zhao, H., Hsu, D. C., Memory of chirality: An emerging strategy for asymmetric synthesis, *Synthesis* **2005**, 1.

[34] Lam, P. C.-H., Carlier, P. R., Experimental and computational studies of ring inversion if 1,4-benzodiazepin-2-ones: Implications for memory of chirality transformations, *J. Org. Chem.* **2005**, *70*, 1530.

[35] Fuji, K., Kawabata, T., Memory of chirality - a new principle in enolate chemistry, *Chem. Eur. J.* **1998**, *4*, 373.

[36] Kawabata, T., Yahiro, K., Fuji, K., Memory of chirality: Enantioselective alkylation reactions at an asymmetric carbon adjacent to a carbonyl group, *J. Am. Chem. Soc* **1991**, *113*, 9694.

[37] Eyring, H., The activated complex and the absolute rate of chemical reactions, *Chem. Rev.* **1935**, *17*, 65.

[38] Lam, P. C.-H., Ph.D. thesis, Virginia Polytechnic Institute and State University, Blacksburg VA, 2004.

[39] Carlier, P. R., Lam, P. C.-H., DeGuzman, J., Zhao, H., Memory of chirality trapping of low inversion barrier 1,4-benzodiazepin-2-one enolates, *Tetrahedron: Asymmetry* **2005**, *16*, 2998.

[40] Eliel, E. L., Wilen, S. H., Mander, L. N. In *John Wiley & Sons*; J. W. Sons, Ed.; John Wiley & Sons: New York, 1994, pp 1142.

[41] Kawabata, T., Wirth, T., Yahiro, K., Suzuki, H., Fuji, K., Direct asymmetric α-alkylation of phenylalanine dervatives using no external chiral sources, *J. Am. Chem. Soc* **1994**, *116*, 10809.

[42] Kawabata, T., Nagae, Y., Suzuki, H., Fuji, K., Chiral nonracemic enolate with dynamic axial chirality: Direct asymmetric α-amino acid derivatives, *Angew. Chem. Int. Ed.* **2000**, *39*, 2155.

[43] Kawabata, T., Chen, J., Suzuki, H., Nagae, Y., Kinoshita, T., Chancharunee, S., Fuji, K., Memory of chirality in diastereoselective α-alkylations of isoleucine and allo-isoleucine derivatives, *Organic Letters* **2000**, *2*, 3883.

[44] Kawabata, T., Kawakami, S.-P., Fuji, K., Enantioselective α-allylation of a phenylalanine derivative under the control of aggregation of a chiral nonracemic enolate, *Tetrahedron Letters* **2002**, *43*, 1465.

[45] Dalgard, J. E., Rychnovsky, S. D., Memory of chirality on the transannular cyclization of cyclodecenyl radicals, *Organic Letters* **2004**, *6*, 2713.

[46] Matsumura, Y., Shirakawa, Y., Satoh, Y., Umino, M., Tanaka, T., Maki, T., Onomura, O., First example of memory of chirality in carbenium ion chemistry, *Organic Letters* **2000**, *2*, 1689.

[47] Griesbeck, A. G., Kramer, W., Lex, J., Diastereo-and enantioselective synthesis of pyrrolo[1,4]benzodiazepines through decarboxylative photocyclization, *Angew. Chem. Int. Ed.* **2001**, *40*, 577.

Chapter 5. Enantioselective Synthesis of Rigid, Quaternary 1,4-Benzodiazepin-2,5-diones.

5.1 Introduction

In chapter 4 we described the medicinal importance of 1,4-benzodiazepin-2,5-diones (Figure 4.1). In particular proline-derived 1,4-benzodiazepin-2,5-diones are extremely useful scaffolds in medicinal chemistry (Figure 4.2). We also noted that very few quaternary 1,4-benzodiazepin-2,5-diones have been described in the literature, and to our knowledge no enantiopure quaternary examples were prepared prior to our work. The Carlier group recently demonstrated the enantioselective preparation of α-alkylated *N*-*i*-Pr-1,4-benzodiazepin-2-ones using a memory of chirality strategy.[1] To determine whether a similar memory of chirality method could be developed for the synthesis of quaternary 1,4-benzodiazepin-2,5-diones, we first explored deprotonation/trapping sequences of proline derivatives (*S*)-**1a-c** (Scheme 5.1) We proposed that upon deprotonation, **1** would proceed through a dynamically chiral enolate intermediate that would "memorize" the original chirality of the ring. Addition of an electrophile would lead to highly enantiopure quaternary products (**2-6**). Retention was envisioned based on our studies of Ala- and Phe-derived 1,4-benzodiazepin-2-ones.[1]

Scheme 5.1 Enantioselective alkylation of proline-derived 1,4-benzodiazepin-2,5-diones utilizing a "memory of chirality" synthesis.

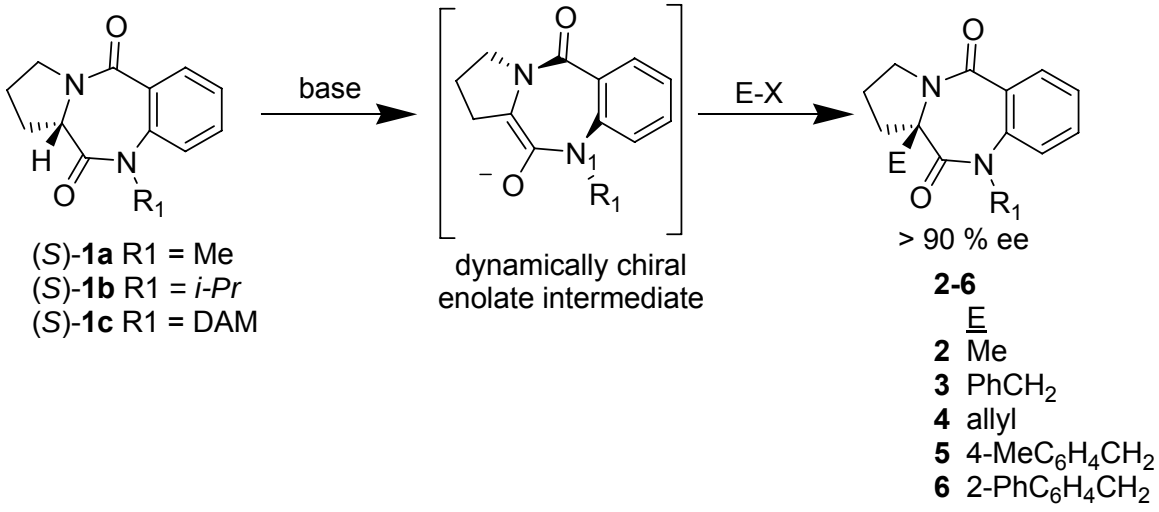

5.2 Synthesis of Quaternary Proline-Derived N-i-Pr 1,4-Benzodiazepin-2,5-diones

We have recently published the successful enantioselective synthesis of quaternary proline-derived *N*-*i*-Pr 1,4-benzodiazepin-2,5-diones.[2] What follows below is an account of how we realized this achievement. Compounds (*S*)-(+)-**8** and (*S*)-(+)-**1a** were prepared following the literature procedure[2] in 75 and 79% yield, respectively (Scheme 5.2). Optical rotation was used to confirm the optical purity of (*S*)-(+)-**8**. Optical rotation and chiral stationary-phase HPLC confirmed the enantiopurity of (*S*)-(+)-**1a**.

Scheme 5.2 Synthesis of *N*-H 1,4-benzodiazepin-2,5-diones

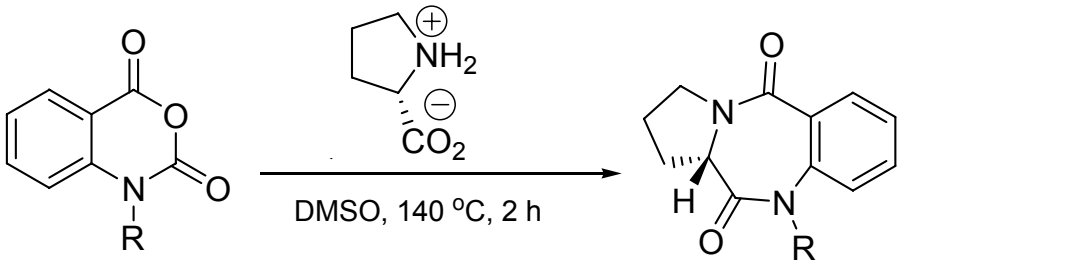

7a R = H
7b R = Me

(*S*)-(+)-**8** R = H 75% (100% ee)
(*S*)-(+)-**1a** R = Me 79% (100% ee)

With (*S*)-(+)-**1a** in hand (Scheme 5.2) we implemented the α-alkylation protocol optimized for the 1,4-benzodiazepin-2-ones,[1] the results are summarized in Table 5.1.

Table 5.1 α-Alkylation of *N*-Me 1,4-benzodiazepin-2,5-dione

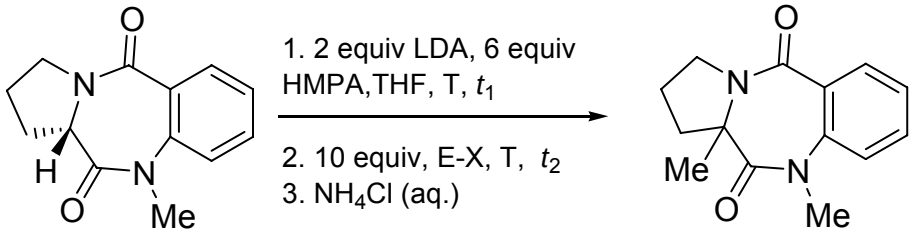

(*S*)-(+)-**1a**

2a

Entry	E-X	Product	T (°C)	t_1 (min)	t_2 (min)	% yield	% ee
1	Me-I	**2a**	-78	10	10	69	0
2	Me-OTf	**2a**	-78	10	10	75	0
3	Me-OTf	**2a**	-78	1	10	21	0
4	Me-OTf	**2a**	-100	1	5	13	0

After a 10 min deprotonation time at -78 °C, addition of methyl iodide afforded the racemic α-methylated product **2a** in 69% (entry 1, Table 5.1). This initial result suggested that the enolate derived from the *N*1-Me derivative has a low inversion barrier

and is racemizing under these conditions. In the case of 1,4-benzodiazepin-2-ones, Lam showed that by employing a more reactive electrophile or by lowering the temperature of the reaction, it is possible to deprotonate and trap low inversion barrier enolates to yield highly enantiopure quaternary products.[3, 4] We tried using MeOTf as a more reactive electrophile (entry 2, Table 5.1) and saw a slight improvement in the yield, however we still obtained racemic product. We attempted a shortened deprotonation time (entry 3, Table 5.1) and a lower temperature reaction (entry 4, Table 5.1) and in both cases we saw no improvement in the % ee. We concluded that the *N*-Me substituent was not large enough to provide a high inversion barrier for the enolate formed upon deprotonation of **1a**.

Previous investigations showed that the inversion barrier of the 1,4-benzodiazepin-2-ones (and the corresponding enolate) is a function of the size of the *N*1 substituent. [1, 4] The *N*-Me group was not large enough to provide conformational stability at –78 ^{o}C for the enolate of the 1,4 benzodiazepin-2-ones and alkylation results in complete racemization. The next logical step was to install a larger substituent such as *i*-Pr at *N*1.

Conversion of (*S*)-(+)-**8** to the *N*-*i*-Pr 1,4-benzodiazepin-2,5-dione (*S*)-(+)-**1b** was achieved by treatment of the sodium salt with isopropyl triflate (Scheme 5.3).[5] Using a very reactive electrophile such as isopropyl triflate (**9**) helped us achieve non-racemizing alkylation at *N*1. Isopropyl triflate was prepared immediately before use from isopropanol and triflic anhydride (Scheme 5.3). Chiral stationary phase HPLC was used to confirm the enantiopurity of (*S*)-(+)-**1b**.

Scheme 5.3 Synthesis of *N*-*i*-Pr 1,4-benzodiazepin-2,5-dione (*S*)-(+)-**1b**

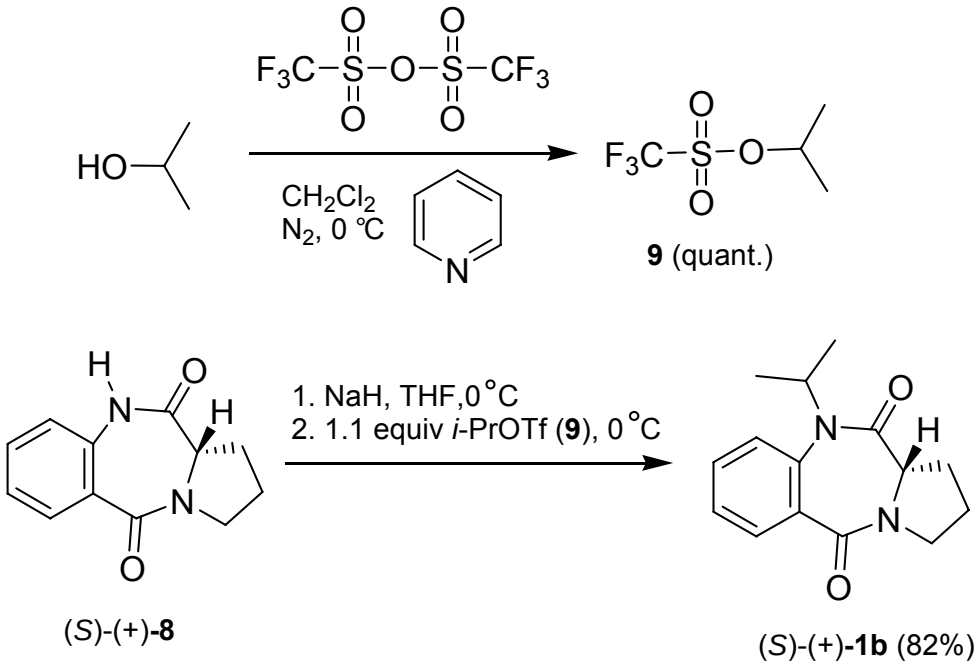

Treatment of (*S*)-(+)-**1b** with LDA in THF at -78 °C for 5 min, followed by subsequent addition of MeI as the electrophile afforded the desired product **2b,** in a low 22% yield, and 0% ee (Table 5.2, entry 1). This disappointing result suggested that with the five minute deprotonation protocol the enolate racemizes. By decreasing the deprotonation time to one minute we were able to obtain the **2b** in 93% ee, but in only 10% yield (Table 5.2, entry 2). To attain both high asymmetric induction and reasonable chemical yields we lowered the reaction temperature to –100 ^{o}C and substituted MeOTf as the electrophile. Use of a 1 minute deprotonation time and a 10 minute reaction time provided **2b** in >99.5% ee and 69% yield (Table 5.2, entry 3). Increasing the reaction time to 15 minutes improved the yield slightly, but caused a slight deterioration of the asymmetric induction (95% ee at t_2 = 15 min). These results indicate the formation of a dynamically chiral enolate intermediate that racemizes rapidly at -78 °C and more slowly

at -100 °C. Table 5.2 shows the variety of electrophiles that were used in the α-alkylation with varying deprotonation and reaction times. Extending the protocol to benzyl and allyl bromide gave the desired products **3b** and **4b** in 78 and 83% ee, respectively (Table 5.2, entries 5 and 7). The lower % ee attained with benzyl and allyl bromide relative to methylation again suggested enolate racemization on the alkylation time scale. We reasoned that an improvement in alkylation rate would reduce racemization, so we repeated the alkylations using benzyl and allyl iodide. Under these conditions the products **3b** and **4b** were obtained in 93 and 99.5% ee (Table 5.2, entries 6 and 8). We also extended the protocol to substituted benzyl iodides, which reacted in excellent % ee and satisfactory yields to afford products **5b** and **6b**. (Table 5.2, entries 9 and 10)

Table 5.2 Sequential deprotonation/alkylation results for compounds (+)-**2b-6b**.

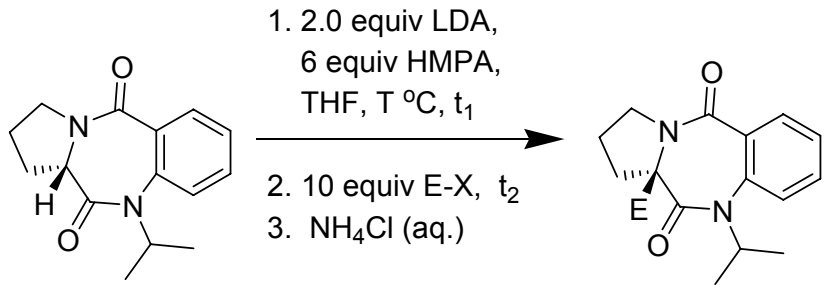

(*S*)-(+)-**1b** (+)-**2b-6b**

Entry	Electrophiles (E-X)	Product	Temp(°C) [a]	t_1(min)	t_2(min)	% yield	%ee[b]
1	Me-I	**2b**	-78	5	10	22	0
2	Me-I	(+)-**2b**	-78	1	10	10	93 *S*
3	Me-OTf	(+)-**2b**	-100	1	10	69	>99.5 *S*
4	Me-OTf	(+)-**2b**	-100	1	15	76	95 *S*
5	$PhCH_2Br$	(+)-**3b**	-100	1	10	64	78 *R*
6	$PhCH_2I$	(+)-**3b**	-100	1	5	77	93 *R*
7	Allyl-Br	(+)-**4b**	-100	1	10	77	83
8	Allyl-I [c]	(+)-**4b**	-100	1	15	89	99.5
9	4-$MeC_6H_4CH_2I$	(+)-**5b**	-100	1	1	63	95 *R* [d]
10	2-$PhC_6H_4CH_2I$	(+)-**6b**	-100	1	5	63	95 *R* [d]

[a] -100 °C obtained using a dry ice and ether bath. [b] % ee measured by chiral stationary phase HPLC (Chiralcel OD,AD). Unless otherwise indicated, absolute stereochemistry was determined by chemical correlation (vide infra). Nearly all results were replicated and %ee varied no more than 1.5 %. [c] reaction performed without added HMPA (section 5.3.1). [d] (*R*)-stereochemistry is assigned to (+)-**5b** and (+)-**6b** on the identical sign and HPLC elution order with the simple benzyl analogue (*R*)-(+)-**3b**.

Use of this sequential deprotonation/alkylation protocol provided *N*-*i*-Pr analogues **2b**-**6b** in high enantioselectivity and moderate yields. We reasoned that the moderate alkylation yields were due to incomplete enolate formation during the 1 minute deprotonation time. Since increasing the deprotonation time would allow enolate racemization to occur, we sought conditions under which the enolate could be immediately trapped as it is formed. Since an in situ strategy was successfully applied to the synthesis of quaternary Ala-derived *N*-PMB 1,4-benzodiazepin-2-ones,[3, 4] we anticipated a straightforward in situ protocol would allow us to prepare the α-alkylated products in both high yields and high enantioselectivity (Table 5.3). Replacement of LDA with KHMDS is necessary in this protocol to prevent the base (present in excess) from reacting with the electrophile before the enolate is formed. Also, less reactive electrophiles such as bromides (rather than iodides) must be used in situ in order to prevent direct reaction of the base with the electrophile before enolate formation, as evidenced by entry 1, Table 5.3. Use of the sequential deprotonation/alkylation protocol (Table 5.2) afforded the benzylated product in **3b** in 93% ee and 77% yield. With a 5 minute in situ reaction time, however, we obtained the benzylated product **3b** in an improved >99.5% ee and a comparable 78% yield (Table 5.3, entry 2). By increasing the in situ reaction time from 5 minutes to 15 minutes **3b** was afforded in an excellent 92% yield with only a slight decrease in enantioselectivity to 96% (Table 5.3, entry 4). Comparison of entry 6 in Table 5.3 with entry 9 in Table 5.2 shows that the in situ method affords the alkylated products **5b** in slightly higher % ee (99% ee versus 95% ee) and significantly higher yields (92% yield versus 63% yield). The 2-phenylbenzylated analogue **6b** was obtained in 95% ee and 63% yield using the sequential method (entry 10, Table 5.2). Implementing the in situ method to obtain **6b** generated the desired

product in 95% ee and a more desirable 82% yield (entry 7, Table 5.3). Application of the in situ protocol for reaction with allyl bromide gave significantly improved enantioselectivity (Table 5.2 entry 7 versus Table 5.3 entry 4). However we achieved 99.5% ee and an improved 89% yield using the sequential method when allyl iodide was used as the electrophile (entry 8, Table 5.2). In addition, the use of very reactive electrophiles such as MeOTf gave very poor yields (Table 5.3, entry 1) suggesting competitive reaction of KHMDS with MeOTf. Based on these experiments we conclude that for methylation and allylation, the sequential method is preferable for obtaining good yields of highly enantiopure products. In all other cases, the in situ protocol gives superior yields and enantioselectivity.

Table 5.3 In situ deprotonation/alkylation results for compounds (+)-**2b**-**6b**.

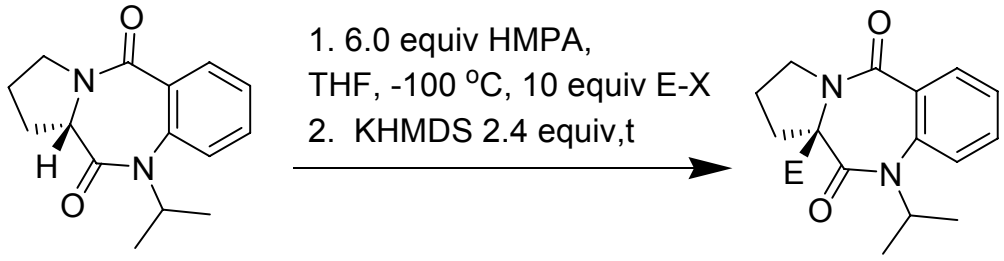

(*S*)-(+)-**1b** (+)-**2b-6b**

Entry	Electrophile (E-X)	Product	t (min)	% yield	% ee [a]
1	Me-OTf	(+)-**2b**	5	24	>99.5 *S*[b]
2	Bn-Br	(+)-**3b**	5	78	>99.5 *R*[b]
3	Bn-Br	(+)-**3b**	10	85	96.3 *R*[b]
4	Bn-Br	(+)-**3b**	15	92	96 *R*[b]
5	Allyl-Br	(+)-**4b**	10	75	98
6	4-Me$C_6H_4CH_2$Br	(+)-**5b**	5	92	99 *R*[c]
7	2-Ph$C_6H_4CH_2$Br	(+)-**6b**	10	82	95 *R*[c]

[a] % ee measured by chiral stationary phase HPLC (Chiralcel OD,AD). Nearly all results were replicated and %ee varied no more than 1.5 %. [b] proven to be (*R*)-stereochemistry by conversion to the known quaternary amino acid [c] (*R*)-stereochemistry is assigned to (+)-**5b** and (+)-**6b** on the identical sign and HPLC elution order with the simple benzyl analogue (*R*)-(+)-**3b**.

As was the case for Ala and Phe-derived 1,4-benzodiazepin-2-ones,[1] the stereochemical outcome for the deprotonation/alkylation of **1b** appears uniformly retentive. Hydrolysis of **2b** and **3b** to the known quaternary amino acids, (*S*)-(-)-α-Me-Pro-OH **10** and (*R*)-(-)-α-Bn-Pro-OH **11** demonstrated retentive alkylation of the enolate (Scheme 5.4). We propose retentive (*R*)-stereochemistry for (+)-**5b** and (+)-**6b** based the

positive rotation of (*R*)-**3b**, and based on the chiral stationary-phase elution order of the major enantiomers.

Scheme 5.4 Hydrolysis to the quaternary amino acid.[6, 7]

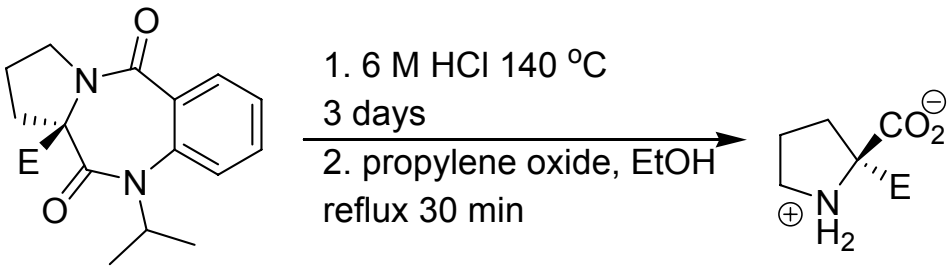

(+)-**2b-3b**

	E	%Yield	$[\alpha]_D$	$[\alpha]_D$(lit)
10	Me	78	-76.2	-83.1
11	$PhCH_2$	85	-18.5	-19.25

Thus our initial goal of achieving MOC deprotonation/alkylation of proline-derived 1,4-benzodiazepin-2,5-diones was realized. However the requirement for a bulky substituent such as *i*-Pr at the N position limits the diversity of the quaternary 1,4-benzodiazepin-2,5-diones that could be prepared. Dr. Hongwu Zhao, a former postdoc in our group, demonstrated that the dianisylmethyl (DAM)[8] group is large enough to prevent racemization during alkylation of the 1,4-benzodiazepine 2-ones and is easily removed afterwards. We thus sought to apply this group to the 1,4-benzodiazepin-2,5-diones.

5.3 Synthesis of Quaternary Proline-Derived N-DAM 1,4-Benzodiazepin-2,5-diones

Dianisylmethyl bromide **11** (DAM-Br) was prepared immediately before use from commercially available 4,4 dimethoxy benzhydrol (Scheme 5.5).[8] Deprotonation of (*S*)-(+)-**8** by NaH, followed by addition of DAM-Br generated (*S*)-(+)-**1c** in 93% yield and 100% ee, as indicated by chiral stationary phase HPLC (Scheme 5.5).

Scheme 5.5 Synthesis of DAM-Br and proline-derived *N*-DAM-1,4-benzodiazepin-2,5-dione (*S*)-(+)-**1c**

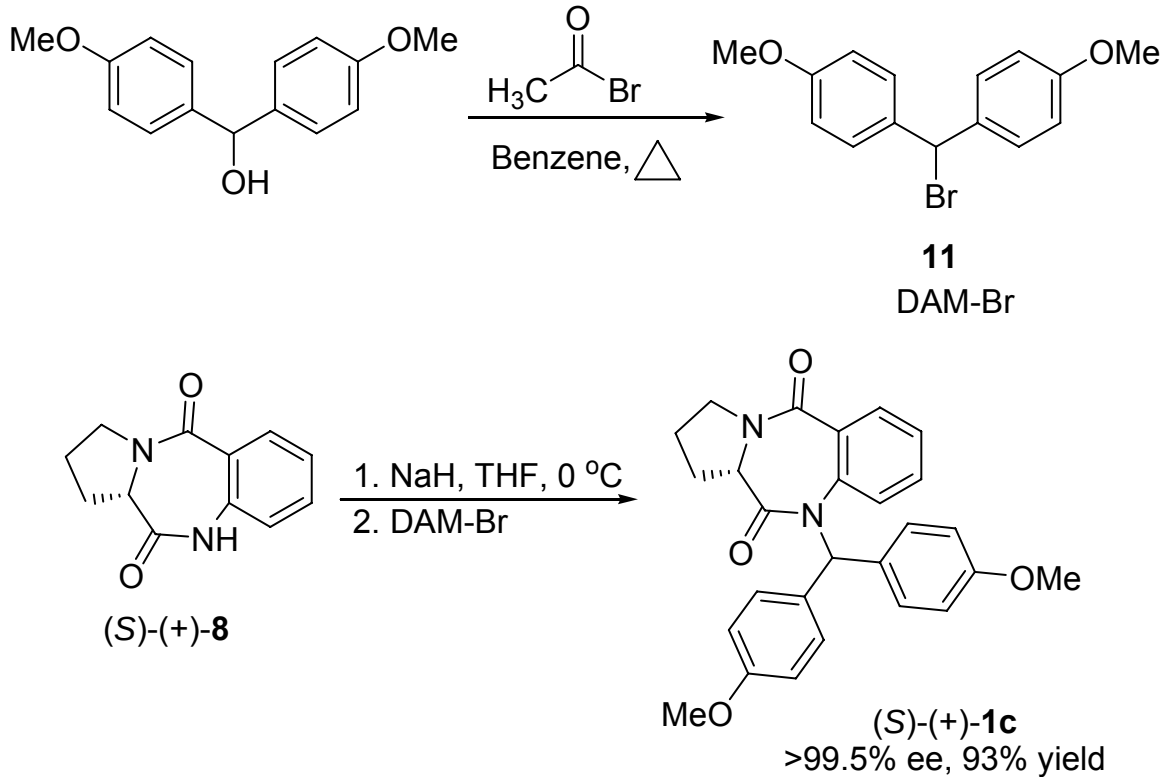

In situ deprotonation/alkylation of the *N*-DAM proline derived 1,4-benzodiazepin-2,5-dione (*S*)-(+)-**1c** afforded α-alkylated products in acceptable yields and high enantioselectivity (Table 5.4). We found the *N*-DAM derived starting material

1c superior to the *N*-*i*-Pr starting material **1b** for a variety of reasons. By increasing the reaction time from 1 minute to 30 minutes (Table 5.4, entries 1-4) we increased the yield of the benzylated *N*-DAM 1,4-benzodiazepin-2,5-dione **3c** without seeing a decrease in the % ee. Increasing the reaction time from 5 minutes to 10 minutes in the *N*-*i*-Pr case lead to an increase in the yield of the benzylated product at the cost of % ee (Table 5.3, entries 2-3). These results suggest that the enolates derived from the *N*-DAM analogues racemize at a slower rate than the enolates derived from the *N*-*i*-Pr analogues. Reaction with allyl bromide produces **4c** in 93% ee and in 65% yield (Table 5.4, entry 5). Substituted benzyl iodides react in reasonable yields and high enantiomeric excess with (*S*)-(+)-**1c** (Table 5.4, entries 6 and 7). Given the apparent slower racemization of the enolate derived from **1c,** we thought it might be possible to conduct deprotonation/alkylation reactions on **1c** at a slightly higher temperature. However deprotonation/benzylation of **1c** at -78 °C gave racemic product (Table 5.4, entry 8).

Table 5.4 Enantioselective in situ deprotonation/alkylation of *N*-DAM-1,4-benzodiazepin-2,5-dione (*S*)-(+)-**1c**

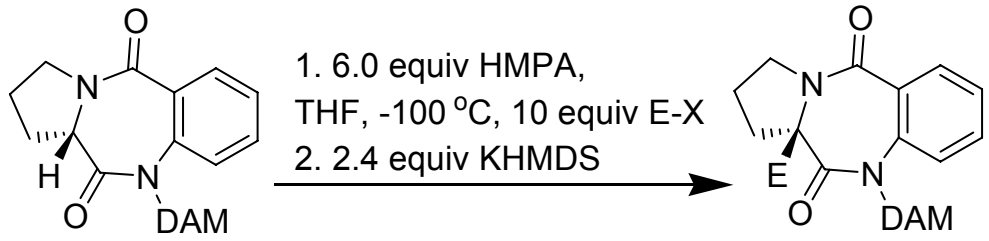

(*S*)-(+)-**1c** (+)-**3c-6c**

Entry	Electrophile	Product	t (min)	% yield	% ee[a]
1	Bn-Br	(+)-**3c**	1	66	96 *R* [b]
2	Bn-Br	(+)-**3c**	5	81	95 *R* [b]
3	Bn-Br	(+)-**3c**	15	93	97 *R* [b]
4	Bn-Br	(+)-**3c**	30	98	98 *R* [b]
5	Allyl-Br	(+)-**4c**	10	65	93
6	4-$MeC_6H_4CH_2Br$	(+)-**5c**	15	93	>99.5 *R* [c]
7	2-$PhC_6H_4CH_2Br$	(+)-**6c**	15	94	99 *R* [c]
8[d]	Bn-Br	**3c**	15	90	0

[a] % ee measured by chiral stationary phase HPLC (Chiralcel OD,AD). Nearly all results were replicated and %ee varied no more than 1.5 %. [b] proven to be (*R*)-stereochemistry by conversion to the known quaternary amino acid [c] (*R*)-stereochemistry is assigned to (+)-**5c** and (+)-**6c** on the identical sign and HPLC elution order with the simple benzyl analogue (*R*)-(+)-**3c**. [d] reaction temperature -78 °C

Treatment of **3c** and **4c** with 25% trifluroacetic acid provided the *N*-H derivatives **12** and **13** in 100% and 97% yield, respectively (Scheme 5.6).

Scheme 5.6 Removal of DAM group from **3c** and **4c**.

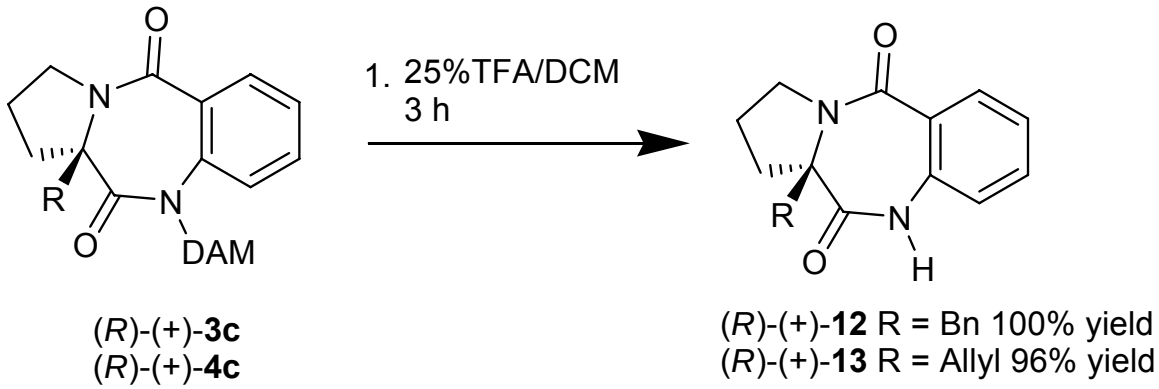

Retentive benzylation was established by hydrolysis of the *N*-H product **12** to the known quaternary amino acid **11** in 100% yield.[7] Previous attempts in our group to hydrolyze C3-allylated 1,4-benzodiazepin-2-ones have been unsuccessful, therefore we did not attempt hydrolysis of **13.**

Scheme 5.7 Hydrolysis of *N*-H C3 benzylated 1,4-benzodiazepin-2,5-dione **12** to (*R*)-(-)-α-Bn-Pro-OH **11**

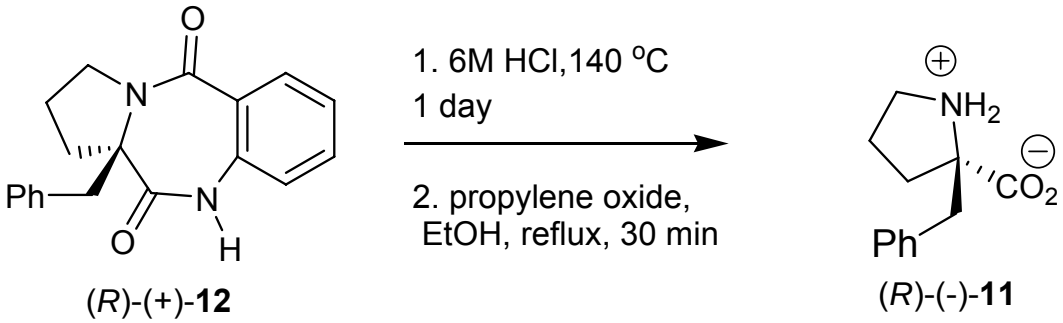

Since alkylation of the *N*-H product could be performed with virtually any electrophile we have demonstrated that the removable bulky DAM substituent facilitates

the preparation of a diverse number of proline-derived quaternary 1,4-benzodiazepin-2,5-diones.

5.3.1 Is HMPA Necessary?

For the 1,4-benzodiazepin-2-ones the inclusion of HMPA (hexamethylphosphoramide) in the deprotonation/alkylation reactions proved to be necessary in order to obtain acceptable yields of α-alkylated products.[1] HMPA is a known animal carcinogen and an anticipated human carcinogen. It is thought to cause birth defects and male infertility, and it is also a potent skin, eye and respiratory irritant. Given the toxicity of HMPA it would be preferable if we could eliminate it from the synthetic protocol. We therefore attempted in situ deprotonation/alkylation of *N*-DAM 1,4-benzodiazepin-2,5-dione **1c** in the absence of HMPA (Table 5.5).

Table 5.5 Enantioselective in situ deprotonation/alkylation of (*S*)-(+)-**1b** and (*S*)-(+)-**1c** without HMPA.

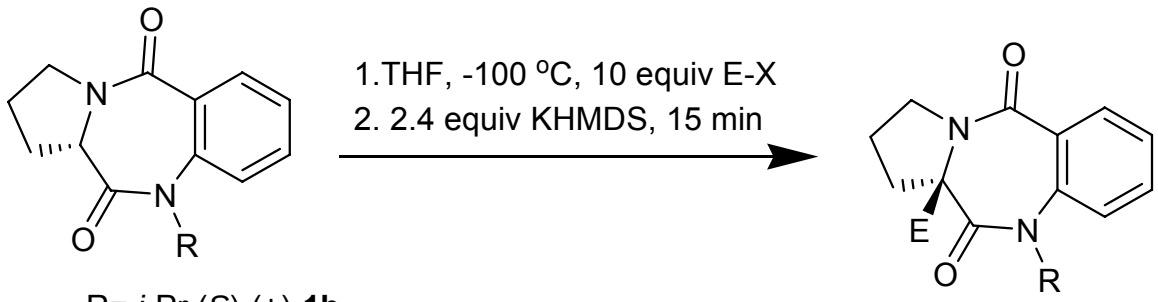

R= *i*-Pr (*S*)-(+)-**1b**
R= DAM (*S*)-(+)-**1c**

(*R*)-(+)-**3b,**
(+)-**3c-6c**

Entry	Electrophile	Product	% yield	% ee[a]
1	Bn-Br	(+)-**3b**	81	90 *R* [b]
2	Bn-Br	(+)-**3c**	83	99 *R* [b]
3	Allyl-Br	(+)-**4c**	90	92
4	4-$MeC_6H_4CH_2Br$	(+)-**5c**	81	99 *R* [c]
5	2-$PhC_6H_4CH_2Br$	(+)-**6c**	87	94 *R* [c]

[a] % ee measured by chiral stationary phase HPLC (Chiralcel OD,AD). Nearly all results were replicated and %ee varied no more than 1.5 %. [b] proven to be (*R*)-stereochemistry by conversion to the known quaternary amino acid [c] (*R*)-stereochemistry is assigned to (+)-**5c** and (+)-**6c** on the identical sign and HPLC elution order with the simple benzyl analogue (*R*)-(+)-**3c**.

In the absence of HMPA we were able to obtain the α-benzylated *N*-*i*-Pr 1,4-benzodiazepin-2,5-dione in 81% yield and 90% ee (Table 5.5, entry 1). We also benzylated the *N*-DAM 1,4-benzodiazepin-2,5-dione **1c** in an excellent 99% ee and a reasonable 83% yield. We attempted the alklyation reactions without HMPA with a variety of other electrophiles and achieved high enantioselectivity and moderate yields for every case (Table 5.5, entries 3-5). These experiments clearly indicate that HMPA is

not necessary for the enantioselective synthesis of quaternary 1,4-benzodiazepin-2,5-diones.

5.4 Synthesis of Quaternary Hydroxy Proline-Derived N-DAM-1,4-Benzodiazepin-2,5-diones

We propose that the highly enantioselective deprotonation/alkylation of *N*-*i*-Pr and *N*-DAM 1,4-benzodiazepin-2,5-diones is due to a memory of chirality mechanism. In order to provide additional evidence for our proposed mechanism we prepared a set of diastereomeric substrates (3*R*,13*S*)-**20** and (3*S*,13*S*)-**23**, that possess an additional chiral center.

Hydroxy proline-derived *N*-H-1,4-benzodiazepin-2,5-diones (3*R*,13*S*)-**16** and (3*S*,13*S*)-**17** were synthesized from commercially available trans-4-hydroxy-L-proline (**14**) and cis-4-hydroxy-D-proline (**15**), respectively according to the literature method (Scheme 5.8).[9] As shown in Scheme 5.8 these diastereomers differ in chirality at C3 but contain the same *S* chirality at the C13 within the proline ring.

Scheme 5.8 Synthesis of derived *N*-H-1,4-benzodiazepin-2,5-diones (3*R*,13*S*)-**16** and (3*S*,13*S*)-**17**

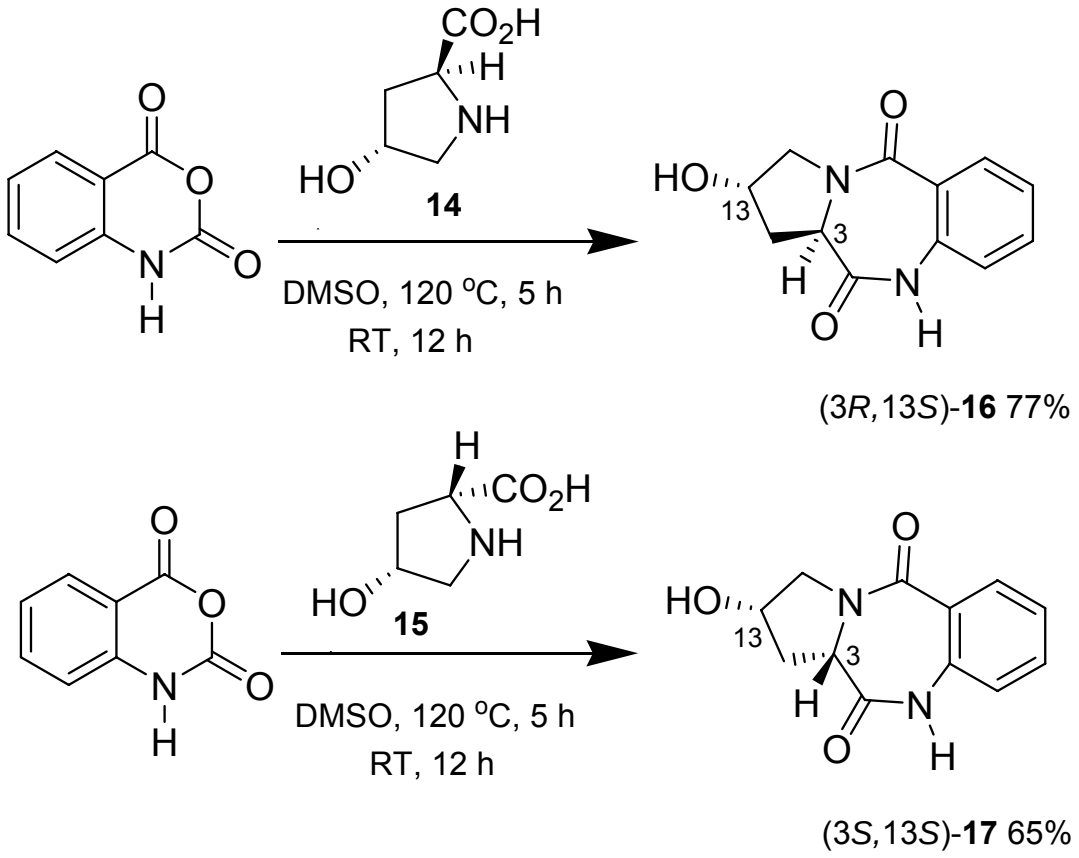

Before we could alkylate at N1 we needed to protect the hydroxy group to prevent competitive O-alkylation. After protecting (3*R*,13*S*)-**16** and (3*S*,13*S*)-**17** with *tert*-butyldimethylsilyl chloride (TBDMSCl) the products (3*R*,13*S*)-**18** and (3*S*,13*S*)-**19** were obtained as outlined in Scheme 5.9.

Scheme 5.9 TBDMS hydroxy group protection of (3*R*,13*S*)-**16** and (3*S*,13*S*)-**17**

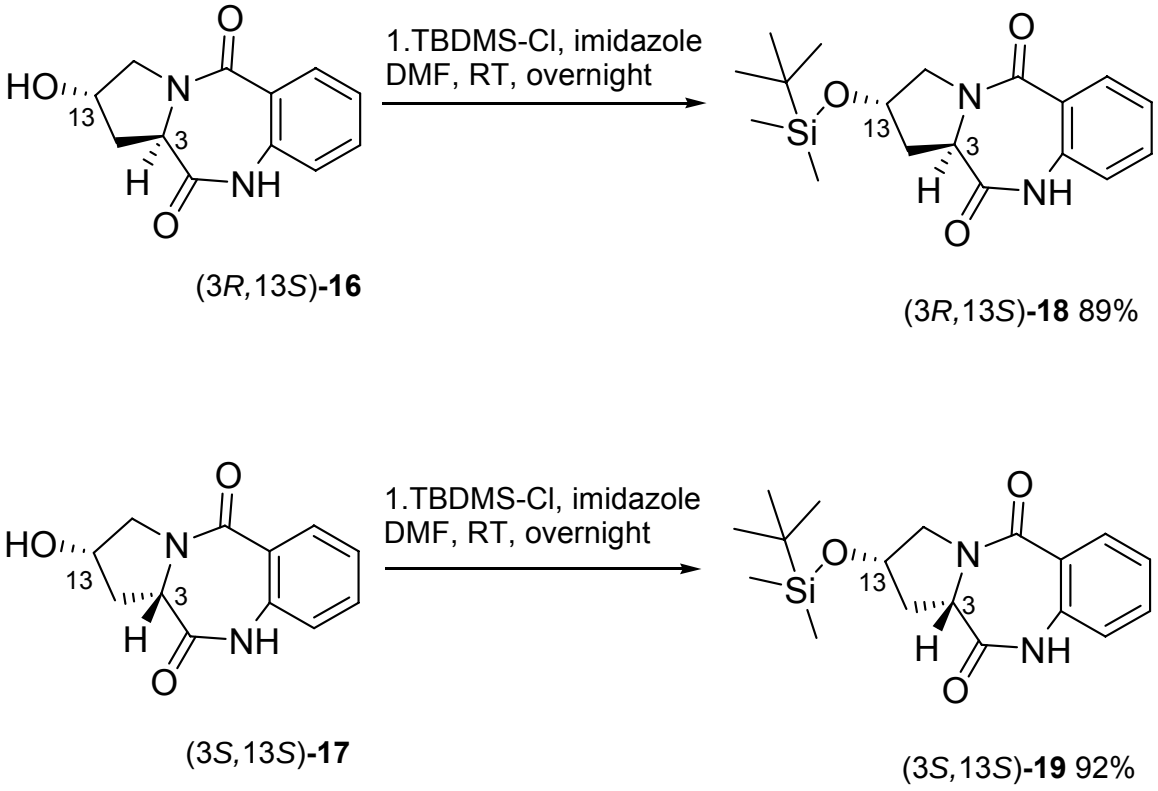

(3*R*,13*S*)-**16**

(3*R*,13*S*)-**18** 89%

(3*S*,13*S*)-**17**

(3*S*,13*S*)-**19** 92%

Incorporation of the DAM group at N1 was achieved using the same reaction conditions outlined for proline-derived 1,4-benzodiazepin-2,5-dione **8** (Scheme 5.5). The *N*-DAM products (3*R*,13*S*)-**20** and (3*S*,13*S*)-**23** were obtained in 82 and 89% yield, respectively (Scheme 5.10). (3*R*,13*S*)-**20** and (3*S*,13*S*)-**23** were formed in >98% de as measured by proton NMR.

Scheme 5.10 N-Alkylation of (3*R*,13*S*)-**18** and (3*S*,13*S*)-**19** with DAM-Br

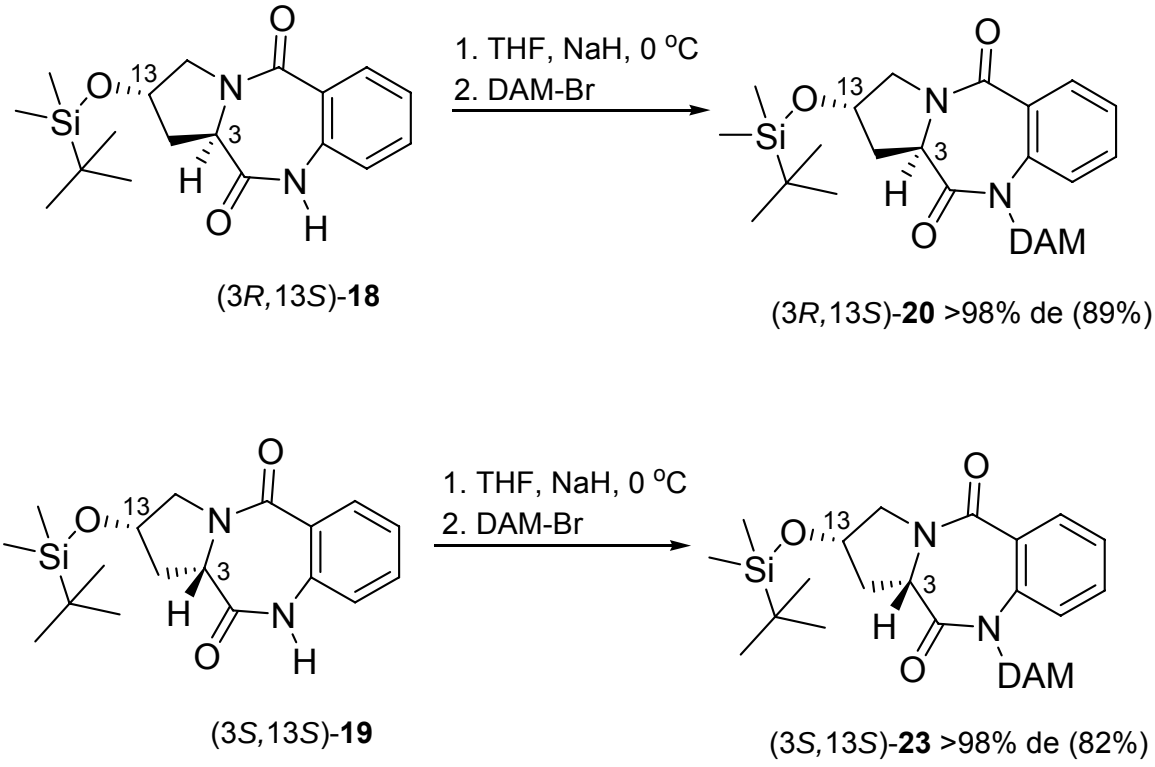

(3*R*,13*S*)-**18**

(3*R*,13*S*)-**20** >98% de (89%)

(3*S*,13*S*)-**19**

(3*S*,13*S*)-**23** >98% de (82%)

In the absence of memory of chirality (*R*,*S*)-**20** and (*S*,*S*)-**23**, would generate the same enolate upon deprotonation (Scheme 5.11). Under such circumstances reaction of the enolate with benzyl bromide would produce the same ratio of diastereomers **22** and **25**, regardless of which starting material (**20** or **23**) was deprotonated.

Scheme 5.11 Expected outcome in the absence of dynamically chiral enolate

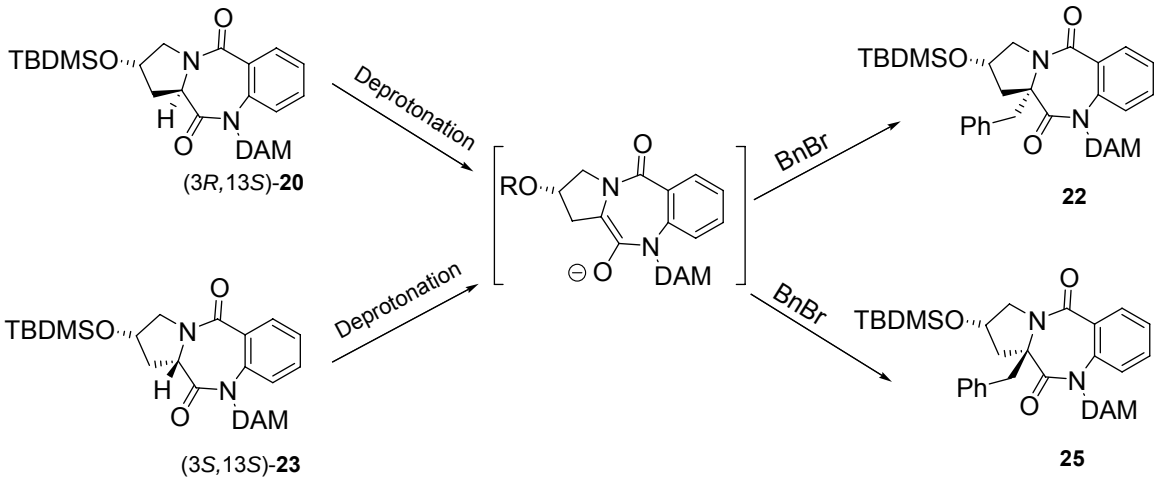

If, however memory of chirality is operative in these transformations, then deprotonation of **20** and **23** will give diastereomeric enolates **21** and **24**, respectively (Scheme 5.12). Assuming non-racemizing retentive addition of the electrophile we would obtain diastereomer **22** from (3*R*,13*S*)-**20**, and **25** from (3*S*,13*S*)-**23.**

Scheme 5.12 Expected outcome with dynamically chiral enolate formation

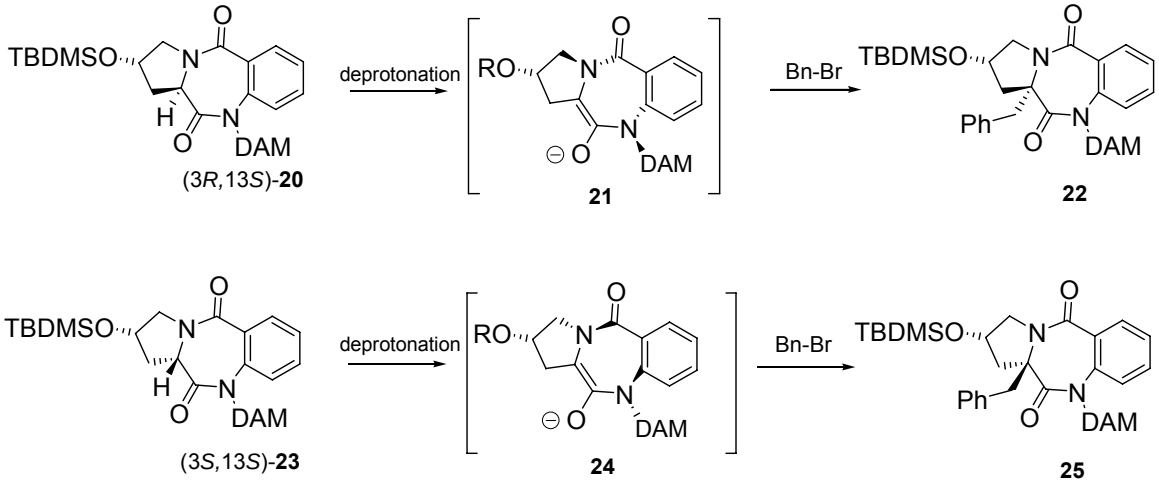

We implemented the in situ deprotonation/alkylation protocol that led to highly enantiopure quaternary 1,4-benzodiazepin-2,5-diones, described in Table 5.3 (Scheme 5.13). Deprotonation and alkylation (benzyl bromide) of (3*R*,13*S*)-**20** gave the retentive benzylated product **22** in 49% yield with a diastereomeric ratio (dr) (**22**:**25**) equal to 92:8. The diastereomeric ratio was determined using both proton NMR and chiral stationary phase HPLC. Upon deprotonation and alkylation of (3*S*,13*S*)-**23** the retentive product, diastereomer **25** was formed in 95% yield with a dr (**22**:**25**) equal to 4:96 (Scheme 5.13). Thus these results provide additional evidence for a MOC mechanism.

Scheme 5.13 Enantioselective in situ deprotonation/alkylation of hydroxyproline derived 1,4-benzodiazepin-2,5-diones at -100 °C

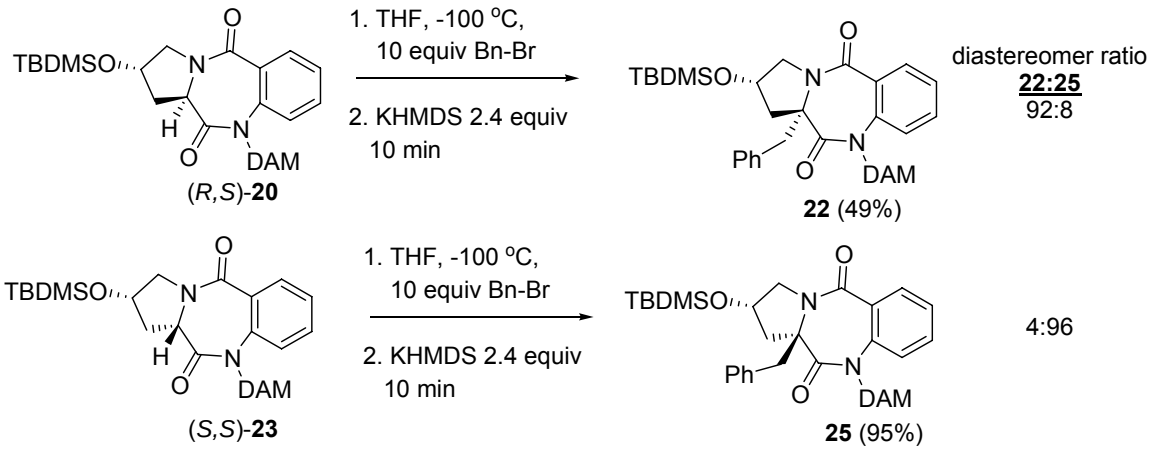

The lower diastereomeric ratios obtained from (3*R*,13*S*)-**20** and (3*S*,13*S*)-**23** (92:8, 4:96) compared to the 99.5:0.5 enantiomeric ratios obtained with (*S*)-**1c** suggests the enolates derived from the hydroxyproline-derived 1,4-benzodiazepin-2,5-diones have a slightly lower inversion barrier. Epimerization of the enolates will result in decreased % de as shown in Scheme 5.13.

Scheme 5.14 Possible interconversion between diastereomeric enolates **21** and **24**

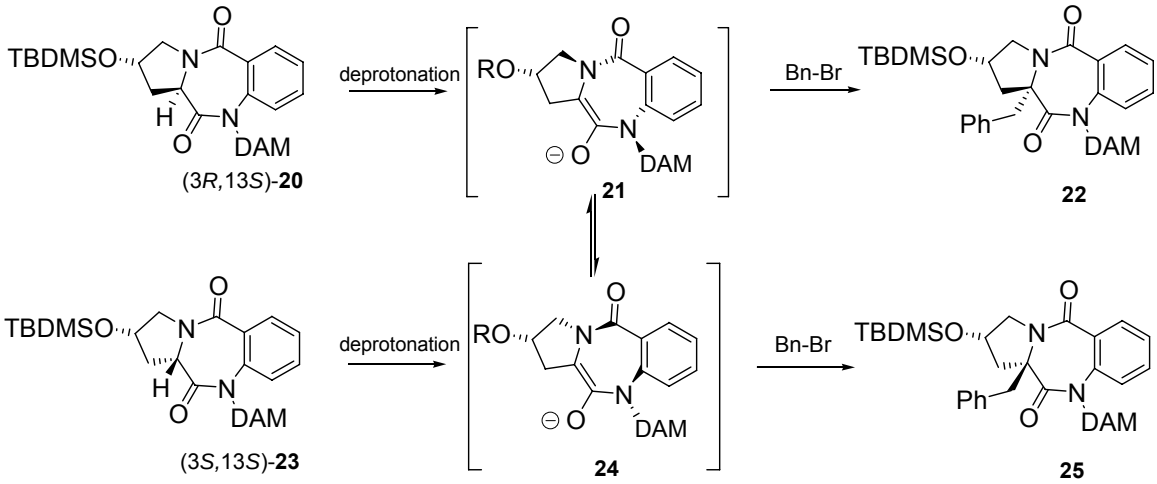

At higher reaction temperatures, the interconversion of the diastereomeric enolates, **21** and **24** would be considerably faster. We showed previously that in situ deprotonation/alkylation of *N*-DAM 1,4-benzodiazepin-2,5-dione (*S*)-**1c** gives racemic product at -78 °C, suggesting enolate racemization is faster than alkylation at this temperature. We therefore carried out deprotonation/alkylation of (3*R*,13*S*)-**20** and (3*S*,13*S*)-**23** at -78 °C (Scheme 5.15). Under these conditions we expected a rapid equilibration of the diastereomeric enolates, and thus identical diastereomeric ratios of **22:25** in both cases. As can be seen in Scheme 5.15 upon deprotonation and benzylation both (3*R*,13*S*)-**20** and (3*S*,13*S*)-**23** gave essentially the same diastereomeric ratios (34:66, 31:69) of **22**:**25**.

Scheme 5.15 Deprotonation/alkylation of hydroxyproline derived 1,4-benzodiazepin-2,5-diones at -78 °C

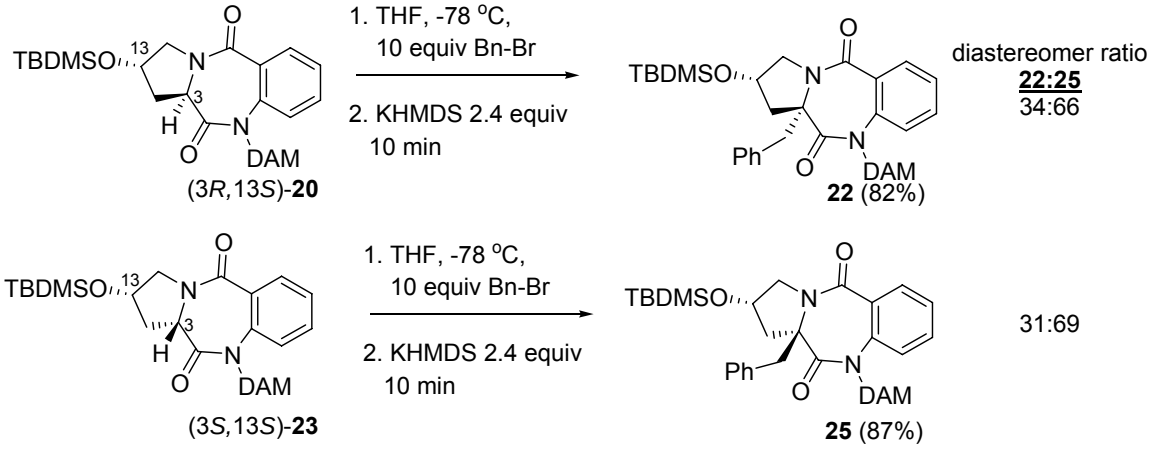

These results demonstrate that the enolates formed from (3*R*,13*S*)-**20** and (3*S*,13*S*)-**23** at -100 °C are different, and that the stereochemistry of the reaction at this

temperature is controlled by the conformation of the dynamically chiral enolate intermediate.

The successful MOC deprotonation/alkylations of proline-derived 1,4-benzodiazepin-2,5-diones prompted us to explore the synthesis of pseudoproline-derived 1,4-benzodiazepin-2,5-diones.

5.5 Synthesis of Quaternary Thioproline-Derived N-DAM- 1,4-Benzodiazepin-2,5-diones 28a,b

Extension of the previously described synthesis of proline-derived *N*-H 1,4-benzodiazepin-2,5-diones (**8**) to the thioproline-derived *N*-H 1,4-benzodiazepin-2,5-diones (*S*)-(+)-**26** is shown in Scheme 5.16. Reaction of commercially available (*S*)-thioproline with isatoic anhydride afforded the desired product (*S*)-(+)-**26** in 87% yield. Conversion of (*S*)-(+)-**26** to the sodium salt, followed by addition of DAM-Br led to thioproline-derived *N*-DAM 1,4-benzodiazepin-2,5-diones (*S*)-(+)-**27** in 89% yield and >99.5% ee (determined by chiral stationary-phase HPLC) (Scheme 5.16).

Scheme 5.16 Synthesis of thioproline-derived *N*-DAM 1,4-benzodiazepin-2,5-diones (*S*)-(+)-**27**

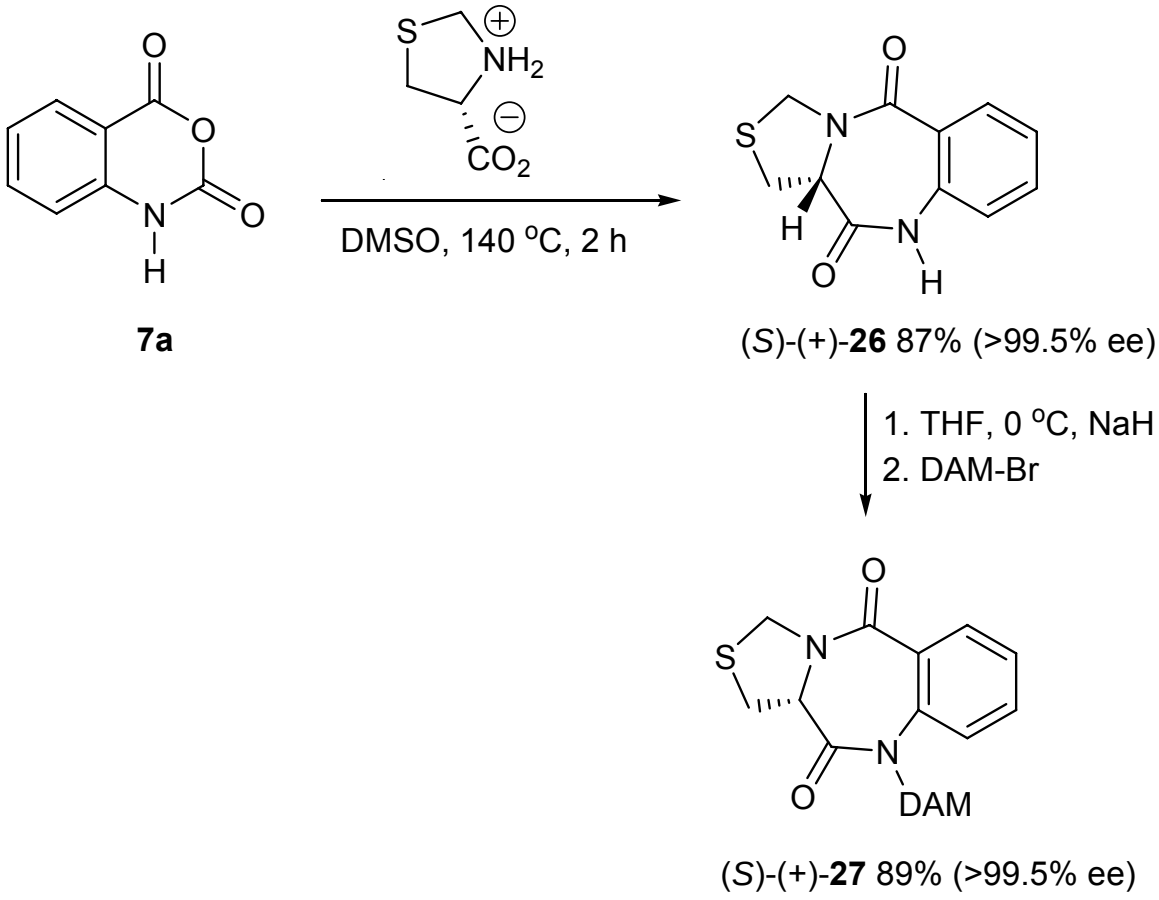

7a

(*S*)-(+)-**26** 87% (>99.5% ee)

(*S*)-(+)-**27** 89% (>99.5% ee)

We carried out the deprotonation/alkylation of (*S*)-(+)-**27** based on the MOC strategy. The details of the results are outlined in Scheme 5.17. C3 alkylation of (*S*)-(+)-**27** was successful for the two reactions we attempted. The C3 alkylated products **28a** and **28b** were synthesized in 99 and 95% ee, respectively.

Scheme 5.17 Enantioselective in situ deprotonation/alkylation of *N*-DAM-1,4-benzodiazepin-2,5-dione **27** (retentive stereochemistry assumed by analogy)

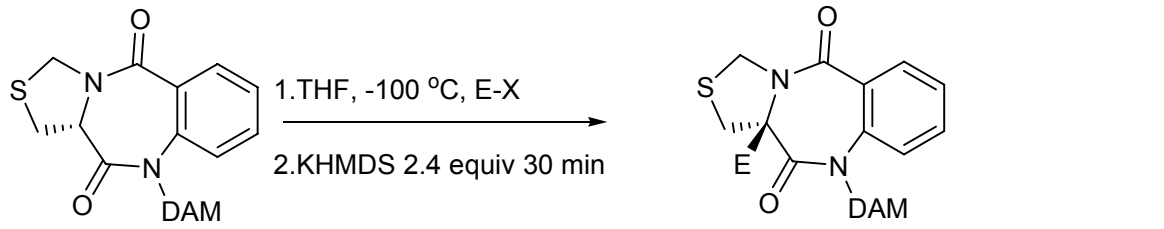

(S)-(+)-**27**

(*S*)-(+)-**28a** E = $PhCH_2$ 99% ee (98% yield)
(*S*)-(+)-**28b** E = allyl 95% ee (89% yield)

Upon noting the ease in which the sulfur-containing proline was incorporated into our MOC strategy we wanted to extend our library of compounds to include an oxygen-containing proline ring (oxaproline).

5.6 Synthesis of Quaternary Oxaproline-Derived N-DAM 1,4-Benzodiazepin-2,5-diones

Our interest in the synthesis of oxaproline-derived 1,4-benzodiazepin-2,5-diones was twofold. First, they would make a nice addition to the library of 1,4-benzodiazepin-2,5-diones that we could enantioselectively deprotonate and alkylate using the MOC strategy. Second, proline-derived 1,4-benzodiazepin-2,5-diones are important scaffolds in medicinal chemistry (Chapter 4). We envision that the oxaproline-derived 1,4-benzodiazepin-2,5-diones may exhibit similar pharmacological properties, therefore the development of an efficient synthesis to these types of compounds would be beneficial to the scientific community.

Oxaproline is not commercially available. However, CBZ-protected oxaproline **29** can be prepared from commercially available (*S*)-serine and formaldehyde as shown in Scheme 5.18.[10]

Scheme 5.18 Synthesis of CBZ-protected oxaproline **29**

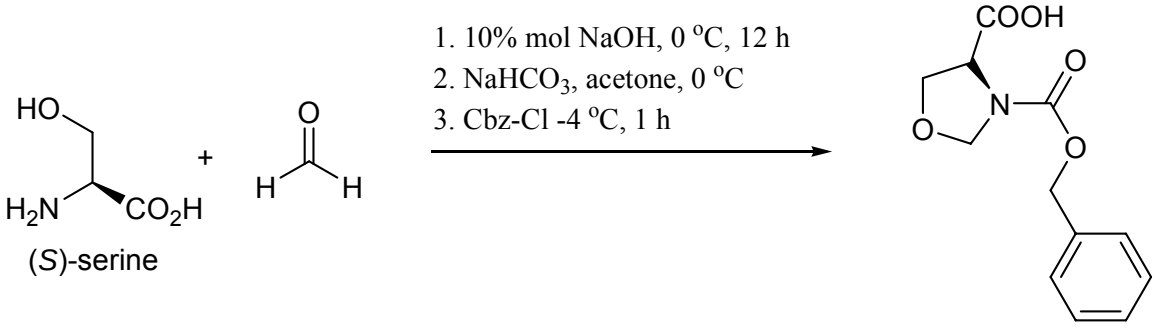

(*S*)-**29** (90%)

In order to incorporate oxaproline into our synthetic method involving isatoic anhydride (Scheme 5.2) we required conversion to the NH-free oxaproline **30**. Removal of the CBZ protecting group was performed by hydrogenation (Pd/C), but synthesis of the 1,4-benzodiazepin-2,5-dione was not successful. A brief search of the literature revealed that NH-free oxaprolines are unstable and exist as tautomeric mixtures with the imine open chain isomer **31**[11, 12] (Scheme 5.19).

Scheme 5.19 NH-free oxaproline tautomerizes between ring and imine open chain

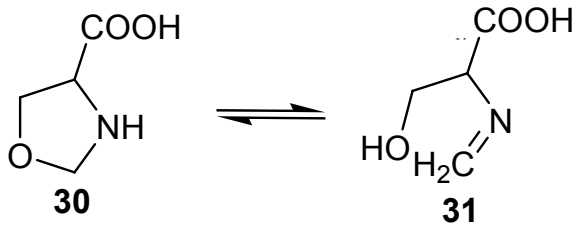

Based on this knowledge we devised a method to synthesize a set of oxaproline-derived 1,4-benzodiazepin-2,5-diones that did not involve NH-free oxaproline (Scheme 5.20).[10]

Scheme 5.20 Oxaproline-derived *N*-H 1,4-benzodiazepin-2,5-diones **34a-b**

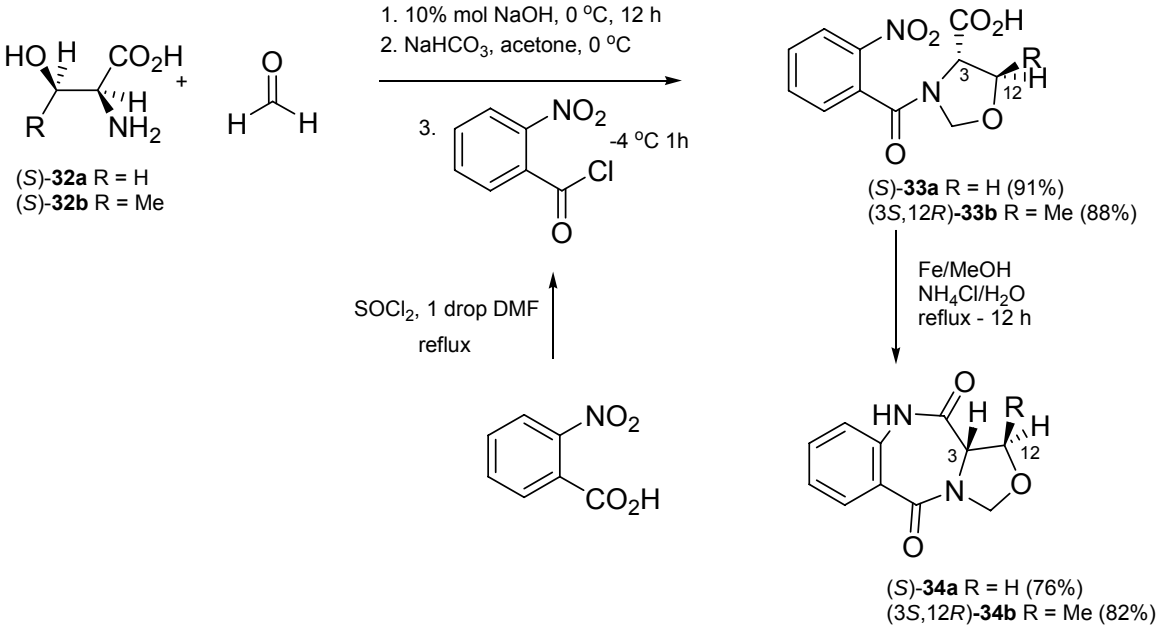

Reacting either (*S*)-serine (**32a**) or (*S*)-threonine (**32b**) with formaldehyde in the presence of base yields the oxaproline in situ, however rather than adding CBZ-Cl at this point we added the acid chloride derived from *p*-nitrobenzoic acid (Scheme 5.20). The acyl protected oxaprolines (*S*)-**33a** and (3*S*,12*R*)-**33b** were formed in 91 and 88% yield, respectively. We intended to reduce the nitro groups of (*S*)-**33a** and (3*S*,12*R*)-**33b** to a primary aromatic amine and then close the rings by heating in DMSO. We were pleased to discover that after refluxing in CH_3OH in the presence of Fe powder and aqueous NH_4Cl for 12 hours[13] the rings closed and the oxaproline-derived *N*-H1,4-benzodiazepin-2,5-diones (*S*)-**34a** and (3*S*,12*R*)-**34b** were obtained in 76 and 82% yield.

Finally, we installed the DAM substituent at the *N*1 position and obtained both *N*-DAM products (**35a-b**) in high yield (Scheme 5.21).

Scheme 5.21 N1 alkylation of (*S*)-**34a** and (3*S*,12*R*)-**34b**

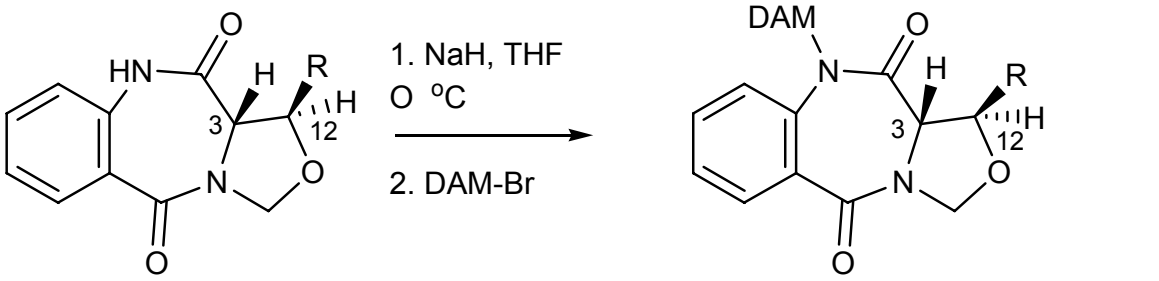

(*S*)-**34a** R = H
(3*S*,12*R*)-**34b** R = Me

(*S*)-**35a** R = H (94%)
(3*S*,12*R*)-**35b** R = Me (92%)

Alkylation reactions were carried out using the MOC protocol developed for 1,4-benzodiazepin-2,5-diones (Table 5.6). As can be seen from Table 5.6, 3,3-disubstituted products were obtained for the serine derived starting material (*S*)-**35a**. Alkylation with Bn-Br at -100 °C for 10 min gave the product **36** in excellent yield but only 25% ee (Table 5.6, entry 1). By decreasing the reaction time to 1 min we saw a slight improvement in the % ee, but we were not yet satisfied. Clearly, the enolate formed upon deprotonation of (*S*)-**35a** has a significantly lower inversion barrier than previously prepared 1,4-benzodiazepin-2,5-diones. Previous success with enantioselective deprotonation and alkylation of low inversion barrier enolates involved lowering the reaction temperature to -109 °C.[3, 4] As shown in Table 5.6 entry 3 we improved the enantioselectivity to 84% by employing this lower temperature procedure. An allyl group was placed at the C3 position of (*S*)-**35a**, however we were not able to obtain the product in reasonable % ee (Table 5.6, entries 4-6). The lower % ee attained with allyl bromide

relative to benzyl bromide may be due to O-allylation followed by a Claisen Rearrangement upon warm up, as shown in Scheme 5.22.

Scheme 5.22 Possible claisen rearrangement of O-allylated product

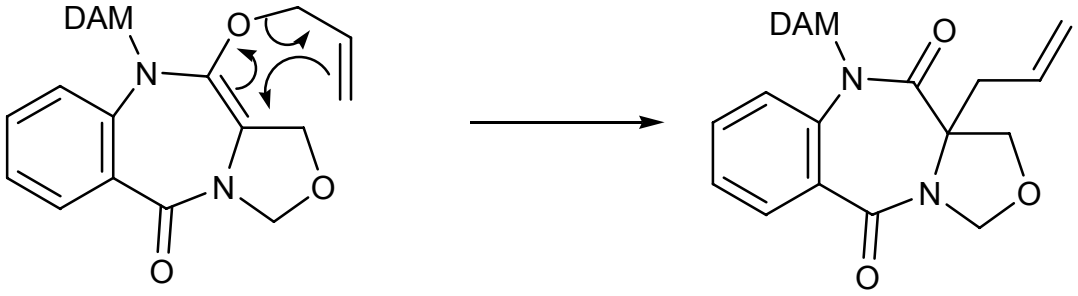

37

Unfortunately, (3*S*,12*R*)-**35b** is unreactive towards alkylation. The same reaction conditions that worked for (*S*)-**35a** resulted in no product formation in the case of (3*S*,12*R*)-**35b**. We tried increasing the reaction temperature to -78 °C (Table 5.6, entry 9) and still recovered all of the starting material. In one final attempt to alkylate (3*S*,12*R*)-**35b** we warmed the reaction to room temperature and unfortunately we were still unable to achieve benzylation at C3 (Table 5.6, entry 10).

Table 5.6 Attempted alkylations of **35a** and **35b**

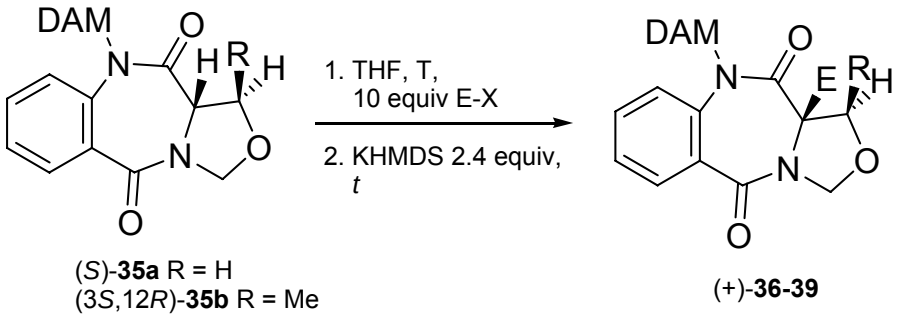

(*S*)-**35a** R = H
(3*S*,12*R*)-**35b** R = Me

(+)-**36-39**

Entry	Starting Material	E-X	Product	T (°C)	t (min)	% Yield	% ee [a]
1	**35a**	Bn-Br	(+)-**36**	-100	10	92	25
2	**35a**	Bn-Br	(+)-**36**	-100	1	71	50
3	**35a**	Bn-I	(+)-**36**	-109	1	82	84 *S* [b]
4	**35a**	allyl-Br	(+)-**37**	-100	10	96	27
5	**35a**	allyl-Br	(+)-**37**	-100	1	51	30
6	**35a**	allyl-Br	(+)-**37**	-109	1	43	45 *S* [b]
7	**35b**	Bn-Br	**38**	-100	10	0	-
8	**35b**	allyl-Br	**39**	-100	10	0	-
9	**35b**	Bn-Br	**38**	-78	30	0	-
10	**35b**	Bn-Br	**38**	RT	30	0	-

[a] % ee measured by chiral stationary phase HPLC (Chiralcel OD,AD). Nearly all results were replicated and %ee varied no more than 1.5 %. [b] the absolute stereochemistry is believed to be (*S*) based on the identical sign and HPLC elution order with the simple benzyl analogue (*S*)-(+)-**33a**

Although the oxaproline-derived 1,4-benzodiazepin-2,5-diones gave less than optimum results, our successes with proline and thioproline-derived analogues motivated

us to extend the enantioselective deprotonation/alkylation MOC strategy to include other amino acid derived 1,4-benzodiazepin-2,5-diones.

5.7 Synthesis of (S)-Alanine-Derived 1,4-Benzodiazepin-2,5-dione.

As we considered preparing 1,4-benzodiazepin-2,5-diones from acyclic, 1° amine containing amino acids, it became clear that N4 would need to be protected for the desired C3 deprotonation/alkylation sequence. As a first step in this direction we explored the reaction of *N*-Me-Ala-OH and *N*-Bn-Ala-OH with isatoic anhydride. Reaction with *N*-Me-Ala-OH has been reported in the literature,[14] and we successfully repeated this result, obtaining (*S*)-(+)-**40** in 90% yield. Surprisingly however, reaction of isatoic anhydride with *N*-Bn-Ala-OH did not give the desired product. Apparently reaction of amines with isatoic anhydride in sensitive to steric bulk at N4.[15]

Compound (*S*)-(+)-**40** was alkylated at the N1 position using the reactions conditions outlined in Scheme 5.23 to yield the *N*4-Me-Ala-derived *N*1-DAM 1,4-benzodiazepin-2,5-dione (*S*)-(+)-**41** in 93% yield and 95% ee.

Scheme 5.23 Synthesis of (*S*)-Ala-1,4-benzodiazepin-2,5-dione (*S*)-(+)-**41**

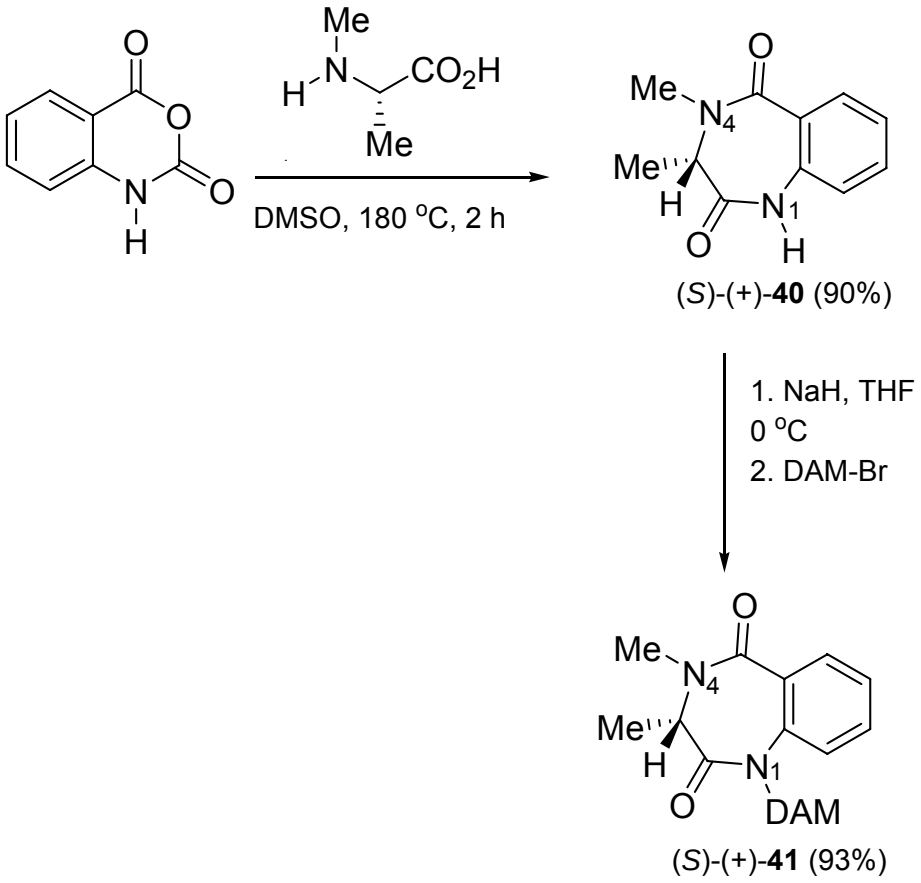

Attempts to carry out C3 alkylation of (*S*)-(+)-**41** were unexpectedly fruitless as can be seen by the results summarized in Table 5.7. Prolonged reaction time, addition of HMPA and running the reaction at room temperature did not produce the intended product **42** but resulted in the formation of the O-alkylated product **43,** as shown in Table 5.7. The typical ^{1}H chemical shift for C3-benzyl protons in quaternary 1,4-benzodiazepin-2,5-diones (e.g. **3b** & **3c**) range from 2.5 ppm to 2.7 ppm. However, the chemical shift observed for the benzyl protons of **43** was significantly higher (4.3, 4.9 ppm) indicating the benzyl group was attached to a more electronegative atom. We confirmed this proposal using Heteronuclear Multiple Bond Correlation (HMBC), which

allows for identification of proton nuclei by observation of 2- and 3-bond coupling to carbon nuclei (Figure 5.1).

Table 5.7 Attempted alkylation of Ala-derived 1,4-benzodiazepin-2,5-dione **41**

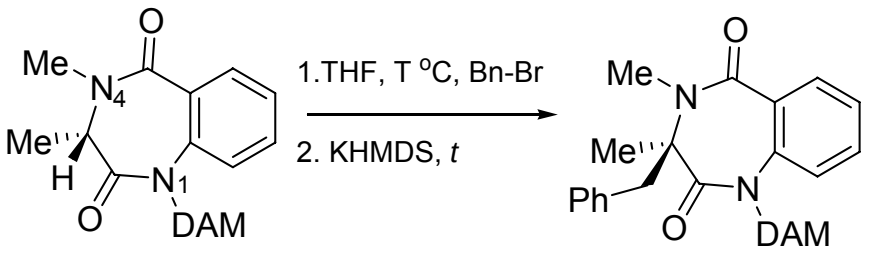

(*S*)-(+)-**41** **42**

Entry	T (°C)	*t* (min)	Equiv Base	HMPA (equiv)	Remarks
1	-100	30	2.4	no	Recovery of **41**
2	-78	30	5	yes (6)	Recovery of **41**
3	RT	60	5	yes (12)	O-alkylation product **43** (87%) based on ^{1}H NMR, confirmed with HMBC NMR

Specifically we examined the protons of the methyl group attached to *N*4. In the case of C3 benzylation (**42**) these protons would be correlated to an sp^2 carbonyl carbon and sp^3 C3. What we observed in the HMBC spectra was the protons from the *N*-Me were correlated to two sp^2 carbons, one carbonyl carbon and one alkene carbon (Figure 5.1). This result is consistent with the proposed O-alkylated structure **43**, but not the C3-alkylated product **42**.

Figure 5.1 C3 alkylated **43** and O-alkylated **42** Ala-derived 1,4-benzodiazepin-2,5-diones and HMBC spectrum.

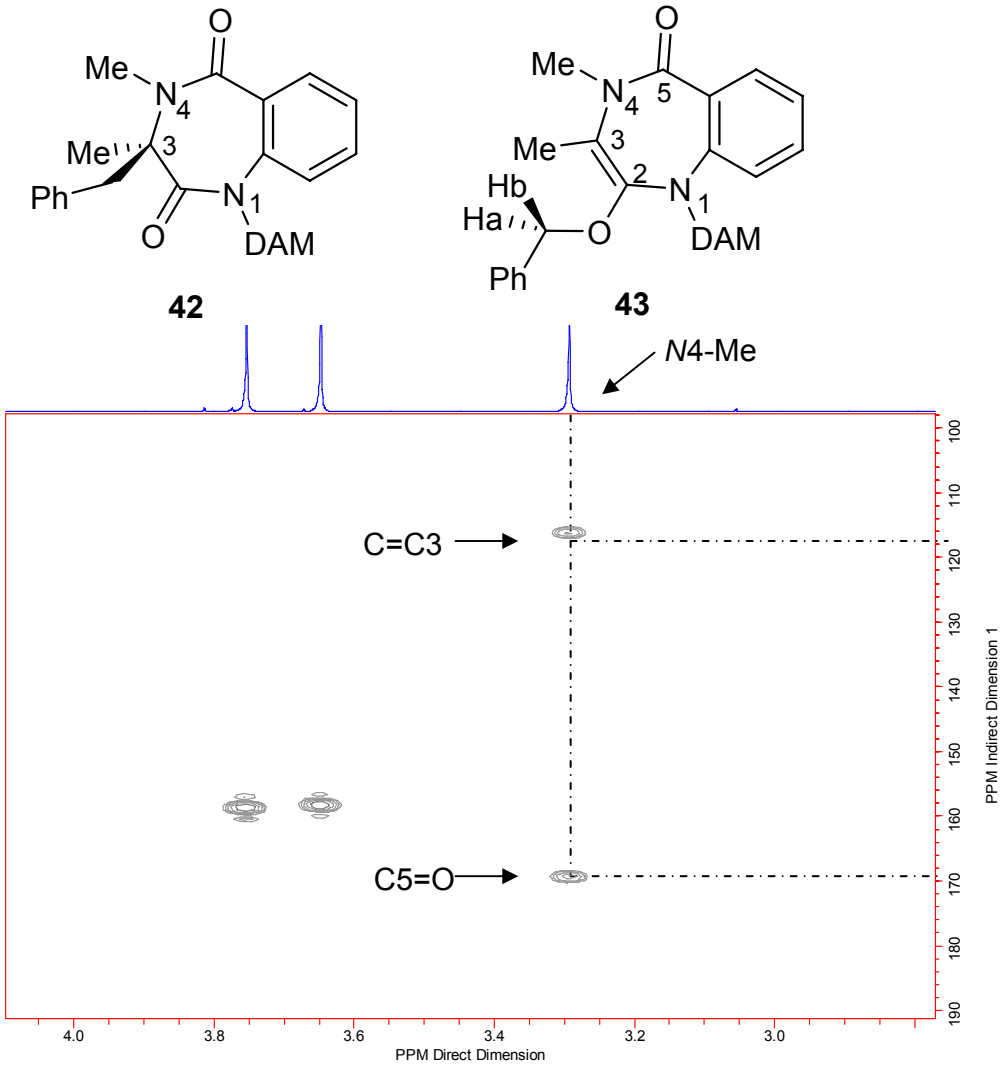

As described in Chapter 4, one of the criteria for a successful MOC strategy is slow racemization of the dynamically chiral intermediate. We have proposed that racemization of the enolate derived from 1,4-benzodiazepin-2,5-diones occurs via ring inversion. The O-alkylation product provided us with the opportunity to investigate the

ring inversion barrier of an enol ether derived from a 1,4-benzodiazepin-2,5-dione, by coalescence of the diastereotopic protons H_a and H_b.

Ring inversion causes these protons to exchange but the process is obviously slow at room temperature. At the coalescence temperature the peaks of interest (H_a/H_b) will merge into a flat topped peak and the inversion barrier could then be determined. We attempted to observe coalescence of H_a and H_b by raising the temperature in 20° intervals (Figure 5.2). Initially it appeared that H_a and H_b were beginning to merge (Figure 5.2, 293 K, 393 K, 413 K). However at 423 K the two doublets for H_a and H_b are gone and a coalescenced peak is not observed. Coalescence was sought up to 453 K, the high temperature limit of the spectrometer. When we subsequently ran the ^{1}H NMR of this sample at room temperature we found that **43** had decomposed. Although we cannot calculate the ring inversion barrier of **43** from this study without the coalescence temperature we can conclude from the data we obtained that the ring inversion barrier of the enol ether **43** is higher than 19.3 kcal/mol because coalescence of H_a and H_b had not occurred by 413 K (Figure 5.2).

Figure 5.2 Variable temperature ^{1}H NMR spectra of Bn-CH_2 (**43**)

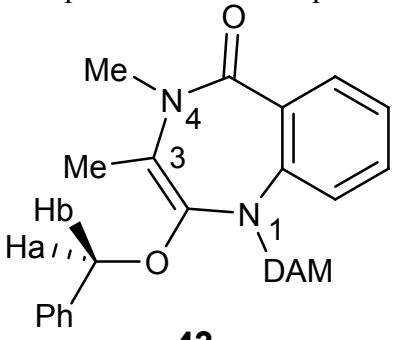

43

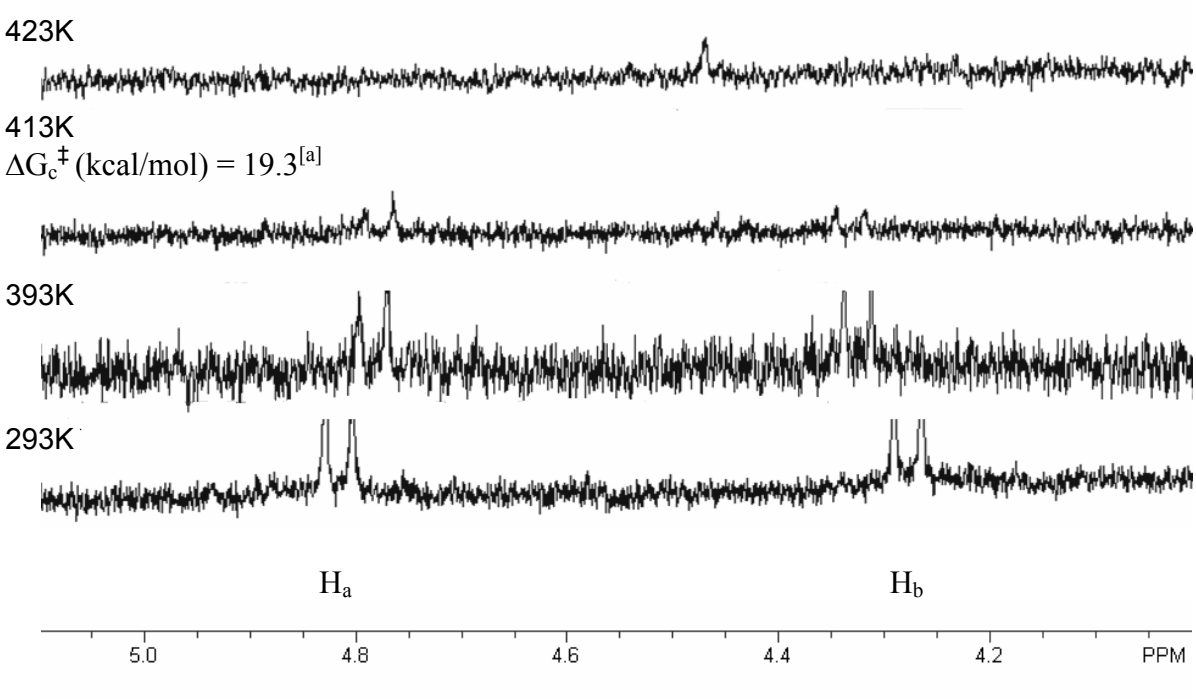

[a] The rate constant k_c at the coalescence temperature is given by $k_c = 2.22\sqrt{(\Delta\nu^2 + 6J_{AB}^2)}$ where $\Delta\nu$ is the separation of two coalescing protons measured in Hz at room temperature (240 Hz) and J_{AB} is the coupling constant between two coalescing protons at room temperature (11.1).
$\Delta G_c^‡$ (kcal/mol) is calculated using the following equation:
$\Delta G_c^‡ = 4.58\ Tc\ (10.32 + \log\ (Tc/kc))$cal mol^{-1} where Tc is the coalescence temperature.[16]

5.8 Synthesis of (R/S)-Pipecolic Acid-Derived 1,4-Benzodiazepin-2,5-diones.

We began the synthesis of pipecolic acid derived 1,4-benzodiazepin-2,5-dione with commercially available *R/S* pipecolic acid **44**. A racemic synthesis was motivated by economic concerns; if successful we planned to resolve the amino acid. Pipecolic acid derived *N*-H 1,4-benzodiazepin-2,5-dione **45** was prepared from reacting *R/S* pipecolic acid with isatoic anhydride in DMSO and heating at 160 °C for 3 hours, followed by stirring at room temperature overnight.[17] Compound **45** was formed in 89% yield. Installation of the DAM substituent at N1 gave the desired *N*-alklyated product **46** in 86% yield (Scheme 5.24).

Scheme 5.24 Synthesis of pipecolic acid derived *N*-DAM 1,4-benzodiazepin-2,5-dione (±)-**46**

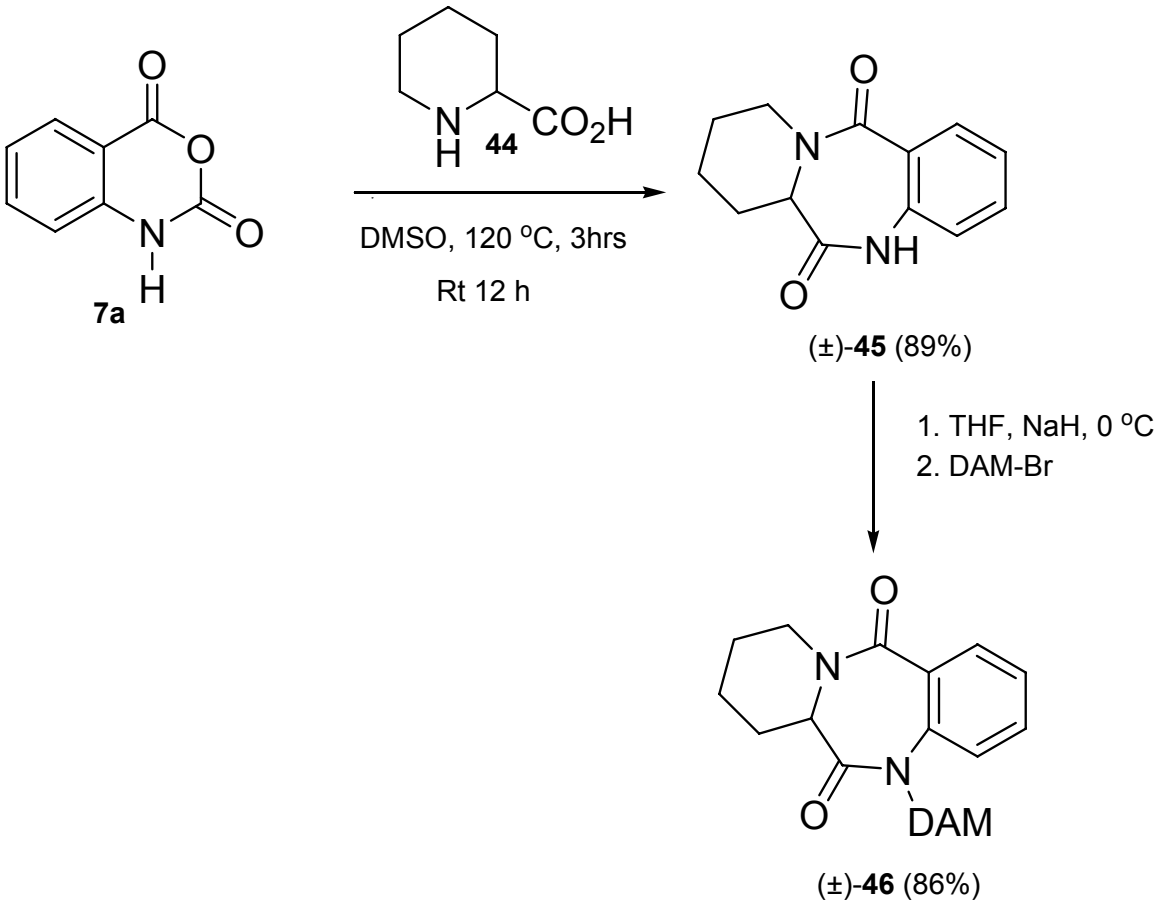

We implemented the typical MOC strategy in an attempt to benzylate (±)-**46** at C3. The results are shown in Table 5.8. As evidenced by entries 1 and 2 we were unable to obtain any product when we ran the deprotonation/alkylation reactions at low temperatures (-100 and -78 °C). Attempting the reaction at room temperature did not yield the expected C3 alkylated product. Once again, however O-alkylation of (±)-**46** was observed under these reaction conditions. We were able to isolate and identify the O-benzylated product **48** using 1H NMR. As mentioned previously the typical chemical shift for C3-benzyl protons ranges from 2.5 ppm to 2.7 ppm. The chemical shift observed for the benzyl protons of **48** was significantly higher (4.4, 4.9 ppm) indicating the benzyl

group was attached to a more electronegative atom. The presence of diastereotopic benzyl protons is also consistent with the chiral structure of **48**. We did not attempt verification of O-alkylation using HMBC in this instance due to the more complex nature of the proton NMR.

Table 5.8 Attempted benzylation of **46**

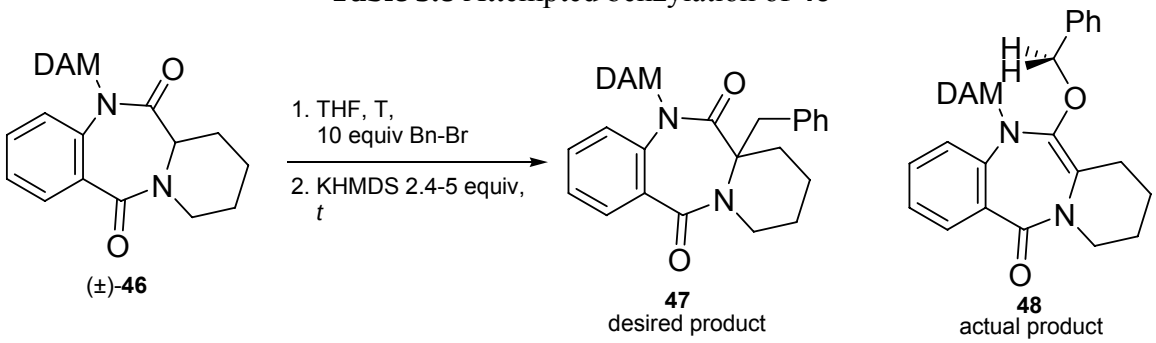

Entry	T (°C)	*t* (min)	Equiv Base	HMPA (equiv)	Remarks
1	-100	15	2.4	no	Recovery of **46**
2	-78	30	5	yes (6)	Recovery of **46**
3	RT	60	5	yes (12)	O-alkylation product **48** (45%) based on H^1 NMR

Again we attempted to determine the coalescence temperature of **48** (Bn-CH_2 protons), the data we obtained is shown in Figure 5.3. Unfortunately the O-alkylated product **48** met the same fate as O-alkylated **43**. We observed decomposition of O-benzylated product **48** around 428 K, consequently we were unable to determine the approximate ring inversion barrier of the enol ether, however based on this experiment we conclude that the ring inversion barrier for **48** is higher than 19.8 kcal/mol. In the future, 2D EXSY ^{1}H NMR should be used to determine the inversion barrier of these enol ethers.

Figure 5.3 Variable temperature ^{1}H NMR of Bn-CH_2 (**48**)

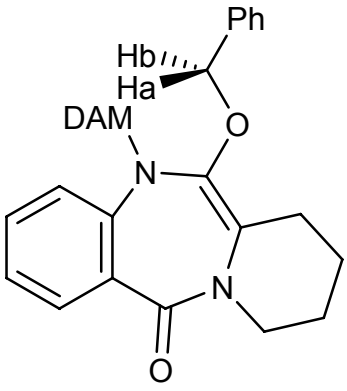

48

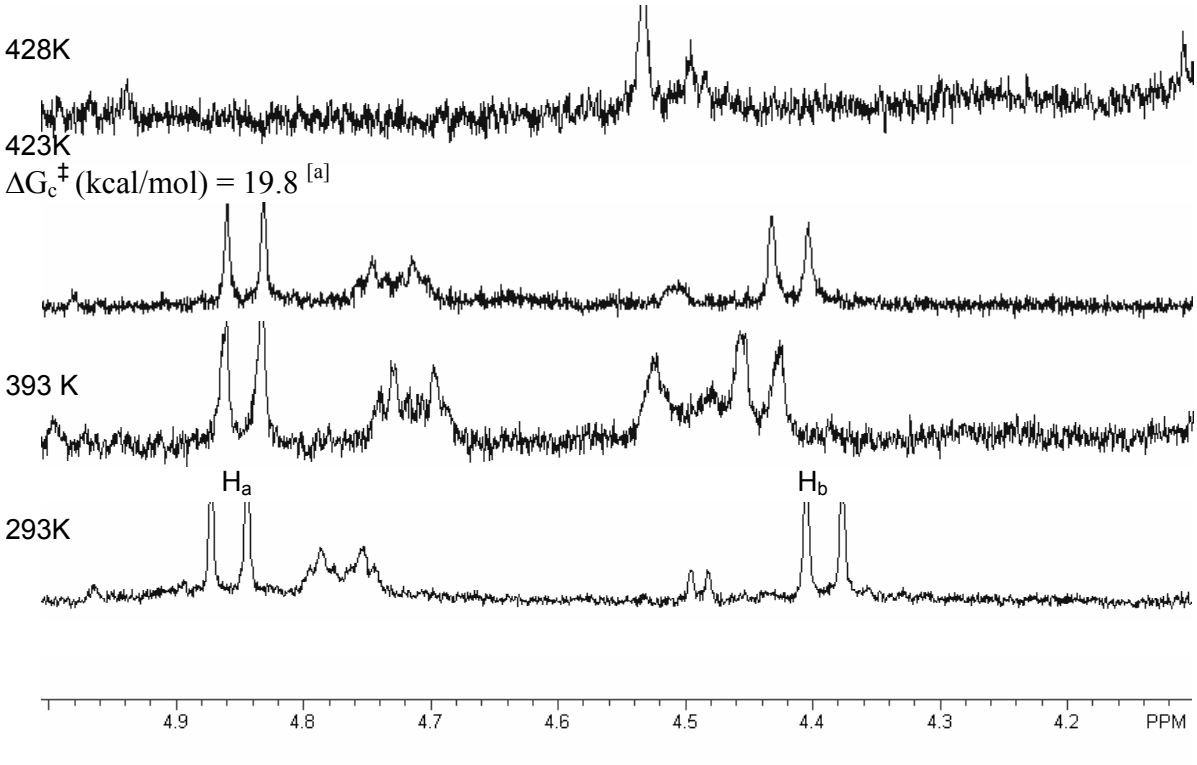

[a] The rate constant k_c at the coalescence temperature is given by $k_c = 2.22\sqrt{(\Delta\nu^2 + 6J_{AB}^2)}$ where $\Delta\nu$ is the separation of two coalescing protons measured in Hz at room temperature and J_{AB} is the coupling constant between two coalescing protons at room temperature.
$\Delta G_c^‡$ (kcal/mol) is calculated using the following equation:
$\Delta G_c^‡ = 4.58\ Tc\ (10.32 + \log\ (Tc/kc))$cal mol^{-1} where Tc is the coalescence temperature.[16]

5.9 Computational Studies of 1,4-Benzodiazepin-2,5-diones

To understand the stereochemical course of the deprotonation/alkylation reactions of proline-derived 1,4-benzodiazepin-2,5-diones, we have undertaken computational studies. X-ray crystallography has established that proline-derived 1,4-benzodiazepin-2,5-diones present the proline ring in the equatorial position.[18] DFT (B3LYP/6-31G*) calculations on (*S*)-(+)-**1b** similarly indicate a 17.8 kcal/mol preference (ΔG) for the equatorial conformer (Figure 5.4). Thus, similar to the 1,4-benzodiazepin-2-ones,[1, 3] (3S)-stereochemistry induces the benzodiazepine ring of **1b** to adopt the (*M*)-conformation. The calculated structures of the equatorial-proline (*M*)-(*S*)- and the axial-proline (*P*)-(*S*)-conformers of **1b** suggest that the significant destabilization of the latter is due primarily to compromised amide resonance (dihedral O-C5-N4-C12 = 30.3°) and concurrent pyramidalization of N4 (sum of angles = 348.5°). The proton at C3 in (*M*)-(*S*)-**1b** appears well disposed for abstraction, unlike that in the high energy conformer (*P*)-(*R*)-**1b** (calculated H-C3-C2-O dihedrals 125.4° and 35.3° respectively).[19] Therefore the stereospecific transformation of (*S*)-**1b** to an (*M*)-enolate appears feasible.

Figure 5.4 Calculated equilibrium geometries (B3LYP/6-31G*) of the proline derived 1,4-benzodiazepin-2,5-dione (*S*)-(+)-**1b**. Molecular structure drawings created by Molecule™

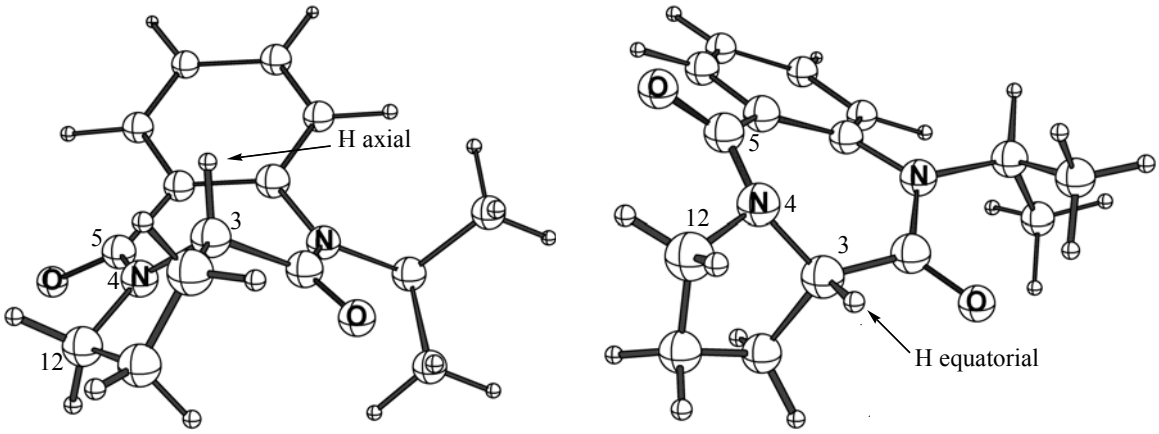

(*M*)-(*S*)-**1b**	(*P*)-(*S*)-**1b**
0.0 kcal/mol	+17.8 kcal/mol
O-C5-N4-C12 1.9°	O-C5-N4-C12 30.0°
Sum of angles at N4 = 359.7°	Sum of angles at N4 = 348.5°

^{1}H and ^{13}C NMR spectroscopy of α-alkylated proline-derived 1,4-benzodiazepin-2,5-diones (**2b-6b, 2c-6c**) indicate a single conformation of the BZD ring, in sharp contrast to the quaternary 1,4-benzodiazepin-2-ones, which exist as a mixture of the (*M*) and (*P*) conformers. The calculated equilibrium geometries (B3LYP/6-31G*)[20] for (*S*)-(+)-**2b** shows a 25.8 kcal/mol preference (ΔG) for proline to occupy the equatorial position ((*M*)-(*S*)-**2b**, Figure 5.5).[2] The energy difference calculated for (*S*)-(+)-**2b** is much larger than that calculated for Ala-derived 1,4-benzodiazepine-2-ones.[1] In addition to the unfavorable trans-annular steric interaction visible in (*P*)-(*S*)-**2b**, other structural distortions are seen**.** Whereas (*M*)-(*S*)-**2b** features a planar N4 (sum of angles = 359°) the axial conformer (*P*)-(*S*)-**2b** features a pyramidalized N4 (sum of angles = 337°). This

strong equatorial preference is in large part due to amide resonance which is retained in (*M*)-(*S*)-**2b** and compromised in (*P*)-(*S*)-**2b**, as evidenced by C3-N4-C5-O5 dihedrals of -174.6 and -73.7°, respectively.[2]

Figure 5.5 Calculated equilibrium geometries (B3LYP/6-31G*) of the proline derived 1,4-benzodiazepin-2,5-dione (*S*)-(+)-**2b**. Molecular structure drawings created by Molecule™

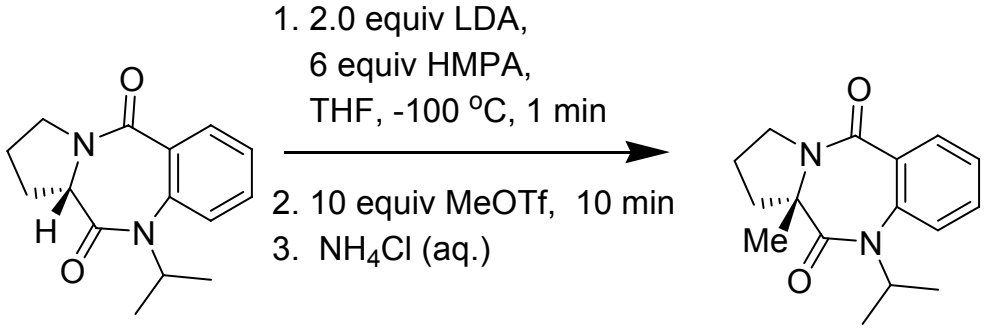

(*S*)-(+)-**1b** (*S*)-(+)-**2b**

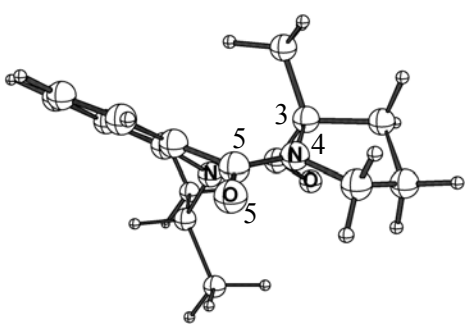

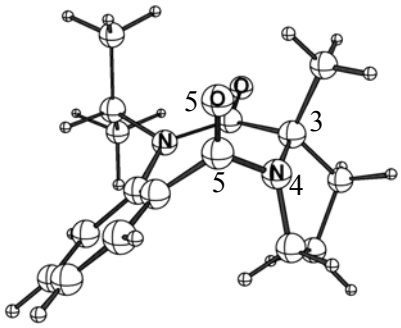

(*M*)-(*S*)-**2b** (*P*)-(*S*)-**2b**

0.0 kcal/mol +25.8 kcal/mol

Sum of angles around N4 = 359° Sum of angles around N4 = 337°

$\tau_{C3\text{-}N4\text{-}C5\text{-}O5}$ = -174.6° $\tau_{C3\text{-}N4\text{-}C5\text{-}O5}$ = -73.7°

The formation of an enantiopure dynamically chiral reactive intermediate that racemizes slowly on the reaction time scale is one of the requirements for a successful MOC transformation. To account for the formation of the enantiomerically pure enolate formed upon deprotonation of (*S*)-**1b** we have computationally modeled the deprotonation of (*S*)-**1b** by dimeric lithium dimethylamide. Collum has recently reported dimer-based mechanisms for deprotonation of ketones and esters in which two molecules of lithium amide are present in the transition structure.[21] As shown in Figure 5.6, transition structures leading to the (*M*)- and (*P*)- enolate were located at B3LYP/6-31G* (single point energies were calculated at B3LYP/6-31+G*). (*M*)-(*S*)-**49b** is the transition structure corresponding to the deprotonation of (*M*)-(*S*)-**1b** and leading to the (*M*)-enolate. (*P*)-(*S*)-**49b** is the transition structure corresponding to deprotonation of (*P*)-(*S*)-**1b** and leading to the (*P*)-enolate. The transition state (*M*)-(*S*)-**49b** that leads to the (*M*)-enolate is favored by 11.9 kcal/mol at 173 K.[2]

Figure 5.6 B3LYP/6-31G* transition structures for deprotonation of (*S*)-**1b** by $(LiNMe_2)_2$. Bond lengths in Å. Relative free energies (173 K) at B3LYP/6-31+G*. Molecular structure drawings created by Molecule^{TM}

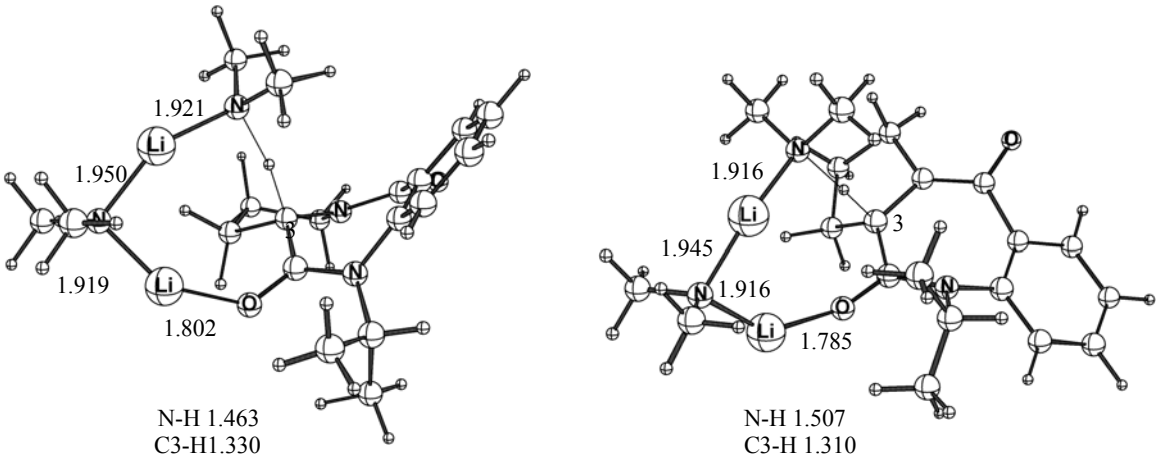

(*M*)-(*S*)-**49b**

0.0 kcal/mol

(*P*)-(*S*)-**49b**

11.9 kcal/mol

In addition, we have also calculated the explicit bis(Me_2O) solvates of the deprotonation transition structures ((*M*)-(*S*)-**50b** and (*P*)-(*S*)-**50b**) shown in Figure 5.7. The calculated energy of (*M*)-(*S*)-**50b** is 9.7 kcal/mol lower than that of (*P*)-(*S*)-**50b** indicating once again there is a distinct preference for the formation of the (*M*)-enolate.[2] Based on these calculated results we conclude that the formation of an enantiopure (*M*)-enolate by deprotonation of (*M*)-(*S*)-**1b** is reasonable.

Figure 5.7 B3LYP/6-31G* transition structures for explicit bis(Me_2O) solvates (*M*)-(*S*)-**50b** and (*P*)-(*S*)-**50b**. Bond lengths in Å. Relative free energies (173 K) at B3LYP/6-31+G*. Molecular structure drawings created by Molecule™

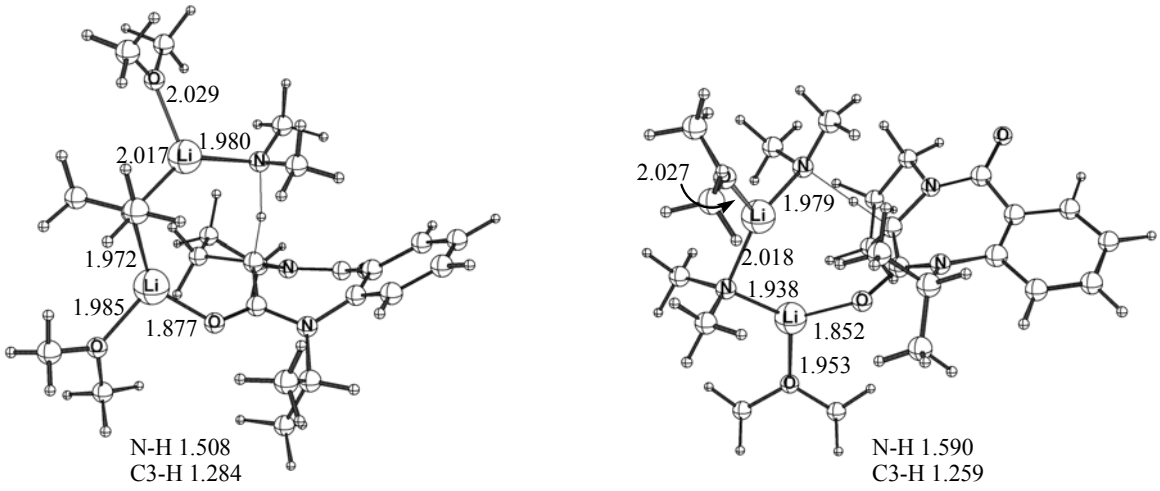

(*M*)-(*S*)-**50b**

0.0 kcal/mol

(*P*)-(*S*)-**507b**

9.7 kcal/mol

The solution structure of the dynamically chiral enolate derived from (*S*)-**1b** is unknown. In order to gain insight into the racemization half life of the enolate derived from (*S*)-**1b** we have located the equilibrium geometry and ring inversion transition structures for the enolate free anion (**51b, 51b***) and the corresponding $Li(OMe_2)_3$ salt (**52b, 52b***).[20] The B3LYP/6-31+G*//B3LYP/6-31G* activation free energy for ring inversion of the enolate free anion **51b** (Figure 5.8) at 173 K is 12.2 kcal/mol, which corresponds to a racemization half life of 4 minutes.[2] The activation free energy for racemization of **52b** at 173 K is equal to 16.0 kcal/mol, corresponding to a racemization half life of 180 days (Figure 5.8). Thus DFT calculations suggest that the enolate derived from (*S*)-**1b** would have sufficient conformationally stability at -100 °C to undergo in situ deprotonation/alkylation reactions without significant racemization. [2]

Figure 5.8 B3LYP/6-31G* equilibrium geometry and ring inversion transition structure for the free enolate anion (**51b**, **51b***)and its Li(OMe$_2$)$_3$ salt (**52b**, **52b***)derived from1,4-benzodiazepin-2,5-dione **1b** (B3LYP/6-31+G*//B3LYP/6-31G*). Bond lengths in Å

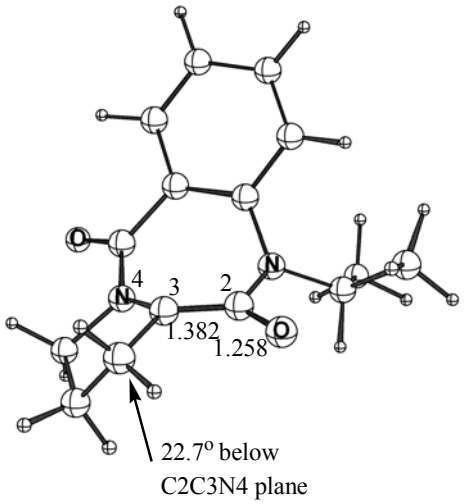

(*M*)- **51b**

equilibrium geometry

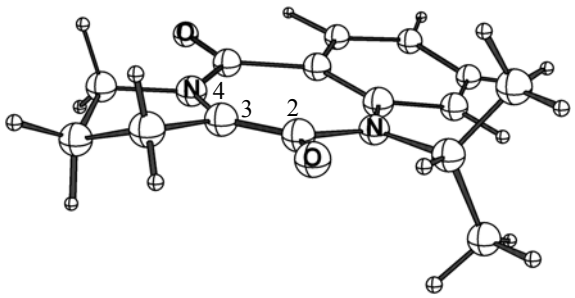

51b*

$\Delta G^{\ddagger}$ (173 K) = 12.2 kcal/mol
ring inversion
transition structure

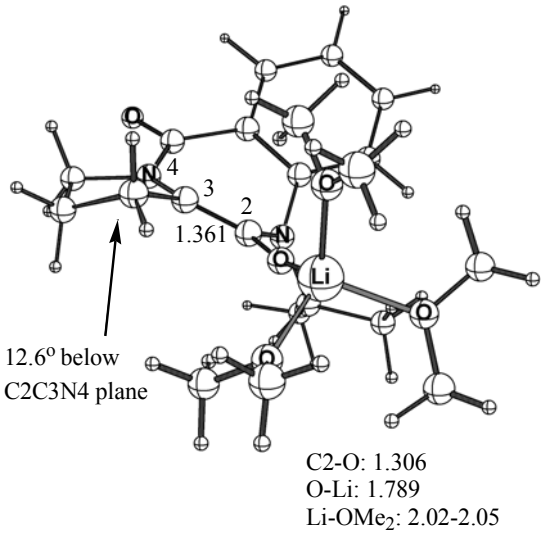

(*M*)- **52b**

equilibrium geometry

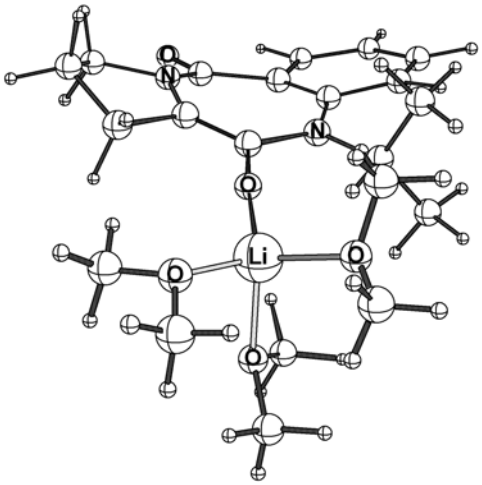

52b*

$\Delta G^{\ddagger}$ (173 K) = 16.0 kcal/mol
ring inversion
transition structure

Therefore up to now we have successfully addressed the first two steps of the MOC mechanism (Chapter 4, Scheme 4.4): formation of an enantiopure, dynamically chiral intermediate and slow racemization of the intermediate on the allkylation reaction time scale. The remaining challenge is to explain why the dynamically chiral intermediate reacts stereoselectively. We experimentally proved retentive alklyation of (*S*)-(+)-**1b** and (*S*)-(+)-**1c**, which necessitates alkylation of the (*M*)-enolate from the top face. The top face of the enolate is the concave face, and is more sterically hindered. It is not yet clear as to why we get contra-steric alkylation, however Seebach has suggested that stereoselectivity of enolate alkylation can be correlated with slight pyramidalization of the reactant toward the electrophile.[22] Examination of the enolate equilibrium geometries **(51b** and **52b**) in Figure 5.8 show that the C3 is slightly pyramidalized. A closer look at the proline attached CH_2 carbon in these structures shows that it is deformed 22.7 and 12.6° below the C2C3N4 plane, therefore the enolate is pyramidalized toward the favored trajectory of the electrophile. [23]

5.10 Future Work

Despite the work that has been completed on this project a number of avenues of research remain unexplored. React IR could be used to study the kinetics involved with deprotonation and alkylation of the 1,4-benzodiazepin-2,5-diones. Specifically, monitoring the disappearance of the amide carbonyl and appearance of the enolate C=C stretch would allow us to follow the rate of enolate formation. Measuring the disappearance of the enolate C=C stretch and the reappearance of the amide carbonyl upon addition of electrophile would provide information on the rate of alkylation. These

studies could clarify the mechanism of the deprotonation and alkylation reactions, and might assist further optimization of the deprotonation/alkylation sequence.

Slow enolate racemization is imperative for achieving highly enantiopure 1,4-benzodiazepin-2,5-diones. We have proposed that enolate racemization occurs through ring inversion. Measuring enolate racemization experimentally, however, has proved difficult. We have successfully developed a method for trapping enolates derived from deprotonation of **41** and **46** leading to enol ethers **43** and **46**. 2D-EXSY ^{1}H NMR may be used to determine the ring inversion barrier for enol ethers **43** and **46**, thereby providing useful information about enolate racemization for the N-Me-Ala and pipecolic acid-derived 1,4-benzodiazepin-2,5-diones.

Deprotonation/alkylation of diastereomeric hydroxy proline-derived 1,4-benzodiazepin-2,5-diones (3*R*,13*S*)-**20** and (3*S*,13*S*)-**23** at -109 °C should result in improved % de. This dependence of % de on temperature would provide additional evidence for a MOC mechanism. It may be possible to use ^{1}H NMR to observe enolate interconversion in the case of enolates **21** and **24** since they should have different ^{1}H and ^{13}C NMR spectra. Since our synthetic results show that enolate interconversion is slow at -100 °C, but fast at -78 °C, ^{1}H and ^{13}C NMR studies in this temperature range could allow determination of the coalescence temperature and direct calculation of the enolate inversion barrier for the proline-derived 1,4-benzodiazepin-2,5-diones.

Finally it may be possible to improve the deprotonation/alkylation protocol for oxaproline-derived 1,4-benzodiazepin-2,5-diones (*S*)-**35a** and (3*S*,12*R*)-**35b** by varying the reaction conditions. Changing the reaction solvent, closely monitoring the reaction temperature or varying the electrophile may be a few ways to improve enantioselectivity and yields.

5.11 Conclusions

We have developed a concise highly enantioselective memory of chirality route to quaternary proline-derived 1,4-benzodiazepin-2,5-diones. Retentive alkylation was established via hydrolysis to the known quaternary amino acids in the case of **2b** and **3b-c**. Diversification at the N1 position of the 1,4-benzodiazepin-2,5-diones is facilitated by the incorporation of the removable DAM substituent. Using the set of diastereomeric hydroxy proline-derived 1,4-benzodiazepin-2,5-diones (3*R*,13*S*)-**20** and (3*S*,13*S*)-**23,** we provide conformation that the enantioselectivity of the MOC transformations at -100 °C is due to the formation of dynamically chiral enolate intermediates.

Our goal to synthesize quaternary pseudo-proline derived 1,4-benzodiazepin-2,5-diones utilizing a MOC strategy was met with the highly enantioselective synthesis of quaternary thioproline-derived 1,4-benzodiazepin-2,5-diones (**26a-b**). (*S*)-Threonine-derived oxaproline 1,4-benzodiazepin-2,5-diones (3*S*,12*R*)-**33b** proved unreactive towards the deprotonation/alkylation protocol while the deprotonation/alkylation of the (*S*)-serine-derived oxaproline 1,4-benzodiazepin-2,5-dione (*S*)-**33a** yielded alkylated products, yet the enantioselectivity was less than optimum. However, the efficient synthetic method developed for the preparation of (*S*)-**32a** and (3*S*,12*R*)-**32b** will facilitate the synthesis of important BZD-based drugs.

Using variable temperature ^{1}H NMR, we estimated the ring inversion of the enol ethers **43** and **48** to be higher than 19.3 kcal/mol and 19.8 kcal/mol, respectively. In the future these compounds could be prepared again and 2D-EXSY NMR may be used to determine the ring inversion barrier.

We studied computational models of **1b** and **2b** to gain insight into the stereochemical outcome of the MOC reactions. Using DFT we have offered an explanation for the preferred formation of the enantiopure (*M*)-enolate of (*S*)-**1b** and also the formation of the retentive alkylated products. The present synthesis provides an efficient method for preparing a diverse library of compounds; the rigid conformation of the benzodiazepine ring makes these compounds appealing synthetic intermediates for drugs that have been previously inaccessible.

References for Chapter 5

[1] Carlier, P. R., Zhao, H., DeGuzman, J., Lam, P. C.-H., Enantioselective synthesis of "quaternary" 1,4-benzodiazepin-2-one scaffolds via memory of chirality, *J. Am. Chem. Soc* **2003**, *125*, 11482.

[2] MacQuarrie-Hunter, S., Carlier, P. R., Highly enantioselective synthesis of rigid, quaternary 1,4-benzodiazepine-2,5-diones derived from proline, *Organic Lett.* **2005**, *7*, 5305.

[3] Carlier, P. R., Lam, P. C.-H., DeGuzman, J., Zhao, H., Memory of chirality trapping of low inversion barrier 1,4-benzodiazepin-2-one enolates, *Tetrahedron: Asymmetry* **2005**, *16*, 2998.

[4] Lam, P. C.-H., Carlier, P. R., Experimental and computational studies of ring inversion if 1,4-benzodiazepin-2-ones: Implications for memory of chirality transformations, *J. Org. Chem.* **2005**, *70*, 1530.

[5] Beard, C. V., Baum, K., Grakaskas, V., Synthesis of some novel trifluoromethanesulfonates and their reactions with alcohols, *J. Org. Chem.* **1973**, *38*, 3673.

[6] Ishikura, M., Mori, M., Terashima, M. B., Y., A new synthesis of anthramycin via palladium-catalyzed carbonylation, *J. Chem. Soc. Chem . Commun.* **1982**, 741.

[7] Seebach, D., Boes, M., Naef, R., Schweizer, B., Alkylation of amino acids without loss of the optical activity: preparation of .alpha.-substituted proline derivatives. A case of self-reproduction of chirality, *J. Am. Chem. Soc.* **1983**, *105*, 5390.

[8] Sekine, M., Iwase, R., Masuda, N., Hata, T., Synthesis of oligoribonucleotides by use fo 4,4', 4"-tris(acyloxy)trityl groups for protection of the 6-amino group of adenosine, *Bull. Chem. Soc. Jpn.* **1988**, *61*, 1669.

[9] Pena, M. R., Stille, J. K., A total synthesis of anthramycin. Application of palladium-catalyzed coupling reactions for the attachment of the acrylic side chain, *J. Am. Chem. Soc* **1989**, *111*, 5417.

[10] Falorno, M., Conti, S., Giacomelli, G., Cossu, S., Soccolini, F., Optically active 4-oxaproline derivatives: New useful chiral synthons derived from serine and threonine, *Tetrahedron* **1995**, *6*, 287.

[11] Selambarom, J., Smadja, J., Pavia, A., Conversion of isomeric 2:3 adducts to N-acyl-pseudoprolines derivatives, *Tetrahedron Lett.* **2005**, *46*, 615.

[12] Brewster, A. G., Jayatissa, J., Mitchell, M. B., Schofield, A., Stoodley, R., Memory of chirality effects in aldol cyclisations of 1-(3-oxobutyryl) derivatives of L-4-oxaproline and L-proline isopropyl esters, *Tetrahedron Lett.* **2002**, *43*, 3919.

[13] Wissner, A., Overbeek, E., Reich, M. F., Floyd, M. B., Johnson, B. D., Mamuya, N., Rosfjord, E. C., Discafani, C., Shi, X.-Q., Rabindran, S. K., Gruber, B. C., Ye, F., Hallett, W. A., Nilakantan, R., Shen, R., Wang, Y.-F., Greenberger, L. M., Tsou, H.-R., Synthesis and structure-activity relationship of 6,7-disubstituted 4-anilinoquinoline-3 carbonitriles., *J. Med. Chem.* **2003**, *46*, 49.

[14] Sabb, A., Vogel, R., Welmaker, G., Sabalski, J., Coupet, J., Dunlop, J., Rosenzweig-Lipson, S., Harrison, B., Cycloalkyl[b][1,4]benzodiazepinoindoles are agonists at the human 5-HT2C receptor., *Bioorg. Med. Chem.* **2004**, *14*, 2603.

[15] Juaristi, E., Leno-Romo, J. L., Quiros, Y., Enantioselective synthesis of α-amino acids from chiral 1,4-benzodiazepin-2,5-diones containing the α-phenethyl group, *J. Org. Chem.* **1999**, *64*, 2914.

[16] Friebolin, H. In *Basic One- and Two Dimensional NMR Spectroscopy*; 2 ed.; D. E. Wille, Ed.; VCH Publishers: New York, 1993; Vol. 1, pp 294.

[17] Jadidi, K., Aryan, R., Mehrdad, M., Lugger, T., Ekkehardt, H., Ng, S., Simple synthesis, structure and ab initio study of 1,4-benzodiazepine-2,5-diones., *Journal of Molecular Structure* **2004**, *692*, 37.

[18] Neidle, S., Webster, G. D., Jones, D. E., Thurston, D., Structures of two DNA minor-groove binders, based on pyrrolo[2,1-c][1,4]benzodiazepines, *Acta Cryst. Sect. C* **1991**, *47*.

[19] Behnam, S. M., Behnam, S. E., Ando, K., Green, N. S., Houk, K. N., Stereoelectronic, torsional, and steric effects on rates of enolization of ketones, *J. Org. Chem.* **2000**, *65*, 8970.

[20] Frisch, M. J., Trucks, G. W., Schlegel, H. B., Scuseria, G. E., Robb, M. A., Cheeseman, J. R., Zakrewski, V. G., Montgomery, J. A., Stratmann, R. E., Burant, J. C., Dapprich, S., Millam, J. M., Daniels, A. D., Kudin, K. N., Strain, M. C., Farkas, O., Tomasi, J., Barone, V., Cossi, M., Cammi, R., Mennucci, B., Pomelli, C., Adamo, C., Clifford, S., Ochterski, J., Petersson, G. A., Ayala, P. Y., Cui, Q., Morokuma, K., Salvador, P., Dannenberg, J. J., Malick, D. K., Rabuck, A. D., Raghavachari, K., Foresman, J. B., Cioslowski, J., Ortiz, J. V., Baboul, A. G., Stefanov, B. B., Liu, G., Liashenko, A., Piskorz, P., Komaromi, I., Gomperts, R., Martin, R. L., Fox, D. J., Keith, T., Al-Laham, M. A., Peng, C. Y., Nanayakkara, A., Challacombe, M., Gill, P. M. W., Johnson, B., W., C., Wong, M. W., Andres, J. L., Gonzalez, C., Head-Gordon, M., Replogle, E. S., Pople, J. A. In *Gaussian 03*; G. Inc, Ed.; Gaussian Inc: Pittsburgh PA, 2003.

[21] Sun, X., Collum, D. B., Lithium diisopropylamide-mediated enolizations: solvent-independent rates, solvent dependent mechanisms, *J. Am. Chem. Soc.* **2000**, *122*, 2452.

[22] Seebach, D., Maetzke, T., Petter, W., Klotzer, B., Plattner, D., Pyramidalization and reactivity of trigonal centers. X-ray crystal structure analysis of two silyl enol ethers from 1-benzoyl- and 1-(methoxycarbonyl)-2-tert-butyl-3,5-dimethyl-4-imidazolidinone (reagents for amino acid synthesis), *J. Am. Chem. Soc.* **1991**, *113*, 1781.

[23] Mai, A., Di Santo, R., Massa, S., Artico, M., Pantaleoni, G. C., Giorgi, R., Coppolino, M. F., Barracchini, A., Pyrrolobenzodiazepines with antinociceptive activity, *Eur. J. Med. Chem.* **1995**, *30*, 593.

Chapter 6. Experimental Procedures for 1,4-Benzodiazepin-2,5-diones

6.1 General Information

THF was distilled from Na/benzophenone immediately before use. *(S)* and (*R*)-proline, trans-4-hydroxy-*R*-proline, cis-4-hydroxy-*S*-proline, (*R/S*)-pipecolic acid, (*S*)-thioproline, (*S*)-serine, and (*S*)-threonine were all purchased from Acros and were used as received. (*S*)-MeAla-OH was purchased from Advanced ChemTech. Systematic names were developed for all novel compounds based on examples described in the literature.[1-3] Enantiomeric excess of all synthesized compounds was assessed by HPLC (Chiralcel AD or OD). ^{1}H NMR Spectra were recorded on JEOL Eclipse 500 and Varian Inova 400 MHz NMR Spectrometers. Variable temperature ^{1}H NMR measurements were performed on a Varian Unity 400 MHz NMR. Identity and purity of the synthesized compounds were further confirmed in the following way. High resolution mass spectra recorded under FAB conditions (NBA. PEG), in each case gave the expected molecular formula (M+1) as the closest match among all possible formulas. Chiral stationary phase HPLC indicated >95% chemical purity in each case.

6.2 Tabulation of HPLC Conditions and Retention Times for 1,4-Benzodiazepin-2,5-diones

Reported retention times are determined from racemic and enantiomerically enriched/pure samples. The HPLC columns are not thermostatted and as a consequence retention times are subject to day-to-day variability.

compound	column	solvent, flow rate	fast enantiomer retention time (config)	slow enantiomer retention time (config)
1a	AD	10% isopropanol-hexane, 1mL/min	26.5 min (*3R*)	34.0 min (*3S*)
2a	AD	20% isopropanol-hexane, 1mL/min	9.2 min (*3R*)	12.1 min (*3S*)
1b	AD	20% isopropanol-hexane, 1mL/min	7.0 min (*3R*)	9.4 min (*3S*)
2b	AD	20% isopropanol-hexane, 1mL/min	6.1 min (*3R*)	8.6 min (*3S*)
3b	AD	20% isopropanol-hexane, 1mL/min	6.4 min (*3S*)	8.5 min (*3R*)
4b	AD	20% isopropanol-hexane, 1mL/min	7.7 min (*3S*)	10.4 min (*3R*)
5b	AD	20% isopropanol-hexane, 1mL/min	7.1 min (*3S*)	9.9 min (*3R*)
6b	AD	20% isopropanol-hexane, 1mL/min	6.9 min (*3R*)	9.1 min (*3S*)
1c	AD	20% isopropanol-hexane, 1mL/min	18.6 min (*3R*)	21.1 min (*3S*)
3c	OD	20% isopropanol-hexane, 1mL/min	8.3 min (*3S*)	9.8 min (*3R*)
4c	OD	20% isopropanol-hexane, 1mL/min	9.2 min (*3S*)	11.3 min (*3R*)
5c	OD	20% isopropanol-hexane, 1mL/min	11.0 min (*3S*)	13.5 min (*3R*)
6c	OD	20% isopropanol-hexane, 1mL/min	7.8 min (*3R*)	10.1 Min (*3S*)
28a	OD	20% isopropanol-hexane, 1mL/min	13.4 min (*3R*)	15.8 min (*3S*) [a]
28b	OD	20% isopropanol-hexane, 1mL/min	7.9 min (*3R*)	9.3 min (*3S*) [a]
36	OD	20% isopropanol-hexane, 1mL/min	11.0 min (*3R*)	14.2 min (*3S*) [a]
37	OD	20% isopropanol-hexane, 1mL/min	9.8 min (*3R*)	12.3 min (*3S*) [a]

[a]the absolute stereochemistry is assigned based on the assumption of retentive alkylation

6.3 Synthetic Procedures

6.3.1 (*S*)-Proline-derived 1,4-benzodiazepin-2,5-dione project

1,2,3,11a(*S*)-tetrahydro-5*H*-pyrrolo[2,1-*c*][1,4]benzodiazepine-5,11(10*H*)-diones (*S*)-(+)-**8** and (*S*)-(+)-**1a** were prepared according to the literature method.[2] Isopropyl triflate was prepared according to the literature method [4] immediately before use and was dispensed as a solution in CCl_4. Dianisylmethyl bromide was synthesized according to the literature method.[5]

General procedure for N1 alkylation with DAM-Br

At 0 °C to a stirred solution of the 1,4-benzodiazepin-2,5-dione (2.768 mmol, 1.0 equiv) in dry THF (10.0 mL) was added NaH (3.10 mmol, 1.12 equiv, 60% suspension in mineral oil) in one portion. The resulting solution was stirred at 0 °C for 30 min before the addition of DAM-Br (8.33 mmol, 3.0 equiv). The reaction mixture was stirred for a further 120 min at 0 °C, at which point TLC (70:30 EtOAc:hexane) indicated the reaction was complete. The reaction was quenched at 0 °C with 40 ml of saturated aqueous NH_4Cl solution, and extracted with CH_2Cl_2 (3 x 60 mL). The combined extracts were dried over anhydrous Na_2SO_4, filtered, and concentrated. The crude product was purified by flash column chromatography on silica gel (70:30 EtOAc:hexane) affording the *N*-DAM 1,4-benzodiazepin-2,5-dione.

General sequential protocol for C3-alkylation

At –78 °C or -100 °C under nitrogen, to a stirred solution of the 1,4-benzodiazepin-2,5-dione (0.15 mmol, 1.0 equiv) and HMPA (0.90 mmol, 6.0 equiv) in anhydrous THF (3.0 mL) was added LDA (0.15 mmol, 1.2 equiv, 1.5 M in hexanes) and the mixture stirred for a further time *t*. The electrophile (1.5 mmol, 10 equiv) was then added dropwise via syringe at –78 °C or -100 °C and the reaction was stirred at this temperature until the starting benzodiazepine was consumed (TLC). The reaction was quenched at –78 °C or -100 °C by the addition of saturated aqueous NH_4Cl (5.0 mL) and extracted with CH_2Cl_2 (3 x 10 mL). The combined extracts were dried over anhydrous Na_2SO_4, filtered, and concentrated. The crude product was purified by flash column chromatography on silica gel (70:30 EtOAc:hexanes).

General in situ protocol for C3-alkylation At -100 °C under nitrogen, to a stirred solution of the 1,4-benzodiazepin-2,5-dione (0.15 mmol, 1.0 equiv) and HMPA (0.90 mmol, 6.0 equiv) in anhydrous THF (3.0 mL) the electrophile was added (1.5 mmol, 10 equiv) and the mixture was stirred for 15 min. KHMDS (0.15 mmol, 1.2 equiv, 0.5 M) was then added via syringe and the mixture stirred at -100 °C until the starting benzodiazepine was consumed (TLC). The reaction was quenched at -100 °C by the addition of saturated aqueous NH_4Cl (5.0 mL) and extracted with CH_2Cl_2 (3 x 10 mL). The combined extracts were dried over anhydrous Na_2SO_4, filtered, and concentrated. The crude product was purified by flash column chromatography on silica gel (70:30 EtOAc:hexanes).

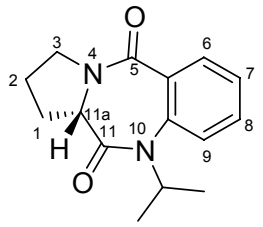

(11a*S*)-(+)-10-isopropyl-1,2,3,11a-tetrahydro-5*H*-pyrrolo[2,1-*c*][1,4]benzodiazepine 5,11(10*H*)-dione (*S*)-(+)-1b

At 0 °C to a stirred solution of 1,2,3,11a(*S*)-tetrahydro-5*H*-pyrrolo[2,1-*c*][1,4]benzodiazepine-5,11(10*H*)-dione (*S*)-(+)-**8** (299 mg, 1.384 mmol, 1.0 equiv) in dry THF (5.0 mL) was added NaH (62.0 mg, 1.550 mmol, 1.12 equiv, 60% suspension in mineral oil) in one portion. The resulting solution was stirred at 0 °C for 30 min before the dropwise addition of *i*-PrOTf (800 mg, 4.152 mmol, 3.0 equiv). The reaction mixture was stirred for a further 20 min at 0 °C, at which point TLC (70:30 EtOAc:hexane) indicated the reaction was complete. The reaction was quenched at 0 °C with 20 mL of saturated aqueous NH_4Cl solution, and extracted with CH_2Cl_2 (3 x 30 mL). The combined extracts were dried over anhydrous Na_2SO_4, filtered, and concentrated. The crude product was purified by flash column chromatography on silica gel (70:30 EtOAc:hexane) affording 292 mg (82%) of (3*S*)-(+)-**1b** as a white foam. Chiral stationary-phase HPLC (Chiralcel AD) indicated >99.5% ee. $[\alpha]_D^{26}$ = +426 (c = 1 in MeOH) ;^{1}H NMR ($CDCl_3$) δ 1.23 (d, *J* = 6.7 Hz, 3H), 1.50 (d, *J* = 7.1 Hz, 3H), 1.97 (m, 2H), 2.11 (m, 1H), 2.69 (m, 1H), 3.53 (m, 1H), 3.77 (m,1H), 3.97 (m, 1H), 4.49 (m, 1H), 7.32 (m, unassigned aromatic protons 2H), 7.46 (m, 1H), 7.85 (dd, *J* = 9.5 Hz, *J* = 1.6 Hz 1H); ^{13}C NMR ($CDCl_3$) δ 14.11, 20.34, 20.95, 21.94, 23.85, 26.37, 46.31, 52.55, 58.09, 60.29, 123.80, 126.23, 129.87, 131.12, 131.83, 165.13,

169.46, 171.02; HRMS (FAB) calcd for $C_{15}H_{18}N_2O_2$ [M + H]+ 259.1368, found 259.1462 (+6.0 ppm, +1.6 mmu).

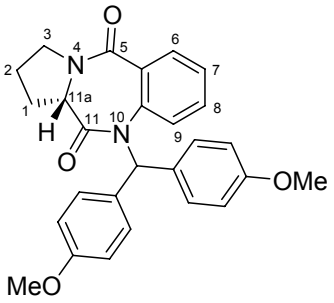

(11a*S*)-(+)-10-dianisylmethyl-1,2,3,11a-tetrahydro-5*H*-pyrrolo[2,1-*c*][1,4]benzodiazepine 5,11(10*H*)-dione (*S*)-(+)-1c

The general method described in Section 6.3 was followed with (*S*)-(+)-**8** (580 mg, 2.768 mmol), NaH (74 mg, 3.10 mmol, 1.12 equiv, 60% suspension in mineral oil) and DAM-Br (2.54 g, 8.33 mmol, 3.0 equiv) in THF (10.0 mL). Purification with flash chromatography on silica gel (70:30 EtOAc:hexane) provided (3*S*)-(+)-**1c** in 93% yield (1.08 g). Chiral stationary-phase HPLC (Chiralcel AD) indicated >99.5% ee. $[\alpha]_D^{26}$ = +189 (c = 1 in MeOH) ; ^{1}H NMR ($CDCl_3$) δ 2.02 (m, 4H), 2.70 (m, 1H), 3.58 (m, 1H), 3.74 (s, 3H), 3.80 (s, 3H), 4.20 (m, 1H), 6.60 (s,1H), 6.73 (dd, *J* = 14.8 Hz, *J* = 4.8 Hz 2H), 6.86 (dd, *J* = 14.8 Hz, *J* = 4.8 Hz, 2H) , 7.13 (m, unassigned aromatic protons 3H), 7.78 (dd, *J* = 9.6 Hz, *J* = 4.0 Hz, 1H); ^{13}C NMR ($CDCl_3$) δ 23.84, 26.62, 46.45, 55.19, 55.29, 58.11, 113.63, 113.68, 124.53, 126.24, 128.99, 129.74, 130.53, 131.08, 131.34, 131.65, 139.29, 158.65, 158.79, 165.29, 169.42 ; HRMS (FAB) 442.189258 calcd for $C_{28}H_{26}N_2O_4$ [M + H]+, found 443.19690(-0.4 ppm, -0.2 mmu).

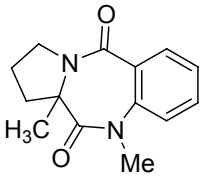

10,11a-dimethyl-1,2,3,11a-tetrahydro-5*H*-pyrrolo[2,1-*c*][1,4]benzodiazepine 5,11(10*H*)-dione 2a

The sequential method described above was followed with compound **1a** (34.6 mg, 0.15 mmol, 1.0 equiv), HMPA (161 μL, 0.90 mmol, 6.0 equiv), LDA (100 μL, 0.15 mmol, 1.2 equiv, 1.5 M in hexanes) and MeOTf (246 μL, 1.5 mmol, 10 equiv) in anhydrous THF (3.0 mL). Purification with flash column chromatography (70:30 EtOAc:hexane) gave 27 mg of **2a** (75% yield). Chiral stationary-phase HPLC (Chiralcel AD) indicated racemic product.

^{1}H NMR ($CDCl_3$) δ 1.01 (s, 3H), 2.04 (m, 3H), 2.75 (m, 1H), 3.43 (s, 3H), 3.58 (m, 1H), 3.88 (m, 1H), 7.23 (dd, *J* = 9.2 Hz, *J* = 0.8 Hz, 1H), 7.24 (t, *J* = 16.0 Hz, 1H), 7.13 (m, unassigned aromatic protons 1H), 7.84 (dd, *J* = 9.2 Hz, *J* = 0.8 Hz, 1H); ^{13}C NMR ($CDCl_3$) δ 20.58, 21.59, 31.70, 34.92, 40.21, 60.55, 124.53, 126.24, 128.99, 129.74, 130.53, 139.30, 169.77, 175.30 ; HRMS (FAB) calcd for $C_{14}H_{16}N_2O_2$ [M + H]+ 245.121178 , found 245.178309 (-0.1 ppm, -0.3 mmu).

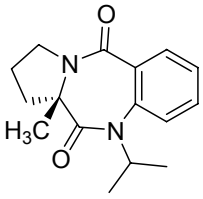

(11a*S*)-(+)-11a-methyl-10-isopropyl-1,2,3,11a-tetrahydro-5*H*-pyrrolo[2,1-*c*][1,4]benzodiazepine 5,11(10*H*)-dione (*3S*)-(+)-2b

The sequential method described above was followed with compound (*S*)-(+)-**1b** (38.8 mg, 0.15 mmol, 1.0 equiv), HMPA (160 μL, 0.90 mmol, 6.0 equiv), LDA (100 μL, 0.15 mmol, 1.2 equiv, 1.5 M in hexanes) and MeOTf (246 μL, 1.5 mmol, 10 equiv) in

anhydrous THF (4.0 mL). Purification with flash column chromatography (70:30 EtOAc:hexane) gave 28 mg of (3*S*)-(+)-**2b** (69% yield).

Chiral stationary-phase HPLC (Chiralcel AD) indicated >99.5% ee. $[\alpha]_D^{26}$ = +137.7 (c = 1.0 in MeOH) ; ^{1}H NMR ($CDCl_3$) δ 1.25 (s, 3H), 1.57 (d, *J* = 6.7 Hz, 3H), 1.77 (d, *J* = 7.1 Hz, 3H), 1.86 (m, 3H), 3.12 (m, 1H), 3.51 (m, 1H), 4.02 (m, 1H), 4.43 (m,1H), 7.32 (m, unassigned aromatic protons 2H), 7.48 (m, 1H), 7.85 (dd, *J* = 9.5 Hz, *J* = 1.6 Hz 1H); ^{13}C NMR ($CDCl_3$) δ 20.58, 21.82, 21.98, 22.39, 40.02, 49.04, 54.01, 65.31, 122.92, 126.01, 130.29, 131.48; HRMS (FAB) calcd for $C_{16}H_{20}N_2O_2$ [M + H]+ 273.1524, found 273.1592 (-4.0 ppm, -1.1 mmu).

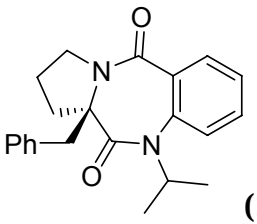

(11a*R*)-(+)-11a-benzyl-10-isopropyl-1,2,3,11a-tetrahydro-5*H*-pyrrolo[2,1-*c*][1,4]benzodiazepine 5,11(10*H*)-dione (3*R*)-(+)-3b

The in situ method described above was followed with compound (*S*)-(+)-**1b** (39.1 mg, 0.15 mmol, 1.0 equiv), HMPA (160 μL, 0.90 mmol, 6.0 equiv), KHMDS (300 μL, 0.15 mmol, 1.2 equiv, 0.5 M in hexanes) and BnBr (141 μL, 1.5 mmol, 10 equiv) in anhydrous THF (3.2 mL). Purification with flash column chromatography (70:30 EtOAc:hexane) gave 41 mg of (3*R*)-(+)-**3b** (78% yield). Chiral stationary-phase HPLC (Chiralcel AD) indicated >99.5% ee. $[\alpha]_D^{26}$ = +259.4 (c = 1.0 in MeOH) ;^{1}H NMR ($CDCl_3$) δ 1.33 (d, *J* = 7.1 Hz, 3H), 1.55 (d, *J* = 5.1 Hz, 3H), 1.65 (m, 1H), 1.73 (m, 1H), 1.95 (m, 1H), 2.46 (d, *J* = 13.5 Hz, 1H), 2.59 (d, *J* = 13.5 Hz, 1H) 2.92 (m, 1H), 3.39 (m,1H), 4.04 (m, 1H), 4.51 (m, 1H) 6.89 (d, *J* = 7.5 Hz, 2H) 7.18 (m, unassigned aromatic protons 4H), 7.35 (m,

1H), 7.54 (m, 1H), 7.98 (d, J = 7.9 Hz, 1H); ^{13}C NMR ($CDCl_3$) δ 20.40, 21.75, 36.85, 39.66, 49.65, 49.65, 54.20, 123.06, 126.28, 127.08, 128.42, 129.59, 130.46, 131.20, 131.78, 135.45, 139.06, 159.19, 165..43, 170.23; HRMS (FAB) calcd for $C_{22}H_{24}N_2O_2$ [M + H]+ 349.1837, found 349.1923 (+2.0 ppm, +0.7 mmu).

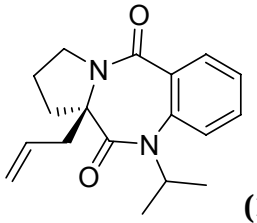

(11a*R*)-(+)-11a-allyl-10-isopropyl-1,2,3,11a-tetrahydro-5*H*-pyrrolo[2,1-*c*][1,4]benzodiazepine 5,11(10*H*)-dione (3*R*)-(+)-4b

The in situ method described above was followed with compound (*S*)-(+)-**1b** (38.6 mg, 0.15 mmol, 1.0 equiv), HMPA (160 μL, 0.90 mmol, 6.0 equiv), KHMDS (300 μL, 0.15 mmol, 1.2 equiv, 0.5 M in hexanes) and allyl-Br (178 μL, 1.5 mmol, 10 equiv) in anhydrous THF (3.5 mL). Purification with flash column chromatography (70:30 EtOAc:hexane) gave 34 mg of (3*R*)-(+)-**4b** (75% yield). Chiral stationary-phase HPLC (Chiralcel AD) indicated 98% ee. $[\alpha]_D^{26}$ = +389.7 (c = 1.0 in MeOH) ;^{1}H NMR ($CDCl_3$) δ 1.33 (d, J = 7.1 Hz, 3H), 1.54 (d, J = 6.7 Hz, 3H), 1.88 (m, 2H), 1.99 (m, 3H), 3.09 (m, 1H), 3.25 (m, 1H), 4.09 (m,1H), 4.49 (m, 1H), 4.77 (dd, J = 18.7 Hz, J = 1.9 Hz , 1H), 5.02 (ddd, J = 11.9, Hz J = 1.9,Hz J = 1.1 Hz, 1H) 7.32 (m, unassigned aromatic protons 2H), 7.51 (m, 1H), 7.88 (dd, J = 9.5 Hz, J = 1.6 Hz 1H); ^{13}C NMR ($CDCl_3$) δ 20.49, 21.78, 21.85, 21.88, 37.01, 38.65, 49.53, 54.02, 68.32, 119.67, 122.84, 126.07, 130.47, 130.84, 131.29, 131.59, 138.92, 165.36, 170.41; HRMS (FAB) calcd for $C_{18}H_{22}N_2O_2$ [M + H]+ 299.1681, found 299.1762 (+0.9 ppm, +0.3 mmu).

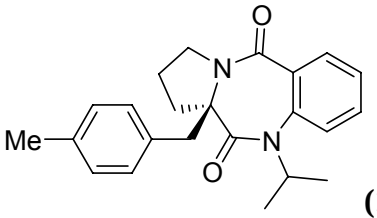

(11a*R*)-(+)-11a-*p*-methylbenzyl-10-isopropyl-1,2,3,11a-tetrahydro-5*H*-pyrrolo[2,1-*c*][1,4]benzodiazepine 5,11(10*H*)-dione (3*R*)-(+)-5b

The in situ method described above was followed with compound (*S*)-(+)-**1b** (38.8 mg, 0.15 mmol, 1.0 equiv), HMPA (160 μL, 0.90 mmol, 6.0 equiv), KHMDS (300 μL, 0.15 mmol, 1.2 equiv, 0.5 M in hexanes) and 4-methyl-benzyl bromide (274 μL, 1.5 mmol, 10 equiv) in anhydrous THF (4.0 mL). Purification with flash column chromatography (70:30 EtOAc:hexane) gave 50 mg of (3*R*)-(+)-**5b** (92% yield). Chiral stationary-phase HPLC (Chiralcel AD) indicated 99% ee. $[\alpha]_D^{26}$ = + 98.6 (c = 1.0 in MeOH) ;^{1}H NMR ($CDCl_3$) δ 1.33 (d, *J* = 7.1 Hz, 3H), 1.54 (d, *J* = 6.7 Hz, 3H), 1.65 (m, 1H), 1.72 (m, 1H), 1.95 (m, 1H), 2.27 (s, 3H), 2.40 (d, *J* = 13.9 Hz, 1H), 2.54 (d, *J* = 13.5 Hz, 1H), 2.87 (m, 1H), 3.41 (m, 1H), 4.03 (m, 1H), 4.50 (m, 1H), 6.77 (d, *J* = 7.9 Hz, 2H), 7.01 (d, *J* = 7.5 Hz, 2H), 7.36 (m, unassigned aromatic protons 2H), 7.53 (m, 1H), 7.95 (dd, *J* = 9.1 Hz, *J* = 1.1 Hz, 1H); ^{13}C NMR ($CDCl_3$) δ 20.36, 20.47, 20.97, 21.14, 21.71, 36.75, 39.14, 49.62, 54.11, 69.54, 123.01, 126.19, 129.07, 129.39, 130.41, 131.70, 132.25, 136.64, 139.05, 165.39, 170.30; HRMS (FAB) calcd for $C_{23}H_{26}N_2O_2$ [M + H]+ 363.1994, found 363.2076 (+1.0 ppm, +0.4 mmu).

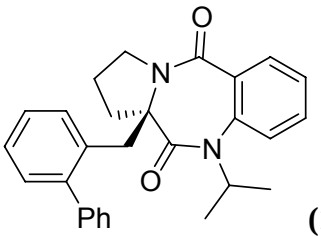

(11a*R*)-(+)-11a-*o*-phenylbenzyl-10-isopropyl-1,2,3,11a-tetrahydro-5*H*-pyrrolo[2,1-*c*][1,4]benzodiazepine 5,11(10*H*)-dione (3*R*)-(+)-6b

The in situ method described above was followed with compound (*S*)-(+)-**1b** (38.8 mg, 0.15 mmol, 1.0 equiv), HMPA (160 μL, 0.90 mmol, 6.0 equiv), KHMDS (300 μL, 0.15 mmol, 1.2 equiv, 0.5 M in hexanes) and 2-phenylbenzyl bromide (369 μL, 1.5 mmol, 10 equiv) in anhydrous THF (4.0 mL). Purification with flash column chromatography (70:30 EtOAc:hexane) gave 52 mg of (3*R*)-(+)-**6b** (82% yield). Chiral stationary-phase HPLC (Chiralcel AD) indicated 95% ee. $[\alpha]_D^{26}$ = +198.6 (c = 1.0 in MeOH) ;^{1}H NMR ($CDCl_3$) δ 1.32 (d, *J* = 7.1 Hz, 3H), 1.25 (m, 1H), 1.49 (m, 2H), 1.55 (d, *J* = 6.7 Hz, 3H), 2.64 (m, 1H), 2.67 (dd, 2H), 3.29 (m, 1H), 3.84 (m, 1H), 4.50 (m, 1H), 6.97 (m,1H), 7.1-7.4 (m, unassigned aromatic protons 11H), 7.54 (m, 1H), 7.91 (dd, *J* = 9.5 Hz, *J* = 1.6 Hz 1H); ^{13}C NMR ($CDCl_3$) δ 20.39, 21.42, 21.77, 34.61, 35.62, 49.49, 54.15, 70.13, 123.09, 126.34, 126.83, 127.09, 127.46, 128.38, 129.09, 129.57, 130.40, 130.64, 131.30, 131.79, 133.28, 138.92, 141.30, 143.02; HRMS (FAB) calcd for $C_{28}H_{28}N_2O_2$ [M + H]+ 425.2150, found 425.2228 (-0.2 ppm, -0.1 mmu).

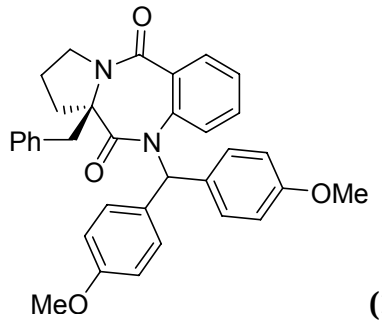

(11a*R*)-(+)-11a-benzyl-10-dianisylmethyl-1,2,3,11a-tetrahydro-5*H*-pyrrolo[2,1-*c*][1,4]benzodiazepine 5,11(10*H*)-dione (3*R*)-(+)-3c

The in situ method described above was followed with compound (*S*)-(+)-**1c** (66.3 mg, 0.15 mmol, 1.0 equiv), HMPA (160 μL, 0.90 mmol, 6.0 equiv), KHMDS (300 μL, 0.15 mmol, 1.2 equiv, 0.5 M in hexanes) and BnBr (142 μL, 1.5 mmol, 10 equiv) in anhydrous THF (5.0 mL). Purification with flash column chromatography (70:30 EtOAc:hexane) gave 78 mg of (3*R*)-(+)-**3c** (98% yield). Chiral stationary-phase HPLC (Chiralcel AD) indicated 98% ee. $[\alpha]_D^{26}$ = +200.3(c = 1.0 in MeOH) ;^{1}H NMR ($CDCl_3$) δ 1.59 (m, 2H), 2.00 (m, 1H), 2.73 (d, *J* = 13.5 Hz, 1H), 2.77 (d, *J* = 13.5 Hz, 1H) 3.01 (m, 1H), 3.39 (m, 1H), 3.81 (s, 3H), 3.82 (s, 3H), 4.04 (m, 1H), 6.41 (s, 1H), 6.89 (d, *J* = 7.5 Hz, 2H) 7.02-7.34 (m, unassigned aromatic protons 14H), 7.98 (dd, *J* = 9.7 Hz, *J* = 1.6 Hz, 1H); ^{13}C NMR ($CDCl_3$) δ 21.66, 37.37, 40.07, 49.63, 55.19, 69.67, 69.79, 113.30, 113.66, 123.78, 126.38, 127.13, 128.45, 128.97, 129.79, 130.00, 130.29, 130.81, 130.86,131.744, 131.91, 131.12, 139.98, 158.47, 158.71, 165.48, 170.22; HRMS (FAB) calcd for $C_{34}H_{32}N_2O_4$ [M + H]+ 533.236208 , found 533.24261(-2.7 ppm, -1.4 mmu).

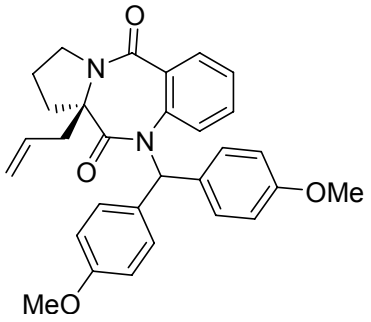

(11a*R*)-(+)-11a-allyl-10-dianisylmethyl-1,2,3,11a-tetrahydro-5*H*-pyrrolo[2,1-*c*][1,4]benzodiazepine 5,11(10*H*)-dione (3*R*)-(+)-4c

The in situ method described above was followed with compound (*S*)-(+)-**1c** (66.0 mg, 0.15 mmol, 1.0 equiv), HMPA (160 μL, 0.90 mmol, 6.0 equiv), KHMDS (300 μL, 0.15 mmol, 1.2 equiv, 0.5 M in hexanes) and allyl-Br (176 μL, 1.5 mmol, 10 equiv) in anhydrous THF (5.0 mL). Purification with flash column chromatography (70:30 EtOAc:hexane) gave 45 mg of (3*R*)-(+)-**4c** (65% yield). Chiral stationary-phase HPLC (Chiralcel AD) indicated 93% ee. $[\alpha]_D^{26}$ = +340.0 (c = 1.0 in MeOH) ;^{1}H NMR ($CDCl_3$) δ 1.30 (m, 1H), 1.78 (m, 1H), 1.92 (m, 1H), 2.09 (m, 1H), 2.21 (m, 1H), 3.04 (m, 1H), 3.44 (m,1H), 3.76 (s, 3H), 3.79 (s, 3H), 4.01 (m, 1H), 4.75 (d, *J* = 16.8 Hz, 1H), 5.09 (d, *J* = 10.4 Hz, 1H), 5.54 (M, 1H), 6.49 (s, 1H), 6.76 (m, unassigned aromatic protons 4H), 7.21 (m,unassigned aromatic protons, 7H), 7.82 (dd, *J* = 9.5 Hz, *J* = 1.6 Hz 1H); ^{13}C NMR ($CDCl_3$) δ 21.72, 36.95, 38.70, 49.53, 54.02, 68.35, 113.35, 113.60, 119.67, 123.47, 126.06, 129.05, 130.07, 130.25, 130.50, 131.17, 131.51, 131.65, 138.92, 158.66 165.36, 170.43; HRMS (FAB) calcd for $C_{30}H_{30}N_2O_4$ [M + H]+, 483.220558 found 483.22745 (-2.1 ppm, -1.0 mmu).

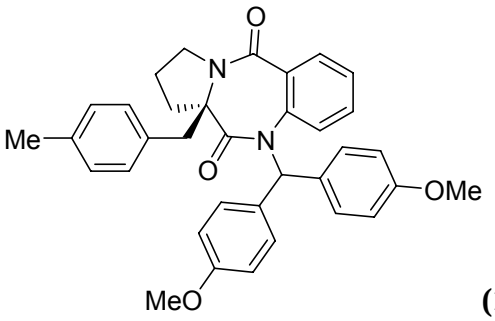

(11a*R*)-(+)-10-dianisylmethyl-11a-*p*-methylbenzyl-1,2,3,11a-tetrahydro-5*H*-pyrrolo[2,1-*c*][1,4]benzodiazepine 5,11(10*H*)-dione (3*R*)-(+)-5c

The in situ method described above was followed with compound (*S*)-(+)-**1c** (66.7 mg, 0.15 mmol, 1.0 equiv), HMPA (160 μL, 0.90 mmol, 6.0 equiv), KHMDS (300 μL, 0.15 mmol, 1.2 equiv, 0.5 M in hexanes) and 4-methyl-benzyl bromide (275 μL, 1.5 mmol, 10 equiv) in anhydrous THF (5.0 mL). Purification with flash column chromatography (70:30 EtOAc:hexane) gave 76 mg of (3*R*)-(+)-**5c** (93% yield). Chiral stationary-phase HPLC (Chiralcel AD) indicated >99.5% ee. $[\alpha]_D^{26}$ = 130.1 (c = 1.0 in MeOH) ;^{1}H NMR ($CDCl_3$) δ 1.42 (m, 1H), 1.99 (m, 1H), 2.32 (s, 1H), 2.63 (d, *J* = 14.0 Hz, 1H), 2.72 (d, *J* = 14.0 Hz, 1H), 2.99 (m, 1H), 3.36 (M, 1H), 3.78 (s, 3H), 3.79 (s, 3H), 6.38 (s, 1H), 6.77 (m, unassigned aromatic protons 5H), 7.53 (m, unassigned aromatic protons 10H), 7.95 (dd, *J* = 9.6 Hz, *J* = 2.0 Hz, 1H); ^{13}C NMR ($CDCl_3$) δ 21.04, 21.69, 37.43, 39.69, 55.16, 69.74, 73.35, 113.26, 113.60, 123.80, 126.34, 128.99, 129.13, 129.66, 129.98, 130.30, 130.78, 131.66, 131.89, 131.97, 136.71, 139.91, 158.45, 158.66, 170.32; HRMS (FAB) calcd for $C_{35}H_{34}N_2O_4$ [M + H]+ 547.251858, found 547.26190(+4.1 ppm, +2.2 mmu).

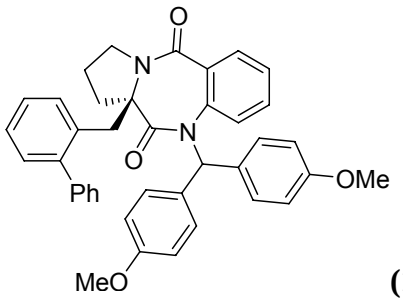

(11a*R*)-(+)-10-dianisylmethyl-11a-*o*-phenylbenzyl 1,2,3,11a-tetrahydro-5*H*-pyrrolo[2,1-*c*][1,4]benzodiazepine 5,11(10*H*)-dione (3*R*)-(+)-6c

The in situ method described above was followed with compound (*S*)-(+)-**1c** (66.1 mg, 0.15 mmol, 1.0 equiv), HMPA (160 μL, 0.90 mmol, 6.0 equiv), KHMDS (300 μL, 0.15 mmol, 1.2 equiv, 0.5 M in hexanes) and 2-phenylbenzyl bromide (370 μL, 1.5 mmol, 10 equiv) in anhydrous THF (5.0 mL). Purification with flash column chromatography (70:30 EtOAc:hexane) gave 88 mg of (3*R*)-(+)-**3c** (94% yield). Chiral stationary-phase HPLC (Chiralcel AD) indicated 99% ee. $[\alpha]_D^{26} = +86.7$ (c = 1.0 in MeOH) ;^{1}H NMR ($CDCl_3$) δ 1.29 (m, 2H), 1.47 (m, 1H), 2.52 (m, 1H), 2.70 (d, *J* = 14.8 Hz, 1H), 2.77 (d, *J* = 14.8 Hz, 1H), 3.25 (m, 1H), 3.74 (s, 3H), 3.75 (s, 3H), 3.85 (m, 1H), 6.37 (s, 1H), 6.73 (m, unassigned aromatic protons 4H), 7.03 (m, unassigned aromatic protons 15H), 7.82 (dd, *J* = 9.6 Hz, *J* = 21.6 Hz, 1H; ^{13}C NMR ($CDCl_3$) δ 21.48, 35.30, 36.12, 49.47, 55.18, 69.62, 70.06, 113.34, 113.70, 123.69, 126.33, 126.78, 127.07, 127.50, 128.25, 128.94, 129.19, 129.37, 129.92, 130.38, 130.52, 131.01, 131.77, 131.84, 133.05, 139.82, 141.08, 142.95, 158.49, 158.74, 170.28; HRMS (FAB) calcd for $C_{40}H_{36}N_2O_4$ [M + H]+ 609.267508, found 609.1228 (-0.4 ppm, -0.1 mmu).

General procedure for hydrolysis of 10-isopropyl-1,2,3,11a-tetrahydro-5*H*-pyrrolo[2,1-*c*][1,4]benzodiazepine 5,11(10*H*)-diones to the corresponding quaternary amino acids.

The 10-isopropyl-1,2,3,11a-tetrahydro-5*H*-pyrrolo[2,1-*c*][1,4]benzodiazepine 5,11(10*H*)-dione to be hydrolyzed (0.1 mmol) was combined with hydrochloric acid (6.0 M, 2.0 mL) in a pressure tube (Teflon screw cap) and heated at 140 °C (bath temperature) for 3 days. Water (2.0 mL) was then added and the mixture was extracted with EtOAc (3 x 3mL) to remove the aminobenzophenone. The water layer was separated, concentrated *in vacuo* and the residue dissolved in EtOH (2.0 mL). Propylene oxide (0.3 mL) was added, and the resulting solution was heated at reflux for 30 minutes. Upon cooling the precipitated solid was collected and washed with ethyl acetate and acetone, affording the corresponding free amino acid.

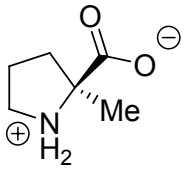

(*S*)-(-)-α-methylproline 10

27.2 mg (0.1 mmol) of (*3S*)-(+)-**7b** was treated as above to afford (*S*)-α-methylproline (78%). ^{1}H NMR (CD_3OD) δ 1.72 (s, 3H), 2.08 (m, 2H), 2.20 (m, 1H), 2.47 (m, 1H), 3.48 (m, 2H); $[\alpha]_D^{18}$ = -76.2° (c= 1, H_2O). Acros (*S*)-α-methylproline is: $[\alpha]_D^{18}$ = -83.1°, (c = 1, H_2O). We thus assign (*S*)-stereochemistry to our synthesized amino acid.

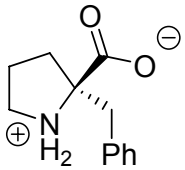

(*R*)-(-)-α-benzylproline 11

34.8 mg (0.1 mmol) of (*3S*)-(+)-**9b** was treated as above to afford (*R)*-α-benzylproline (85%). ^{1}H NMR (D_2O) δ 1.80 (m, 1H), 1.97 (m, 2H), 2.19 (m, 1H), 2.94 (d, *J* = 14.3 Hz 1H), 3.26 (m, 1H), 3.38 (d, *J* = 14.7 Hz, 1H); $[\alpha]_D^{25}$ = -18.15° (c= 1.2, H_2O). Literature rotation value for (*R*)-α-benzylproline is $[\alpha]_D$ = -19.25°, (c = 1.2, H_2O, 25°C).[6]

General procedure for removal of DAM from (11a*R*)-(+)-10-dianisylmethyl-1,2,3,11a-tetrahydro-5*H*-pyrrolo[2,1-*c*][1,4]benzodiazepine 5,11(10*H*)-diones (3*R*)-(+)-3c and (3*R*)-(+)-4c

The benzodiazepin-2,5-dione (0.1 mmol) was combined with trifluoroacetic acid (2.5 mL) and dichloromethane (7.5 mL). The reaction is stirred at ambient temperature for 3 hours. Volatiles were removed under reduced pressure to afford an orange oil which was purified by preparatory thin layer chromatography (80:20 EtOAc:hexanes).

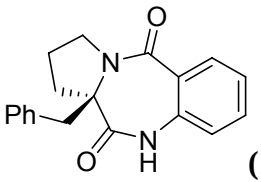

(11a*R*)-benzyl-1,2,3,11a-tetrahydro-5*H*-pyrrolo[2,1-*c*][1,4]benzodiazepine 5,11(10*H*)-dione (*R*)-(+)-12

Compound (3*R*)-(+)-**3c** (60.0 mg, 0.10 mmol) was treated as described above to quantitatively yield the desired compound **12**. $[\alpha]_D^{26}$ = +105.6 (c = 1.0 in MeOH); ^{1}H NMR ($CDCl_3$) δ 1.64 (m, 2H), 2.08 (m, 1H), 2.84 (d, *J* = 14.0 Hz, 1H), 2.85 (d, *J* = 14.0 Hz, 1H), 2.95 (m, 1H), 3.49 (m, 1H), 4.01 (m, 1H), 6.98 (m, unassigned aromatic protons 3H), 7.27 (m, unassigned aromatic protons 5H), 7.52 (t, *J* = 8.0 Hz, 1H), 8.32 (bs, 1H);

^{13}C NMR ($CDCl_3$) δ 21.46, 35.33, 39.29, 50.49, 68.19, 119.74, 125.09, 126.47, 127.37, 128.63, 129.85, 131.57, 132.94, 134.81, 135.12, 165.19, 172.02; HRMS (FAB) calcd for $C_{19}H_{18}N_2O_2$ [M + H]+ 307.136828, found 307.1329 (-1.0 ppm, -0.8 mmu).

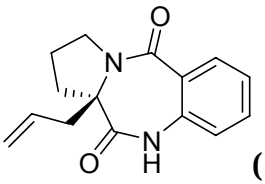

(11a*R*)-allyl-1,2,3,11a-tetrahydro-5*H*-pyrrolo[2,1-*c*][1,4]benzodiazepine 5,11(10*H*)-dione (*R*)-(+)-13

Compound (3*R*)-(+)-**4c** (60.0 mg, 0.10 mmol) was treated as described above to afford compound **13** in 96%.$[\alpha]_D^{26}$ = +54.2 (c = 1.0 in MeOH); ^1H NMR ($CDCl_3$) δ 1.80 (m, 1H), 1.93 (m, 1H), 2.02 (m, 1H), 2.10 (m, 1H), 2.32 (m, 1H), 3.09 (m, 1H), 3.58 (m, 1H), 3.60 (m, 1H), 4.04 (m, 1H), 4.90 (d, *J* = 16.8 Hz, 1H), 5.12 (dd, *J* = 10.8 Hz, *J* = 0.8 Hz ,1H), 5.78 (m, 1H), 6.98 (d, *J* =8.0 Hz, 1H), 7.29 (m, unassigned aromatic proton 1H), 7.49 (m, unassigned aromatic proton, 1H), 8.04 (dd, *J* = 8.8 Hz, *J* = 1.2 Hz ,1H), 8.34 (bs, 1H); ^{13}C NMR ($CDCl_3$) δ 21.68, 35.49, 38.15, 50.40, 66.95, 119.58, 120.41, 124.83, 126.11, 130.69, 131.51, 132.76, 135.12, 165.13, 172.11); HRMS (FAB) calcd for $C_{15}H_{16}N_2O_2$ [M + H]+ 257.113353, found 257.1284 (-1.9 ppm, -0.5 mmu).

6.3.2 Hydroxy proline-derived 1,4-benzodiazepin-2,5-dione project

2-hydroxy-1,2,3,11a-tetrahydro-5*H*-pyrrolo[2,1-*c*][1,4]benzodiazepine 5,11(10*H*)-diones (3*R*,13*S*)-**16** and (3*S*,13*S*)-**17** were prepared according to the literature method in 77 and 65% yield, respectively.[3] Dianisylmethyl bromide was also synthesized according to the literature method.[5]

General synthesis for TBDMS protection of 2-hydroxy-1,2,3,11a-tetrahydro-5*H*-pyrrolo[2,1-*c*][1,4]benzodiazepine 5,11(10*H*)-diones (3*R*,13*S*)-18 and (3*S*,13*S*)-19[3]

(3*R*,13*S*)-**16** or (3*S*,13*S*)-**17** (0.9 mmol, 1 equiv) was combined with *tert*-butyldimethylsilyl chloride (2.0 mmol, 2.2 equiv) and imidazole (4.5 mmol, 5.0 equiv) in DMF and stirred at room temperature for 12 hours. The reaction mixture was partitioned between CH_2Cl_2 (2 x 50 mL) and H_2O (50 mL). The organic layers were dried (Na_2SO_4), filtered and the solvent was evaporated under reduced pressure. The crude was purified using flash column chromatography (50:50 EtOAc:hexane) on silica gel to yield the desired products (3*R*,13*S*)-**18** (89%) and (3*S*,13*S*)-**19** (92%) as white solids.

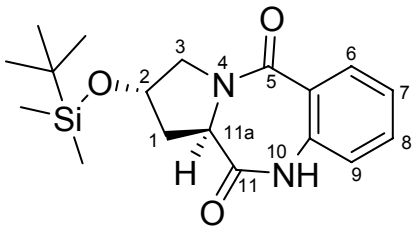

(2*S*,11a*R*)-(-)-2-[(*tert*-butyldimethylsilyl)oxy]-1,2,3,11a-tetrahydro-5*H*-pyrrolo[2,1-*c*][1,4]benzodiazepine 5,11(10*H*)-dione (3*R*,13*S*)-18[3]

(3*R*,13*S*)-**16** (213.0 mg, 0.918 mmol) was reacted with TBDMS-Cl (304.0 mg, 2.01 mmol) and imidazole (312.9 mg, 4.57 mmol) in DMF to afford the title compound (3*R*,13*S*)-**18** (218.0 mg, 89%). ^{1}H NMR indicated >98% de. $[\alpha]_D^{26}$ = -215.9 (c = 1.0 in MeOH); ^{1}H NMR ($CDCl_3$) δ 0.04 (s, 3H), 0.05 (s, 3H), 0.82 (s, 9H), 2.05 (m, 1H), 2.80 (m, 1H), 3.72 (m,2H), 4.19 (m, 1H), 4.57 (m, 1H), 6.96 (d, *J* =8.0 Hz, 1H), 7.22 (m,

unassigned aromatic proton, 1H), 7.44 (m, unassigned aromatic proton, 1H), 7.98 (dd, *J* = 9.2 Hz, *J* = 1.6 Hz ,1H), 8.42 (bs, 1H); ^{13}C NMR ($CDCl_3$) δ -1.19, -0.09, 17.95, 25.72, 35.45, 54.36, 55.64, 69.39, 120.90, 125.15, 126.79, 131.49, 132.34, 135.30, 165.80, 170.92; HRMS (FAB) calcd for $C_{18}H_{26}N_2O_3Si$ [M + H]+ 347.171271, found 347.1768 (-6.6 ppm, -2.3 mmu).

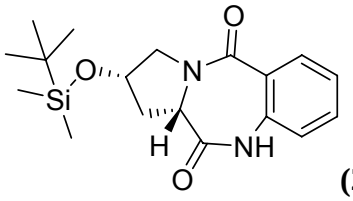

(2*S*,11a*S*)-(+)-2-[(*tert*-butyldimethylsilyl)oxy]-1,2,3,11a-tetrahydro-5*H*-pyrrolo[2,1-*c*][1,4]benzodiazepine 5,11(10*H*)-dione (3*S*,13*S*)-19

(3*S*,13*S*)-**17** (212.4 mg, 0.915 mmol) was reacted with TBDMS-Cl (303.5 mg, 2.01 mmol) and imidazole (311.6 mg, 4.57 mmol) in DMF to afford the title compound (3*R*,13*S*)-**19** (282.0 mg, 92%). Proton NMR indicated >98% de. $[\alpha]_D^{26}$ = +311.7 (c = 1.0 in MeOH); ^{1}H NMR ($CDCl_3$) δ 0.03 (s, 3H), 0.04 (s, 3H), 0.80 (s, 9H), 2.20 (m, 1H), 2.82 (m, 1H), 3.49 (dd, *J* = 17.2 Hz, *J* = 5.2 Hz ,1H), 3.93 (dd, *J* = 17.2 Hz, *J* = 5.2 Hz , 1H), 4.05 (m, 1H), 4.42 (m, 1H), 7.02 (d, *J* =8.0 Hz, 1H), 7.20 (m, unassigned aromatic proton, 1H), 7.43 (m, unassigned aromatic proton, 1H), 7.98 (dd, *J* = 9.2 Hz, *J* = 1.6 Hz ,1H), 9.08 (bs, 1H); ^{13}C NMR ($CDCl_3$) δ 0.00, 0.80, 22.90, 30.57, 39.62, 59.93, 60.89, 74.04, 125.88, 129.68, 130.71, 136.23, 137.52, 140.67, 171.02, 176.56; HRMS (FAB) calcd for $C_{18}H_{26}N_2O_3Si$ [M + H]+ 347.171271, found 347.1768 (-6.6 ppm, -2.3 mmu).

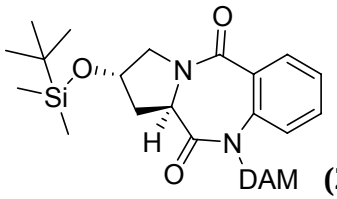

(2*S*,11a*R*)-(-)-2-[(*tert*-butyldimethylsilyl)oxy]-10-dianisylmethyl-1,2,3,11a-tetrahydro-5*H*-pyrrolo[2,1-*c*][1,4]benzodiazepine 5,11(10*H*)-dione (3*R*,13*S*)-(-)-20

The DAM group was installed at the N1 position according to the general method previously described in Section 6.3. (3*R*,13*S*)-**16** (934 mg, 2.76 mmol), NaH (75 mg, 3.10 mmol, 1.12 equiv, 60% suspension in mineral oil) and DAM-Br (2.54 g, 8.33 mmol, 3.0 equiv) in THF (10.0 mL). Purification with flash chromatography on silica gel (70:30 EtOAc:hexane) provided 137 mg of the title compound (3*R*,13*S*)-(-)-**20** (89% yield). Proton NMR indicated >98% de $[\alpha]_D^{26}$ = -190.1 (c = 1.0 in MeOH); ^{1}H NMR ($CDCl_3$) δ 0.03 (s, 6H), 0.81 (s, 9H), 1.98 (m, 1H), 2.80 (m, 1H), 3.56 (m,1H), 3.68 (s, 3H), 3.76 (s, 3H), 4.30 (m, 1H), 4.57 (m, 1H), 6.63 (s, 1H), 6.67 (dd, *J* =8.0 Hz, *J* =1.6 Hz, 1H), 6.82 (m, unassigned aromatic proton, 1H), 6.90-7.15 (m, unassigned aromatic proton, 9H), 7.74 (dd, *J* = 8.0 Hz, *J* = 1.6 Hz ,1H); ^{13}C NMR ($CDCl_3$) δ -0.02, 0.96, 20.13, 32.61, 40.36, 57.30, 60.03, 62.48, 71.01, 74.31, 118.57, 118.74, 131.33, 133.18, 133.66, 134.05, 134.06, 135.33, 135.36, 135.46, 136.09, 144.17, 163.55, 165.71, 170.85, 173.47 ; HRMS (FAB) calcd for $C_{33}H_{41}N_2O_5Si$ [M + H]+ 574.270651, found 574.1259 (-1.2 ppm, -0.5 mmu).

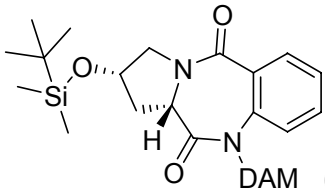

(2*S*,11a*S*)-(+)-2-[(*tert*-butyldimethylsilyl)oxy]-10-dianisylmethyl-1,2,3,11a-tetrahydro-5*H*-pyrrolo[2,1-*c*][1,4]benzodiazepine 5,11(10*H*)-dione (3*S*,13*S*)-(+)-23

The DAM group was installed at the N1 position according to the general method previously described in Section 6.3. (3*S*,13*S*)-**16** (935 mg, 2.76 mmol), NaH (75 mg, 3.10 mmol, 1.12 equiv, 60% suspension in mineral oil) and DAM-Br (2.51 g, 8.33 mmol, 3.0 equiv) in THF (10.0 mL). Purification with flash chromatography on silica gel (70:30 EtOAc:hexane) provided 126 mg of the title compound (3*S*,13*S*)-(+)-**23** (82% yield). Proton NMR indicated >98% de. $[\alpha]_D^{26}$ = +214.6 (c = 1.0 in MeOH); ^{1}H NMR ($CDCl_3$) δ 0.00 (s, 3H), 0.08 (s, 3H), 0.86 (s, 9H), 2.57 (m, 1H), 2.84 (m, 1H), 3.24 (m,1H), 3.73 (s, 3H), 3.79 (s, 3H), 4.14 (m, 2H), 4.37 (m, 1H), 6.63 (s, 1H), 6.72 (dd, *J* =8.0 Hz, *J* =1.6 Hz, 1H), 6.87 (m, unassigned aromatic proton, 1H), 7.18-7.24 (m, unassigned aromatic proton, 9H), 7.76 (dd, *J* = 8.0 Hz, *J* = 1.6 Hz ,1H); ^{13}C NMR ($CDCl_3$) δ 0.00, 0.76, 22.93, 30.64, 39.36, 57.40, 60.06, 61.48, 72.23, 74.31, 118.57, 118.74, 129.33, 131.18, 132.66, 134.05, 134.76, 135.33, 135.36, 135.46, 136.09, 144.17, 163.55, 163.71, 170.65, 173.47 HRMS (FAB) calcd for $C_{33}H_{41}N_2O_5Si$ [M + H]+ 574.270651, found 574.1259 (-1.2 ppm, -0.5 mmu).

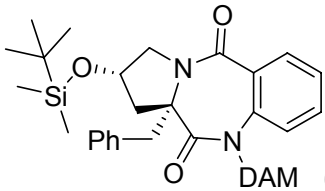

(2*S*,11a*R*)-(+)-2-[(*tert*-butyldimethylsilyl)oxy]-11a-benzyl-10-dianisylmethyl-1,2,3,11a-tetrahydro-5*H*-pyrrolo[2,1-*c*][1,4]benzodiazepine 5,11(10*H*)-dione (13*S*,3*R*)-(+)-22

The general in situ protocol described in Section 6.3 was implemented (without HMPA-see Chapter 5, section 5.3). (3*R*,13*S*)-**20** (85.2 mg, 0.15 mmol, 1.0 equiv), KHMDS (300 μL, 0.15 mmol, 1.2 equiv, 0.5 M in hexanes) and BnBr (143 μL, 1.5 mmol, 10 equiv) in anhydrous THF (4.0 mL). Purification with flash column chromatography (70:30 EtOAc:hexane) gave 48 mg of (13*S*,3*R*)-(+)-**22** (49% yield). $[\alpha]_D^{26}$ = +250.1 (c = 1.0 in MeOH); HLPC (20:80 *i-Pr*-OH:hexane, CHIRALPAK AD, 4.6 x 250 mm: 1.0 ml/min; UV detection at 254 nm) : 11.6 min, 92% de; ^{1}H NMR ($CDCl_3$) δ -0.04 (s, 3H), -0.03 (s, 3H), 0.79 (s, 9H), 2.02 (m, 1H), 2.67 (d, *J* =14.4 Hz, 1H), 2.85 (d, *J* =14.4 Hz, 1H) 3.05 (m, 1H), 3.26 (m,1H), 3.73 (s, 3H), 3.78 (s, 3H), 4.01 (m, 1H), 6.18 (s, 1H), 6.72 (dd, *J* =8.0 Hz, *J* =1.6 Hz, 1H), 6.81-7.34 (m, unassigned aromatic proton, 16H), 7.90 (dd, *J* = 7.6 Hz, *J* = 2 Hz ,1H); ^{13}C NMR ($CDCl_3$) δ 0.00, 0.06, 23.10, 30.83, 45.96, 50.17, 60.18, 60.25, 60.30, 72.34, 74.33, 75.77, 118.17, 118.77, 128.80, 131.76, 132.31, 133.58, 134.16, 134.31, 134.87, 135.10, 135.19, 135.62, 137.75, 137.12, 137.15, 140.06, 145.46, 163.62, 163.82, 170.74, 174.88 HRMS (FAB) calcd for $C_{40}H_{46}N_2O_5Si$ [M + H]+ 662.31760, found 663.3255 (+0.1ppm, +0.1 mmu).

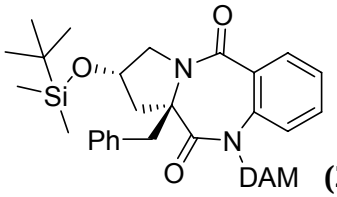

(2*S*,11a*S*)-(-)-2-[(*tert*-butyldimethylsilyl)oxy]-11a-benzyl-10-dianisylmethyl-1,2,3,11a-tetrahydro-5*H*-pyrrolo[2,1-*c*][1,4]benzodiazepine 5,11(10*H*)-dione (13*S*,3*S*)-(-)-25

The general in situ protocol described in Section 6.3 was implemented (without HMPA-see Chapter 5, section 5.3). (13*S*,3*S*)-**23** (86.0 mg, 0.15 mmol, 1.0 equiv), KHMDS (300 μL, 0.15 mmol, 1.2 equiv, 0.5 M in hexanes) and BnBr (144 μL, 1.5 mmol, 10 equiv) in anhydrous THF (4.0 mL). Purification with flash column chromatography (70:30 EtOAc:hexane) gave 94 mg of (13*S*,3*S*)-(-)-**25** (95% yield). $[\alpha]_D^{26}$ = -148.4 (c = 1.0 in MeOH); HLPC (20:80 *i-Pr*-OH:hexane, CHIRALPAK AD, 4.6 x 250 mm: 1.0 ml/min; UV detection at 254 nm) : 10.1 min, 96% de; ^{1}H NMR ($CDCl_3$) δ -0.12 (s, 3H), -0.04 (s, 3H), 0.77 (s, 9H), 2.20 (m, 1H), 2.48 (d, *J* =14.4 Hz, 1H), 2.91 (d, *J* =14.4 Hz, 1H) 3.48 (m, 2H), 3.69 (s, 3H), 3.74 (m,1H), 3.78 (s, 3H), 6.67 (s, 1H), 6.69 (dd, *J* =8.0 Hz, *J* =1.6 Hz, 1H), 6.84-7.22 (m, unassigned aromatic proton, 16H), 7.89 (dd, *J* = 7.6 Hz, *J* = 2 Hz ,1H); ^{13}C NMR ($CDCl_3$) δ 0.00, 0.22, 23.17, 30.92, 44.31, 49.14, 60.28, 60.33, 60.41, 60.46, 61.51, 71.72, 73.02, 74.27, 74.44, 118.78, 118.82, 118.88, 118.94, 129.28, 131.29, 132.53, 133.70, 133.87, 134.27,134.43, 134.98, 135.12, 135.22, 135.30, 135.54, 135.84, 135.89, 136.17, 136.50, 140.19, 143.75, 163.70, 163.87, 170.83, 175.91 HRMS (FAB) calcd for $C_{40}H_{46}N_2O_5Si$ [M + H]+ 662.31760, found 663.3255 (+0.1ppm, +0.1 mmu).

6.3.3 Thioproline-derived 1,4-benzodiazepin-2,5-dione project

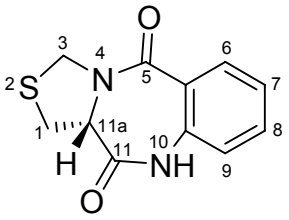

(11a*S*)-1,2,3,11a-tetrahydro-5*H*-(3-thiazolindine)[2,1-*c*][1,4]benzodiazepine 5,11(10*H*)-dione (*S*)-(+)-26

Commercially available (*S*)-thioproline (1.79 g, 13.49 mmol, 1.1 equiv) and isatoic anhydride (2.00 g, 12.29 mmol, 1 equiv) were heated at 115 °C in DMSO (7 mL) for 2 hours. The hot reaction mixture was poured into ice cold water (150 mL) and extracted with $CHCl_3$ (3 x 150 mL). The organic layers were combined and washed with brine (150 mL), and the dried over Na_2SO_4. The solvent was evaporated under reduced pressure to yield a yellow solid. The crude was recrystallized from ethanol and the desired product was obtained as a yellow solid in 87% yield (2.49 g). $[\alpha]_D^{26}$ = + 430.90 (c = 1.0 in MeOH); ^{1}H NMR ($CDCl_3$) δ 3.24 (dd, *J* = 12.0 Hz, *J* = 6.8 Hz, 1H), 3.85 (dd, *J* = 12.0 Hz, *J* = 6.8 Hz, 1H), 4.87 3.24 (dd, *J* = 12.0 Hz, *J* = 6.8 Hz, 1H), 4.72 (d, *J* = 10.8 Hz, 1H), 4.87 (d, *J* =10.8 Hz, 1H), 7.03 (dd, *J* =8.8 Hz, *J* = 1.6 Hz 1H), 7.27 (m, 1H), 7.49 (m, 1H), 7.98 (dd, *J* =8.8 Hz, *J* = 1.6 Hz 1H), 8.74 (bs, 1H); ^{13}C NMR ($CDCl_3$) δ 31.30, 50.27, 58.38, 120.99, 125.37, 126.21, 131.43, 133.01, 134.87, 169.74; HRMS (FAB) calcd for $C_{11}H_{10}N_2O_2S$ [M + H]+ 235.046300 found 235.1516 (-1.2 ppm, -0.5 mmu).

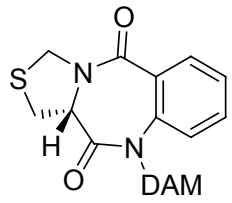

(11a*S*)-(+)-10-dianisylmethyl-1,2,3,11a-tetrahydro-5*H*-(3-thiazolindine)[2,1-*c*][1,4]benzodiazepine 5,11(10*H*)-dione (*S*)-(+)-27

The DAM group was installed at the N1 position according to the general method previously described in Section 6.3. (*S*)-(+)-**26** (63 mg, 2.76 mmol), NaH (73 mg, 3.10 mmol, 1.12 equiv, 60% suspension in mineral oil) and DAM-Br (2.53 g, 8.33 mmol, 3.0 equiv) in THF (5.0 mL). Purification with flash chromatography on silica gel (70:30 EtOAc:hexane) provided 288 mg of the title compound (*S*)-(+)-**27** (89% yield). $[\alpha]_D^{26}$ = + 184.4 (c = 1.0 in MeOH); HLPC (20:80 *i-Pr*-OH:hexane, CHIRALPAK OD, 4.6 x 250 mm: 1.0 ml/min; UV detection at 254 nm) : 15.2 min, 99.5% ee; ^{1}H NMR ($CDCl_3$) δ 3.14 (m, 1H), 3.66 (s, 3H), 3.76 (s, 3H), 3.84 (m, 1H), 4.4 (m, 1H), 4.53 (d, *J* =10.8 Hz, 1H), 4.88 (d, *J* =10.8 Hz, 1H), 6.64 (s, 1H) 6.67 (dd, *J* =8.8 Hz, *J* = 1.6 Hz 1H), 6.82 (d, *J* =8.8 Hz, 2H), 7.02 (d, *J* =8.8 Hz, 2H), 7.13 (m, unassigned aromatic proton, 6H), 7.76 (dd, *J* = 8.8 Hz, *J* = 1.6 Hz ,1H); ^{13}C NMR ($CDCl_3$) δ 31.55, 49.24, 55.12, 55.23, 59.40, 67.16, 113.68, 113.80, 124.61, 126.41, 128.95, 129.05, 129.98, 130.10, 130.32, 130.52, 130.78, 130.84, 131.46, 138.74, 158.71, 158.85, 164.51, 167.67 HRMS (FAB) calcd for $C_{26}H_{23}N_2O_4S$ [M + H]+ 461.145679, found 461.1516 (-3.5 ppm, -1.6 mmu).

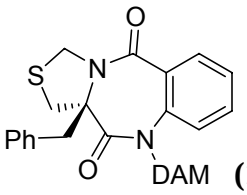

(11a*S*)-(+)-11a-benzyl-10-dianisylmethyl-1,2,3,11a-tetrahydro-5*H*-(3-thiazolindine)[2,1-*c*][1,4]benzodiazepine 5,11(10*H*)-dione (*S*)-(+)-28a

The general in situ protocol described in Section 6.3 was implemented (without HMPA-see Chapter 5, section 5.3). (*S*)-(+)-**27** (69.0 mg, 0.15 mmol, 1.0 equiv), KHMDS (300 μL, 0.15 mmol, 1.2 equiv, 0.5 M in hexanes) and BnBr (143 μL, 1.5 mmol, 10 equiv) in anhydrous THF (3.0 mL). Purification with flash column chromatography (70:30 EtOAc:hexane) gave 79 mg of (*S*)-(+)-**28a** (98% yield). Chiral stationary-phase HPLC (Chiralcel OD) indicated 99% ee. $[\alpha]_D^{26}$ = +89.7 (c = 1.0 in MeOH); ^{1}H NMR ($CDCl_3$) δ 3.62 (d, *J* = 14.4 Hz, 1H), 3.69 (d, *J* = 14.4 Hz, 1H), 3.70 (s, 3H), 3.74 (s, 3H), 4.49 (d, *J* =10.8 Hz, 1H), 4.97 (d, *J* =10.8 Hz, 1H), 5.42 (d, *J* =1.2 Hz, 1H), 5.70 (d, *J* =1.2 Hz, 1H), 6.44 (s, 1H) 6.77 (m, 4H), 7.20-7.32 (m, 10H), 7.07 (d, *J* =8.8 Hz, 2H), 7.13 (m, unassigned aromatic proton, 6H), 7.76 (dd, *J* = 8.8 Hz, *J* = 1.6 Hz ,1H) ; ^{13}C NMR ($CDCl_3$) δ 35.78, 51.12, 55.17, 67.59, 94.77, 113.53, 113.79, 117.85, 123.47, 126.18, 126.96, 128.36, 129.14, 129.71, 130.07, 130.24, 131.50; HRMS (FAB) calcd for $C_{33}H_{29}N_2O_4S$ [M + H]+ 550.184805, found 550.1255 (+4.1ppm, +2.2 mmu).

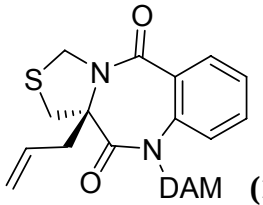

(11a*S*)-(+)-11a-allyl-10-dianisylmethyl-1,2,3,11a-tetrahydro-5*H*-(3-thiazolindine)[2,1-*c*][1,4]benzodiazepine 5,11(10*H*)-dione (*S*)-(+)-28b

The general in situ protocol described in Section 6.3 was implemented (without HMPA-see Chapter 5, section 5.3). (*S*)-(+)-**27** (70.1 mg, 0.15 mmol, 1.0 equiv), KHMDS (300 μL, 0.15 mmol, 1.2 equiv, 0.5 M in hexanes) and allyl-Br (176 μL, 1.5 mmol, 10 equiv) in anhydrous THF (3.5 mL). Purification with flash column chromatography (70:30 EtOAc:hexane) gave 66 mg of (*S*)-(+)-**28b** (89% yield). Chiral stationary-phase HPLC (Chiralcel OD) indicated 94% ee. $[\alpha]_D^{26}$ = +102.7 (c = 1.0 in MeOH); ^{1}H NMR ($CDCl_3$) δ 3.10 (m, 2H), 3.74 (s, 3H), 3.75 (m, 3H), 4.57 (d, *J* =14.0 Hz , 1H) 4.84 (d, *J* =14.0 Hz, 1H), 5.08 (d, *J* =14.0 Hz , 1H), 5.20 (d, *J* =14.0 Hz, 1H), 5.47 (d, *J* =1.6 Hz, 1H), 5.69 (d, *J* =1.6 Hz, 1H), 5.69 (m, 1H), 6.41 (s, 1H), 6.79- 6.82 (m, unassigned aromatic proton, 3H), 7.14-7.28 (m, unassigned aromatic proton, 8H), 7.66 (dd, *J* = 7.6 Hz, *J* = 2 Hz ,1H); ($CDCl_3$) δ 31.35, 38.41, 50.05, 53.12, 56.23, 60.20, 68.23, 113.68, 113.80, 114.52, 125.61, 126.71, 129.05, 130.15, 129.98, 130.10, 130.32, 130.52, 130.78, 130.84, 131.46, 138.36, 138.74, 158.71, 159.85, 165.51, 170.01 HRMS (FAB) calcd for $C_{29}H_{27}N_2O_4S$ [M + H]+ 500.176980, found 500.1747 (+4.5ppm, -2.3 mmu).

6.3.4 Oxaproline-derived 1,4-benzodiazepin-2,5-dione project

General procedure for the preparation of 3-(2-Nitro-benzoyl)-oxazolidine-4-carboxylic acids

The amino acid (serine or threonine, 47.57 mmol, 1 equiv) is stirred with formaldehyde (61.85 mmol, 1.3 equiv) and NaOH (10% mol) at 0 °C for 12 hours. The reaction mixture is cooled to -4 °C and $NaHCO_3$ (47.57 mmol, 1 equiv) dissolved in H_2O/acetone is added to the flask. Prepared *o*-nitrobenzoic acid chloride (52.37, 1.1 equiv) is added dropwise and the reaction is stirred for 1 hour. The reaction mixture was partitioned between ether (50 mL) and water (50 mL). The water layer is acidified with HCl (2 N) and extracted with ether (3 x 50 mL). The organic layers were combined and dried over Na_2SO_4, filtered and concentrated on vacuum to yield the desired product which was then used immediately without further purification.

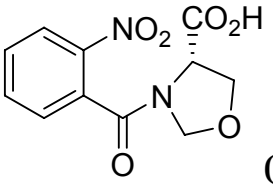

(4*S*)-3-(2-Nitro-benzoyl)-oxazolidine-4-carboxylic acid 33a

(*S*)-Serine (5.00 g, 47.57 mmol, 1 equiv) was reacted as described above with 40 % formaldehyde/water (6.15 mL, 61.85 mmol, 1.3 equiv), NaOH (0.22 g, 10% mol), $NaHCO_3$ (3.90 g, 47.57 mmol, 1 equiv) and *o*-nitrobenzoic acid chloride (9.68 g, 52.37 mmol, 1.1 equiv) to yield 9.31 g of **33a** (91%). The product was determined by ^{1}H NMR and used immediately without further purification. ^{1}H NMR ($CDCl_3$) δ 4.17 (m, 0.25H), 4.34 (m, 1.75H), 4.56 (d, *J* =3.6 Hz , 0.70H) 4.79 (d, *J* =3.6 Hz, 0.70H), 4.94 (m, 1H), 5.21 (d, *J* =3.6 Hz , 0.30H), 5.35 (d, *J* =3.6 Hz, 0.30H), 7.22-7.80- 6.82 (m, unassigned aromatic proton, 3H), 8.19 (m, unassigned aromatic proton, 1H), 10.20 (bs, 1H); ($CDCl_3$)

δ 18.43, 18.51, 62.80, 64.30, 78.71, 79.68, 94.77, 123.80, 124.87, 128.31, 130.36, 130.79, 131.02, 131.24, 132.59, 134.70, 165.56, 173.00 ; HRMS (FAB) calcd for $C_{11}H_{10}N_2O_3$ [M + H]+ 219.069143, found 219.0786 (+7.9 ppm, +1.7 mmu).

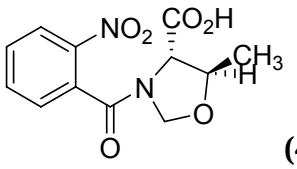

(4*S*,5*R*)-5-Methyl-3-(2-nitro-benzoyl)-oxazolidine-4-carboxylic acid (3*S*,12*R*)-33b

(*S*)-Threonine (5.66 g, 47.57 mmol, 1 equiv) was reacted with 40 % formaldehyde/water (6.14 mL, 61.85 mmol, 1.3 equiv), NaOH (0.22 g, 10% mol), $NaHCO_3$ (3.90 g, 47.57 mmol, 1 equiv) and *o*-nitrobenzoic acid chloride (9.72 g, 52.37 mmol, 1.1 equiv) to yield 8.72 g of **33b** (88%). The product was determined by ^{1}H NMR and used immediately without further purification. ^{1}H NMR ($CDCl_3$) δ 1.25 (d, *J* = 6.4 Hz, 1H), 1.40 (d, *J* = 6.4 Hz, 2H), 3.43 (m, 0.30H), 3.63 (d, *J* = 4.0 Hz, 0.30), 4.28 (m, 1.40H), 4.65 (d, *J* = 4.4 Hz, 0.70H), 4.70 (d, *J* = 4.4 Hz, 0.70H), 4.92 (d, *J* = 4.4 Hz, 0.30H), 5.48 (d, *J* = 4.4 Hz, 0.30H) 7.34-7.64 (m, unassigned aromatic proton, 3H), 8.05 (m, unassigned aromatic proton, 1H), 11.40 (bs, 1H); ($CDCl_3$) δ18.01, 60.23, 76.61, 79.18, 121.38, 125.08, 125.27, 131.24, 133.03, 135.23, 163.96, 169.93; HRMS (FAB) calcd for $C_{12}H_{12}N_2O_3$ [M + H]+ 233.084793, found 233.0927 (+0.8 ppm, +0.2 mmu).

General protocol for 7 membered oxaproline-derived benzodiazepine ring closure

To a mixture of **33a** or **33b** (9.32 mmol, 1 equiv) and Fe powder (66.17 mmol 7 equiv), CH_3OH (50 mL) and NH_4Cl (85.0 mmol, 9.1 equiv) in H_2O (30 mL) were added. The yellow suspension was heated to reflux for 12 hours. The black precipitate was

immediately filtered off the hot solution and the washed with hot CH_3OH (50 mL). The methanol was evaporated under reduced pressure, and the residue was partitioned between CH_2Cl_2 (2 x 150 mL) and 10% $NaHCO_3$ (150 mL). The organic layers were combined, dried ($NaSO_4$), filtered and the solvent was removed under vacuum. The crude yellow oil was purified via flash column chromatography (10:90 CH_3OH:CH_2Cl_2) to afford the desired product (**34a** or **34b**).

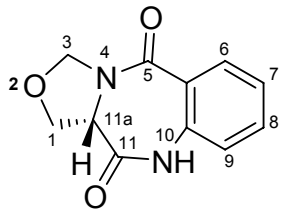

(11a*S*)-(+)-1,2,3,11a-tetrahydro-5*H*-(3-oxazolindine)[2,1-*c*][1,4]benzodiazepine 5,11(10*H*)-dione (*S*)-(+)-34a

33a (2.48 g, 9.32 mmol, 1equiv) and Fe powder (3.69 g, 66.17 mmol, 7 equiv) were refluxed as described above to yield the desired *N*-H 1,4-benzodiazepin-2,5-dione **34a** in 76% yield. $[\alpha]_D^{26}$ = +335.2 (c = 1.0 in MeOH); ^{1}H NMR ($CDCl_3$) δ 4.12 (m, 1H), 4.19 (m, 1H), 4.89 (m, 1H), 5.18 (d, *J* = 5.2 Hz, 1H), 5.23 (d, *J* = 5.2 Hz, 1H), 7.00 (d, *J* =8.0 Hz, 1H), 7.23 (m, 1H), 7.48 (m, 1H), 8.01 (dd, *J* =8.0 Hz, *J* =1.2 Hz, 1H), 8.41 (bs, 1H); ^{13}C NMR ($CDCl_3$) δ; 54.47, 68.09, 80.21, 94.77, 121.21, 125.46, 131.27, 133.13 HRMS (FAB) calcd for $C_{11}H_{10}N_2O_3$ [M + H]+ 219.069143, found 219.1603 (+0.8 ppm, -0.2 mmu).

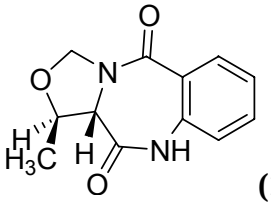

(1*R*,11a*S*)-(+)-1-methyl-1,2,3,11a-tetrahydro-5*H*-(3-oxazolindine)[2,1-*c*][1,4]benzodiazepine 5,11(10*H*)-dione (3*S*,12*R*)-(+)-34b

33b (2.61 g, 9.32 mmol) and Fe powder (3.69 g, 66.17 mmol) were refluxed as described above to yield the desired *N*-H 1,4-benzodiazepin-2,5-dione (3*S*,12*R*)-(+)-**34b** in 82% yield. $[\alpha]_D^{26}$ = +349.75 (c = 1.0 in MeOH); ^{1}H NMR ($CDCl_3$) δ 1.36 (d, *J* = 6.0 Hz , 3H), 3.61 (d, *J* = 6.4, 1H), 4.82 (m, 2H), 5.44 (d, *J* = 6.0 Hz, 1H), 7.06 (d, *J* =8.0, 1H), 7.18 (m, 1H), 7.42 (m, 1H), 7.92 (dd, *J* = 8.0 Hz, *J* = 1.2 Hz, 1H), 9.84 (bs, 1H); ^{13}C NMR ($CDCl_3$) δ 27.95, 54.47, 68.09, 80.21, 94.77, 121.21, 125.46, 129.25, 131.27, 133.13; HRMS (FAB) calcd for $C_{12}H_{12}N_2O_3$ [M + H]+ 233.084793, found 232.13092 (+5.1ppm, +2.2 mmu).

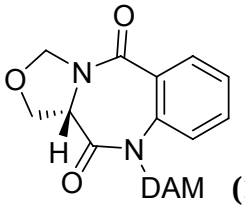

(11a*S*)-(+)-10-dianisylmethyl-1,2,3,11a-tetrahydro-5*H*-(3-oxazolindine)[2,1-*c*][1,4]benzodiazepine 5,11(10*H*)-dione (*S*)-(+)-35a

The general method described in Section 6.3 was followed with (*S*)-(+)-**34a** (494 mg, 2.768 mmol), NaH (74 mg, 3.10 mmol, 1.12 equiv, 60% suspension in mineral oil) and DAM-Br (2.54 g, 8.33 mmol, 3.0 equiv) in THF (10.0 mL). Purification with flash chromatography on silica gel (70:30 EtOAc:hexane) provided (*S*)-(+)-**35a** in 94% yield

(1.18 g). $[\alpha]_D^{26}$ = +191.0 (c = 1.0 in MeOH); HLPC (20:80 *i-Pr*-OH:hexane, CHIRALPAK AD, 4.6 x 250 mm: 1.0 ml/min; UV detection at 254 nm) : 20.2 min, 99.5% ee; ^{1}H NMR ($CDCl_3$) δ 3.68 (s, 3H), 3.76 (s, 3H), 4.12 (m, 1H), 4.21 (m, 1H), 4.81 (m, 1H), 5.12 (d, *J* =5.2 Hz, 1H), 5.13 (d, *J* = 5.2 Hz, 1H), 6.64 (s, 1H), 6.67 (d, *J* = 8.8 Hz, 2H), 6.82 (d, *J* =8.8 Hz, 2H), 7.02 (d, *J* = 8.8 Hz , 2H), 7.13 (d, *J* = 8.8 Hz, 2H), 7.22 (m, 3H), 7.79 (dd, *J* = 7.6 Hz, *J* = 2 Hz ,1H); ^{13}C NMR ($CDCl_3$) δ 31.30, 50.27, 58.38, 120.99, 125.37, 126.21, 131.43, 133.01, 134.87, 169.74; HRMS (FAB) calcd for $C_{26}H_{24}N_2O_5$ [M + H]+ 445.168523, found 445.1735 (-6.8 ppm, -3.0 mmu).

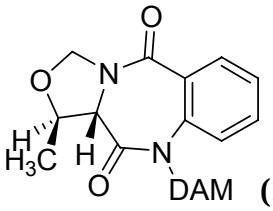

(1*R*,11a*S*)-(+)-1-methyl-10-dianisylmethyl-1,2,3,11a-tetrahydro-5*H*-(3-oxazolindine)[2,1-*c*][1,4]benzodiazepine 5,11(10*H*)- (3*S*,12*R*)-(+)-35b

The general method described in Section 6.3 was followed with (3*S*,12*R*)-(+)-**34b** (623 mg, 2.768 mmol), NaH (74 mg, 3.10 mmol, 1.12 equiv, 60% suspension in mineral oil) and DAM-Br (2.54 g, 8.33 mmol, 3.0 equiv) in THF (10.0 mL). Purification with flash chromatography on silica gel (70:30 EtOAc:hexane) provided (3*S*,12*R*)-(+)-**35b** in 92% yield (1.23 g). $[\alpha]_D^{26}$ = +225.2 (c = 1.0 in MeOH); HLPC (20:80 *i-Pr*-OH:hexane, CHIRALPAK OD, 4.6 x 250 mm: 1.0 ml/min; UV detection at 254 nm) : 11.30 min, 99.5% ee; ^{1}H NMR ($CDCl_3$) δ 1.35 (d, *J* = 6.0 Hz , 3H), 3.67 (s, 3H), 3.74 (s, 3H), 4.87 (m, 2H), 5.42 (d, *J* = 6.0 Hz, 1H), 6.59 (s, 1H), 6.69 (d, *J* = 8.8 Hz, 2H), 6.82 (d, *J* =8.8 Hz, 2H), 7.06 (d, *J* = 8.8 Hz , 2H), 7.15 (d, *J* = 8.8 Hz, 2H), 7.22 (m, 3H), 7.79 (dd, *J* = 7.6 Hz, *J* = 2 Hz ,1H); ^{13}C NMR ($CDCl_3$) δ 14.14, 17.86, 20.97, 55.09, 55.18, 60.13,

61.45, 67.46, 78.57, 113.63, 113.67, 124.81, 126.50, 129.02, 129.87, 129.96, 130.42, 130.84, 131.61, 138.97, 158.68, 158.82, 163.69, 167.53; HRMS (FAB) calcd for $C_{27}H_{26}N_2O_5$ [M + H]+ 459.184173, found 459.1951(+6.8 ppm, +3.1 mmu).

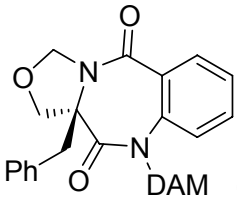

(11a*S*)-(+)-11a-benzyl-10-dianisylmethyl-1,2,3,11a-tetrahydro-5*H*-(3-oxazolindine)[2,1-*c*][1,4]benzodiazepine 5,11(10*H*)-dione (*S*)-(+)-36

The general in situ protocol described in Section 6.3 was implemented (without HMPA-see Chapter 5, section 5.3). (*S*)-**35a** (66.6 mg, 0.15 mmol, 1.0 equiv), KHMDS (300 μL, 0.15 mmol, 1.2 equiv, 0.5 M in hexanes) and BnBr (143 μL, 1.5 mmol, 10 equiv) in anhydrous THF (3.0 mL). Purification with flash column chromatography (70:30 EtOAc:hexane) gave 64 mg of (*S*)-(+)-**36** (82% yield). Chiral stationary-phase HPLC (Chiralcel OD) indicated 84% ee. $[\alpha]_D^{26}$ = +140.1 (c = 1.0 in MeOH); ^{1}H NMR ($CDCl_3$) δ 2.67 (d, *J* =14.0 Hz, 1H), 2.82, (d, *J* =14.0 Hz, 1H), 3.72 (s, 3H), 3.76 (s, 3H), 4.12 (d, *J* = 9.2 Hz , 1H) 4.89 (d, *J* = 9.2 Hz, 1H), 4.97 (d, *J* =5.6 Hz , 1H), 5.32 (d, *J* = 5.6 Hz, 1H), 6.51 (s, 1H), 6.67 (d, *J* = 8.8 Hz, 2H), 6.77 (d, *J* =8.8 Hz, 2H), 6.83 (m, 2H), 6.96 (m, 4H), 7.13 (d, *J* = 8.0 Hz, 1H), 7.24 (m, 5H), 7.66 (dd, *J* = 7.6 Hz, *J* = 2 Hz ,1H); ^{13}C NMR ($CDCl_3$) δ 14.01, 34.91, 55.12, 55.23, 55.69, 67.27, 76.32, 79.33, 113.64, 113.67, 124.98, 125.22, 126.51, 128.98, 129.39, 129.78, 129.96, 130.52, 130.7, 131.59, 138.82, 138.89, 158.70, 158.83, 163.39, 167.58; HRMS (FAB) calcd for $C_{33}H_{30}N_2O_5$ [M + H]+ 535.215473, found 535.2242 (+1.7 ppm, +0.9 mmu).

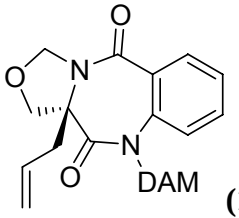

(11a*S*)-(+)-11a-allyl-10-dianisylmethyl-1,2,3,11a-tetrahydro-5*H*-(3-oxazolindine)[2,1-*c*][1,4]benzodiazepine 5,11(10*H*)-dione (*S*)-(+)-37

The general in situ protocol described in Section 6.3 was implemented (without HMPA-see Chapter 5, section 5.3). (*S*)-**35a** (67.8 mg, 0.15 mmol, 1.0 equiv), KHMDS (300 μL, 0.15 mmol, 1.2 equiv, 0.5 M in hexanes) and allyl bromide (178 μL, 1.5 mmol, 10 equiv) in anhydrous THF (3.0 mL). Purification with flash column chromatography (70:30 EtOAc:hexane) gave 31 mg of (*S*)-(+)-**37** (43% yield). Chiral stationary-phase HPLC (Chiralcel OD) indicated 45% ee. $[\alpha]_D^{26}$ = +15.1 (c = 1.0 in MeOH); ^{1}H NMR ($CDCl_3$) δ 2.19 (m, 2H), 3.70 (s, 3H), 3.78 (s, 3H), 4.01 (d, *J* = 9.2 Hz , 1H) 4.89 (d, *J* = 9.2 Hz, 1H), 4.94 (d, *J* =5.6 Hz , 1H), 5.06 (m, 2H), 5.36 (d, *J* =5.6 Hz , 1H), 5.58 (m, 1H), 6.51 (s, 1H), 6.68 (d, *J* = 8.8 Hz, 2H), 6.82 (d, *J* =8.8 Hz, 2H), 7.03 (d, *J* =8.8 Hz, 2H), 7.10 (d, *J* =8.8 Hz, 2H), 7.13-7.23 (m, 3H), 7.66 (dd, *J* = 7.6 Hz, *J* = 2 Hz ,1H);^{13}C NMR ($CDCl_3$) δ 14.23, 32.64, 55.02, 55.24, 55.71, 68.20, 68.25, 80.11, 80.33, 113.65, 113.67, 113.99, 123.78, 124.61, 128.98, 129.78, 129.96, 130.52, 130.7, 131.59, 138.02, 138.82, 158.70, 158.83, 163.39, 168.12; HRMS (FAB) calcd for $C_{29}H_{28}N_2O_5$ [M + H]+ 485.199823, found 485.2079 (-0.3 ppm, -0.2 mmu).

6.3.5 (*S*)-Alanine-derived 1,4-benzodiazepin-2,5-dione project

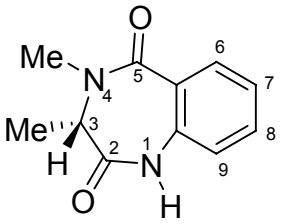

(3*S*)-(+)-3,4-dimethyl-1,4-benzodiazepin-2,5-dione (*S*)-(+)-40

(+)-**40** was prepared from *N*-methyl-(*S*)-alanine (500 mg, 4.4 mmol, 1 equiv) and isatoic anhydride (719 mg, 4.8 mmol, 1.1 equiv) based on the literature method described for (*R/S*)-alanine.[7] The crude was purified via flash column chromatography (10:90 CH_3OH:CH_2Cl_2) and the pure product (+)-**40** was afforded in 90% yield (881 mg). $[\alpha]_D^{26}$ = +210.8 (c = 1.0 in MeOH); ^{1}H NMR ($CDCl_3$) δ 1.49 (d, *J* = 6.8 Hz, 3H), 3.07 (s, 3H), 4.17 (q, *J* = 6.8 Hz, 1H), 7.06 (dd, *J* =8.8 Hz, *J* = 1.6 Hz 1H), 7.29 (m, 1H), 7.41 (m, 1H), 7.92 (dd, *J* =8.8 Hz, *J* = 1.6 Hz 1H), 9.77(bs, 1H); ^{13}C NMR ($CDCl_3$) δ 14.89, 29.92, 57.22, 120.20, 123.32, 126.76, 127.34, 129.72, 141.12, 166.43, 172.72; HRMS (FAB) calcd for $C_{11}H_{12}N_2O_2$ [M + H]+ 205.089878, found 205.0912 (+1.0ppm, -0.2 mmu).

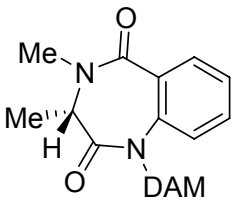

(3*S*)-(+)-1-dianisylmethyl-3,4-dimethyl-1,4-benzodiazepin-2,5-dione (*S*)-(+)-41

The general method described in Section 6.3 was followed with (*S*)-(+)-**40** (550 mg, 2.768 mmol), NaH (73 mg, 3.10 mmol, 1.12 equiv, 60% suspension in mineral oil) and DAM-Br (2.55 g, 8.33 mmol, 3.0 equiv) in THF (10.0 mL). Purification with flash chromatography on silica gel (70:30 EtOAc:hexane) provided (*S*)-(+)-**41** in 93% yield

(1.05 g). Chiral stationary-phase HPLC (Chiralcel OD) indicated 95% ee. $[\alpha]_D^{26} = +131.6$ (c = 1.0 in MeOH); ^{1}H NMR ($CDCl_3$) δ 1.47 (d, *J* = 6.8 Hz, 3H), 3.02 (s, 3H), 3.79 (s, 3H), 3.80 (s, 3H), 4.36 (q, *J* = 6.8 Hz, 1H), 6.55 (s, 1H), 7.01 (dd, *J* =8.8 Hz, *J* = 1.6 Hz, 2H), 7.11 (dd, *J* =8.8 Hz, *J* = 1.6 Hz, 2H), 7.12-7.26 (m, unassigned aromatic protons, 7H), 7.76 (dd, *J* =8.8 Hz, *J* = 1.6 Hz 1H); ^{13}C NMR ($CDCl_3$) δ 15.09, 28.83, 56.01, 57.22, 58.88, 113.21, 113.52, 120.18,120.20, 123.32, 126.76, 127.34, 129.65, 129.72, 135.33, 141.12, 149.09, 166.43, 172.72; HRMS (FAB) calcd for $C_{25}H_{27}N_2O_4$ [M + H]+ 420.197083, found 420.08772 (+1.2ppm, -0.4 mmu).

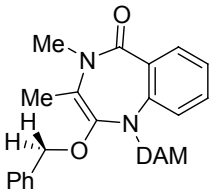

2-benzyloxy-11-dianisylmethyl-3,4-dimethyl-1,4-benzodiazepin-2,5-dione 43

At room temperature under nitrogen, to a stirred solution of the 1,4-benzodiazepin-2,5-dione (+)-**41** (64.5 mg, 0.15 mmol, 1.0 equiv) and HMPA (312 μL, 1.80 mmol, 12.0 equiv) in anhydrous THF (1.5 mL) benzyl bromide was added (179 μL, 1.5 mmol, 10 equiv) and the mixture was stirred for 15 min. KHMDS (1.5 mL, 7.5 mmol, 5 equiv, 0.5 M) was then added via syringe and the mixture stirred at room temperature for 1 hour. The reaction was quenched by the addition of saturated aqueous NH_4Cl (1.0 mL) and extracted with CH_2Cl_2 (3 x 5 mL). The combined extracts were dried over anhydrous Na_2SO_4, filtered, and concentrated. The crude product was purified by flash column chromatography on silica gel (70:30 EtOAc:hexane) and the O-benzylated product **43** was obtained in 87% yield. ^{1}H NMR ($CDCl_3$) δ 1.43 (s, 3H), 3.25 (s, 3H), 3.60 (s, 3H), 3.71 (s, 3H), 4.23 (d, *J* =11.1 Hz, 1H), 4.83 (d, *J* =11.1 Hz, 1H), 5.76 (s, 1H), 6.60 (d, *J* =

8.8 Hz, 2H), 6.74 (d, *J* =8.8 Hz, 2H), 6.98 (m, 2H), 7.01 (m, 1H), 7.15 (d, *J* =8.8 Hz, 2H), 7.17-7.23 (m, 5H), 7.31 (d, *J* =8.8 Hz, 2H), 7.66 (dd, *J* = 7.6 Hz, *J* = 2 Hz ,1H); HRMS (FAB) calcd for $C_{32}H_{33}N_2O_4$ [M + H]+ 510.244033, found 510.187563 (+1.2ppm, -0.4 mmu).

6.3.6 Pipecolic acid-derived 1,4-benzodiazepin-2,5-dione project

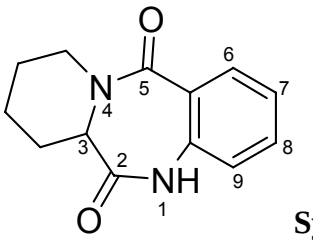

Synthesis of (±)-pyrido[2,1-*c*]-1,4-benzodiazepine-2,5-dione (±)-45[7]

Commercially available (±)-pipecolic acid (5.73 g, 35.19 mmol, 1.1 equiv) and isatoic anhydride (5.00 g, 38.70 mmol, 1 equiv) were heated at 100 °C in DMSO (7 mL) for 2 hours. The hot reaction mixture was poured into ice cold water (150 mL), the brown solid that formed was collected and recrystallized from ethanol to yield the desired product (±)-**45** as an off-white solid in 89% yield (7.19 g). The ^{1}H and ^{13}C spectra closely matched the spectra for compound **45** found in the literature.[7] ^{1}H NMR ($CDCl_3$) δ 1.68 (m, 5H), 2.21 (m, 1H), 2.98 (m, 1H), 4.15 (m, 1H), 4.51 (m, 1H) 6.89 (dd, *J* =8.0 Hz, *J* = 1.2 Hz 1H), 7.21 (m, 1H), 7.43 (m, 1H), 7.90 (dd, *J* = 8.0 Hz, *J* = 1.2 Hz, 1H), 7.95 (bs, 1H); ^{13}C NMR ($CDCl_3$) δ 19.19, 22.81, 23.21, 40.37, 51.14, 120.30, 125.22, 127.73, 131.30, 132.16, 135.72, 168.49, 171.78; HRMS (FAB) calcd for $C_{13}H_{14}N_2O_2$ [M + H]+ 231.105528, found 231.1130 (-1.5 ppm, -0.3 mmu).

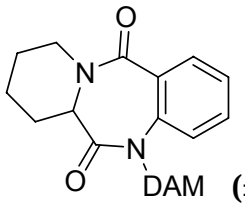

(±)-1-Dianisylmethyl-pyrido[2,1-*c*]-1,4-benzodiazepine-2,5-dione (±)-46

The general method described in Section 6.3 was followed with (±)-**45** (661 mg, 2.768 mmol), NaH (75 mg, 3.10 mmol, 1.12 equiv, 60% suspension in mineral oil) and DAM-Br (2.55 g, 8.33 mmol, 3.0 equiv) in THF (10.0 mL). Purification with flash chromatography on silica gel (70:30 EtOAc:hexane) provided (±)-**46** in 86% yield (1.02 g). ^{1}H NMR ($CDCl_3$) δ 1.59 (m, 5H), 2.19 (m, 1H), 2.76 (m, 1H), 3.71 (s, 3H), 3.75 (s, 3H), 4.25 (m, 1H), 4.51 (m, 1H), 6.46 (s, 1H), 6.72 (dd, *J* =8.0 Hz, *J* = 1.2 Hz 2H), 6.81 (dd, *J* =8.0 Hz, *J* = 1.2 Hz, 2H), 7.03-7.15 (m, 7H), 7.70 (dd, *J* = 8.0 Hz, *J* = 1.2 Hz, 1H); ^{13}C NMR ($CDCl_3$) δ 19.11, 23.21, 23.56, 40.29, 51.90, 55.13, 55.22, 113.51, 113.69, 123.30, 126.21, 129.08, 129.50, 130.21, 130.60, 130.92, 131.01, 131.43, 140.09, 158.59, 158.75, 168.61, 169.57; HRMS (FAB) calcd for $C_{28}H_{28}N_2O_4$ [M + H]+ 457.204908, found 457.0753 (-3.1 ppm, -1.2 mmu).

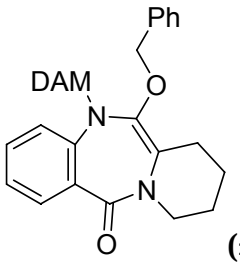

(±)-2-Benzyloxy-11-dianisylmethyl-pyrido[2,1-*c*][1,4] benzodiazepine-2,5-dione 48

At room temperature under nitrogen, to a stirred solution of the 1,4-benzodiazepin-2,5-dione **46** (69.7 mg, 0.15 mmol, 1.0 equiv) and HMPA (312 μL, 1.80 mmol, 12.0 equiv) in anhydrous THF (1.5 mL) benzyl bromide was added (179 μL, 1.5 mmol, 10 equiv) and the mixture was stirred for 15 min KHMDS (1,5 mL ,7.5 mmol, 5 equiv, 0.5 M) was then added via syringe and the mixture stirred at room temperature for 1 hour. The reaction was quenched by the addition of saturated aqueous NH_4Cl (1.0 mL) and extracted with CH_2Cl_2 (3 x 5 mL). The combined extracts were dried over anhydrous Na_2SO_4, filtered, and concentrated. The crude product was purified by flash column chromatography on silica gel (50:50 EtOAc:hexane) and the O-benzylated product **48** was obtained in 45% yield (36.0 mg); ^{1}H NMR ($CDCl_3$) δ 1.20 (m, 5H), 2.21 (m, 1H), 2.98 (m, 1H), 3.60 (s, 3H), 3.71 (s, 3H), 4.48 (d, *J* = 13.9 Hz, 1H), 4.67 (m, 1H), 4.77 (d, *J* = 13.9 Hz, 1H), 4.98 (m, 1H), 5.76 (s, 1H), 6.61 (dd, *J* =8.0 Hz, *J* = 1.2 Hz 2 H), 6.63 (dd, *J* =8.0 Hz, *J* = 1.2 Hz 2 H), 6.85 (m, 2H), 7.01 (m, 1H), 7.15 (m, 2H), 7.17-7.23 (m, 5H), 7.31 (d, *J* =8.8 Hz, 2H), 7.66 (dd, *J* = 7.6 Hz, *J* = 2 Hz ,1H); ^{13}C NMR ($CDCl_3$) δ 13.55, 29.92, 33.25, 55.26, 55.33, 65.40, 72.71, 114.10, 114.38, 121.55, 123.22, 127.87, 128.34, 128.39, 128.55, 130.73, 131.45, 168.49, 171.77; HRMS (FAB) calcd for $C_{35}H_{34}N_2O_4$ [M + H]+ 547.251858, found 547.3209 (+2.1 ppm, -0.8 mmu)**.**

6.4 Computational Details

Geometry optimizations and frequency calculations were performed using Gaussian03[8] at B3LYP/6-31G*; B3LYP electronic energies (ε_0) were calculated at the indicated basis set. Vibrational frequency analysis was used to identify stationary points as minima (number of imaginary frequencies (nimag) = 0) or transition states (nimag = 1). The displacement of the imaginary frequencies corresponded to the expected molecular motion for deprotonation and ring inversion transition structures. B3LYP/6-31G* Zero-point vibrational energies and Gibbs free energy correction (G_{corr}) were calculated from corrected frequencies (correction factor = 0.9804). Gibbs free energy G(*T*) is defined as the sum of ε_0 and G_{corr} (*T*). Thermodynamic corrections at 173K unless otherwise stated. Single point electronic energies were calculated at the B3LYP/6-31+G*//B3LYP/6-31G* level.

Structure	Energy Basis (B3LYP)	ε_0 (nimag) (hartrees)	Corr ZPVE (hartrees)	G_{corr} (*T*) (hartrees)	G(*T*) (hartrees)	Δ G (*T*)[b] (kcal/mol)
(M)-(S)-**1b**	6-31G*	-842.4254469 (0)	0.306643 (298K)	0.269422 (298K)	-842.162429	0 (298 K)
(P)-(S)-**1b**	6-31G*	-842.3968614 (0)	0.306795 (298K)	0.268863 (298K)	-842.134406	17.6 (298K)
(M)-(S)-**2b**	6-31G*	-881.734819 (0)	0.333882 (298 K)	0.289159 (298K)	-881.445660	0 (298K)
(P)-(S)-**2b**	6-31G*	-881.692183 (0)	0.332856 (298 K)	0.287567 (298K)	-881.404616	25.8 (298K)
(M)-(S)-**49b**	6-31G*	-1126.684672 (1)	0.464055	0.436840	-1126.247832	0.0
(M)-(S)-**49b**	6-31 + G*	-1126.716452	0.464055	0.436840	-1126.279612	0.0

(P)-(S)-**49b**	6-31G*	-1126.665622 (1)	0.464585	0.436722	-1126.228900	11.9
(P)-(S)-**49b**	6-31 + G*	-1126.697438	0.464585	0.436722	-1126.260716	11.9
(M)-(S)-**50b**	6-31G*	-1436.774273 (1)	0.624174	0.589601	-1436.167705	0.0
(M)-(S)-**50b**	6-31 + G*	-1436.813602	0.624710	0.590772	-1436.183501	0.0
(P)-(S)-**50b**	6-31G*	-1436.758723 (1)	0.624710	0.590772	-1436.222830	9.5
(P)-(S)-**50b**	6-31 + G*	-1436.797744	0.625265	0.590427	-1436.168296	9.7
(M)-**51b**	6-31G*	-841.820306 (0)	0.625265	0.590427	-1436.207317	0.0
(M)-**51b**	6-31 + G*	-841.864176	0.291016	0.270099	-841.550207	0.0
(M)-**51b*** [a]	6-31G*	-841.803209 (1)	0.291016	0.270099	-841.594077	11.0
(M)-**51b***	6-31 + G*	-841.845129	0.291285	0.270543	-841.532666	12.2
(M)-**52b**	6-31G*	-1314.510547 (0)	0.291285	0.270543	-841.574586	0.0
(M)-**52b**	6-31 + G*	-1314.549748	0.536242	0.504102	-1314.006445	0.0
(M)-**52b***[a]	6-31G*	-1314.487770 (1)	0.536242	0.504102	-1314.045646	15.5
(M)-**52b***	6-31 + G*	-1314.526140	0.536846	0.505978	-1313.981792	16.0

[a] One of a pair of enantiomeric ring inversion transition states.
[b] Relative free energies, calculated at the same basis/geometry

Cartesian Coordinates of (11a*S*)-(+)-10-isopropyl-1,2,3,11a-tetrahydro-5*H*-pyrrolo[2,1-*c*][1,4]benzodiazepine 5,11(10*H*)-dione (*M*)-(*S*)-1b

C	-2.344838098342	-0.250425028962	-0.978502512100
C	-2.182357482308	-0.639143061901	1.744159337060
C	-1.069934174786	-0.359299795758	-0.389913559179
C	-3.510080442891	-0.345786558481	-0.228247725676
C	-3.432234848855	-0.554343535692	1.148445143580
C	-0.986168572603	-0.531376325470	1.008289489863
H	-4.473222441322	-0.252855024532	-0.722596807054
H	-4.331744482190	-0.642091486905	1.750428619710
H	-2.084821773193	-0.800288478905	2.811183456241
N	0.053883501748	-0.352276347291	-1.269450856397
C	1.183718207676	0.406631025731	-1.072278687724
O	1.974315733451	0.631452829053	-1.984215641042
C	1.567697280623	0.948730813624	0.302938270903
N	1.390275330930	0.110652788054	1.494593199311
C	2.074412993097	0.885325623454	2.549717907555
H	1.724475673190	0.544207637617	3.522286293360
H	3.153977286981	0.712398311287	2.484581954214
C	1.128384665201	2.350197653564	0.778645928800
H	1.521626859122	3.144372022284	0.138355469973
H	0.036229955494	2.428152015431	0.793668887594
C	1.719118185287	2.374240012341	2.220321012272
H	2.610321406105	3.007256143807	2.273721216382
H	0.993773325935	2.769063039233	2.937581090962
H	2.653961294190	1.008408463886	0.172969148900
H	-2.419498345169	-0.081052364093	-2.045941520826
C	0.239751066089	-0.550909417355	1.883941042289
O	0.173649708757	-1.056183357879	3.001878552233
C	-0.066836672745	-1.103637208232	-2.565578809550
H	-0.979829253567	-1.690349730429	-2.442766132342
C	-0.232303816773	-0.197861064820	-3.794206961286
H	0.681973275921	0.365189662622	-3.984512575002
H	-1.054239738847	0.514911375268	-3.665546574233
H	-0.457516384602	-0.816416313437	-4.670915574917
C	1.085547787832	-2.104622016154	-2.730157633625
H	2.038488138844	-1.596814908783	-2.886325356101
H	0.883797715827	-2.740738862314	-3.599516870402
H	1.166155661865	-2.750469052123	-1.849387875459

Cartesian Coordinates of (11a*S*)-(+)-10-isopropyl-1,2,3,11a-tetrahydro-5*H*-pyrrolo[2,1-*c*][1,4]benzodiazepine 5,11(10*H*)-dione (*P*)-(*S*)-1b

H	0.609123176632	-1.966703208074	2.582889050295
C	0.298399255189	-0.927491810728	2.551636445492

C	-0.472411963238	1.733217466958	2.484379814166
C	-0.001990233258	-0.340273957271	1.309723867552
C	0.211364614918	-0.200957552876	3.734256606954
C	-0.184477830139	1.138173172298	3.706076132020
C	-0.371313132201	1.023094718084	1.278423474470
H	0.455335927721	-0.683208280773	4.676884306929
H	-0.264563627037	1.709849309747	4.625951890357
H	-0.797055053493	2.767007323668	2.426935081816
N	0.011093068344	-1.180647225816	0.149873899556
C	-0.697549906458	1.804922669878	0.036304365194
C	0.639882273265	-0.837276666177	-1.027823615360
O	0.709201833726	-1.594727116559	-1.989806214362
O	-1.559686658891	2.682844574855	0.029447830415
N	0.061421385183	1.527487694539	-1.059223836590
C	1.198106190484	0.593931168843	-1.084601406661
H	1.859162122373	0.770786474072	-0.227891597831
C	-0.131411485287	2.233611838620	-2.332512078774
H	-1.191961072625	2.245638369499	-2.597102896015
H	0.193964381785	3.277852044362	-2.231050345389
C	0.750108132949	1.442333994073	-3.308372485762
H	0.190046991187	0.600304240261	-3.727212094435
H	1.109683977481	2.059956688211	-4.136408984684
C	1.888462149415	0.907457567396	-2.420824323196
H	2.647716692891	1.680881850441	-2.258865949661
H	2.369326308259	0.020456301502	-2.836019300970
C	-0.690842835110	-2.503416577614	0.238390460495
H	-1.130804401881	-2.507339639260	1.238248612343
C	-1.848896404700	-2.586530394388	-0.765759411680
H	-2.417984605120	-3.505636986441	-0.584851819947
H	-1.481348905917	-2.600431431197	-1.793021769854
H	-2.529128593742	-1.736985363405	-0.642753687806
C	0.271858628740	-3.693299115414	0.133576674453
H	1.073096798985	-3.623706261880	0.878148577137
H	0.724335611944	-3.742827890137	-0.858201880076
H	-0.278393030227	-4.623695618108	0.315392322415

Cartesian Coordinates of (11a*S*)-(+)-11a-methyl-10-isopropyl-1,2,3,11a-tetrahydro-5*H*-pyrrolo[2,1-*c*][1,4]benzodiazepine 5,11(10*H*)-dione (*M*)-(*S*)-2b

C	-1.482247939228	-2.199360274041	-0.779054126301
C	-2.294469522187	-1.152968069369	1.651756427253
C	-0.945797908773	-0.969134258751	-0.357047072154
C	-2.408747285258	-2.888099964186	-0.003841845666
C	-2.828300238209	-2.359960712591	1.218999522255
C	-1.342724173650	-0.454435576541	0.892388386511
H	-2.799858143529	-3.838214378375	-0.357329802861

H	-3.559365360521	-2.884771682815	1.826830910085
H	-2.606345117565	-0.706338330972	2.589849177500
N	-0.069757462333	-0.276980100306	-1.249363347965
C	1.136874412666	0.291924188008	-0.893113746457
O	1.890966788763	0.757006896927	-1.740900822999
C	1.518076205067	0.363484721098	0.611549334134
N	0.480392271017	1.124022559989	1.354291979158
C	1.016732480142	2.312910555443	2.036983599668
H	0.785393921920	3.218638820968	1.460064496464
H	0.538426377330	2.414302674497	3.013272026217
C	2.767496567281	1.272241782575	0.781177539973
H	3.687844032867	0.681931867540	0.788820416294
H	2.829102800633	1.958609113222	-0.065566179084
C	2.518904542198	2.037590642849	2.086457140254
H	2.760891158838	1.420786002839	2.960354529934
H	3.111012447806	2.955129508911	2.153070220589
H	-1.159395408766	-2.620788574415	-1.724972699720
C	-0.840442197596	0.817121667263	1.508704489355
O	-1.586606763995	1.519680846705	2.192452589745
C	-0.494980385307	-0.189719610608	-2.688547804551
H	-1.488580346674	-0.642809823872	-2.696690063539
C	-0.669901342210	1.268932487824	-3.134450290678
H	0.287327705480	1.789676123210	-3.184128884855
H	-1.332385552288	1.805930835169	-2.447087039007
H	-1.129583706772	1.286027225239	-4.129380628260
C	0.403844986215	-0.996006458781	-3.635180175276
H	1.401937820413	-0.559612359373	-3.693812630666
H	-0.038317537820	-0.999297908823	-4.638311626806
H	0.498729089124	-2.036882585869	-3.305509351319
C	1.810944640937	-1.031118721091	1.207391203131
H	0.936153509619	-1.680606778634	1.246219999824
H	2.195171528411	-0.918011471587	2.226710257370
H	2.580939870028	-1.526911838299	0.605646830816

Cartesian Coordinates of (11a*S*)-(+)-11a-methyl-10-isopropyl-1,2,3,11a-tetrahydro-5*H*-pyrrolo[2,1-*c*][1,4]benzodiazepine 5,11(10*H*)-dione (*P*)-(*S*)-2b

H	0.296306256066	-2.056349882401	2.605670035440
C	0.021713318554	-1.007356660360	2.575295497716
C	-0.648690902365	1.679020969237	2.519442060171
C	-0.184220740030	-0.386291713513	1.329654301014
C	-0.108980091931	-0.300502290236	3.765927672264
C	-0.454527429213	1.052488395992	3.743696361421
C	-0.500947881473	0.987255520733	1.307691156486
H	0.062185479794	-0.809897924158	4.710335687670
H	-0.567923361354	1.609626297534	4.668925581789

H	-0.932766303663	2.724592567370	2.463121189749
N	-0.115430911724	-1.198726266342	0.154559512192
C	-0.739167853426	1.792838080646	0.066848322992
C	0.578224928079	-0.872322278548	-0.995228720300
O	0.688946371880	-1.671844813458	-1.919120778131
O	-1.585331687102	2.687843038332	0.047447809521
N	0.038318252980	1.523156016693	-1.020858119176
C	1.165806368368	0.561652813603	-1.117464995815
C	-0.252722133194	2.200684278039	-2.295447984986
H	-1.333778018878	2.292160687087	-2.420911517109
H	0.163307675201	3.217516693871	-2.285490813946
C	0.438153714104	1.310794453288	-3.330319527073
H	-0.210927682402	0.474301420722	-3.609627450617
H	0.703414068513	1.856897853696	-4.240407117290
C	1.660869809152	0.790436248806	-2.567882621281
H	2.445688027777	1.555995949427	-2.548504634112
H	2.074905616033	-0.128357768227	-2.983263072628
C	-0.831341486371	-2.519830477419	0.197403115825
H	-1.339450535621	-2.512935649956	1.164059259138
C	-1.924379851064	-2.600945782036	-0.877388015290
H	-2.516532595732	-3.509544205973	-0.718217079188
H	-1.496421858437	-2.635576670560	-1.880100190266
H	-2.599456784666	-1.741312687467	-0.806910509320
C	0.121385676567	-3.722234381757	0.169065088732
H	0.878548473424	-3.649262221566	0.958099871022
H	0.630791286187	-3.795626626640	-0.792746621469
H	-0.450950651120	-4.642298514895	0.335320895853
C	2.326251907985	0.817077072235	-0.134578255742
H	2.085798286324	0.603417160639	0.906996807814
H	2.637934872587	1.864135467877	-0.206863418903
H	3.175634760494	0.186938509913	-0.422293642660

Cartesian Coordinates of the transition structure for deprotonation of (11a*S*)-(+)-10-isopropyl-1,2,3,11a-tetrahydro-5*H*-pyrrolo[2,1-*c*][1,4]benzodiazepine 5,11(10*H*)-dione by $(LiNMe_2)_2$. (*M*)-(*S*)-49b

H	-1.938513544341	2.435003996382	-1.784236950117
C	-1.698710985046	2.590328885966	-0.738924348507
C	-1.075590344681	3.023701285207	1.921135903821
C	-1.498086427694	1.478796103051	0.100278088035
C	-1.590716950856	3.890313932405	-0.255993674852
C	-1.277298146810	4.114512942255	1.085624514044
C	-1.166981477417	1.705400810992	1.447998460240
H	-1.749903131532	4.725411246328	-0.932855728946
H	-1.197789384049	5.125588059075	1.474191163859

H	-0.864935285928	3.156357363410	2.976939859352
N	-1.685387268901	0.171003613820	-0.468022955973
C	-0.973933268219	0.634884510008	2.479745672811
C	-0.731189030985	-0.819826243648	-0.363395571369
N	-0.377664803743	-0.512870762180	2.076789168258
C	0.209689810001	-0.822256195846	0.756432380488
C	0.902924818743	-2.186086483971	0.972300288627
H	1.851360333337	-2.258424362152	0.423298617640
C	1.118658592796	-2.274928639956	2.491551166617
C	-0.115142584333	-1.571175435374	3.058319293169
H	0.027624344713	-1.122244385963	4.042685087753
H	-0.974398158534	-2.254935279079	3.122041277295
O	-1.330777884596	0.821299268397	3.648026347413
H	0.263277398830	-3.011696103303	0.632590120438
H	2.022082451336	-1.728085918466	2.782621985242
H	1.217066107460	-3.306014334555	2.844631206832
C	-2.860106786589	-0.026098242093	-1.374691996938
H	-3.483762227577	0.849447664165	-1.177912224577
C	-2.536628228564	-0.046381585549	-2.878206234074
H	-2.058441946342	-0.984115772689	-3.165095107290
H	-1.873397335831	0.775609754222	-3.166379063158
H	-3.468074867287	0.058354926027	-3.447346026698
C	-3.670594811404	-1.258336366842	-0.948848373923
H	-3.107272139170	-2.180931342307	-1.109222044520
H	-4.590833451188	-1.312556070857	-1.541522752302
H	-3.948267300082	-1.192827795335	0.108034839153
H	1.230455856184	-0.035052089701	0.429487363490
N	2.483923359797	0.600739708589	0.024688079330
Li	2.972928894077	-0.625966895843	-1.370846578411
N	2.647116955261	-2.089430834614	-2.617765456362
O	-0.646080419450	-1.683080037362	-1.288756759691
Li	0.816132653205	-2.349640284255	-2.104576115256
C	3.325752683208	0.685737116041	1.213992359320
H	4.260898289129	1.246604948334	1.029508505590
H	3.612623365623	-0.318406225173	1.555190337582
H	2.823073573574	1.190036084694	2.060818692757
C	2.123917287341	1.946781713550	-0.412876383926
H	3.005066788334	2.534588967661	-0.730425267454
H	1.620164031878	2.535574483656	0.374879890193
H	1.436067498805	1.899916307379	-1.268144953620
C	2.806601988876	-1.659323399740	-4.006233055634
H	3.842507830250	-1.344311124334	-4.250171947559
H	2.151301665655	-0.803093858635	-4.226237405352
H	2.559510427894	-2.452887927207	-4.741074045845
C	3.531697458240	-3.227078334653	-2.375589076848
H	4.604123938984	-2.989192827360	-2.534560165532
H	3.321087387468	-4.093144144242	-3.036121182170

H	3.433479996389	-3.583396858099	-1.339041016184

Cartesian Coordinates of the transition structure for deprotonation of (11a*S*)-(+)-10-isopropyl-1,2,3,11a-tetrahydro-5*H*-pyrrolo[2,1-*c*][1,4]benzodiazepine 5,11(10*H*)-dione by $(LiNMe_2)_2$. (*P*)-(*S*)-49b

H	-2.592052963699	-3.218675321079	-0.225244767011
C	-3.090092861668	-2.269189261663	-0.079675200163
C	-4.408046686435	0.125684330504	0.243697498461
C	-2.326620343179	-1.109383566582	0.157568187556
C	-4.478594238549	-2.234209276263	-0.144287967345
C	-5.150521501347	-1.024895297045	0.019689929339
C	-3.003126533815	0.117166900317	0.310014761766
H	-5.026022175057	-3.154674752193	-0.328960280198
H	-6.234600350358	-0.978067175874	-0.024001114630
H	-4.893013027559	1.082338102557	0.397371931988
N	-0.902087692980	-1.261101486758	0.250857622213
C	-2.416757578266	1.483594211826	0.548235415655
C	-0.042223432173	-0.462603470146	-0.486133102282
N	-1.145045472708	1.769512960356	0.151678140163
C	-0.089418702370	0.987088282399	-0.479856340836
C	-0.126307629326	3.222628172352	-1.439520475024
C	-0.774994002899	3.180455197090	-0.032413368088
H	-1.672495256632	3.789322294419	0.065568400270
H	-0.066002727428	3.486185664892	0.744117857552
O	-3.135301036892	2.364040312168	1.031190321858
H	-0.830966740929	3.627095833015	-2.172452647788
C	0.231990075554	1.750417615405	-1.782590372941
H	-0.376842766037	1.380062846859	-2.616245494316
H	1.283365056478	1.633466689543	-2.060654542626
H	0.756154333154	3.868237490685	-1.443447935912
C	-0.380741894852	-2.530489952330	0.848206901362
H	-1.224558611124	-2.894767931880	1.438627317862
C	0.013332229797	-3.641405415442	-0.145494134527
H	1.023824135141	-3.491114951533	-0.531202322700
H	-0.664532911364	-3.690493054981	-1.002170481998
H	-0.012932392183	-4.610767929634	0.366753468571
C	0.750473832978	-2.236138287543	1.840023525023
H	1.631006473434	-1.828730843147	1.334872988334
H	1.049533116988	-3.164955595770	2.338966939660
H	0.425129977775	-1.525049570438	2.604985319665
H	0.953181201954	1.223434828542	0.204823485097
N	2.283767604670	1.583022791406	0.977445034057
Li	3.455236358892	0.250250909975	0.268664227059
N	4.308158533031	-0.940505361689	-1.030827559368
Li	2.567120645573	-1.295464178405	-1.715171094692

O	0.953726240665	-1.010014799746	-1.045981621163
C	2.807358760890	2.893422783971	0.608098052039
H	3.122845195014	2.903812256709	-0.445721465536
H	3.687976615487	3.184913044966	1.214331287977
H	2.076153918438	3.715986902965	0.734914327991
C	1.868948164848	1.609325857762	2.373793034321
H	1.106756524782	2.383982882835	2.586724002649
H	2.711462375242	1.811277675238	3.063665053230
H	1.436516470520	0.643312731887	2.662723303691
C	5.249804951545	-0.224037142633	-1.886438026076
H	4.763664796509	0.640802677576	-2.362815534709
H	5.662656511307	-0.852160697854	-2.701926827790
H	6.131113682179	0.165271353418	-1.335820559045
C	4.994479808062	-2.080048147506	-0.428752869017
H	5.397249299527	-2.793143379409	-1.176838978890
H	4.311265114553	-2.648516686221	0.220704424535
H	5.862487163451	-1.785753210220	0.197138486625

Cartesian Coordinates of the transition structure for explicit bis(Me_2O) solvate (*M*)-(*S*)-50b

H	2.853729752922	0.389451403434	-3.022651969576
C	3.134693508678	-0.314167911880	-2.248537614613
C	3.869399102802	-2.134630800258	-0.302875558026
C	2.775971737257	-0.040192274054	-0.908505043646
C	3.824737959658	-1.468413345708	-2.604097354013
C	4.179777890360	-2.404359527274	-1.630219788713
C	3.181400381032	-0.972203606815	0.081943701374
H	4.076063500992	-1.638530252227	-3.648549458080
H	4.716001808775	-3.310568407615	-1.897649460437
H	4.200356621684	-2.795841932587	0.491429619631
N	2.080942538368	1.144725401374	-0.594346757501
C	3.097682864010	-0.764585707758	1.570693730252
C	0.871442055723	1.092752801393	0.192048200900
N	2.070150165053	-0.020141854954	2.064498110993
C	0.886637079108	0.426931708231	1.382790099129
C	-0.264930649223	0.413361116781	2.369485300933
H	-1.154095773599	-0.134093963251	2.020168217300
C	0.340032539639	-0.237976986560	3.634484980064
C	1.844232810520	0.056574480092	3.510197575292
H	2.495130923691	-0.656163616086	4.016474450892
H	2.077942068452	1.068031237556	3.871872053207
O	3.951420688216	-1.273929590072	2.308169097037
H	-0.605104351034	1.439843240374	2.584065757105
H	0.185800656206	-1.324198145957	3.612552542064

H	-0.092589363143	0.142300752601	4.565394250637
C	2.403073691738	2.394987929851	-1.313559482226
H	3.423806774634	2.243695314687	-1.683095778165
C	1.511102102221	2.733709903008	-2.525007492655
H	0.504600955957	2.992766778666	-2.194611415682
H	1.423448660559	1.891376380897	-3.218105127203
H	1.941232971430	3.580621942908	-3.075323962241
C	2.445892564793	3.569859177983	-0.323826797075
H	1.451952427461	3.756575783816	0.094900091412
H	2.782089821249	4.482394514436	-0.830754982590
H	3.134323964868	3.355016883184	0.499562944214
H	-0.048018398268	-1.240992618062	-0.097835866883
N	-0.556371987352	-2.058118365076	-0.458205407012
Li	-2.536873963441	-1.496663290302	-0.429273668364
N	-3.412642245688	0.236315867510	-0.534352397329
O	-0.183385692605	1.667671351554	-0.295946427589
Li	-1.979304376338	1.595543280014	-0.181054461194
C	-0.098769970098	-3.227215613944	0.310183923330
H	-0.640641897905	-4.119758176476	-0.023040969580
H	-0.303248431442	-3.070347724618	1.374349534759
H	0.978577164516	-3.410539759657	0.189922993552
C	-0.211738835204	-2.192726454872	-1.887258815553
H	-0.766611639737	-3.036482655560	-2.315791053693
H	0.861398202646	-2.363339292579	-2.049480220573
H	-0.497267638875	-1.278980806265	-2.418164165490
C	-3.900055650614	0.604046098628	-1.856096508234
H	-4.705241692646	-0.062998211645	-2.241822952825
H	-3.083153976575	0.574750114545	-2.593507075656
H	-4.333611709224	1.627182428762	-1.897237841876
C	-4.523296964667	0.301858999750	0.399659595215
H	-5.352495934801	-0.404077503339	0.163082737779
H	-5.010061867768	1.301152972498	0.442181411513
H	-4.188541878442	0.066185729880	1.422234032207
O	-2.662059388075	3.482264456665	0.082311762562
C	-3.355360117547	3.865350725095	1.262560972718
H	-4.055748626758	4.685974744894	1.052876171005
H	-2.652272900152	4.185446381244	2.045119728004
H	-3.916411702358	2.994342266005	1.605363624261
C	-1.893769908462	4.548367346668	-0.465644622591
H	-2.550028025517	5.379342760999	-0.760364055430
H	-1.377407106225	4.156474339597	-1.342153737486
H	-1.149991846825	4.909521292802	0.257131304175
O	-3.677826151562	-3.136423275096	-0.320973012387
C	-3.767043229438	-3.987654902287	0.817399344708
H	-3.906239485146	-5.032901650542	0.510069014313
H	-4.602842693879	-3.686677214822	1.463631569808
H	-2.828131685235	-3.897460166277	1.366367379777

C	-4.850794505600	-3.184885904220	-1.132305587736
H	-4.981856786187	-4.189780590748	-1.555680718234
H	-4.718251535341	-2.459527281955	-1.936598310983
H	-5.739697990195	-2.914681660147	-0.548068670316

Cartesian Coordinates of transition structure for explicit bis(Me_2O) solvate (*P*)-(*S*)-50b

H	3.247336518546	2.091582560415	2.352086274581
C	3.819378463782	1.447544606453	1.697723015598
C	5.337902192100	-0.159792542933	0.045570855771
C	3.160947631983	0.429479312571	0.972886603859
C	5.189580003268	1.662038401170	1.588953367020
C	5.961681429996	0.866182662073	0.743389282660
C	3.958399648080	-0.399811377777	0.142434871190
H	5.648555402470	2.463123223165	2.163955302649
H	7.031583250436	1.027859620719	0.646959748739
H	5.912163757288	-0.840751669623	-0.573257199531
N	1.767490119301	0.223566640612	1.126879015063
C	3.503648393520	-1.637552473131	-0.579688768947
C	0.933777285954	0.209793330968	-0.056564809481
N	2.204383797227	-1.712416316584	-0.994797195217
C	1.231607502945	-0.662277165786	-1.060185412551
C	1.193252362708	-1.957937514329	-3.106514197527
C	1.805633800467	-2.757356870709	-1.938898928741
H	2.675151210347	-3.358666082965	-2.203576707788
H	1.054303216857	-3.412768441022	-1.471209728347
O	4.299310855336	-2.562508617397	-0.781761637124
H	1.986260305326	-1.687054544770	-3.812175958710
C	0.607142888403	-0.680738451502	-2.443046062378
H	0.858178924009	0.216780112989	-3.027944012758
H	-0.491321091339	-0.707354305748	-2.408054684658
H	0.446202289482	-2.536446525158	-3.660539359174
C	1.146219979482	0.544344744680	2.429253035929
H	1.953470294596	0.404475881208	3.156624362895
C	0.587457831413	1.973044456037	2.619896101446
H	-0.353713038291	2.098180226122	2.083611603663
H	1.276175696107	2.737304281494	2.250720841463
H	0.415414420463	2.159004366106	3.688696019687
C	0.067206847333	-0.493535351519	2.766674069315
H	-0.781920711593	-0.391343107050	2.082677884755
H	-0.296657770778	-0.344803822259	3.790914277709
H	0.471938234939	-1.507673760570	2.684371837351
H	-0.991458456424	-1.739714987276	-0.458248012414
N	-1.883737757445	-2.223173560563	-0.291896921269

Li	-3.197482818618	-0.686609153739	0.166733614463
N	-3.486491720167	1.136953483438	-0.456479753452
Li	-1.592464107340	1.745923238429	-0.674636466707
O	-0.038781591590	1.066721154337	-0.118019730517
C	-2.329452327317	-2.824612197503	-1.561294966717
H	-2.474835351655	-2.042570025398	-2.312794567726
H	-3.285750528088	-3.336432822708	-1.402898946494
H	-1.612364729057	-3.558948456316	-1.958848186742
C	-1.637505685367	-3.263795591166	0.719449855536
H	-0.926176007920	-4.028320416487	0.372068395991
H	-2.583313073015	-3.758068355851	0.965695046154
H	-1.231992947626	-2.807476439357	1.625512979103
C	-4.267483706217	1.154284872573	-1.682267693722
H	-3.764653396138	0.578193446814	-2.474182722685
H	-4.433747367114	2.175195643059	-2.090841405606
H	-5.291991283888	0.727125043003	-1.574201002777
C	-4.140285669875	1.987042413093	0.525233050069
H	-4.251968603955	3.041943863474	0.191414562835
H	-3.564579042500	2.012607559139	1.463145316450
H	-5.172652463676	1.662697670016	0.789540164066
O	-1.207432938469	3.525755273015	-1.482137046645
C	0.146830447407	3.976268499268	-1.469414672113
H	0.238257563045	4.901634088298	-0.883439483653
H	0.500643284747	4.161386517600	-2.493305954630
H	0.724845867396	3.176847409878	-1.005424661299
C	-2.107891079699	4.479904734109	-2.023884208257
H	-2.097706656458	5.407923175022	-1.434250247954
H	-3.105696862793	4.039346450276	-1.990042030561
H	-1.847066359149	4.716957150284	-3.065354636124
O	-4.605039016551	-1.546634686514	1.331477806154
C	-5.971653911258	-1.333872048539	0.976140086983
H	-6.338699517645	-0.381387117867	1.378192297721
H	-6.594624359623	-2.157175530985	1.350377494577
H	-6.021436042315	-1.305558868243	-0.113908694426
C	-4.412585617638	-1.580807973861	2.744300529257
H	-4.680056836390	-0.617472747489	3.199144820384
H	-3.356165604343	-1.789473900690	2.922768791554
H	-5.018913167445	-2.376856176620	3.196447562444

Cartesian Coordinates of the equilibrium geometry for the enolate free anion derived from (11a*S*)-(+)-10-isopropyl-1,2,3,11a-tetrahydro-5*H*-pyrrolo[2,1-*c*][1,4]benzodiazepine 5,11(10*H*)-dione. (*M*)-51b

C	-1.468866676076	0.007297085251	0.540398672064
C	-1.396123878945	-0.395741625370	3.312197113439

C	-0.235873178781	-0.354206293067	1.147008109655
C	-2.622620143097	0.138379910505	1.324850346624
C	-2.605143596464	-0.054673373413	2.702399030899
C	-0.239286558550	-0.533141325595	2.550645460479
H	-3.545807068098	0.367830486155	0.801308228364
H	-3.515576574853	0.052119001477	3.288252802301
H	0.690301471748	-0.775611032687	3.048342457887
H	-1.346309684250	-0.549383994945	4.389341453305
N	0.919141181510	-0.575684347468	0.374794982340
C	1.030870556641	2.282518864473	-2.201159787387
H	2.120239228768	2.373449960200	-2.243335592244
H	0.618942156788	3.289627704912	-1.993919575305
N	-0.654620849815	0.732269679712	-1.640693990333
C	-1.672404771055	0.199669794277	-0.933232135914
O	-2.765846485973	-0.085650053990	-1.469262872652
C	0.410256391055	1.743002719922	-3.513782149340
H	0.223730020642	2.512224129388	-4.275439414445
H	1.082062957321	0.993556505715	-3.949705059984
C	-0.895963617151	1.068701720187	-3.054534303376
H	-1.763158268184	1.739442308295	-3.122969976689
H	-1.150230911190	0.168938194402	-3.626831294969
C	1.877199461457	-1.652820386638	0.676264117107
H	2.492254026976	-1.693992848600	-0.228698618390
C	2.884008825264	-1.411270483873	1.825938643721
H	3.252905712653	-0.386870959052	1.754459246681
H	3.735266731090	-2.098360053808	1.714146338948
H	2.458171156259	-1.592164565754	2.820495828986
C	1.164306337883	-3.004939554367	0.817661546528
H	0.535364478788	-3.203701420826	-0.056895309027
H	0.523399102656	-3.037301671236	1.705828882492
H	1.902966091456	-3.812457121706	0.908750734654
C	1.504117434967	0.551354339751	-0.396852268442
C	0.619810996512	1.241395927869	-1.204442434376
O	2.729360429425	0.786074320601	-0.234736858186

Cartesian Coordinates of the ring inversion transition structure of the enolate free anion derived from (11a*S*)-(+)-10-isopropyl-1,2,3,11a-tetrahydro-5*H*-pyrrolo[2,1-*c*][1,4]benzodiazepine 5,11(10*H*)-dione. (*M*)-51b[*]

C	-1.475895009994	-0.012965076144	0.534461559645
C	-1.482146869291	-0.117813058963	3.350968411710
C	-0.205995453031	-0.101857929670	1.209974071485
C	-2.658068333923	-0.051923602804	1.296900656463
C	-2.700833636477	-0.121930330582	2.682708110917
C	-0.293911644317	-0.099461757267	2.634958190728
H	-3.572663915669	0.003649859741	0.718571900626
H	-3.649504436209	-0.150399666192	3.213218641630

H	0.612921375063	-0.087841317161	3.211672100795
H	-1.436053342022	-0.126847718140	4.439516301940
N	1.068240244391	-0.205344672594	0.647631032371
C	1.451168485601	-0.160396658851	-0.804395055579
C	0.579200773206	0.112896353884	-1.824978359878
C	1.079567480645	0.168384167415	-3.245027819745
H	1.144182353401	-0.828750148909	-3.723308050129
H	2.085354492909	0.596526311220	-3.296445134258
N	-0.837084021192	0.347674171631	-1.851140287133
C	-1.804195719649	0.208249166073	-0.928924330935
O	2.678437449916	-0.381242423398	-1.047083977266
O	-3.002058091039	0.327451610903	-1.279306264118
C	0.014848754751	1.018723460027	-3.958321684732
H	0.227753977569	2.085722462634	-3.812501189994
H	-0.058235497533	0.834326036756	-5.037581428292
C	-1.275688978299	0.645325147700	-3.223703572999
H	-2.035233193337	1.430860398315	-3.205522143427
H	-1.750366653273	-0.245687432705	-3.660583568214
C	2.257539555107	-0.467251841248	1.494145187644
H	3.017091042645	-0.609386788561	0.722254614011
C	2.760626315695	0.749335704802	2.296929918923
H	2.882282856219	1.597828592522	1.614777038496
H	3.747687916794	0.518591273893	2.721747873216
H	2.118031201627	1.075470810438	3.121327778480
C	2.233804429198	-1.801471704508	2.263902324200
H	1.982710411311	-2.611233118348	1.569826617816
H	1.534700242767	-1.855384711088	3.103242717393
H	3.240091838989	-2.000477076896	2.657886997232

Cartesian Coordinates of the equilibrium geometry for the $Li(OMe_2)_3$ salt of the enolate derived from (11a*S*)-(+)-10-isopropyl-1,2,3,11a-tetrahydro-5*H*-pyrrolo[2,1-*c*][1,4]benzodiazepine 5,11(10*H*)-dione. (*M*)-52b

C	-3.071458822197	0.459211106814	0.589414282139
C	-2.683201778826	0.843864933771	3.338443324014
C	-2.013535065104	-0.219673645367	1.239242753083
C	-3.908060471033	1.309854008492	1.326294045129
C	-3.723281541037	1.512423808676	2.689577799188
C	-1.838516276294	0.000052787001	2.621466039012
H	-4.730590756464	1.779249013097	0.796482218790
H	-4.386350763393	2.173186141804	3.241514796116
H	-1.022656326013	-0.497733691650	3.131477938586
H	-2.521490423078	0.983607320702	4.405095743651
N	-1.175911089600	-1.105019451820	0.525112209097
C	-0.458871825750	0.510244103846	-2.883836763045
H	0.559637105874	0.147418805726	-3.046133299938

H	-0.433995290672	1.612107324101	-2.949145367947
N	-2.465025142207	-0.000738879220	-1.756481269637
C	-3.445726490746	0.277600680112	-0.853975901460
O	-4.621671268860	0.416222126043	-1.219175807487
C	-1.468337243501	-0.044050366313	-3.915916287156
H	-1.483086926615	0.513543156551	-4.858570517151
H	-1.218358929989	-1.086239438385	-4.145922639494
C	-2.822803180421	0.024775925840	-3.187051693594
H	-3.373041395027	0.948637721698	-3.401887506670
H	-3.490519417178	-0.807113946843	-3.433620218935
C	-0.868402335265	-2.473041207034	0.975088028406
H	-0.477503422250	-2.960552547373	0.074041567724
C	0.232043254749	-2.615847206854	2.048608099277
H	1.087842696787	-1.992991186680	1.779579691576
H	0.561918684439	-3.661953136061	2.103995074678
H	-0.120805953094	-2.337204984600	3.048247157438
C	-2.146906323274	-3.215674754150	1.386069142597
H	-2.884748044725	-3.192498473095	0.578007910286
H	-2.603669562942	-2.766191339891	2.274533036053
H	-1.917369794760	-4.261958716712	1.620633043105
C	-0.379684673505	-0.578405111812	-0.556255054114
C	-1.040227374957	0.014092707072	-1.588587480458
O	0.916683856138	-0.700743826710	-0.460973061791
Li	2.411971934771	0.224726780367	-0.132304246325
O	3.499251151633	-0.096436114483	1.564712015518
O	3.784196412175	-0.367318000920	-1.514780239442
O	2.220334046082	2.222437427149	0.049474992674
C	4.202382321745	-1.326594776704	1.709237502523
H	4.533342610343	-1.618281310473	0.711553280272
H	3.547002836353	-2.105638899108	2.120210898817
H	5.072681834820	-1.200629984653	2.368639563359
C	2.966825966295	0.377904659627	2.798790088882
H	2.419017985937	1.294098753088	2.574409628752
H	3.775650874863	0.591586317376	3.511650946044
H	2.281846651606	-0.359105833311	3.236948717067
C	3.266534863204	3.165577319072	0.219006714736
H	3.028405551857	3.875755539553	1.023843675774
H	3.445226319159	3.729398635370	-0.707767833947
H	4.166386762232	2.607557246825	0.488091592830
C	0.963362738739	2.835223122660	-0.252643628484
H	0.653384384533	3.491705052356	0.571731111250
H	0.235171636760	2.033283073421	-0.385707793876
H	1.037794575078	3.426428428437	-1.175498596675
C	3.288844261657	-1.298420426747	-2.480324053714
H	2.303392902812	-1.601354063409	-2.123761436972
H	3.963612573549	-2.162574675016	-2.558601291593
H	3.201883566974	-0.819968276233	-3.465718517351

C	5.039298985801	0.187696764094	-1.870235153859
H	5.334591004614	0.868265738931	-1.068251703192
H	4.972097784636	0.745443044323	-2.815274829851
H	5.801908962293	-0.597332314905	-1.976863890201

Cartesian Coordinates of the ring inversion transition structure for the Li(OMe$_2$)$_3$ salt of the enolate derived from (11a*S*)-(+)-10-isopropyl-1,2,3,11a-tetrahydro-5*H*-pyrrolo[2,1-*c*][1,4]benzodiazepine 5,11(10*H*)-dione. (*M*)-52b[*]

C	3.429541945044	0.284070006967	0.292511918116
C	4.770573605413	-2.185072383546	0.254966992713
C	2.696649255855	-0.877590441762	-0.123203453368
C	4.744558301427	0.127531021242	0.766961387585
C	5.422421562806	-1.082023870135	0.794208356131
C	3.461877085680	-2.072365310471	-0.194338605263
H	5.235557480499	1.040949594878	1.080763301459
H	6.437810050134	-1.144881681727	1.174047476970
H	3.016074881387	-2.956763970418	-0.612831040160
H	5.270867714390	-3.147733004653	0.172852977786
N	1.322416992492	-0.974035795140	-0.415018006594
C	0.382803771325	0.136919610048	-0.562647057479
C	0.695563474296	1.456381888198	-0.604622653990
C	-0.356165095745	2.509080539697	-0.868069714538
H	-0.863984142525	2.836470393045	0.057002379114
H	-1.133399215744	2.140951610142	-1.544904686869
N	1.950319641746	2.139791454848	-0.475857408280
C	3.091533139885	1.751202492588	0.143873442187
O	3.914946719521	2.615339461715	0.477993133014
C	0.453452145343	3.678841412859	-1.453271122691
H	0.618040244020	3.518050139100	-2.525394519406
H	-0.026009687776	4.655608735371	-1.327189638637
C	1.780925885142	3.584814164942	-0.700482930076
H	2.640285811411	3.979906760853	-1.247584846638
H	1.744013398674	4.112067602179	0.263041735067
C	0.667224647792	-2.306356136721	-0.524343793617
H	-0.381783809301	-2.027469004670	-0.525908232267
C	0.875404571120	-3.009898095043	-1.880677534292
H	0.631571207201	-2.314301231574	-2.690988824085
H	0.192013312646	-3.866850921559	-1.956887593450
H	1.884958593492	-3.388455863531	-2.062188920884
C	0.812950113325	-3.221010168672	0.708050449274
H	0.570642732190	-2.657761451885	1.616315927200
H	1.797798511531	-3.668442993763	0.852468292028
H	0.087846241436	-4.040346883372	0.618157453010
O	-0.880650477953	-0.216522249676	-0.669240519138
Li	-2.471014754884	-0.107595163158	0.124172577723
O	-3.527295132348	-1.690602005762	-0.682286979061

O	-2.347766114040	-0.006793916155	2.127914885483
O	-3.939950007399	1.315855023005	-0.045791120290
C	-4.498946938455	-2.564824857208	-0.131475014595
H	-4.852066135462	-2.116919325848	0.800329700813
H	-4.064825583007	-3.551808148519	0.081907554568
H	-5.349813210692	-2.693503064002	-0.816045817302
C	-2.990692154935	-2.179859915116	-1.913873439528
H	-2.190258716266	-1.496081503921	-2.197548990587
H	-3.774398224000	-2.211257889456	-2.684166303253
H	-2.577988351222	-3.188723965218	-1.779733636948
C	-4.839943807163	1.321601967529	-1.148929665233
H	-4.510688009345	2.033681093266	-1.918121752908
H	-5.857207157252	1.586699945408	-0.823573757004
H	-4.842639253866	0.312153798360	-1.560595948024
C	-3.819720693456	2.602859273402	0.552420417842
H	-3.446650507445	3.337455305088	-0.172608964834
H	-3.107031023349	2.507024579362	1.371933602548
H	-4.791304541854	2.939455221430	0.941697751532
C	-1.061946470616	-0.048300669150	2.752321719755
H	-0.324975955052	0.170600558253	1.979351926024
H	-0.872561600548	-1.040920998880	3.182338624315
H	-1.003733795573	0.706448883823	3.548434221459
C	-3.427394188359	-0.183446394312	3.029706696946
H	-4.347720590224	-0.069326470813	2.449656719489
H	-3.404295630323	0.574262134784	3.825795101573
H	-3.398558049800	-1.181277427045	3.490555323927

References for Chapter 6

[1] Madani, H., Thompson, A., Threadgill, M. D., An expedient synthesis of 7-O-functionalized pyrrolo-1,4-benzodiazepine-2,11-diones, *Tetrahedron* **2002**, *58*, 8107.

[2] Wright, W., Brabander, H., Greenblatt, E., Day, I., Hardy, R., Derviatives of 1,2,3,11a-tetrahydro-5H-pyrrolo[2,1-c][1,4]benzodiazepine-5,11(10H)-dione as anxiolytic agents, *J. Med. Chem.* **1978**, *21*, 1087-1089.

[3] Pena, M. R., Stille, J. K., A total synthesis of anthramycin. Application of palladium-catalyzed coupling reactions for the attachment of the acrylic side chain, *J. Am. Chem. Soc.* **1989**, *111*, 5417.

[4] Beard, C. V., Baum, K., Grakaskas, V., Synthesis of some novel trifluoromethanesulfonates and their reactions with alcohols *J. Org. Chem.* **1973**, *38*, 3673.

[5] Sekine, M., Iwase, R., Masuda, N., Hata, T., Synthesis of oligoribonucleotides by use fo 4,4', 4"-tris(acyloxy)trityl groups for protection of the 6-amino group of adenosine, *Bull. Chem. Soc. Jpn.* **1988**, *61*, 1669.

[6] Seebach, D., Boes, M., Naef, R., Schweizer, B., Alkylation of amino acids without loss of the optical activity: preparation of α-substituted proline derivatives. A case of self-reproduction of chirality, *J. Am. Chem. Soc.* **1983**, *105*, 5390.

[7] Jadidi, K., Aryan, R., Mehrdad, M., Lugger, T., Ekkehardt, H., Ng, S., Simple synthesis, structure and ab initio study of 1,4-benzodiazepine-2,5-diones, *Journal of Molecular Structure* **2004**, *692*, 37.

[8] Frisch, M. J., Trucks, G. W., Schlegel, H. B., Scuseria, G. E., Robb, M. A., Cheeseman, J. R., Zakrewski, V. G., Montgomery, J. A., Stratmann, R. E., Burant, J. C., Dapprich, S., Millam, J. M., Daniels, A. D., Kudin, K. N., Strain, M. C., Farkas, O., Tomasi, J., Barone, V., Cossi, M., Cammi, R., Mennucci, B., Pomelli, C., Adamo, C., Clifford, S., Ochterski, J., Petersson, G. A., Ayala, P. Y., Cui, Q., Morokuma, K., Salvador, P., Dannenberg, J. J., Malick, D. K., Rabuck, A. D., Raghavachari, K., Foresman, J. B., Cioslowski, J., Ortiz, J. V., Baboul, A. G., Stefanov, B. B., Liu, G., Liashenko, A., Piskorz, P., Komaromi, I., Gomperts, R., Martin, R. L., Fox, D. J., Keith, T., Al-Laham, M. A., Peng, C. Y., Nanayakkara, A., Challacombe, M., Gill, P. M. W., Johnson, B., W., C., Wong, M. W., Andres, J. L., Gonzalez, C., Head-Gordon, M., Replogle, E. S., Pople, J. A. *Gaussian 03* Pittsburgh PA, 2003.